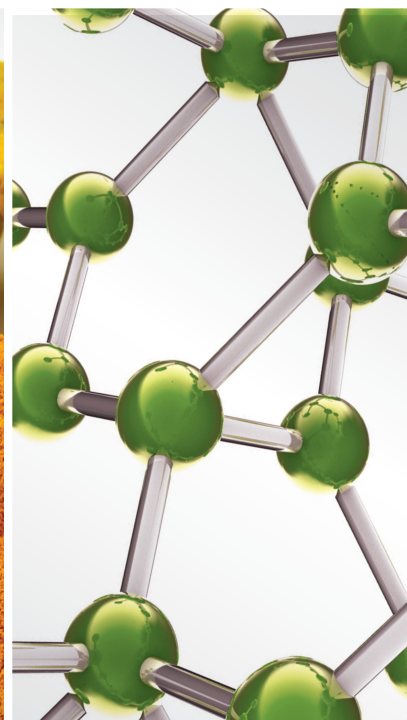
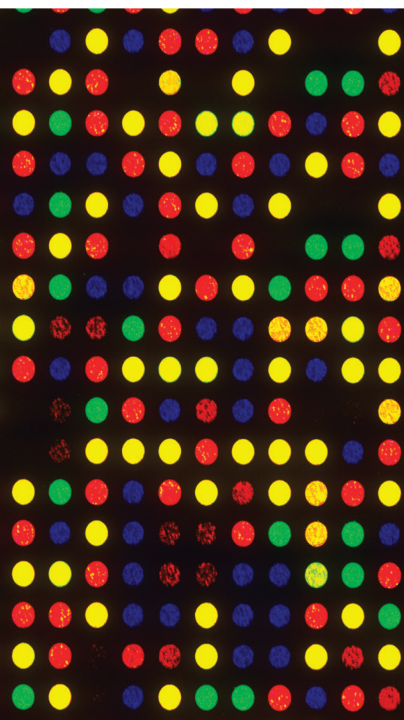



Application of Natural Products in Experimental and Cheminformatics-Based Therapy for Neurological and Metabolic Disorders 2021

Lead Guest Editor: Rajeev K Singla

Guest Editors: Rupesh K Gautam and Christos Tsagkaris





**Application of Natural Products in
Experimental and Cheminformatics-Based
Therapy for Neurological and Metabolic
Disorders 2021**

Evidence-Based Complementary and Alternative Medicine

**Application of Natural Products in
Experimental and Cheminformatics-
Based Therapy for Neurological and
Metabolic Disorders 2021**

Lead Guest Editor: Rajeev K Singla

Guest Editors: Rupesh K Gautam and Christos
Tsagkaris



Copyright © 2022 Hindawi Limited. All rights reserved.

This is a special issue published in "Evidence-Based Complementary and Alternative Medicine." All articles are open access articles distributed under the Creative Commons Attribution License, which permits unrestricted use, distribution, and reproduction in any medium, provided the original work is properly cited.

Chief Editor

Jian-Li Gao , China






Associate Editors

Hyunsu Bae , Republic of Korea
Raffaele Capasso , Italy
Jae Youl Cho , Republic of Korea
Caigan Du , Canada
Yuewen Gong , Canada
Hai-dong Guo , China
Kuzhuvelil B. Harikumar , India
Ching-Liang Hsieh , Taiwan
Cheorl-Ho Kim , Republic of Korea
Victor Kuete , Cameroon
Hajime Nakae , Japan
Yoshiji Ohta , Japan
Olumayokun A. Olajide , United Kingdom
Chang G. Son , Republic of Korea
Shan-Yu Su , Taiwan
Michał Tomczyk , Poland
Jenny M. Wilkinson , Australia

Academic Editors

Eman A. Mahmoud , Egypt
Ammar AL-Farga , Saudi Arabia
Smail Aazza , Morocco
Nahla S. Abdel-Azim, Egypt
Ana Lúcia Abreu-Silva , Brazil
Gustavo J. Acevedo-Hernández , Mexico
Mohd Adnan , Saudi Arabia
Jose C Adsuar , Spain
Sayeed Ahmad, India
Touqeer Ahmed , Pakistan
Basiru Ajiboye , Nigeria
Bushra Akhtar , Pakistan
Fahmida Alam , Malaysia
Mohammad Jahoor Alam, Saudi Arabia
Clara Albani, Argentina
Ulysses Paulino Albuquerque , Brazil
Mohammed S. Ali-Shtayeh , Palestinian Authority
Ekram Alias, Malaysia
Terje Alraek , Norway
Adolfo Andrade-Cetto , Mexico
Letizia Angiolella , Italy
Makoto Arai , Japan

Daniel Dias Rufino Arcanjo , Brazil
Duygu AĞAGÜNDÜZ , Turkey
Neda Baghban , Iran
Samra Bashir , Pakistan
Rusliza Basir , Malaysia
Jairo Kenupp Bastos , Brazil
Arpita Basu , USA
Mateus R. Beguelini , Brazil
Juana Benedí, Spain
Samira Boulbaroud, Morocco
Mohammed Bourhia , Morocco
Abdelhakim Bouyahya, Morocco
Nunzio Antonio Cacciola , Italy
Francesco Cardini , Italy
María C. Carpinella , Argentina
Harish Chandra , India
Guang Chen, China
Jianping Chen , China
Kevin Chen, USA
Mei-Chih Chen, Taiwan
Xiaojia Chen , Macau
Evan P. Cherniack , USA
Giuseppina Chianese , Italy
Kok-Yong Chin , Malaysia
Lin China, China
Salvatore Chirumbolo , Italy
Hwi-Young Cho , Republic of Korea
Jeong June Choi , Republic of Korea
Jun-Yong Choi, Republic of Korea
Kathrine Bisgaard Christensen , Denmark
Shuang-En Chuang, Taiwan
Ying-Chien Chung , Taiwan
Francisco José Cidral-Filho, Brazil
Daniel Collado-Mateo , Spain
Lisa A. Conboy , USA
Kieran Cooley , Canada
Edwin L. Cooper , USA
José Otávio do Amaral Corrêa , Brazil
Maria T. Cruz , Portugal
Huantian Cui , China
Giuseppe D'Antona , Italy
Ademar A. Da Silva Filho , Brazil
Chongshan Dai, China
Laura De Martino , Italy
Josué De Moraes , Brazil

Arthur De Sá Ferreira , Brazil
Nunziatina De Tommasi , Italy
Marinella De leo , Italy
Gourav Dey , India
Dinesh Dhamecha, USA
Claudia Di Giacomo , Italy
Antonella Di Sotto , Italy
Mario Dioguardi, Italy
Jeng-Ren Duann , USA
Thomas Effërth , Germany
Abir El-Alfy, USA
Mohamed Ahmed El-Esawi , Egypt
Mohd Ramli Elvy Suhana, Malaysia
Talha Bin Emran, Japan
Roger Engel , Australia
Karim Ennouri , Tunisia
Giuseppe Esposito , Italy
Tahereh Eteraf-Oskouei, Iran
Robson Xavier Faria , Brazil
Mohammad Fattahi , Iran
Keturah R. Faurot , USA
Piergiorgio Fedeli , Italy
Laura Ferraro , Italy
Antonella Fioravanti , Italy
Carmen Formisano , Italy
Hua-Lin Fu , China
Liz G Müller , Brazil
Gabino Garrido , Chile
Safoora Gharibzadeh, Iran
Muhammad N. Ghayur , USA
Angelica Gomes , Brazil
Elena González-Burgos, Spain
Susana Gorzalczany , Argentina
Jiangyong Gu , China
Maruti Ram Gudavalli , USA
Jian-You Guo , China
Shanshan Guo, China
Narcís Gusi , Spain
Svein Haavik, Norway
Fernando Hallwass, Brazil
Gajin Han , Republic of Korea
Ihsan Ul Haq, Pakistan
Hicham Harhar , Morocco
Mohammad Hashem Hashempur , Iran
Muhammad Ali Hashmi , Pakistan

Waseem Hassan , Pakistan
Sandrina A. Heleno , Portugal
Pablo Herrero , Spain
Soon S. Hong , Republic of Korea
Md. Akil Hossain , Republic of Korea
Muhammad Jahangir Hossen , Bangladesh
Shih-Min Hsia , Taiwan
Changmin Hu , China
Tao Hu , China
Weicheng Hu , China
Wen-Long Hu, Taiwan
Xiao-Yang (Mio) Hu, United Kingdom
Sheng-Teng Huang , Taiwan
Ciara Hughes , Ireland
Attila Hunyadi , Hungary
Liaqat Hussain , Pakistan
Maria-Carmen Iglesias-Osma , Spain
Amjad Iqbal , Pakistan
Chie Ishikawa , Japan
Angelo A. Izzo, Italy
Satveer Jagwani , USA
Rana Jamous , Palestinian Authority
Muhammad Saeed Jan , Pakistan
G. K. Jayaprakasha, USA
Kyu Shik Jeong, Republic of Korea
Leopold Jirovetz , Austria
Jeeyoun Jung , Republic of Korea
Nurkhalida Kamal , Saint Vincent and the
Grenadines
Atsushi Kameyama , Japan
Kyungsu Kang, Republic of Korea
Wenyi Kang , China
Shao-Hsuan Kao , Taiwan
Nasiara Karim , Pakistan
Morimasa Kato , Japan
Kumar Katragunta , USA
Deborah A. Kennedy , Canada
Washim Khan, USA
Bonglee Kim , Republic of Korea
Dong Hyun Kim , Republic of Korea
Junghyun Kim , Republic of Korea
Kyungho Kim, Republic of Korea
Yun Jin Kim , Malaysia
Yoshiyuki Kimura , Japan

Nebojša Kladar , Serbia
Mi Mi Ko , Republic of Korea
Toshiaki Kogure , Japan
Malcolm Koo , Taiwan
Yu-Hsiang Kuan , Taiwan
Robert Kubina , Poland
Chan-Yen Kuo , Taiwan
Kuang C. Lai , Taiwan
King Hei Stanley Lam, Hong Kong
Faniel Lampiao, Malawi
Ilaria Lampronti , Italy
Mario Ledda , Italy
Harry Lee , China
Jeong-Sang Lee , Republic of Korea
Ju Ah Lee , Republic of Korea
Kyu Pil Lee , Republic of Korea
Namhun Lee , Republic of Korea
Sang Yeoup Lee , Republic of Korea
Ankita Leekha , USA
Christian Lehmann , Canada
George B. Lenon , Australia
Marco Leonti, Italy
Hua Li , China
Min Li , China
Xing Li , China
Xuqi Li , China
Yi-Rong Li , Taiwan
Vuanghao Lim , Malaysia
Bi-Fong Lin, Taiwan
Ho Lin , Taiwan
Shuibin Lin, China
Kuo-Tong Liou , Taiwan
I-Min Liu, Taiwan
Suhuan Liu , China
Xiaosong Liu , Australia
Yujun Liu , China
Emilio Lizarraga , Argentina
Monica Loizzo , Italy
Nguyen Phuoc Long, Republic of Korea
Zaira López, Mexico
Chunhua Lu , China
Ângelo Luís , Portugal
Anderson Luiz-Ferreira , Brazil
Ivan Luzardo Luzardo-Ocampo, Mexico

Michel Mansur Machado , Brazil
Filippo Maggi , Italy
Juraj Majtan , Slovakia
Toshiaki Makino , Japan
Nicola Malafronte, Italy
Giuseppe Malfa , Italy
Francesca Mancianti , Italy
Carmen Mannucci , Italy
Juan M. Manzanque , Spain
Fatima Martel , Portugal
Carlos H. G. Martins , Brazil
Maulidiani Maulidiani, Malaysia
Andrea Maxia , Italy
Avijit Mazumder , India
Isac Medeiros , Brazil
Ahmed Mediani , Malaysia
Lewis Mehl-Madrona, USA
Ayikoé Guy Mensah-Nyagan , France
Oliver Micke , Germany
Maria G. Miguel , Portugal
Luigi Milella , Italy
Roberto Miniero , Italy
Letteria Minutoli, Italy
Prashant Modi , India
Daniel Kam-Wah Mok, Hong Kong
Changjong Moon , Republic of Korea
Albert Moraska, USA
Mark Moss , United Kingdom
Yoshiharu Motoo , Japan
Yoshiki Mukudai , Japan
Sakthivel Muniyan , USA
Saima Muzammil , Pakistan
Benoit Banga N'guessan , Ghana
Massimo Nabissi , Italy
Siddavaram Nagini, India
Takao Namiki , Japan
Srinivas Nammi , Australia
Krishnadas Nandakumar , India
Vitaly Napadow , USA
Edoardo Napoli , Italy
Jorddy Neves Cruz , Brazil
Marcello Nicoletti , Italy
Eliud Nyaga Mwaniki Njagi , Kenya
Cristina Nogueira , Brazil

Sakineh Kazemi Noureini , Iran
Rômulo Dias Novaes, Brazil
Martin Offenbaecher , Germany
Oluwafemi Adeleke Ojo , Nigeria
Olufunmiso Olusola Olajuyigbe , Nigeria
Luís Flávio Oliveira, Brazil
Mozaniel Oliveira , Brazil
Atolani Olubunmi , Nigeria
Abimbola Peter Oluyori , Nigeria
Timothy Omara, Austria
Chiagoziem Anariochi Otuechere , Nigeria
Sokcheon Pak , Australia
Antônio Palumbo Jr, Brazil
Zongfu Pan , China
Siyaram Pandey , Canada
Niranjan Parajuli , Nepal
Gunhyuk Park , Republic of Korea
Wansu Park , Republic of Korea
Rodolfo Parreira , Brazil
Mohammad Mahdi Parvizi , Iran
Luiz Felipe Passero , Brazil
Mitesh Patel, India
Claudia Helena Pellizzon , Brazil
Cheng Peng, Australia
Weijun Peng , China
Sonia Piacente, Italy
Andrea Pieroni , Italy
Haifa Qiao , USA
Cláudia Quintino Rocha , Brazil
DANIELA RUSSO , Italy
Muralidharan Arumugam Ramachandran,
Singapore
Manzoor Rather , India
Miguel Rebollo-Hernanz , Spain
Gauhar Rehman, Pakistan
Daniela Rigano , Italy
José L. Rios, Spain
Francisca Rius Diaz, Spain
Eliana Rodrigues , Brazil
Maan Bahadur Rokaya , Czech Republic
Mariangela Rondanelli , Italy
Antonietta Rossi , Italy
Mi Heon Ryu , Republic of Korea
Bashar Saad , Palestinian Authority
Sabi Saheed, South Africa




Mohamed Z.M. Salem , Egypt
Avni Sali, Australia
Andreas Sandner-Kiesling, Austria
Manel Santafe , Spain
José Roberto Santin , Brazil
Tadaaki Satou , Japan
Roland Schoop, Switzerland
Sindy Seara-Paz, Spain
Veronique Seidel , United Kingdom
Vijayakumar Sekar , China
Terry Selfe , USA
Arham Shabbir , Pakistan
Suzana Shahar, Malaysia
Wen-Bin Shang , China
Xiaofei Shang , China
Ali Sharif , Pakistan
Karen J. Sherman , USA
San-Jun Shi , China
Insop Shim , Republic of Korea
Maria Im Hee Shin, China
Yukihiro Shoyama, Japan
Morry Silberstein , Australia
Samuel Martins Silvestre , Portugal
Preet Amol Singh, India
Rajeev K Singla , China
Kuttulebbai N. S. Sirajudeen , Malaysia
Slim Smaoui , Tunisia
Eun Jung Sohn , Republic of Korea
Maxim A. Solovchuk , Taiwan
Young-Jin Son , Republic of Korea
Chengwu Song , China
Vanessa Steenkamp , South Africa
Annarita Stringaro , Italy
Keiichiro Sugimoto , Japan
Valeria Sulsen , Argentina
Zewei Sun , China
Sharifah S. Syed Alwi , United Kingdom
Orazio Tagliatalata-Scafati , Italy
Takashi Takeda , Japan
Gianluca Tamagno , Ireland
Hongxun Tao, China
Jun-Yan Tao , China
Lay Kek Teh , Malaysia
Norman Temple , Canada

Kamani H. Tennekoon , Sri Lanka
Seong Lin Teoh, Malaysia
Menaka Thounaojam , USA
Jinhui Tian, China
Zipora Tietel, Israel
Loren Toussaint , USA
Riaz Ullah , Saudi Arabia
Philip F. Uzor , Nigeria
Luca Vanella , Italy
Antonio Vassallo , Italy
Cristian Vergallo, Italy
Miguel Vilas-Boas , Portugal
Aristo Vojdani , USA
Yun WANG , China
QIBIAO WU , Macau
Abraham Wall-Medrano , Mexico
Chong-Zhi Wang , USA
Guang-Jun Wang , China
Jinan Wang , China
Qi-Rui Wang , China
Ru-Feng Wang , China
Shu-Ming Wang , USA
Ting-Yu Wang , China
Xue-Rui Wang , China
Youhua Wang , China
Kenji Watanabe , Japan
Jintanaporn Wattanathorn , Thailand
Silvia Wein , Germany
Katarzyna Winska , Poland
Sok Kuan Wong , Malaysia
Christopher Worsnop, Australia
Jih-Huah Wu , Taiwan
Sijin Wu , China
Xian Wu, USA
Zuoqi Xiao , China
Rafael M. Ximenes , Brazil
Guoqiang Xing , USA
JiaTuo Xu , China
Mei Xue , China
Yong-Bo Xue , China
Haruki Yamada , Japan
Nobuo Yamaguchi, Japan
Junqing Yang, China
Longfei Yang , China

Mingxiao Yang , Hong Kong
Qin Yang , China
Wei-Hsiung Yang, USA
Swee Keong Yeap , Malaysia
Albert S. Yeung , USA
Ebrahim M. Yimer , Ethiopia
Yoke Keong Yong , Malaysia
Fadia S. Youssef , Egypt
Zhilong Yu, Canada
RONGJIE ZHAO , China
Sultan Zahiruddin , USA
Armando Zarrelli , Italy
Xiaobin Zeng , China
Y Zeng , China
Fangbo Zhang , China
Jianliang Zhang , China
Jiu-Liang Zhang , China
Mingbo Zhang , China
Jing Zhao , China
Zhangfeng Zhong , Macau
Guoqi Zhu , China
Yan Zhu , USA
Suzanna M. Zick , USA
Stephane Zingue , Cameroon



Contents

Pharmacological Potential of the Standardized Methanolic Extract of *Prunus armeniaca* L. in the Haloperidol-Induced Parkinsonism Rat Model

Uzma Saleem , Liaqat Hussain , Faiza shahid, Fareeha Anwar, Zunera Chauhdary , and Aimen Zafar


Research Article (15 pages), Article ID 3697522, Volume 2022 (2022)

Potential Targets and Action Mechanism of Gastrodin in the Treatment of Attention-Deficit/Hyperactivity Disorder: Bioinformatics and Network Pharmacology Analysis

Zhe Song , Guangzhi Luo, Chengen Han, Guangyuan Jia, and Baoqing Zhang 





Research Article (12 pages), Article ID 3607053, Volume 2022 (2022)

The Inhibitory Effect of Polyphenon 60 from Green Tea on Melanin and Tyrosinase in Zebrafish and A375 Human Melanoma Cells

Mehar Ali Kazi, Reshma Sahito, Qamar Abbas, Sana Ullah, Abdul Majid, Abdul Rehman Phull , Md. Mominur Rahman , and Song Ja Kim 

Research Article (9 pages), Article ID 7739023, Volume 2022 (2022)

***Tridax procumbens* Ameliorates Streptozotocin-Induced Diabetic Neuropathy in Rats via Modulating Angiogenic, Inflammatory, and Oxidative Pathways**

Munish Kakkar, Tapan Behl , Celia Vargas-De-La Cruz, Hafiz A. Makeen , Mohammed Albratty, Hassan A. Alhazmi , Abdulkarim M. Meraya , Ghadeer M. Albadrani, and Mohamed M. Abdel-Daim


Research Article (12 pages), Article ID 1795405, Volume 2022 (2022)

The Effects of Er Xian Decoction Combined with Baduanjin Exercise on Bone Mineral Density, Lower Limb Balance Function, and Mental Health in Women with Postmenopausal Osteoporosis: A Randomized Controlled Trial

Keqiang Li , Hongli Yu, Xiaojun Lin, Yuying Su, Lifeng Gao, Minjia Song, Hongying Fan, Daniel Krokosz, Huixin Yang, and Mariusz Lipowski 



Research Article (13 pages), Article ID 8602753, Volume 2022 (2022)

Elucidating the Neuroprotective Effect of *Tecoma stans* Leaf Extract in STZ-Induced Diabetic Neuropathy

Amit Gupta, Tapan Behl , Aayush Sehgal, Sukhbir Singh, Neelam Sharma, Shivam Yadav, Khalid Anwer, Celia Vargas-De-La Cruz, Sridevi Chigurupati, Abdullah Farasani, and Saurabh Bhatia






Research Article (13 pages), Article ID 3833392, Volume 2022 (2022)

Neurobehavioral and Biochemical Evidences in Support of Protective Effect of Marrubiin (Furan Labdane Diterpene) from *Marrubium vulgare* Linn. and Its Extracts after Traumatic Brain Injury in Experimental Mice




Nidhi, Govind Singh, Rekha Valecha, Govind Shukla, Deepak Kaushik, Mohammad Akhlaquer Rahman, Rupesh K. Gautam, Kumud Madan, Vineet Mittal , and Rajeev K. Singla 

Research Article (13 pages), Article ID 4457973, Volume 2022 (2022)

In Vivo Anti-Inflammatory, Analgesic, Muscle Relaxant, and Sedative Activities of Extracts from *Syzygium cumini* (L.) Skeels in Mice

Abdur Rauf , Yahya S. Al-Awthan , Imtaiz Ali Khan, Naveed Muhammad, Syed Uzair Ali Shah, Omar Bahattab , Mohammed A. Al-Duais, Rohit Sharma , and Md. Mominur Rahman 
Research Article (7 pages), Article ID 6307529, Volume 2022 (2022)

Biogenic Phytochemicals Modulating Obesity: From Molecular Mechanism to Preventive and Therapeutic Approaches

Vikram Kumar , Desh Deepak Singh, Sudarshan Singh Lakhawat, Nusrath Yasmeen , Aishwarya Pandey, and Rajeev K. Singla 
Review Article (20 pages), Article ID 6852276, Volume 2022 (2022)

Research Article

Pharmacological Potential of the Standardized Methanolic Extract of *Prunus armeniaca* L. in the Haloperidol-Induced Parkinsonism Rat Model

Uzma Saleem ¹, Liaqat Hussain ¹, Faiza shahid,¹ Fareeha Anwar,²
Zunera Chauhdary ¹ and Aimen Zafar³

¹Department of Pharmacology, Faculty of Pharmaceutical Sciences, Government College University Faisalabad, Faisalabad, Pakistan

²Riphah Institute of Pharmaceutical Sciences, Riphah International University, Raiwind Road Lahore, Pakistan

³University Institute of Food Science & Technology, The University of Lahore, Raiwind Road Lahore, Lahore, Pakistan

Correspondence should be addressed to Uzma Saleem; uzma95@gmail.com and Liaqat Hussain; liaqat.hussain@gcuf.edu.pk

Received 6 July 2022; Revised 10 September 2022; Accepted 13 September 2022; Published 29 September 2022

Academic Editor: Rupesh K. Gautam

Copyright © 2022 Uzma Saleem et al. This is an open access article distributed under the Creative Commons Attribution License, which permits unrestricted use, distribution, and reproduction in any medium, provided the original work is properly cited.

Parkinson's disease (PD) is a complex, age-related neurodegenerative disease that causes neuronal loss and dysfunction over time. An imbalance of redox potential of oxidative stress in the cell causes neurodegenerative diseases and dysfunction of neurons. Plants are a rich source of bioactive substances that attenuate oxidative stress in a variety of neurological disorders. The aim of the present study was to evaluate the *Prunus armeniaca* L. methanolic extract (PAME) for anti-Parkinson activity in rats. PD was induced with haloperidol (1 mg/kg, IP). The PAME was administered orally at 100, 300, and 800 mg/kg dose levels for 21 days. Behavioral studies (catalepsy test, hang test, open-field test, narrow beam walk, and hole-board test), oxidative stress biomarkers (SOD, CAT, GSH, and MDA) levels, neurotransmitters (dopamine, serotonin, and noradrenaline) levels, and acetylcholinesterase activity were quantified in the brain homogenate. Liver function tests (LFTs), renal function tests (RFTs), complete blood count (CBC), and lipid profiles were measured in the blood/serum samples to note the side effects of PAME at the selected doses. Histopathological analysis was performed on the brain (anti-PD study), liver, heart, and kidney (to check the toxicity of PAME on these vital organs). Motor functions were improved in the behavioral studies. Dopamine, serotonin, and noradrenaline levels were significantly increased ($P < 0.001$), whereas the level of acetylcholinesterase was decreased significantly ($P < 0.001$). The levels of superoxide dismutase (SOD), catalase (CAT), and reduced glutathione (GSH) were increased, while malondialdehyde (MDA) and nitrite levels were decreased in the PAME-treated groups significantly compared with the disease control group, hence reducing oxidative stress. The incidence of toxicity was determined by biochemical analysis of LFT and RFT biomarkers testing. The histopathological analysis indicated that neurofibrillary tangles and plaques decreased in a dose-dependent manner in the PAME-treated groups. Based on the data, it is concluded that PAME possessed good anti-Parkinson activity, rationalizing the plant's traditional use as a neuroprotective agent.

1. Introduction

Neurological diseases are a divergent group of diseases of the sensory system that include the brain, peripheral nerves, and spinal cord [1]. Proteostasis, strain, neuroinflammation, apoptosis, and oxidative stress are involved in the pathology of neurodegenerative disorders, which are all responsible for continuous neuronal damage and destruction [2]. Dementia,

Parkinson's disease (PD), and motor neuron dysfunction are important neurodegenerative disorders. It is estimated that, in Pakistan, 450,000 people are suffering from PD. According to the WHO, the death rate associated with PD in Pakistanis is 1.87% of the total population.

PD is a complex neurodegenerative disease that happens due to continuous damage of dopaminergic neurons projecting from the substantia nigra (pars compacta) to the

corpus striatum. The disease was explicated for the first time by Dr. James Parkinson in 1817 in his “Essay on the shaking palsy”. There are two forms of PD: familial (genetically inherited) and sporadic (idiopathic). It is a slowly progressive degenerative disorder with both motor and non-motor features. Signs and symptoms of PD include tremor at rest, postural or gait abnormalities, muscle rigidity, and bradykinesia [3]. The pathological characteristic of PD is Lewy bodies. They are α -synuclein-immunoreactive clusters of proteins that majorly cause proteolysis. These include ubiquitin and reduction in the level of dopaminergic neurons in the striatum, expressed as a reduction in voluntary movements. As PD progresses, the spread of Lewy bodies expands to the neocortical and cortical regions [4].

The disease usually begins at the age of 65 to 70 years and is more occurring in men than women [5]. The neuropathological mechanisms of PD are multifactorial and involve genetic as well as nongenetic and environmental factors. Protein aggregate accumulation, mitochondrial damage, impaired protein clearance pathways, neuroinflammation, oxidative stress, excitotoxicity, and genetic mutations are the main pathological mechanisms [6]. Cases of PD involve genetics-based origin, only constituting 5–10 in number out of 100 cases. Some of the variant genes control a cluster of molecular pathways, and when they are disturbed, they cause neurological dysfunction leading to PD [7]. Tremendous genome-wide association studies (GWASs) propose a specific acquired encoding for proteins that are linked to these molecular pathways and play a role in sporadic PD. Examples of different pathways are mitochondrial function abnormality and neuronal inflammation [8].

The current medication of PD treats only symptoms; neither slows down the progression of the disease nor halts the dopaminergic neuron degradation [9]. Regarding the treatment of PD, many guidelines are available in which dopamine agonists are used in treating young-onset patients and levodopa for older patients. For initial therapy, patients who go through first motor fluctuations, MAO-B inhibitors act as a better treatment option. Similarly, COMT inhibitors enhance the action of levodopa if any wearing-off symptoms present [10]. Treatments such as pharmacological dopamine replacement and the use of deep brain stimulation are extremely effective. In recent decades, PD has been effectively managed by enhancing one’s quality of life [11]. Different strategies will be developed in the future to identify people who are at high risk to develop PD [12]. Newer formulations are also under development to enhance the efficacy and reduce the toxicity of available drugs [13]. A novel compound such β -asarone also showed good potential against PD [14].

There are a number of plant species that have been recognized to have excellent therapeutic potential against neurodegenerative disorders [4]. These have been found to exert a diverse range of protective effects that mitigate the devastating neurodegeneration [15]. Generally, plant species with antioxidant properties have been broadly recognized to ameliorate the disease process [16–19]. *P. armeniaca* L. contains various flavonoids such as quercetin, a potent antioxidant that has been credited to protect neurons from

free radical-associated cellular degeneration in PD [20]. However, there is a long list of isolated bioactive compounds from therapeutic plants that have been found to ameliorate the neurodegenerative disorders [21].

P. armeniaca L. (apricot) is a significant plant species from the family *Rosaceae* and is traditionally used for treating different ailments [22]. This plant is found in China, Turkey, Iran, Italy, France, Morocco, Pakistan, Spain, USA, and India [23]. Apricots are high in oils, proteins, fatty acids, vitamins, carotenoids (β -carotene, γ -carotene), minerals (calcium, Na^+ , K^+ , PO_4^{3-} , Mg^{2+} , Fe^{2+} , Zn^{2+}), polyphenols, and flavonoids [24,25]. According to the Unani system, it is utilized as an antidiarrheal, emetic, and anthelmintic in liver disorders, ear infection, and deafness and as an expectorant for dry throat, laryngitis, lung ailments, and abscesses [24]. The present study was designed to assess the potential of *P. armeniaca* L. methanolic extract (PAME) for the management of PD on the basis of scientific grounds by using a haloperidol-induced PD animal model.

2. Materials and Methods

2.1. Plant Collection and Identification. Fresh kernels of *P. armeniaca* were obtained from the local market of Faisalabad, they were verified by the Botany Department of Government College University Faisalabad by Taxonomist Dr. Qasim Ali under authentication number 279-BOT-21, and the voucher specimen was placed in the herbarium.

2.2. Plant Extract Preparation. The fresh kernels were collected, washed to remove filth, superfluous substances, and dried under shade for 1 month. Then, the dried kernels were crushed into powder by utilizing an electronic blender. The powder of *P. armeniaca* was weighed in three beakers of 1000 mL capacity. The microwave was adjusted at 9000 watts. In the 1st cycle, 100 g of powder and 750 mL methanol were added in all beakers. Then, these beakers were placed in a microwave oven and the oven was heated for two minutes; then stopped the oven and opened it for 30 seconds. This specific method was repeated for 5 times. At the end, the supernatant was filtered by using filtered paper or muslin cloth. In the 2nd cycle, again 500 mL methanol was added in each beaker and then all beakers were placed in a microwave oven. The oven heated up for 2 minutes and stopped for 30 seconds. The same method was repeated for 5 times. And the supernatant was filtered by using muslin cloth. In the 3rd cycle, 500 mL methanol was added in each beaker, and the same method was repeated for 5 times. Filtrates were pooled in the same reservoir. In the rotary evaporator, the distillate was evaporated under reduced pressure at 4 rpm. After the evaporation of the solvent, the semisolid material of *Prunus armeniaca* L. methanolic extract (PAME) was formed [4].

2.3. Plant Characterization

2.3.1. Physicochemical Analysis. The physical and chemical properties of the powder plant material were investigated to calculate the moisture content, total ash, acid indissoluble

ash, aqueous indissoluble ash, water, alcohol dissoluble extractives, and sulfated ash content; all these analysis were performed according to established protocols and already performed in our previous published articles [26].

2.3.2. Phytochemical Analysis. To investigate the alkaloid, phenolic, and flavonoid contents of the plant extract, the phytochemical analysis was performed according to previous published protocols [4,26].

Estimation of Total Phenolic Content (TPC). Folin–Ciocalteu’s phenol reagent (0.2 mL) was mixed in the test tubes with the sample and standard solution (0.2 mL), and after 4 minutes, 1 mL of sodium bicarbonate solution (15%) was added into these test tubes. For the next 2 hours, the solution was kept at room temperature, and various concentrations of standard reference at 10, 20, 30, 40, 50, and 60 $\mu\text{g}/\text{mL}$ were formed to build up a linear regression equation. Then, the absorbance was taken at 760 nm. The test tube standard had all reagents except the analyte, and for drawing the standard curve gallic acid was used [27]. As a result, the total phenolic content of the test sample was measured as mg of gallic acid equivalents (GAEqs)/g of the extract and is calculated using the following equation:

$$\begin{aligned} &\text{total phenolic content} \\ &= \frac{\text{gallic acid equivalents} \times \text{extract volume}}{\text{sample (g)}} \end{aligned} \quad (1)$$

Estimation of Total Flavonoid Content (TFC). 10% aluminum nitrate solution (0.1 mL), 1 M potassium acetate (0.1 mL), and 4.6 mL distilled water were mixed with the sample (0.2 mL) and standard solution (0.2 mL) in test tubes (0.2 mL). Then, for the next 45 minutes, the mixture prepared was placed at room temperature for incubation. The test tube standard has all reagents except analyte, and quercetin (QTN) will be used for drawing the standard curve. Standard curves for reference sample solution were taken at different concentrations 10, 20, 30, 40 50, and 60 $\mu\text{g}/\text{mL}$ and at 415 nm, and the absorbance was measured [27]. The TFC was measured as mg of quercetin equivalents/g (QEqs/g) of the extract and is determined using the following equation:

$$\begin{aligned} &\text{total flavonoid content} \\ &= \frac{\text{QTN equivalents} \times \text{extract volume}}{\text{sample (g)}} \end{aligned} \quad (2)$$

Estimation of Total Alkaloids. The gallic acid solution in 5% methanol (100 L), concentrated H_2SO_4 (2 L), and sample/standard alcoholic solution (100 L) were combined in a test tube. For the next 10 minutes, the solution was boiled, and at 660 nm the absorbance was measured. The test tube standard has all reagents except the sample. For drawing the standard curve, atropine was used. Standard atropine solutions at different concentrations 10, 20, 30, 40, 50, and 60 $\mu\text{g}/\text{mL}$ were made. Presence of total alkaloids in the extract was

measured as milligrams of atropine equivalents (AEqs/g) of the extract, and total alkaloids are figured out using the following equation [28]:

$$\begin{aligned} &\text{total alkaloids} \\ &= \frac{\text{piperine equivalents} \times \text{extract volume}}{\text{sample (g)}} \end{aligned} \quad (3)$$

Determination of Antioxidant Activity Using DPPH Assay. Various concentrations of the sample will be used to determine the antioxidant activity. DPPH will be dissolved in methanol. In a total volume of 4 mL methanol, 200 μL of 0.05% DPPH will be mixed with 80 μL of the sample. And for the next 30 minutes it was kept in darkness. The results will be expressed as a percentage of inhibition using the percent inhibition relationship [22]:

$$\begin{aligned} &\% \text{scavenging effect} \\ &= \frac{\text{absorbance of control} - \text{absorbance of sample}}{\text{absorbance of control}} \times 100. \end{aligned} \quad (4)$$

2.4. Experimental Animals. Thirty-six healthy albino Wistar rats weighing 150–200 g of either sex were used for *in vivo* anti-Parkinson activity. The rats were acquired and placed in an animal house under proper conditions (12-hour light and dark cycle, room temperature 25°C) in polypropylene cages. Animals were divided into 6 groups after one-week normal feeding with water ad libitum. The study was started after getting ethical approval (Ref. No. GCUF/ERC/2222) from the Institutional Review Board of Government College University Faisalabad ruling under the regulation of the Institute of Laboratory Animal Resources, Commission on Life Sciences, National Research Council (1996).

2.5. Evaluation of Anti-Parkinson Activity

2.5.1. Disease Induction. In rats, haloperidol (1 mg/kg) was given once daily (intraperitoneally) for twenty-one days to induce Parkinson’s disease except the normal control group. It was injected before one hour of extract treatment [15].

2.5.2. Study Design. Thirty-six healthy albino Wistar rats (almost equal from each sex) were divided into 6 groups ($n=6$ each group). Group 1 was served as normal control and was given the vehicle only. Group 2 or the disease control group received 1 mg/kg of haloperidol via intraperitoneal injection. Group 3 or the standard group received 100 mg/kg of levodopa and 25 mg/kg carbidopa [29]. Groups 4, 5, and 6 or treatment groups received the kernel extract of PAME at doses 100, 300, and 800 mg/kg.

All the groups were treated for consecutive 21 days. Behavioral and weight alterations were measured at the beginning, during, and end of the study. After 21 days of

treatment, all the rats were euthanized and observations were recorded by biochemical and histological experiments. Brains from all the groups were separated and rinsed with normal saline and preserved in chilled phosphate buffer (pH 7.4) for measurement of neurotransmitters (dopamine, serotonin, norepinephrine) and oxidative stress biomarkers. Blood samples of the animals were taken by cardiac puncture. LFTs and RFTs were performed on blood plasma and serum, respectively. The vital organs such as brain, liver, heart, and kidney were preserved in 10% buffered formalin for further toxicity studies and histopathological observations.

2.5.3. Behavioral Analysis. The catalepsy, open field, hang, hole board, swim, narrow beam walk, elevated plus maze, and Y-maze tests were conducted to investigate the behavioral analysis [29].

Catalepsy Test. Catalepsy is the inability of rats to respond to external stimuli and rigidity of muscles. Briefly, the rats were placed on a wooden bar (1 cm diameter and 3–9 cm elevated) with their forelimbs after giving haloperidol and the time taken to correct the imposed posture was recorded as a catalepsy indicator. Catalepsy ends when either the rats climb up the bar or their forelimbs touched the floor. These observations were noted after 30, 60, 90, and 120 minutes [29]. All findings were done in a quiet environment at 23–25 degrees Celsius, with a 5-minute cut-off time [30].

The scoring of catalepsy was as follows:

- (i) Score 0: when the rats were placed on the table, they moved normally
- (ii) Score 0.5: when pushed or touched, the rats behaved normally
- (iii) Score 2: in 10 seconds, the rats were unable to correct the imposed posture; 1 score for every paw

Open-Field Test. This test was conducted to evaluate the locomotor and exploratory behavior patterns of experimental rats. For this test, a square-shaped wooden box (100 cm width \times 100 cm diameter \times 45 cm height) was made of plywood material painted with white color and black-line-coated floor has been splinted into 25 blocks. Ethanol was used to wash the apparatus. For 5 minutes, the rats were positioned in the center of the field and let them enter the box freely, and then both central and horizontal numbers of squares crossed and the number of crossings, time of stretch attend, defecation, freezing, and postures were recorded [29].

Hole Board Test. For the evaluation of behavioral components of the experimental animals, the hole board test is used. The apparatus consisted of a (30 cm length (L) \times 30 cm width (W)) square-shaped area that contained 16 equidistant holes. On the 20th day of dosing, each animal was acclimatized for 30 minutes near the apparatus before being placed in the center of the hole board apparatus for the evaluation of test. Focused (edge sniffing and head dipping),

horizontal (walking and immobile sniffing), and vertical (climbing and rearing) exploratory activities, as well as immobility events, were observed during a 120-second session with each animal [4].

Narrow Beam Walk Test. This said test was carried out to analyze the motor coordination and balance in the Parkinson's model. The rats were taught to walk for 120 seconds through a narrow stationary flat wooden plank measuring 100 cm in length and 4 cm in width. The time it took to cross a narrow beam with two ends pointing in opposite directions was recorded as a measure of motor coordination and balance [29].

Swim Test. It is the characteristic test for the observation of depression in the animal, therefore called behavior despair test. The test was designed in a cylindrical setting (16 cm H \times 40 cm L \times 25 cm W) that was filled with water to check the immobility or mobility potential of the animal. The typical observation of this test was that the animal remains immobile with its head above the surface of water. It was a 2-day procedure, after the first trial on 20th day, and the final trial was done on the 21st day of experiment. The rats were placed individually in a cylinder containing 19 cm of water, and the temperature was kept constant at 23°C. Each animal was subjected to a 6-minute swim test. The swimming behavior was examined, and the duration of immobility in the last four minutes was recorded, followed by 2 minutes of acclimatization [31].

Y-Maze Test. In the Y-maze test, spontaneous alterations were used as an index of working short-term memory. The maze was considered of a triangular central area with three A, B, and C equilateral arms of (35 cm L \times 25 cm H \times 10 cm W) each rat was placed in the central area facing one of the arms. When all four paws of the rat were in the arm, the entry was scored. Consecutive entries (ABC, BCA, or CAB but not CAC) into all three arms were defined as spontaneous alterations in behavior. Maximum spontaneous alteration (total number of arms entered) and percentage of spontaneous alteration (actual/maximum alterations \times 100) were calculated [32].

2.5.4. Evaluation of Biochemical Parameters. The levels of oxidative stress biomarkers GSH, SOD, CAT, and MDA were quantified in the brain, liver, heart, and kidney homogenates; whereas acetylcholinesterase activity and dopamine, serotonin, and norepinephrine levels were measured in the brain tissue homogenate [15].

Established protocols as already published and employed in our previous studies were followed for the estimation of catalase activity (CAT), dismutase activity (SOD), glutathione (GSH), and malondialdehyde (MDA) levels in brain homogenates [29].

2.5.5. Estimation of Total Protein. **Solution A** was prepared by adding 2% Na₂CO₃ in 0.1 N NaOH; **solution B**, 1% sodium potassium tartrate in H₂O; **solution C**, 0.5% CuSO₄ in H₂O; **reagent 1**, 48 mL of solution A, 1 mL of solution B,

and 1 mL of solution C; and **reagent 2**, 1 part of Folin phenol in part of water in 1:1 ratio.

Bovine serum albumin (BSA) 0.2 mL was added as a standard in 5 test tubes, and 0.8 mL distilled water was added. Then, in each test tube, reagent 1 (4.5 mL) was added and incubated for 10 minutes. Following the initial incubation, 0.5 mL of reagent 2 was added and incubated for another 30 minutes. At 660 nm, the absorbance was taken and a standard graph was drawn. The standard curve was constructed by BSA, and the values were expressed in mg/mL [33]. The following regression line was used:

$$\text{absorbance (Y)} = 0.00007571x + 0.00004762. \quad (5)$$

2.5.6. Measurement of Nitrite Levels. Quantification of nitric oxide can be done in the form of nitrite levels. The tissue homogenate and Griess reagent (36 mL) were mixed in equal amounts and incubated for 10 minutes for this assay. The absorbance of the reaction mixture was measured at 546 nm [4,29]. The following regression line was used:

$$\text{absorbance (Y)} = 0.003432 + 0.0366. \quad (6)$$

2.5.7. Evaluation of Acetylcholinesterase Activity. In this assay, 2.6 mL phosphate buffer (pH 8) was added to (0.1 M) 2,4-di-thio-bis-nitrobenzoic acid (100 L) and 0.4 mL tissue homogenate was mixed with acetylthiocholine iodide (20 L). The resultant mixture became yellow in appearance due to the reaction of DTNB with acetylthiocholine iodide. At 412 nm, the absorbance was recorded. Change in absorbance was measured after every 2 minutes till the 10 minutes of duration [4,34]. AChE activity was determined by using the following formula:

$$R = 5.74 \times 10^{-4} \times \frac{A}{C_0}, \quad (7)$$

where C_0 is the original concentration of tissue (mg/mL), A is expressed as the variation in absorbance/minute, and R is the rate in moles of substrate hydrolyzed/min/gram of tissue.

2.5.8. Tests for the Estimation of Neurotransmitter Levels

Aqueous Phase Preparation. The brains of all sacrificed rats were isolated and weighed. The homogenate of brain tissue was preserved in 5 mL of HCL-butanol and centrifuged for 10 minutes at 2000 rpm. After centrifugation, an aliquot of the supernatant was taken, 0.31 mL of HCL (0.1 M) and 2.5 mL of heptane were added, and the mixture was shaken for 10 minutes. The mixture was centrifuged at 2000 rpm for 10 minutes. Two layers were separated after centrifugation, and the temperature was kept at 0°C throughout the procedure. The liquid phase (0.2 mL) was used for the determination of neurotransmitter levels [35].

Estimation of Serotonin Levels. 0.25 mL O-phthalaldehyde was added to the liquid phase (0.2 mL). To make a fluorophore, the prepared solution was heated to 100°C. The

solution was then allowed to cool to room temperature before the absorbance was measured. The emission wavelength for the fluorescence method is 340 nm, and the excitation wavelength is 305 nm [34].

$$\text{Absorbance (Y)} = 0.0299x + 0.0918. \quad (8)$$

Estimation of Dopamine and Noradrenaline Levels. A 0.2 mL sample of the aqueous phase was mixed with 0.05 mL HCL (0.4 M) and 0.1 mL sodium acetate/ethylenediaminetetraacetic acid buffer (pH 6.9). After mixing, 0.1 mL of Na_2SO_3 solution was added to carry out the oxidation reaction for 1.5 minutes, followed by 0.1 mL of acetic acid. The solution was heated to 100°C for 6 minutes before cooling to room temperature. The absorbance of dopamine and noradrenaline was measured at 350 nm and 450 nm, respectively [34].

$$\text{absorbance of dopamine (Y)} = 0.0314x + 0.1067. \quad (9)$$

2.6. Histopathological Analysis. The brains of all animals were silver stained, while other organs such as liver, heart, and kidney were also processed for by using H&E staining [36].

2.7. Statistical Analysis. The results were presented as means \pm SEM. In GraphPad Prism, version 6, data were analyzed using one-way/two-way ANOVA followed by Bonferroni's multiple comparison as a post hoc test, with P values of <0.05 considered significant.

3. Results

3.1. Plant Characterization

3.1.1. Physicochemical Analysis. PAME was characterized for physicochemical parameters that are shown in Table 1. The moisture content was found to be 7%, the total ash content was 22%, and the sulfated ash content was 52%. The water-insoluble ash content (39%) was found higher compared with alcohol-insoluble ash (19%); while water- and alcohol-soluble extractives were 1.6% and 5.8%, respectively.

3.1.2. Phytochemical Analysis. Phytochemical screening of plant extracts showed different quantities such as polyphenolic content (26.07 ± 0.71 mg/g), total alkaloid content (43 ± 0.28 mg/g), and total flavonoids (70.66 ± 0.45 mg/g). These constituents may be possibly responsible for the biological activities of *P. armeniaca* L. Alkaloids were quantified using the gallic acid standard curve with linear regression equation " $y = 0.0006x$ and $R^2 = 0.9957$," while flavonoids and polyphenols were quantified using the quercetin standard curve with linear regression equation " $y = 0.001x$ and $R^2 = 0.9748$ " and piperine standard curve with linear regression equation " $y = 0.00396x$ and $R^2 = 0.9954$," respectively. The results are expressed in Table 2.

TABLE 1: Physicochemical analysis of *P. armeniaca* L.

Sr. no.	Physicochemical parameters	Percentage
1	Moisture content	7
2	Total ash content	22
3	Sulfated ash	52
4	Water-insoluble ash	39
5	Alcohol-insoluble ash	19
6	Water-soluble extractives	1.6
7	Alcohol-soluble extractives	5.8

TABLE 2: Phytochemical analysis of *P. armeniaca* L.

Phytochemical parameters	Quantity (mg/g)
Polyphenols	26.07 ± 0.71
Total alkaloids	43 ± 0.28
Total flavonoids	70.66 ± 0.45

3.1.3. Determination of Antioxidant Activity Using DPPH Assay. The antioxidant activity of the phytoconstituents analyzed increased as the concentration of the extracts increased, according to the 2,2-diphenyl-1-picrylhydrazine (DPPH) finding. From the curve drawn between concentration and residual DPPH, the extract's IC₅₀ value was determined. The plant extract had an IC₅₀ value of 60.32 ± 2.73, while ascorbic acid had an IC₅₀ value of 47.51 ± 1.92.

3.2. Behavioral Analysis for the Evaluation of Anti-Parkinson's Effect of PAME

3.2.1. Catalepsy Test. On the 7th, 14th, and 21st days, all experimental rats in the respective groups were tested for cataleptic reaction. Each animal's cataleptic reaction was recorded at 30, 60, 90, and 120 minutes following treatment in all experimental groups. The results are expressed in Figure 1. In contrast to the normal control group, the time spent substantially ($P < 0.001$) rose in the haloperidol (HAL) group, which was noted on the 7th, 14th, and 21st days of treatment. In comparison with the group treated with haloperidol only, the induced cataleptic outcome of haloperidol was dose- and time-dependent ($P < 0.001$) reversed by oral administration of levodopa and carbidopa (standard anti-parkinsonian drugs). The cataleptic response was reduced in all PAME-treated groups in a dose-dependent manner. When compared with the disease group, the 800 mg/kg dose demonstrated a significant ($P < 0.001$) reduction in catalepsy and the lowest score was noted on the 21st day.

3.2.2. Narrow Beam Walk Test. The latency period for a narrow beam test conducted was examined as a marker of motor function as well as coordination on the 21st day following the administration of doses, whereas the number of padded faults was utilized to measure balance. The delay time and number of foot mistakes in the haloperidol-treated group were substantially ($P < 0.001$) higher than those in the

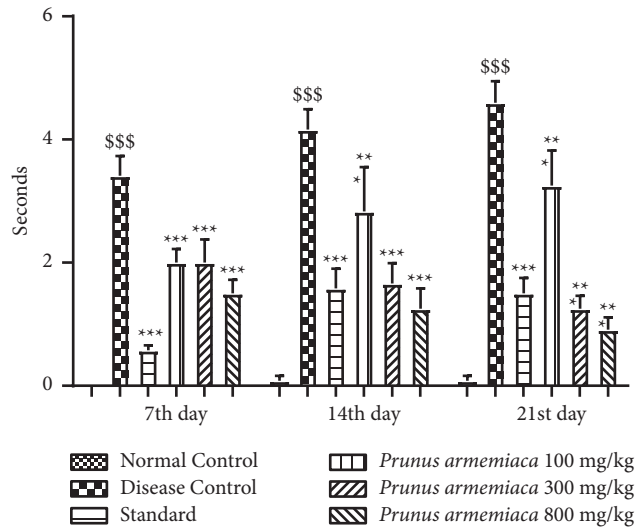


FIGURE 1: Effects of *P. armeniaca* L. on measurement of cataleptic scores. Data are presented as mean ± SEM ($n = 6$), where $^{\$}P < 0.05$, $^{\$\$}P < 0.01$, and $^{\$ \$ \$}P < 0.001$ compared with the normal control group. $^*P < 0.05$, $^{**}P < 0.01$, and $^{***}P < 0.001$ compared with the disease control group.

normal control group. Therapy with levodopa and carbidopa reduced the crossing time approximately identically to the control group ($P < 0.001$), indicating that treatment eliminated the haloperidol effect. Compared with the disease control group, the 100 and 300 mg/kg extract-treated groups had substantially shorter latency times and fewer foot slip mistakes ($P < 0.01$). When compared with the disease control group, the 800 mg/kg dosage level of PAME significantly ($P < 0.001$) reduced the number of foot slip mistakes. The results are shown in Figure 2.

3.2.3. Open-Field Test. The effects of PAME on the number of lines crossed and exploratory behavior are shown in Figures 3(a) and 3(b). The treatment groups had a significant influence on the number of squares traversed, as well as the central and peripheral explorations ($P < 0.001$). Post-test analysis revealed that plant extract at 100 mg/kg and 300 mg/kg resulted in a substantial increase ($P < 0.01$) and the most significant improvement ($P < 0.01$) in central area explorations. Although, in terms of the number of squares traversed, animals in the plant-treated groups showed dose-dependent recovery, $P < 0.05$, $P < 0.01$, and $P < 0.001$, respectively, at all treatment dosages. As a result, the rats demonstrated a dose-dependent increase in locomotor activity, as well as an increase in exploratory behavior and crossings. An indication of anxiolytic impact was a substantial ($P < 0.001$) reduction in the frequency of both central and horizontal explorations in the disease control group.

3.2.4. Hole Board Test. The hole board test was performed to evaluate the antianxiety potential and focused horizontal and vertical exploratory activities in all the groups of

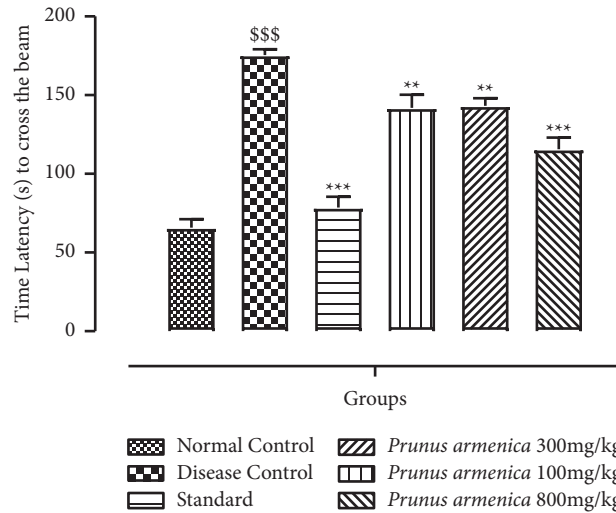


FIGURE 2: Effects of *P. armeniaca* L. on time latency (seconds) in the narrow beam walk test. Data are presented as mean ± SEM ($n = 6$). \$\$\$ $P < 0.001$ compared with the normal control group. ** $P < 0.01$ and *** $P < 0.001$ compared with the disease control group.

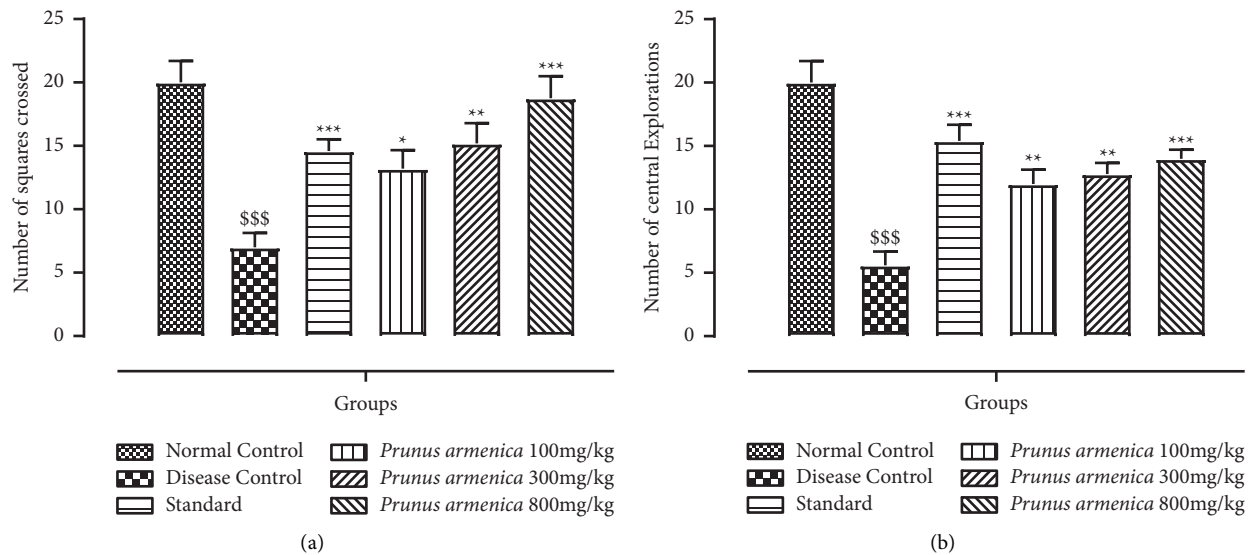


FIGURE 3: Effects of *P. armeniaca* L. on the (a) number of squares crossed and (b) number of central explorations in the open-field test. Data are presented as mean ± SEM ($n = 6$). \$\$\$ $P < 0.001$ compared with the normal control group. * $P < 0.05$, ** $P < 0.01$, and *** $P < 0.001$ compared with the disease control group.

experimental animals. And the number of rats putting their heads into the holes is a sign of curiosity. Furthermore, compared with the only haloperidol-treated group, post hoc analysis indicated a substantial ($P < 0.001$) reduction in the number of hole exploration. The number of focused (head dipping, edge sniffing) and vertical exploring behaviors decreased significantly ($P < 0.001$) in the disease group (Figures 4(a) and 4(b)). All the treatment groups showed an increase in their exploratory behaviors, with the 100 mg/kg and 300 mg/kg dosage groups showing fairly significant recovery ($P < 0.01$) and the 800 mg/kg dose group of PAME showing a substantial ($P < 0.001$) improvement in climbing and rearing. The plant extract's dose-dependent impact suggests that it can protect against dopaminergic depletion.

3.2.5. Swim Test. In the Parkinson disease model, the severity of parkinsonian signs was evaluated through swimming scores after haloperidol and treatment dose administration as displayed in Table 3. All the treatment groups increased their exploratory behaviors, with the 100 mg/kg and 300 mg/kg dosage groups showing fairly significant recovery ($P < 0.01$) and the 800 mg/kg dose group of PAME showing a substantial ($P < 0.001$) improvement in climbing and rearing. The plant extract's dose-dependent impact suggests that it can guard against dopaminergic depletion. In addition, a dose-related significant reduction ($P < 0.001$) in the duration of immobility was noticed, compared with the disease control group. The standard treatment group also showed a significant ($P < 0.001$) improvement in swimming. In addition, compared with the

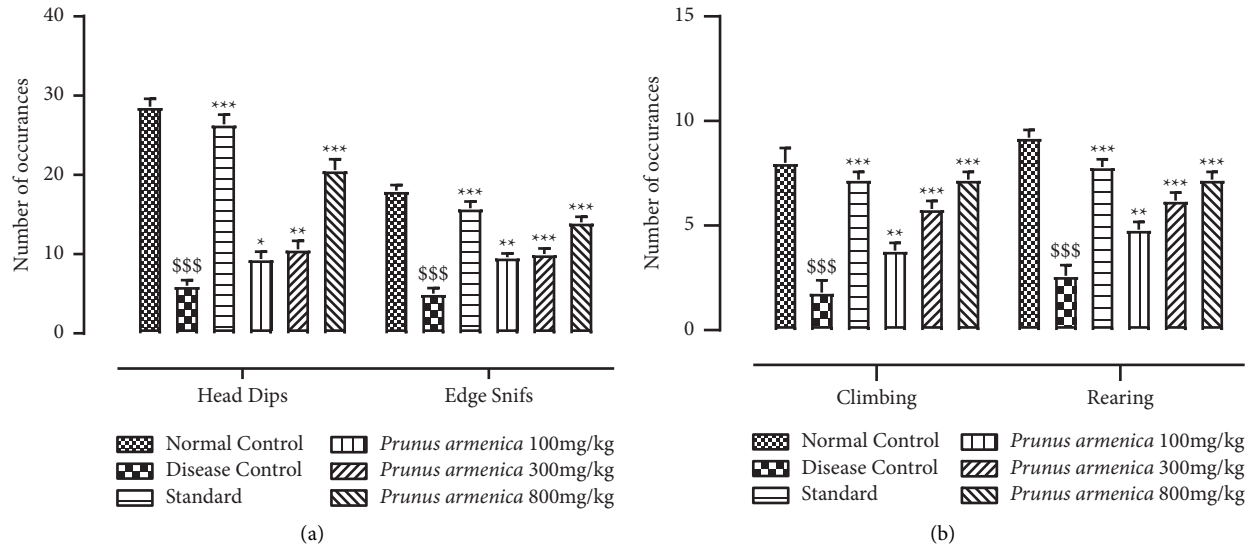


FIGURE 4: Effects of *P. armeniaca* L. on the (a) number of focused exploratory activities and (b) number of vertical exploratory activities in the hole board test. Data are presented as mean \pm SEM ($n = 6$). $^{***}P < 0.001$ compared with the normal control group. $^{*}P < 0.05$, $^{**}P < 0.01$, and $^{***}P < 0.01$ compared with the disease control group.

TABLE 3: Effects of *P. armeniaca* L. on the forced swim test.

Groups	Dose (mg/kg)	Swimming (sec)	Climbing (sec)	Immobility (sec)
Normal control	—	146 \pm 3.65	28.50 \pm 3.17	65.50 \pm 5.05
Disease control (Haloperidol)	1	98.50 \pm 6.08 ***	15.50 \pm 2.40 $^{\$}$	121 \pm 6.77 ***
Standard (Levodopa + Carbidopa)	100/25	145.50 \pm 4.20 ***	27.66 \pm 2.87 ***	79.83 \pm 5.44 ***
<i>Prunus armeniaca</i> L. (PAME)	100	125.16 \pm 3.95 *	25.67 \pm 2.96 **	109.16 \pm 6.17 *
	300	138 \pm 2.84 **	18.5 \pm 3.65 **	93.5 \pm 10.54 **
	800	142.83 \pm 3.04 ***	21.5 \pm 3.45 ***	84.16 \pm 4.81 ***

Data are presented as mean \pm SEM ($n = 6$). $^{\$}P < 0.05$, and $^{***}P < 0.001$ in comparison with the normal control group. $^{*}P < 0.05$, $^{**}P < 0.01$, and $^{***}P < 0.001$ in comparison with the disease control group.

disease control group, there was a dose-related substantial decrease ($P < 0.001$) in the length of immobility. Swimming performance was also significantly improved ($P < 0.001$) in the standard treatment group.

3.2.6. Y-Maze Test. The impact of PAME on short-term memory or working memory was evaluated using the spontaneous alternation behavior Y-maze test, as stated previously. In comparison with the normal control group, a significant ($P < 0.001$) decrease in spontaneous alternation behavior after haloperidol administration was revealed. The decrease in the relative proportion of spontaneous alternation behavior caused by haloperidol was significantly reversed dose dependently ($P < 0.05$, $P < 0.01$, and $P < 0.001$) upon administration of PAME (100, 300, and 800 mg/kg). Haloperidol administration also reduced the number of arm entries in the disease control group. The treatment groups, on the other hand, showed a significant ($P < 0.001$) recovery of memory loss. The percentage of spontaneous alterations increased significantly ($P < 0.001$) in the standard and 800 mg/kg dosage groups. All the results are shown in Figures 5(a)–5(c).

3.3. Estimation of Neurotransmitter Levels in the Brain

3.3.1. Estimation of Dopamine and Noradrenaline Levels.

The levels of dopamine and noradrenaline were measured in brain's tissue homogenate. The treatment groups, on the other hand, showed a significant ($P < 0.001$) recovery of memory loss. The percentage of spontaneous alterations increased significantly ($P < 0.001$) in the standard and 800 mg/kg dosage groups. In the standard as well as plant extract-treated groups, a significant improvement was seen in the level of both neurotransmitters, which was a comparable potential to the haloperidol-treated group. However, all the treatment groups exhibited a dose-dependent recovery in the levels of dopamine and noradrenaline ($P < 0.05$, $P < 0.01$) at 100 mg/kg and 300 mg/kg, with a significant ($P < 0.001$) increase at the highest dose level 800 mg/kg, as shown in Figures 6(a) and 6(b).

3.3.2. Estimation of Serotonin Level. When compared with the disease control group, which had a substantial reduction in serotonin levels, animals in the levodopa plus carbidopa

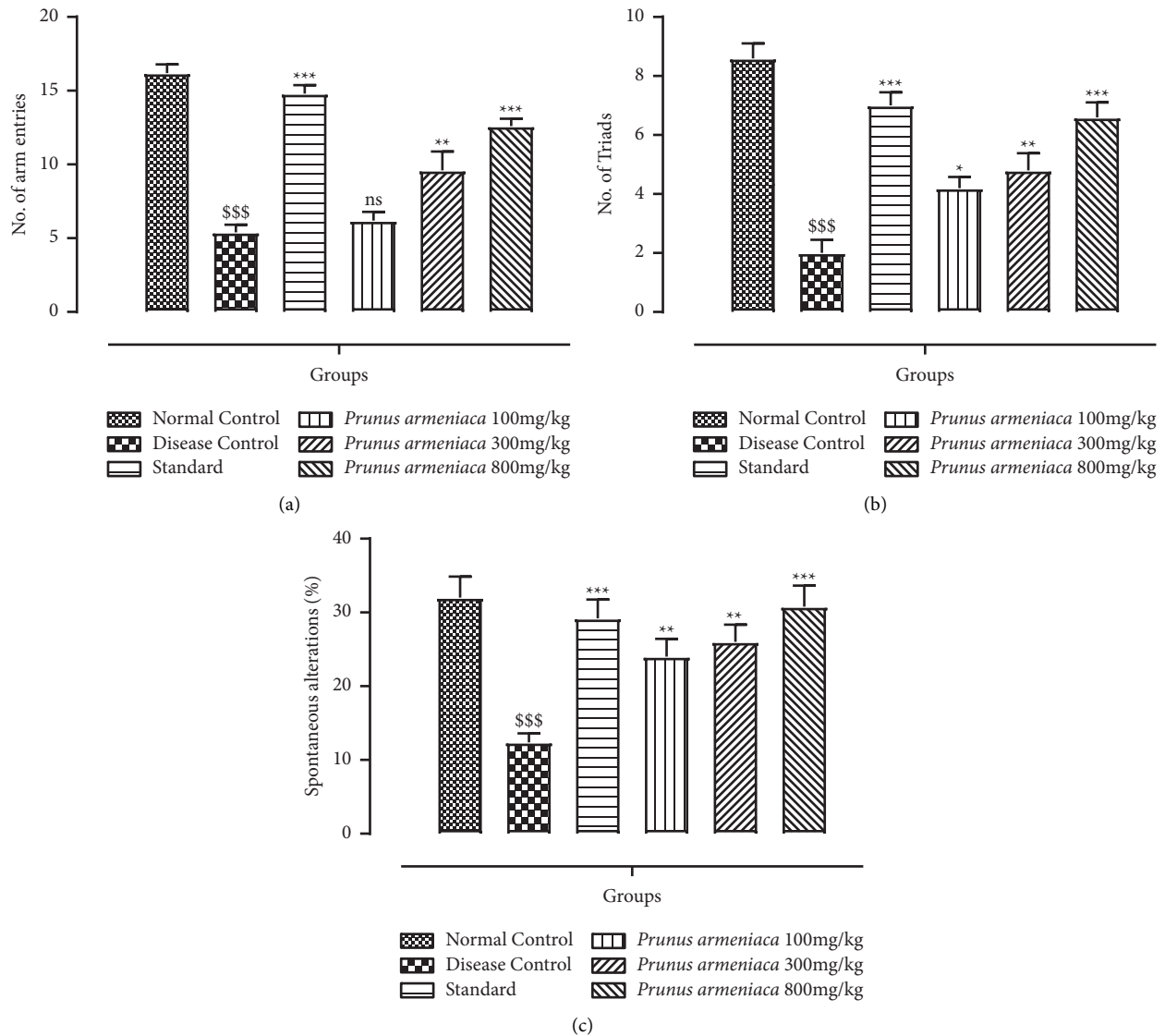


FIGURE 5: Effects of *P. armeniaca* L. on (a) arm entries, (b) the number of Triads, and (c) spontaneous alterations (%) in the Y-maze test. Data are presented as mean \pm SEM ($n = 6$). \$\$\$\$ $P < 0.001$ compared with the normal control group. * $P < 0.05$, ** $P < 0.01$, and *** $P < 0.001$ compared with the disease control group.

(standard)-treated group showed a highly significant ($P < 0.001$) improvement in serotonin levels (Figure 6(c)). The decrease in serotonin levels in Parkinson's disease is correlated with dyskinesia and mood disturbance. All dosage levels of PAME restored the diminished level of serotonin in a dose-dependent way with a substantially significant ($P < 0.001$) increase at the highest dose level, i.e., 800 mg/kg.

3.3.3. Evaluation of Acetyl Cholinesterase (AChE) Activity. The AChE level was substantially increased ($P < 0.001$) in the disease control group. The standard treatment group showed a decrease in AChE levels ($P < 0.001$). A highly significant ($P < 0.001$) reduction in AChE levels was seen in the 800 mg/kg dose group of PAME, whereas, in the case of dose levels of 100 mg/kg and 300 mg/kg, a significant ($P < 0.05$) improvement was seen (Figure 7).

3.4. Evaluation of Oxidative Stress Parameters in the Brain

3.4.1. Superoxide Dismutase (SOD) Levels. A significant reduction was found in the SOD levels of brain tissue homogenates after 21 days of experimentally induced parkinsonism with haloperidol ($P < 0.001$), but groups treated with PAME of 800 mg/kg had significantly enhanced the level of SOD after 21 days ($P < 0.001$) (Table 4). Even though the level of SOD was improved significantly with levodopa and carbidopa in haloperidol-treated rats, but this increment was not significant compared with extract-treated animals.

3.4.2. Evaluation of Catalase (CAT) Level. As depicted in Table 4, when comparing the haloperidol-treated group with the normal control group for 21 days, there was a statistically significant ($P < 0.001$) reduction in catalase levels. The

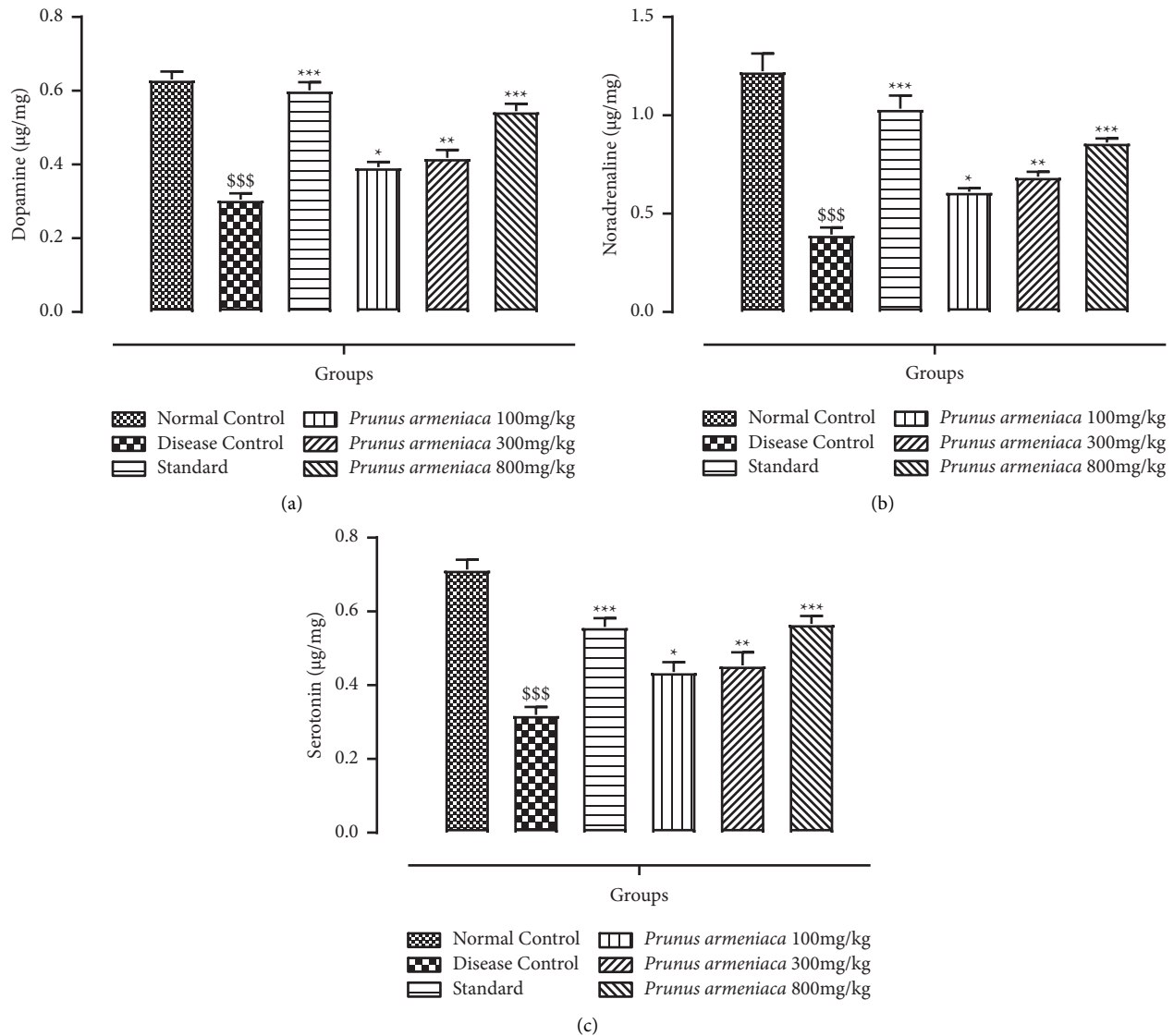


FIGURE 6: Effects of *P. armeniaca* L. on (a) dopamine, (b) noradrenaline, and (c) serotonin levels in brain homogenates. Data are presented as mean \pm S.E.M. ($n=6$). \$\$\$ $P < 0.001$ compared with the normal control group. * $P < 0.05$, ** $P < 0.01$, and *** $P < 0.001$ compared with the disease control group.

standard group significantly reversed the change in CAT levels caused by haloperidol. However, a dose-dependent significant improvement was observed in all the treatment groups such as 100 mg/kg ($P < 0.001$), 300 ($P < 0.001$), and 800 mg/kg dose levels ($P < 0.001$) when aqueous methanolic extract of PAME was administered for 21 days along with haloperidol administration.

3.4.3. Evaluation of Reduced Glutathione (GSH) Level. Administration of haloperidol resulted in a significant depletion of GSH levels in brain tissue homogenates of the disease control group ($P < 0.001$), as shown in Table 4. The glutathione level reached near normal in the Parkinson's group who received levodopa plus carbidopa along with haloperidol. The recovery of GSH content in the treatment group with a dose of 800 mg/kg was highly

significant ($P < 0.001$), while the other treatment doses (100 and 300 mg/kg) showed moderately significant improvement ($P < 0.01$), which was comparable to the replenishment of GSH level in the standard group ($P < 0.05$).

3.4.4. Determination of Malondialdehyde (MDA) Levels. There was a significant ($P < 0.001$) increase in the level of MDA after exposure of rats to haloperidol in comparison with the normal control group. Concurrent treatment with aqueous methanolic extract of the plant had significantly reduced MDA levels ($P < 0.05$) at all the treatment doses. However, the standard treatment group exhibited a significant decrease after receiving treatment with levodopa plus carbidopa for 21 days, which was close to the normal control group (Table 5).

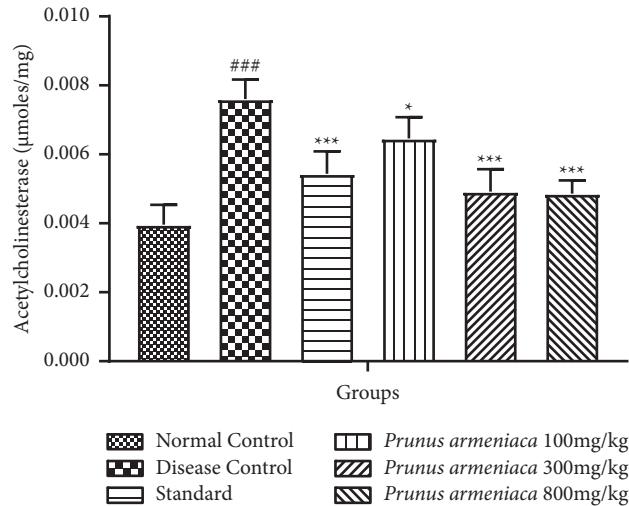


FIGURE 7: Effects of *P. armeniaca* L. on acetylcholinesterase levels in brain homogenates. Data are presented as mean \pm S.E.M. ($n = 6$). $^{\text{###}}P < 0.001$ compared with the normal control group. $^*P < 0.05$, $^{**}P < 0.01$, and $^{***}P < 0.001$ compared with the disease control group.

TABLE 4: Estimation of SOD, CAT, and GSH levels in brain homogenates.

Groups	Dose	SOD ($\mu\text{g}/\text{mg}$ of protein)	CAT ($\mu\text{mol}/\text{min}/\text{mg}$ of protein)	GSH ($\mu\text{g}/\text{mg}$ of protein)
Normal control	—	2.189 \pm 0.02	30.18 \pm 0.1	12.186 \pm 0.1
Disease control	1 mg/kg	1.324 \pm 0.01 $^{\text{SSS}}$	21.58 \pm 0.1 $^{\text{SSS}}$	9.366 \pm 0.1 $^{\text{SSS}}$
Standard (levodopa + carbidopa)	100/25 mg/kg	2.171 \pm 0.01 ***	28.64 \pm 0.1 ***	11.664 \pm 0.1 **
<i>Prunus armeniaca</i> L. (PAME)	100 mg/kg	1.569 \pm 0.01 *	23.01 \pm 0.3 *	9.779 \pm 0.7 **
	300 mg/kg	1.832 \pm 0.01 **	25.71 \pm 0.3 **	10.437 \pm 0.5 **
	800 mg/kg	2.035 \pm 0.01 ***	27.09 \pm 0.4 ***	11.172 \pm 0.5 ***

Data are presented as mean \pm SEM ($n = 6$). $^{\text{SSS}}P < 0.001$ in comparison with the normal control group. $^*P < 0.05$, $^{**}P < 0.01$, and $^{***}P < 0.001$ in comparison with the disease control group.

TABLE 5: Estimation of MDA, nitrite, and protein levels in brain homogenates.

Groups	Dose	MDA (nmol/mg of protein)	Nitrite ($\mu\text{g}/\text{mg}$ of protein)	Protein ($\mu\text{g}/\text{mg}$)
Normal control	—	728 \pm 2.4	2.01 \pm 0.2	310.8 \pm 1.2
Disease control	1 mg/kg	865 \pm 1.5 $^{\text{SSS}}$	3.89 \pm 0.2 $^{\text{SSS}}$	214.8 \pm 1.5 $^{\text{SSS}}$
Standard (levodopa + carbidopa)	100/25 mg/kg	741 \pm 1.7 ***	2.23 \pm 0.2 ***	295.9 \pm 1.2 ***
<i>Prunus armeniaca</i> L.	100 mg/kg	823 \pm 1.5 **	3.42 \pm 0.2 **	240.2 \pm 1.6 *
	300 mg/kg	791 \pm 1.2 **	2.97 \pm 1.2 ***	273.1 \pm 1.6 **
	800 mg/kg	765 \pm 1.2 **	2.48 \pm 0.2 ***	287.7 \pm 1.6 ***

Data are presented as mean \pm SEM ($n = 6$). $^{\text{SSS}}P < 0.001$ in comparison with the normal control group. $^*P < 0.05$, $^{**}P < 0.01$, and $^{***}P < 0.001$ in comparison with the disease control group.

3.4.5. Measurement of Nitrite Levels. PAME when injected at 100 mg/kg indicated a significant reduction ($P < 0.05$), whereas 300 and 800 mg/kg dose levels exhibited a significant decrease in nitrite levels ($P < 0.001$), as shown in Table 5. A significant reduction in the nitrite level was observed in the standard treatment group ($P < 0.001$). However, haloperidol was able to decrease the level of nitrite in the disease control group.

3.4.6. Estimation of Total Protein Levels. When compared with the normal control group, tissue protein levels in the disease control group were significantly lower after treatment with haloperidol alone ($P < 0.001$). The groups of animals treated with different doses of plant extract showed

recovery in the level of protein. The highest dose of PAME 800 mg/kg showed the statistically maximum improvement in the level of protein ($P < 0.05$). A more significant increase was observed in the protein level of the standard treatment group after treatment with haloperidol and concurrent administration of levodopa plus carbidopa ($P < 0.001$) (Table 5).

3.4.7. Histopathological Examination of Brain Tissue. The histopathological changes in brain specimens from various treated groups are displayed in Figure 8. Microscopic examination with a light microscope at 40 \times of brain tissues from the normal control group showed an intact histological structure and no histopathological alterations. Animals in

the disease control group, on the other hand, showed neuronal degeneration, mild congestion in blood vessels, and slight hemorrhage. In the brain tissues, neurofibrillary tangles and plaques were also noticed in the haloperidol-treated group. Furthermore, an improvement in histological alterations was seen in groups treated with PAME at 100, 300, and 800 mg/kg dose levels. The standard treatment group was significantly replaced with health active neurons.

4. Discussion

Parkinson's disease is a complex, age-related nervous system disorder featured by reduction in the level of dopamine and the loss of nerve cells in the substantia nigra pars compacta [5]. Presently, PD is considered the second most prevalent neurodegenerative disorder [37]. Clinically, motor dysfunction and dementia have been widely attributed to PD. Neurodegeneration and neuronal dysfunction are considerably modulated by oxidative stress and neuroinflammation, leading to the reduction of various antioxidants. The reported prevalence of PD increases from 1 to 5% with an increase in age from 65 to 85 years, respectively, and is more occurring in men than women [5,38], and this gender discrimination is attributed to the neuroprotective effect of estrogen in females [39–41]. The neuropathological mechanisms of PD are multifactorial and include genetic and nongenetic as well as environmental factors, while the etiology of PD is still largely unknown. Protein aggregate accumulation, mitochondrial damage, impaired protein clearance pathways, neuroinflammation, oxidative stress, excitotoxicity, and genetic mutations are the main pathological mechanisms. The current medication of PD treats only symptoms, neither slows down nor halts the dopaminergic neurodegeneration [42]. Numerous efforts have been made to discover, identify, and formulate disease-modifying agents, but these efforts are still restricted to symptomatic treatment. Regarding the treatment of PD, many guidelines are available in which dopamine agonist is used in treating young-onset patients and levodopa for older patients. For initial therapy, patients who go through first motor fluctuations, MAO-B inhibitors act as a better treatment option. Similarly, COMT inhibitors enhance the action of levodopa if any wearing-off symptoms present [10]. There are many side effects of the currently available anti-Parkinson drugs, so the current approaches for treatment focuses on newer agents that will either inhibit or terminate the progression of the ailment and be economical. Therefore, the need of developing new drugs from plant origin has preventive yet lesser side effects against Parkinson's disease. Plants with potent antioxidant activities have been a long-established source of potential bioactivity moieties with neuropharmacological activities. Quercetin, a potent antioxidant flavonoid, is present in *Prunus armeniaca*. Quercetin, a flavonoid-derived plant flavanol, has recently been discovered to have neuroprotective properties against neurodegenerative diseases. It has been proposed as a Parkinson's disease supplemental therapy, and the role of flavonoids in PD treatment has been extensively researched. It has pharmacological effects in PD by regulating various

molecular pathways [43]. It also has therapeutic potential for the prevention and treatment of neurodegenerative diseases such as Alzheimer's disease (AD) and Parkinson's disease (PD) due to its antioxidant and anti-inflammatory properties, as well as its ability to cross the blood-brain barrier [20].

This research was carried out to assess the neuroprotective potential of the methanolic extract of *Prunus armeniaca* (PAME), and the standard drug that was used throughout the study was L-dopa plus carbidopa to compare the neuroprotective effect of our methanolic extract with current strategies and medications being used conventionally. Catalepsy is a key biomarker for the evaluation of Parkinson's disease, and this behavior was found to be improved and attenuated upon treatment with PAME (Figure 1). The extract under study improved the muscle strength of experimental rats in a dose-dependent manner. It was found that, in a hanging test, PAME improved neuromuscular strength, which was compromised by prolonged haloperidol administration. The motor coordination was also found to be improved by extract administration as it was shown to increase the horizontal bar test time (Figures 2 and 3). The hazardous effects of oxidative stress are inhibited by the natural antioxidants present in different plants owing to the presence of phenolic compounds, flavonoids. The current study suggested that physical strength, balance, and coordination were improved and maintained by administration of extract. In this study, the preliminary qualitative analysis has revealed large fractions of compounds such as polyphenols, flavonoids, and alkaloids in the PAME, which were also present abundantly in different plants in previous studies showing neuroprotective effects [44]. Considering the antioxidant potential of *P. armeniaca* L. plant, we conducted an antioxidant assay of the extract to confirm the presence of this compound in sufficient quantity to show antioxidant properties. The antioxidant capacity of the extract was determined using the DPPH assay, and it was confirmed that PAME has an excellent antioxidant potential (Table 5). Different behavior analyses such as open field, hole board, narrow beam, swim, elevated plus maze, and catalepsy tests were performed, and the changes in the behavior of experimental animals were evaluated (Figures 3–6). All behavior parameters of experimental animals were improved in response to administration of PAME and standard drugs. Administration of the extract resulted in improvement of locomotor activity, motor coordination, exploratory activities, and reduction in depression, anxiety, and reduced episodes of catalepsy (Figures 3–6). Numerous previous studies have shown that increased oxidative stress in the body and antioxidant enzyme imbalance can be related to development of neurodegenerative disorders [45]. Provoked oxidative stress and disturbed normal state of cells can lead to production of free radicals and peroxides, leaving toxic effects on brain cells. The increased level of free radicals and peroxides can lead to damaging of all cell components including lipids, proteins, and DNA. Haloperidol has been reported to deteriorate the levels of normal storage of antioxidant enzymes in the body by increasing oxidative stress on administration, which was indicated by increased lipid

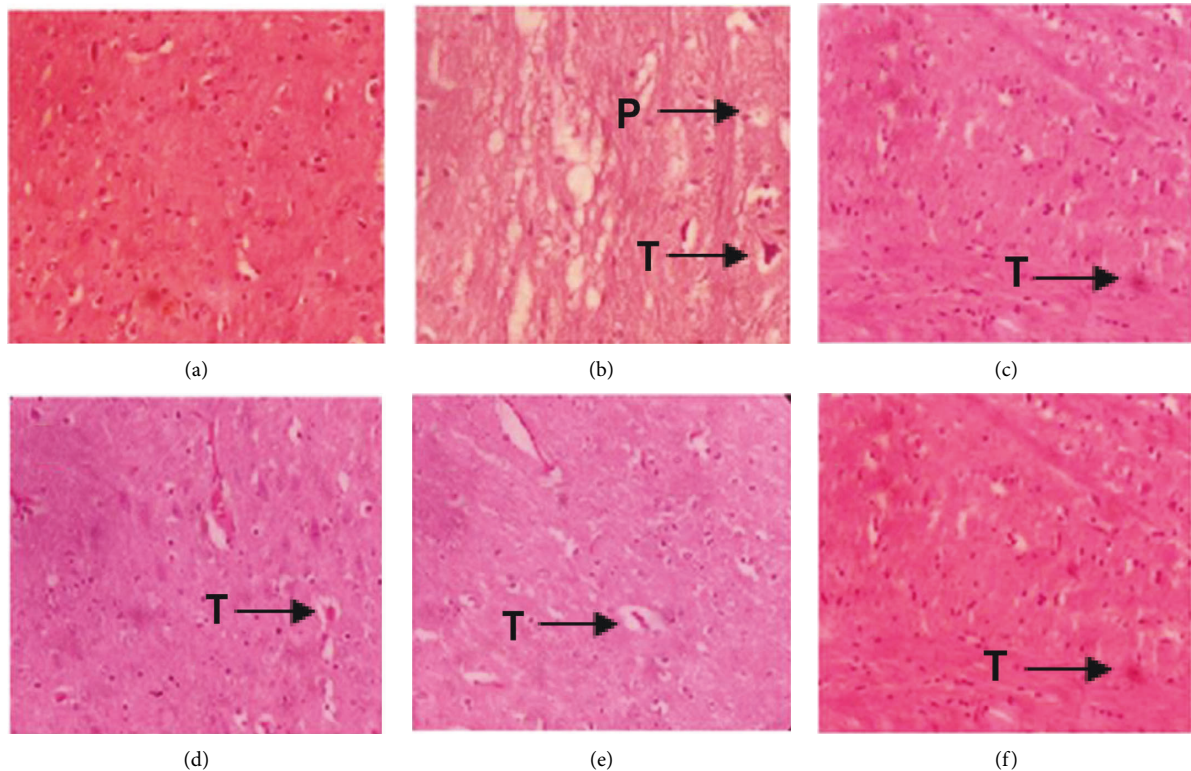


FIGURE 8: Histopathological examination of brain tissue: (a) normal control; (b) disease control; (c) standard; (d) extract 100 mg/kg; (e) extract 300 mg/kg; and (f) extract 800 mg/kg. The pictures were taken at 40 \times . T: neurofibrillary tangles; P: plaques.

peroxidation and decreased SOD, CAT, and GSH that guard against oxidative stress [46]. One of the major causes of neurodegeneration is oxidative stress, and to evaluate the test doses, the levels of all oxidative stress biomarkers were measured. In the current study, PAME significantly restored the levels of antioxidant enzymes including SOD, CAT, and GSH (Table 4) in the body and reduced the elevated levels of nitrites and MDA (Table 5). As antioxidant enzymes were recovered within the body, it might be the reason of improvement in behavior and different brain functions. In the current study, different parameters were evaluated to estimate the neurotransmitter levels in the body and the results showed that the levels of neurotransmitters including dopamine, serotonin, and noradrenaline were significantly increased ($P < 0.001$), whereas the level of acetylcholinesterase was decreased significantly ($P < 0.001$) (Figures 6 and 7). Histopathological data showed improvement in histological alterations, such as neurofibrillary tangles and plaques (Figure 8). Data regarding the toxicity study performed on heart, kidney, and liver are given in supplementary data (Tables S1–S6). The incidence of side effects was inquired by biochemical analysis via LFTs and RFTs, and none of the abnormally raised values were determined (Tables S7 and S8). Nonsignificant differences in values among different groups were seen. Furthermore, the histopathological examinations also revealed normal histological findings for all vital organs such as heart, kidney, and liver (Figures S1–S3).

5. Conclusion

In this study, the therapeutic potential of PAME in Parkinson's disease was investigated. The antioxidant potential of PAME was evaluated through behavioral, biochemical, and histological analyses and estimation of neurotransmitter levels, and its anti-Parkinson's activity was confirmed. It has been found to improve motor function deficits, behavioral disturbances, and neurotransmitter levels in a haloperidol-induced PD rat model. It has been observed that, in this disease, oxidative stress can be reduced and antioxidant enzymes can be recovered. It was also discovered to inhibit the acetylcholinesterase enzyme's activity in the brain tissue. Therefore, it can be concluded that this PAME might have a potential in the treatment of PD, and further research in this regard may open a new era of research if the study can be extended to the molecular level.

Data Availability

The data used to support the findings of this study are available from the corresponding author upon reasonable request.

Conflicts of Interest

The authors declare no conflicts of interest.

Supplementary Materials

Prunus armeniaca L. methanolic extract (PAME) and toxicity studies performed on the heart, liver, and kidney. All the toxicity data are provided in the supplementary material file and cited in the relevant section of the main text and supplementary material file. (*Supplementary Materials*)

References

- [1] R. Fischer and O. Maier, "Interrelation of oxidative stress and inflammation in neurodegenerative disease: role of TNF," *Oxidative Medicine and Cellular Longevity*, vol. 2015, Article ID 610813, 18 pages, 2015.
- [2] P. Narne, V. Pandey, P. K. Simhadri, and P. B. Phanithi, "Poly (ADP-ribose) polymerase-1 hyperactivation in neurodegenerative diseases: the death knell tolls for neurons," in *Seminars in Cell & Developmental Biology* Elsevier, Amsterdam, Netherlands, 2017.
- [3] C. Colosimo, L. Morgante, A. Antonini et al., "Non-motor symptoms in atypical and secondary parkinsonism: the PRIAMO study," *Journal of Neurology*, vol. 257, no. 1, pp. 5–14, 2010.
- [4] D. G. T. Parambi, U. Saleem, M. A. Shah et al., "Exploring the therapeutic potentials of highly selective oxygenated chalcone based MAO-B inhibitors in a haloperidol-induced murine model of Parkinson's disease," *Neurochemical Research*, vol. 45, no. 11, pp. 2786–2799, 2020.
- [5] O.-B. Tysnes and A. Storstein, "Epidemiology of Parkinson's disease," *Journal of Neural Transmission*, vol. 124, no. 8, pp. 901–905, 2017.
- [6] P. Maiti, J. Manna, and G. L. Dunbar, "Current understanding of the molecular mechanisms in Parkinson's disease: targets for potential treatments," *Translational Neurodegeneration*, vol. 6, no. 1, pp. 28–35, 2017.
- [7] T. Porter, "The role of genetics in Alzheimer's disease and Parkinson's disease," *Genetics, Hormones, and Lifestyle*, pp. 443–498, 2019.
- [8] M. A. Nalls, N. Pankratz, C. M. Lill et al., "Large-scale meta-analysis of genome-wide association data identifies six new risk loci for Parkinson's disease," *Nature Genetics*, vol. 46, no. 9, pp. 989–993, 2014.
- [9] W. Dauer and S. Przedborski, "Parkinson's disease: mechanisms and models," *Neuron*, vol. 39, no. 6, pp. 889–909, 2003.
- [10] H. Reichmann, "Modern treatment in Parkinson's disease, a personal approach," *Journal of Neural Transmission*, vol. 123, no. 1, pp. 73–80, 2016.
- [11] A. Ascherio and M. A. Schwarzschild, "The epidemiology of Parkinson's disease: risk factors and prevention," *The Lancet Neurology*, vol. 15, no. 12, pp. 1257–1272, 2016.
- [12] L. M. de Lau, P. C. Giesbergen, M. C. de Rijk, A. Hofman, P. J. Koudstaal, and M. M. Breteler, "Incidence of parkinsonism and Parkinson disease in a general population: the Rotterdam Study," *Neurology*, vol. 63, no. 7, pp. 1240–1244, 2004.
- [13] N. Mishra, S. Sharma, R. Deshmukh, A. Kumar, and R. Sharma, "Development and characterization of nasal delivery of selegiline hydrochloride loaded nanolipid carriers for the management of Parkinson's disease," *Central Nervous System Agents in Medicinal Chemistry*, vol. 19, no. 1, pp. 46–56, 2019.
- [14] M. Gupta, K. Kant, R. Sharma, and A. Kumar, "Evaluation of in silico anti-Parkinson potential of β -asarone," *Central Nervous System Agents in Medicinal Chemistry*, vol. 18, no. 2, pp. 128–135, 2018.
- [15] U. Saleem, Z. Chauhdary, Z. Raza et al., "Anti-Parkinson's activity of tribulus terrestris via modulation of AChE, α -synuclein, TNF- α , and IL-1 β ," *ACS Omega*, vol. 5, no. 39, pp. 25216–25227, 2020.
- [16] S. M. Iqbal, L. Hussain, M. Hussain et al., "Nephroprotective potential of a standardized extract of bambusa arundinacea: in vitro and in vivo studies," *ACS Omega*, vol. 7, no. 21, pp. 18159–18167, 2022.
- [17] A. Bashir, M. Asif, M. Saadullah et al., "Therapeutic potential of standardized extract of melilotus indicus (L.) all. And its phytochemicals against skin cancer in animal model: in vitro, in vivo, and in silico studies," *ACS Omega*, vol. 7, no. 29, pp. 25772–25782, 2022.
- [18] L. H. Zeng, S. Rana, L. Hussain et al., "Polycystic ovary syndrome: a disorder of reproductive age, its pathogenesis, and a discussion on the emerging role of herbal remedies," *Frontiers in Pharmacology*, vol. 13, Article ID 874914, 2022.
- [19] L. Hussain, M. S. H. Akash, M. Tahir, and K. Rehman, "Hepatoprotective effects of Sapium sebiferum in paracetamol-induced liver injury," *Bangladesh Journal of Pharmacology*, vol. 10, no. 2, pp. 393–398, 2015.
- [20] M. A. Ansari, H. M. Abdul, G. Joshi, W. O. Opii, and D. A. Butterfield, "Protective effect of quercetin in primary neurons against A β (1–42): relevance to Alzheimer's disease," *The Journal of Nutritional Biochemistry*, vol. 20, no. 4, pp. 269–275, 2009.
- [21] M. Berk, R. Post, A. Ratheesh et al., "Staging in bipolar disorder: from theoretical framework to clinical utility," *World Psychiatry*, vol. 16, no. 3, pp. 236–244, 2017.
- [22] S. Wani, N. Jan, T. A. Wani, M. Ahmad, F. Masoodi, and A. Gani, "Optimization of antioxidant activity and total polyphenols of dried apricot fruit extracts (*Prunus armeniaca* L.) using response surface methodology," *Journal of the Saudi Society of Agricultural Sciences*, vol. 16, no. 2, pp. 119–126, 2017.
- [23] A. B. Fadhil, "Evaluation of apricot (*Prunus armeniaca* L.) seed kernel as a potential feedstock for the production of liquid bio-fuels and activated carbons," *Energy Conversion and Management*, vol. 133, pp. 307–317, 2017.
- [24] S. Sharma, B. Kaur, A. Suttee, H. M. Mukhtar, and V. Kalsi, "Evaluation of antianxiety effect of dried fruits of *Prunus Americana* marsh," *Asian Journal of Pharmaceutical and Clinical Research*, vol. 10, no. 16, p. 67, 2017.
- [25] D. Shrivastav and D. Lata, "A Review on phytochemical and pharmacological studies of fruit *Prunus armeniaca* linn," *International Journal of Pharmaceutical & Biological Archives*, vol. 10, no. 4, pp. 242–250, 2019.
- [26] U. Saleem, K. Hussain, M. Ahmad, N. I. Bukhari, A. Malik, and B. Ahmad, "Report: physicochemical and phytochemical analysis of *Euphorbia helioscopia* (L.)," *Pakistan Journal of Pharmaceutical Sciences*, vol. 27, no. 3, pp. 577–585, 2014.
- [27] A. Younas, L. Hussain, A. Shabbir, M. Asif, M. Hussain, and F. Manzoor, "Effects of fagonia indica on letrozole-induced polycystic ovarian syndrome (PCOS) in young adult female rats," *Evidence-based Complementary and Alternative Medicine*, vol. 2022, Article ID 1397060, 13 pages, 2022.
- [28] C. H. Lee, T. H. Lee, P. Y. Ong et al., "Integrated ultrasound-mechanical stirrer technique for extraction of total alkaloid content from *Annona muricata*," *Process Biochemistry*, vol. 109, pp. 104–116, 2021.
- [29] U. Saleem, Z. Raza, F. Anwar, Z. Chaudary, and B. Ahmad, "Systems pharmacology based approach to investigate the in-

- vivo therapeutic efficacy of *Albizia lebbek* (L.) in experimental model of Parkinson's disease," *BMC Complementary and Alternative Medicine*, vol. 19, no. 1, pp. 352–416, 2019.
- [30] N. Chaitra, A. Joy, and M. Handral, "ANTIPARKINSON'S activity of vigna vexillata seed extract in haloperidol induced cataleptic rats," *World Journal of Pharmaceutical Research*, vol. 5, no. 7, pp. 729–746, 2016.
- [31] R. Haobam, K. M. Sindhu, G. Chandra, and K. P. Mohanakumar, "Swim-test as a function of motor impairment in MPTP model of Parkinson's disease: a comparative study in two mouse strains," *Behavioural Brain Research*, vol. 163, no. 2, pp. 159–167, 2005.
- [32] P. Pal and A. Ghosh, "Antioxidant, anti-alzheimer and anti-Parkinson activity of *Artemisia nilagirica* leaves with flowering tops," *Pharmaceutical and Biosciences Journal*, vol. 6, pp. 12–23, 2018.
- [33] O. H. Lowry, N. Rosebrough, A. L. Farr, and R. Randall, "Protein measurement with the Folin phenol reagent," *Journal of Biological Chemistry*, vol. 193, no. 1, pp. 265–275, 1951.
- [34] S. Hira, U. Saleem, F. Anwar, Z. Raza, A. U. Rehman, and B. Ahmad, "In silico study and pharmacological evaluation of Eplerinone as an Anti-Alzheimer's drug in STZ-induced Alzheimer's disease model," *ACS Omega*, vol. 5, no. 23, pp. 13973–13983, 2020.
- [35] S. Hira and U. Saleem, F. Anwar, Z. Raza, A. U. Rehman, and B. Ahmad, *In Silico Study and Pharmacological Evaluation of Eplerinone as an Anti-alzheimer's Drug in STZ-Induced Alzheimer's Disease Model*, ACS Omega, Washington, DC, USA, 2020.
- [36] U. Saleem, Z. Raza, F. Anwar, B. Ahmad, S. Hira, and T. Ali, "Experimental and computational studies to characterize and evaluate the therapeutic effect of *Albizia lebbek* (L.) seeds in Alzheimer's disease," *Medicina*, vol. 55, no. 5, p. 184, 2019.
- [37] S. Takahashi and K. Mashima, "Neuroprotection and disease modification by astrocytes and microglia in Parkinson disease," *Antioxidants*, vol. 11, no. 1, p. 170, 2022.
- [38] A. Saeed, L. Shakir, M. A. Khan, A. Ali, and A. A. Zaidi, "Haloperidol induced Parkinson's disease mice model and motor-function modulation with Pyridine-3-carboxylic acid," *Biomedical Research and Therapy*, vol. 4, no. 05, pp. 1305–1317, 2017.
- [39] N. Ball, W. P. Teo, S. Chandra, and J. Chapman, "Parkinson's disease and the environment," *Frontiers in Neurology*, vol. 10, p. 218, 2019.
- [40] F. Manzoor, M. U. Nisa, A. Shakoore, L. Hussain, A. Mahmood, and A. Younas, "Effect of sodium alginate supplementation on weight management and reproductive hormones in polycystic females," *Food & Function*, 2022.
- [41] L. Hussain, K. Abbas, B. Ahmad, M. Baber, S. A. Muhammad, and M. I. Qadir, "Report: analgesic and anti-inflammatory activity of aqueous-methanolic extract of *Aerva javanica*," *Pakistan Journal of Pharmaceutical Sciences*, vol. 30, no. 1, pp. 213–215, 2017.
- [42] F. Sancho-Bielsa, "Parkinson's disease: present and future of cell therapy," *Neurology Perspectives*, vol. 2, pp. S58–S68, 2022.
- [43] O. R. Tamtaji, T. Hadinezhad, M. Fallah et al., "The therapeutic potential of quercetin in Parkinson's disease: insights into its molecular and cellular regulation," *Current Drug Targets*, vol. 21, no. 5, pp. 509–518, 2020.
- [44] Q. F. Liu, J. H. Lee, Y. M. Kim et al., "In vivo screening of traditional medicinal plants for neuroprotective activity against $\text{A}\beta_{42}$ cytotoxicity by using drosophila models of alzheimer's disease," *Biological and Pharmaceutical Bulletin*, vol. 38, 2015.
- [45] A. E. Pukhalskaia, A. S. Diatlova, N. S. Linkova, and I. M. Kvetnoy, "Sirtuins: role in the regulation of oxidative stress and the pathogenesis of neurodegenerative diseases," *Neuroscience and Behavioral Physiology*, vol. 52, pp. 164–174, 2022.
- [46] E. A. Abdel-Sattar, S. M. Mouneir, G. F. Asaad, and H. M. Abdallah, "Protective effect of *Calligonum comosum* on haloperidol-induced oxidative stress in rat," *Toxicology and Industrial Health*, vol. 30, no. 2, pp. 147–153, 2014.

Research Article

Potential Targets and Action Mechanism of Gastrodin in the Treatment of Attention-Deficit/Hyperactivity Disorder: Bioinformatics and Network Pharmacology Analysis

Zhe Song ¹, Guangzhi Luo,² Chengen Han,³ Guangyuan Jia,³ and Baoqing Zhang ³

¹The First Clinical Medical College, Shandong University of Traditional Chinese Medicine, Jinan 250355, Shandong, China

²College of Traditional Chinese Medicine, Shandong University of Traditional Chinese Medicine, Jinan 250355, Shandong, China

³Department of Pediatrics, Affiliated Hospital of Shandong University of Traditional Chinese Medicine, Jinan 250011, Shandong, China

Correspondence should be addressed to Baoqing Zhang; baoping09009@126.com

Received 11 May 2022; Revised 8 August 2022; Accepted 18 August 2022; Published 12 September 2022

Academic Editor: Rajeev K. Singla

Copyright © 2022 Zhe Song et al. This is an open access article distributed under the Creative Commons Attribution License, which permits unrestricted use, distribution, and reproduction in any medium, provided the original work is properly cited.

Objective. Gastrodin is a main medicinal component of traditional Chinese medicine (TCM) *Gastrodia elata* Blume (*G. elata*), presenting the potential for the treatment of attention-deficit/hyperactivity disorder (ADHD). However, the underlying targets and action mechanisms of the treatment have not been identified. **Methods.** The gastrodin-related microarray dataset GSE85871 was obtained from the GEO database and analyzed by GEO2R to obtain differentially expressed genes (DEGs). Subsequently, the targets of gastrodin were supplemented by the Encyclopedia of Traditional Chinese Medicine (ETCM), PubChem, STITCH, and SwissTargetPrediction databases. ADHD-associated genes were collected from six available disease databases (i.e., TTD, DrugBank, OMIM, PharmGKB, GAD, and KEGG DISEASE). The potential targets of gastrodin during ADHD treatment were obtained by mapping gastrodin-related targets with ADHD genes, and their protein-protein interaction (PPI) relationship was constructed by the STRING database. The GO function and KEGG pathway enrichment analyses were performed using the ClueGO plug-in in the Cytoscape software and DAVID database, respectively. Finally, the binding affinity between gastrodin and important targets was verified by molecular docking. **Results.** A total of 460 gastrodin-related DEGs were identified from GSE85871, and 124 known gastrodin targets were supplemented from 4 databases, including ETCM. A total of 440 genes were collected from the above 6 disease databases, and 267 ADHD-relevant genes were obtained after duplicate removal. Through mapping the 584 gastrodin targets to the 267 ADHD genes, 16 potential therapeutic targets were obtained, among which the important ones were DRD2, DRD4, CHRNA3, CYP1A1, TNF, IL6, and KCNJ3. The enrichment analysis results indicated that 16 potential targets were involved in 25 biological processes (e.g., dopamine (DA) transport) and 22 molecular functions (e.g., postsynaptic neurotransmitter receptor activity), which were mainly localized at excitatory synapses. The neuroactive ligand-receptor interaction, cholinergic synapse, and dopaminergic synapse might be the core pathways of gastrodin in ADHD treatment. Through molecular docking, it was preliminarily verified that gastrodin showed good binding activity to seven important targets and formed stable binding conformations. **Conclusions.** Gastrodin might exert an anti-ADHD effect by upgrading the dopaminergic system and central cholinergic system, inhibiting the inflammatory response and GIRK channel, and exerting a synergistic effect with other drugs on ADHD. For this reason, gastrodin should be considered a multitarget drug for ADHD treatment.

1. Introduction

Attention-deficit/hyperactivity disorder (ADHD) is a common neurodevelopmental disorder clinically, mainly characterized by inattention, hyperactivity, and impulsiveness [1].

According to the results of the latest meta-analysis, the global prevalence of ADHD in children and adults was 7.2% and 6.76%, respectively [2, 3], indicating persistent lifetime symptoms in most ADHD patients. Additionally, ADHD is often accompanied by other psychiatric conditions, such as

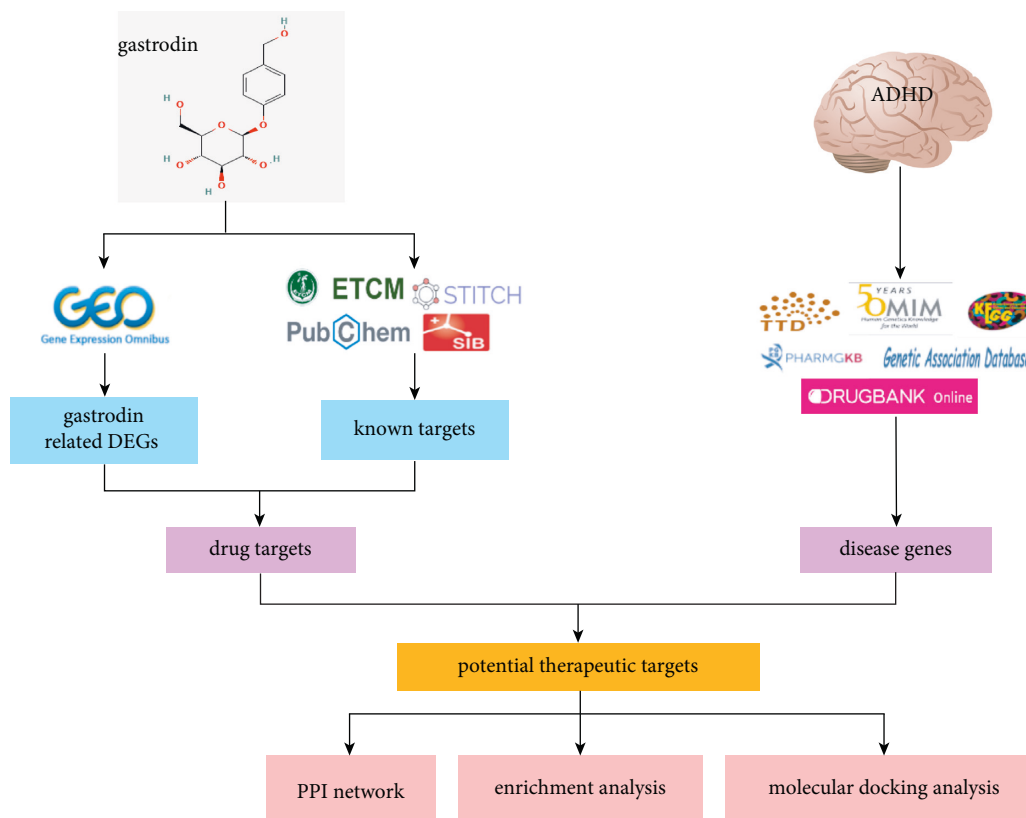


FIGURE 1: Flowchart of the study on the molecular mechanism of gastrodin in attention-deficit/hyperactivity disorder (ADHD) treatment.

depression disorder, severe anxiety, and oppositional defiant disorder [4]. With the rising incidence in recent years, ADHD has become a global public health concern [5].

ADHD has been defined as a complex, multifactorial disorder, with its etiology and pathogenesis not well understood [6]. Among many hypotheses of ADHD, the abnormalities in the functions of monoamine neurotransmitters have been the research focus; especially, the “dopamine deficit theory” has been confirmed [7, 8]. At present, methylphenidate (MPH) is the most commonly used drug in clinical practice and shows a significant advantage in the temporary control of ADHD symptoms [9]. Unfortunately, MPH is a stimulant that produces potential digestive and cardiovascular side effects. It also causes recurrent symptoms after discontinuation, resulting in poor compliance of patients with treatment [10–12]. Therefore, it is essential to explore a more efficient and safer drug for ADHD treatment.

Considering the clear curative effect, multiple targets, and other advantages of traditional Chinese medicine (TCM) with a long history, Chinese herbs and their main active ingredients have gradually become the major resources of new drugs, represented by artemisinin from *Artemisia annua* [13, 14]. *Gastrodia elata* Blume (*G. elata*) is a high-frequency herb used in the TCM prescription for ADHD treatment [15]. Gastrodin, chemically known as 4-hydroxymethylphenyl β -D-glucopyranoside, is the key characteristic medicinal component of *G. elata* [16]. Modern pharmacological studies have revealed that gastrodin has the properties of the regulation of monoamine neurotransmitters

[17], anti-inflammation [18], antioxidation [19], antianxiety [20], neuron protection [21], etc., closely related to the known ADHD pathogenesis. Moreover, gastrodin exhibits excellent oral bioavailability, rapid penetration of the blood-brain barrier, and almost nontoxicity [22, 23]. However, the mechanism of gastrodin, as a potential drug for ADHD treatment, on ADHD still remains unclear.

Recent years have seen the emerging bioinformatics and network pharmacology in the field of life science and pharmacology, which offer new methods to elucidate the molecular mechanisms of diseases and drug therapy targets [24]. On this basis, this study was designed to use bioinformatics coupled with network pharmacology to screen and predict the potential targets and signal pathways of gastrodin in ADHD treatment and to verify the predicted results by molecular docking. This study is expected to lay a basis for the follow-up experiment and novel drug development. A flowchart of our study is presented in Figure 1.

2. Materials and Methods

2.1. Identification of Gastrodin Targets. The microarray dataset GSE85871 was obtained by searching the gene expression omnibus (GEO) database (<https://www.ncbi.nlm.nih.gov/geo/>) with “gastrodin” as the keyword. The data of GSE85871 were based on the affymetrix human genome U133A 2.0 array (GPL571), containing the gene expression data of 102 TCM ingredient-treated MCF7 cells. Dimethyl sulfoxide (DMSO) treatment was used as a control. Only

data from the two gastrodin intervention groups and the two DMSO control groups were extracted and subsequently analyzed. GEO2R (<https://www.ncbi.nlm.nih.gov/geo/geo2r/>) was used to standardize the raw data and investigate the differentially expressed genes (DEGs). Genes with $P < 0.01$ and $|\text{fold change (FC)}| < 2$ were considered DEGs, all of which were displayed by the heatmap and volcano plot.

Afterward, the Encyclopedia of Traditional Chinese Medicine (ETCM) (<https://www.tcmip.cn/ETCM/>), PubChem (<https://pubchem.ncbi.nlm.nih.gov/>), STITCH (<https://stitch.embl.de/>), and SwissTargetPrediction (<https://www.swisstargetprediction.ch/>) databases were retrieved with “gastrodin” as the keyword, respectively. Then the gastrodin-related drug targets were gained by combining the targets obtained from the above four databases with the DEGs analyzed by the dataset GSE85871.

2.2. Collection of ADHD Disease Genes. By retrieving the Therapeutic Target Database (TTD, <https://bidd.nus.edu.sg/group/cjttd/>), DrugBank (<https://go.drugbank.com/>), Online Mendelian Inheritance in Man (OMIM, <https://www.omim.org/>), Pharmacogenomics Knowledge Base (PharmGKB, <https://www.pharmgkb.org/>), Genetic Association Database (GAD, <https://geneticassociationdb.nih.gov/>), and KEGG DISEASE (<https://www.kegg.jp/kegg/disease/>), the ADHD disease genes were collected.

2.3. Construction of Protein-Protein Interaction (PPI) Network. The potential targets of gastrodin in ADHD treatment could be obtained by mapping drug targets with disease genes. These potential therapeutic targets were uploaded to the STRING database (<https://cn.string-db.org/>) with a minimum interaction score of 0.4 to obtain the PPI relationship. Then, they were visualized by the Cytoscape software.

2.4. Enrichment Analysis. To further explore the main mechanism of gastrodin in ADHD treatment, the ClueGO plug-in in the Cytoscape software was employed for gene ontology (GO) enrichment analysis, covering biological process (BP), molecular function (MF), and cell composition (CC). Moreover, the Kyoto Encyclopedia of Genes and Genomes (KEGG) pathway enrichment analysis was carried out using the DAVID database (<https://david.ncifcrf.gov/>), with $P < 0.05$ as the cut-off criterion and the result displayed by the barplot.

2.5. Molecular Docking Analysis. The key therapeutic targets were selected for molecular docking with gastrodin to preliminarily verify the mechanism of gastrodin for ADHD treatment. Briefly, the molecular structure of gastrodin was downloaded from the PubChem database, and the format transformation and energy minimization were carried out by the Chem3D software. The obtained structure was imported into the Schrödinger software and saved as the ligand database of molecular docking after hydrogenation, structure optimization, and energy minimization. The crystal

structures of the key targets were obtained from the RCSB PDB database (<https://www.rcsb.org/>) and imported into the Maestro 11.9 platform. The proteins were pretreated by the Protein Preparation Wizard module in Schrödinger software. Constrained energy minimization and geometric structure optimization were performed by the OPLS3e force field. Finally, using the default software parameters, the standard precision (SP) method was selected to dock gastrodin with key therapeutic targets. The docking results were visualized by the PyMOL software.

3. Results

3.1. Identification of DEGs and Target Collection of Gastrodin. With $P < 0.01$ and $|\text{FC}| > 2$ as the threshold, 460 DEGs (Supplementary Table 1) were identified from the microarray dataset GSE85871, including 253 up-regulated genes and 207 down-regulated genes between the gastrodin intervention groups and control groups. The heatmap and volcano plot were utilized to display the distribution of all DEGs (Figure 2).

By database retrieval, 16, 7, 6, and 103 gastrodin targets (Supplementary Table 2) were obtained in ETCM, PubChem, STITCH, and SwissTargetPrediction, respectively. These targets were combined with 460 DEGs, with the duplicate values deleted. Finally, 584 gastrodin-associated drug targets were obtained (Supplementary Table 3).

3.2. Screening of ADHD Disease Genes. A total of 440 known genes of ADHD were collected from 6 existing databases, and 267 ADHD disease genes were obtained after duplicate removal (Supplementary Table 4).

3.3. Identification of Therapeutic Targets and Construction of PPI Network. Among the 584 drug targets and 267 disease genes, 16 common targets were found. By uploading the 16 targets to the STRING database, a PPI network including 14 interactive nodes and 2 independent nodes was obtained and visualized by the Cytoscape software (Table 1 and Figure 3). The NetworkAnalyzer plug-in was employed to evaluate the degree value (i.e., the number of edges linked to a node) of each node. A greater degree value indicates a more significant target in the PPI network and greater biological functions of the target [25]. Only targets with a degree greater than the average value (3.0) were considered important, including DRD2, DRD4, CHRNA3, CYP1A1, TNF, IL6, and KCNJ3.

3.4. GO Function and KEGG Pathway Enrichment. The ClueGO plug-in in the Cytoscape software was utilized to perform the enrichment analysis of BP, MF, and CC on the above 16 targets. As shown in Figure 4(a), 25 biological processes were obtained and clustered into 3 groups: membrane repolarization during ventricular cardiac muscle cell action potential, dopamine (DA) transport, and response to nicotine. Among the three groups, DA transport had close ties to the pathological mechanism of ADHD,

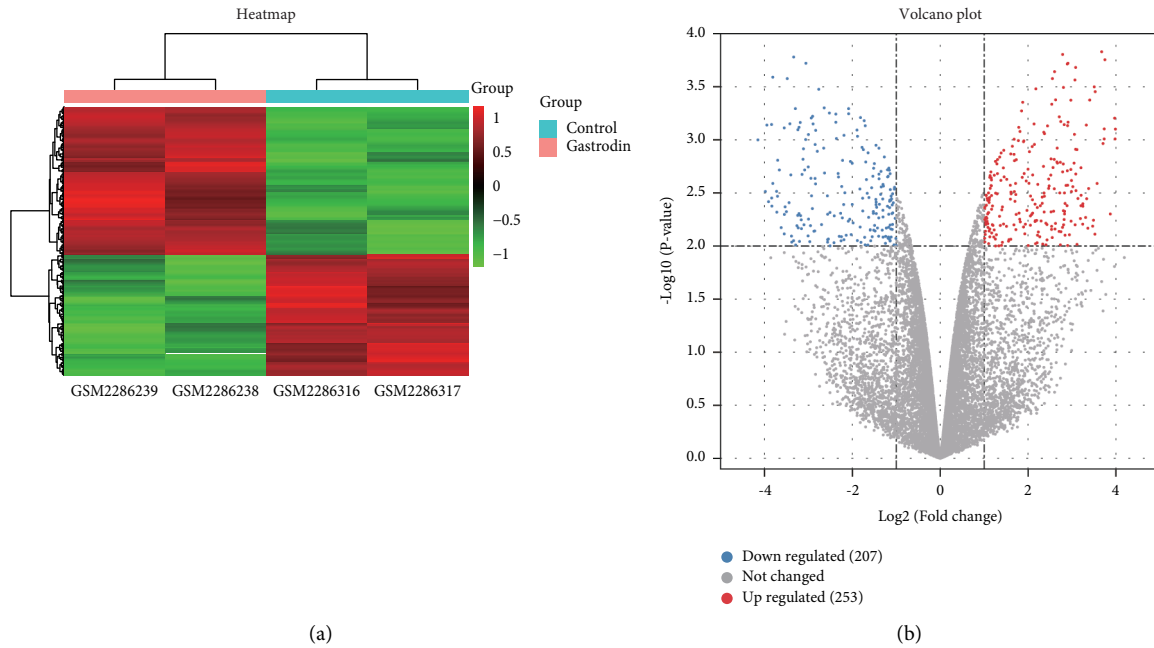


FIGURE 2: Heatmap and volcano plot of differentially expressed genes (DEGs). (a) Heatmap of 460 DEGs identified with the threshold of $P < 0.01$ and $|\logFC| > 1$. Pink and blue indicate gastrodin intervention groups and DMSO control groups, respectively. The color gradient from red to green represents differential expression values from high to low. Red represents the up-regulated genes, while green denotes the down-regulated genes. (b) Volcano plot of all genes. The red dots indicate up-regulated genes, the blue dots indicate down-regulated genes, and the gray dots indicate genes with no significant difference.

TABLE 1: Basic information of 16 potential therapeutic targets.

No.	Gene symbol	Gene name	Degree	logFC
1	DRD2	Dopamine receptor D2	6	2.4680278
2	DRD4	Dopamine receptor D4	5	—
3	CHRNA3	Cholinergic receptor nicotinic alpha 3 subunit	4	2.5349484
4	CYP1A1	Cytochrome P450 family 1 subfamily A, member 1	4	-3.8387415
5	TNF	Tumor necrosis factor	4	—
6	IL6	Interleukin 6	4	—
7	KCNJ3	Potassium inwardly rectifying channel, subfamily J, member 3	4	-1.1164583
8	CYP2E1	Cytochrome P450 family 2, subfamily E, member 1	3	2.7216362
9	SLC6A2	Solute carrier family 6, member 2	3	2.5546023
10	TPH1	Tryptophan hydroxylase 1	3	2.1948648
11	NTRK2	Neurotrophic receptor tyrosine kinase 2	3	2.7099514
12	KCND3	Potassium voltage-gated channel subfamily D, member 3	2	3.0669291
13	KCNH2	Potassium voltage-gated channel subfamily H, member 2	2	1.127879
14	CHRM5	Cholinergic receptor muscarinic 5	1	1.8235883
15	GGH	Gamma-glutamyl hydrolase	0	—
16	NLGN3	Neurologin 3	0	-1.8037092

covering 44.0% of all BP terms. As can be seen in Figure 4(b), 16 targets mediated 22 molecular functions, which were also clustered into three groups, i.e., the postsynaptic neurotransmitter receptor activity, arachidonic acid monooxygenase activity, and voltage-gated potassium channel activity involved in ventricular cardiac muscle cell action potential repolarization. Among them, the postsynaptic neurotransmitter receptor activity was the main enriched molecular function, covering 54.55% of all MF terms. The CC result demonstrated that the potential targets of gastrodin during ADHD treatment were located on 14 cell compositions clustered into 8 groups (Figure 4(c)). Among them, the

excitatory synapse was the main enriched area (covering 50%). The KEGG pathway enrichment analysis indicated 16 targets associated with 7 pathways ($P < 0.05$), mainly including the neuroactive ligand-receptor interaction, cholinergic synapse, and dopaminergic synapse (Figure 5).

3.5. Molecular Docking of Gastrodin with Important Therapeutic Targets. Gastrodin was docked with DRD2, DRD4, CHRNA3, CYP1A1, TNF, IL6, and KCNJ3, respectively, to evaluate the binding affinity between gastrodin and these target proteins. Generally, binding energy less than 0

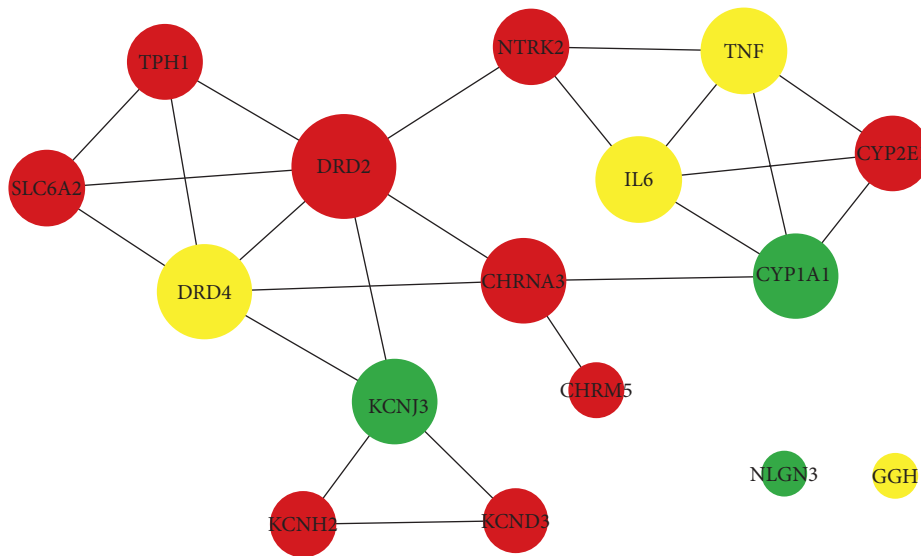


FIGURE 3: Protein-protein interaction (PPI) network diagram of potential therapeutic targets. Each node in the network represents a target. The node size represents the degree value, and the different color represents differential expression values. Red indicates the up-regulated targets, green indicates the down-regulated targets, yellow indicates targets supplemented by four drug databases, and there is no logFC value.

indicates that the ligand can bind to the receptor spontaneously [26]; binding energy less than -5.00 kcal/mol implies strong binding activity [27]. As can be seen from Table 2, the binding energies of gastrodin and seven important targets were all less than -6.00 kcal/mol. As shown in Figure 6, gastrodin could form stable complexes with seven target proteins mainly through the formation of hydrogen bonds or hydrophobic interaction. In short, the docking results provide data support for the subsequent verification of the regulatory relationship between gastrodin and these targets.

4. Discussion

ADHD was previously considered a behavioral disorder only in childhood, with the symptoms disappearing with age. Nevertheless, growing evidence has revealed that more than half of patients will continue to suffer from ADHD until adulthood and even throughout life [28, 29]. ADHD leads to declining academic performance, cognitive impairment, various emotional problems, and increasing social crime and suicide rates [30, 31], resulting in significant negative consequences for individual patients, their families, and society [32]. Due to the complex etiology and pathogenesis, it is difficult to eliminate the symptoms using the existing therapeutic drugs, which have many side effects and thus pose severe challenges to clinical treatment [33]. Fortunately, Chinese herbs and their active ingredients bring new opportunities for drug research and development, represented by a frequently used herb *G. elata* in ADHD treatment, with gastrodin as its key component [34]. Therefore, elucidation of the specific mechanism of gastrodin during ADHD treatment can provide guidance for new drug development and clinical treatment.

This study systematically analyzed potential targets and signal pathways of gastrodin during ADHD treatment. By

retrieving the GEO database, several drug databases, and disease databases, 16 potential therapeutic targets were identified, among which the important were DRD2, DRD4, CHRMA3, CYP1A1, TNF, IL6, and KCN3. Both DRD2 and DRD4 belonged to DA D2-like receptors, participating in DA transmission [35]. DA is a key neurotransmitter regulating physical movement, emotion, and neuroendocrine activities [36], stored in the synaptic vesicles of dopaminergic neurons after synthesis. When nerve impulses are afferent, DA is released into the synaptic cleft and binds to DA receptors to perform multiple functions [37]. A genome-wide association study of first-line pharmacotherapeutics for ADHD suggested that DRD2 might be a secondary target of MPH and amphetamine (AMP) [38]. Decreased DRD2 expression could lead to hyperactive behavior in mice [39]. A neuroimaging experiment has also confirmed that the decreasingly available DA D2 autoreceptors were closely related to impulsive traits [40]. According to our results (Table 1 and Figure 3), gastrodin might promote DRD2 expression, suggesting the potential ameliorative effects of gastrodin on the impulsive and hyperactive symptoms of ADHD by increasing the number of DRD2 or its sensitivity to DA. Regarded as a therapeutic target for ADHD [41], DRD4 represented a lower density in multiple brain regions of ADHD patients than that of normal individuals [42, 43]. The application of highly selective DRD4 agonists could significantly improve the cognitive ability of ADHD model rats; moreover, it did not increase the risk of substance abuse compared with psychostimulant therapy [44, 45]. To our knowledge, the targeting relationship between gastrodin and DRD4 has not been reported. Our molecular docking results showed a strong binding affinity of gastrodin with DRD4 (binding energy: -7.13 kcal/mol). As shown in Figure 6(b), gastrodin could interact with multiple amino acid residues of DRD4 through hydrophobic interaction and hydrogen bonding. Therefore, DRD4 might become a new target for

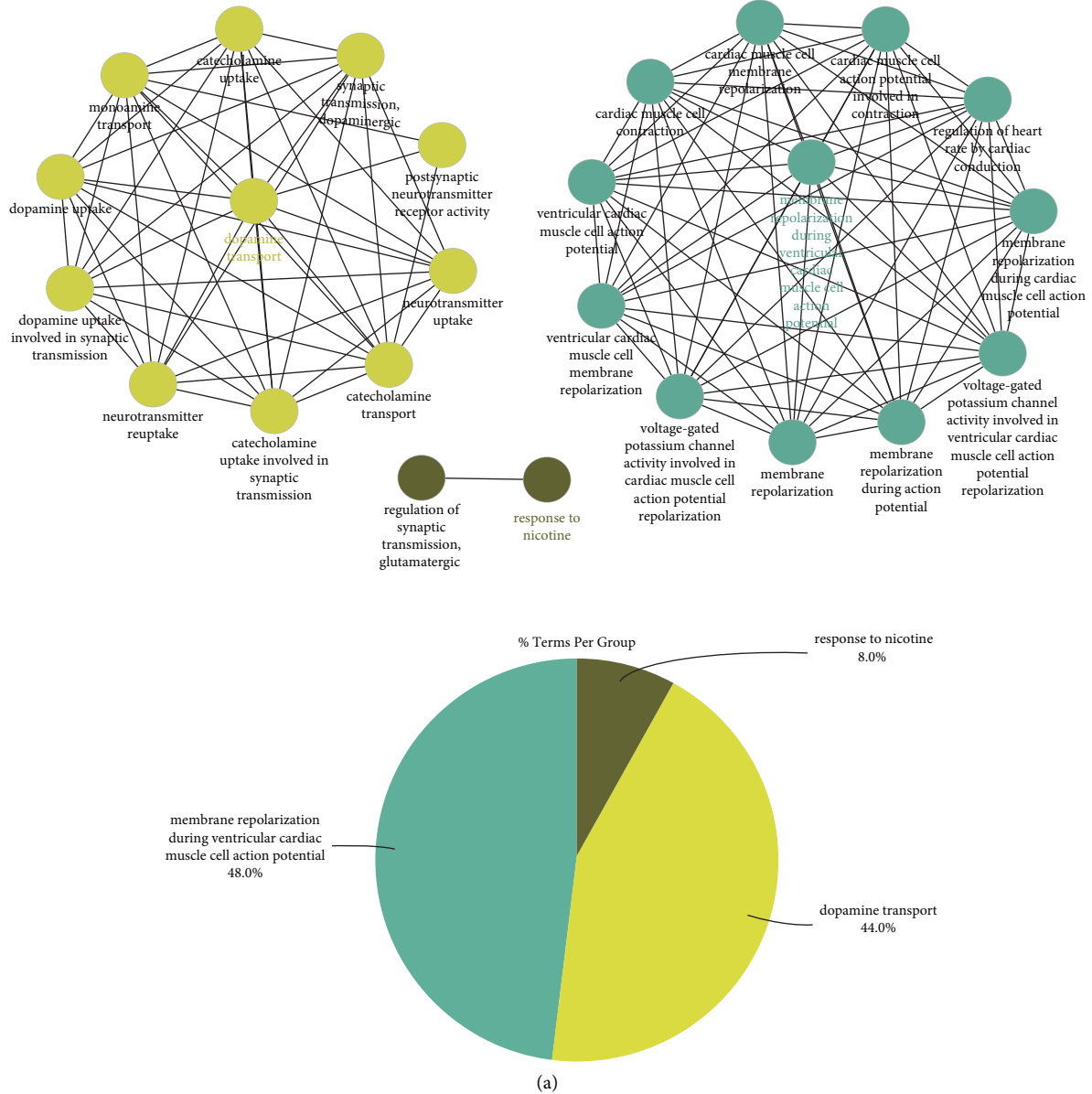
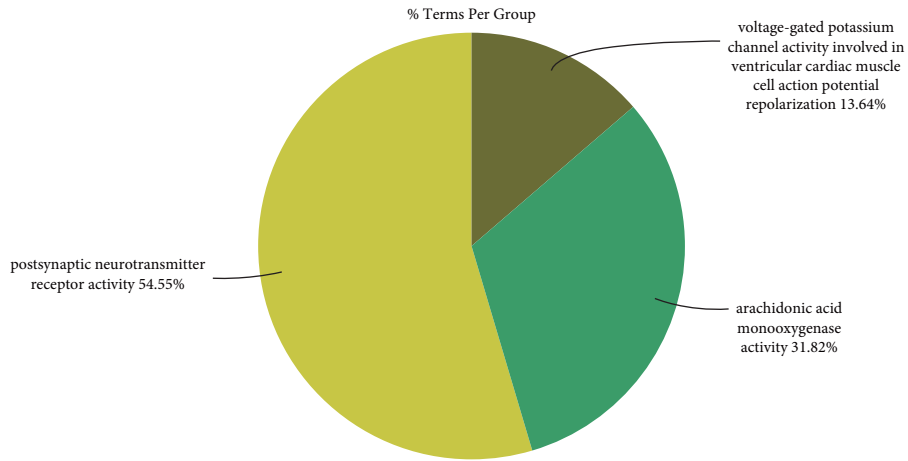
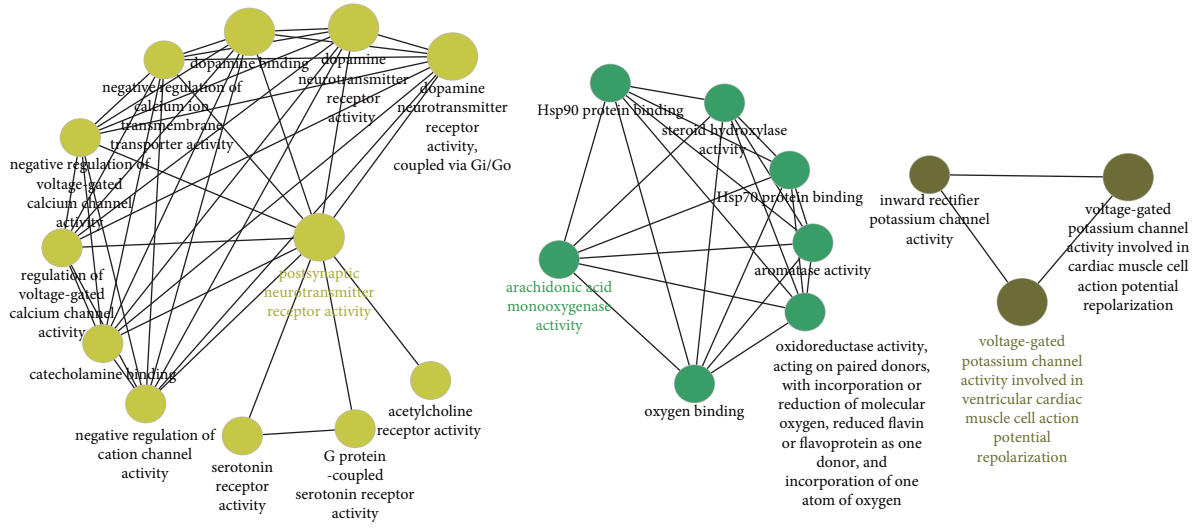


FIGURE 4: Continued.



(b)
FIGURE 4: Continued.



FIGURE 4: Results of gene ontology (GO) function enrichment analysis. The cluster network and the pie chart of (a) biological process (BP), (b) molecular function (MF), and (c) cell composition (CC). In the cluster network, each node represents a GO term, with the most important term in each group highlighted. The pie chart shows the proportion of each cluster group.

gastrodin in disease treatment. Particularly in ADHD treatment, gastrodin might play a role similar to that of a DRD4 agonist. CHRNA3 is a member of the nicotinic acetylcholine receptor (nAChR) family, and nAChR dysfunction plays an important role in the pathological mechanism of attention deficit [46]. Several novel nAChR agonists have been developed, such as AZD3480, ABT-894,

and ABT-089. They can improve adult ADHD symptoms to a certain extent according to the randomized controlled phase II clinical trials [47–49], indicating the feasibility of using gastrodin to treat ADHD by increasing CHRNA3 expression. CYP1A1 is an important paralog of CYP1A2, both of which are members of the cytochrome P450 (CYP450) superfamily [50]. CYP450 is among the most

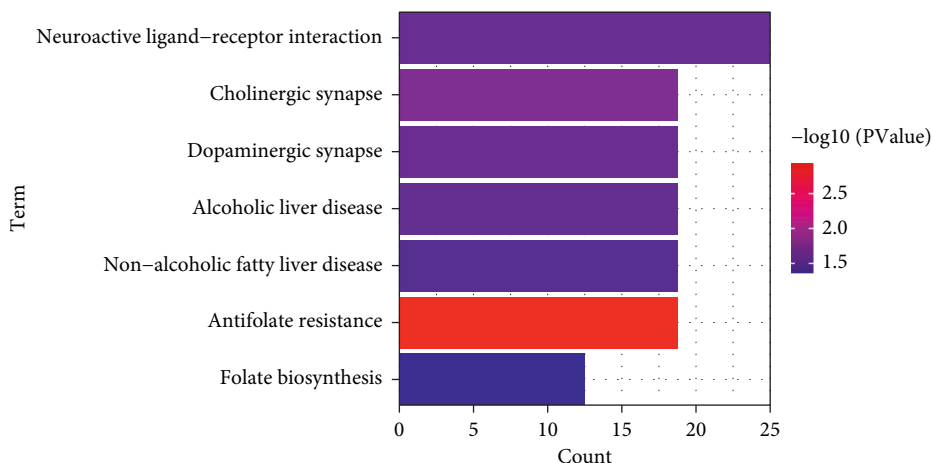


FIGURE 5: Barplot of the KEGG pathway enrichment. The horizontal axis represents the gene ratio, and the vertical axis represents the KEGG pathways. The color gradient of bars from red to blue indicates the (P) values from low to high.

TABLE 2: The result of molecular docking.

Target	PDB ID	Binding energy (kcal/mol)
DRD2	6CM4	-7.46
DRD4	5WIV	-7.13
CHRNA3	4ZK4	-7.93
CYP1A1	4I8V	-7.33
TNF	7KPA	-8.35
IL6	4O9H	-6.64
KCNJ3	2QKS	-6.52

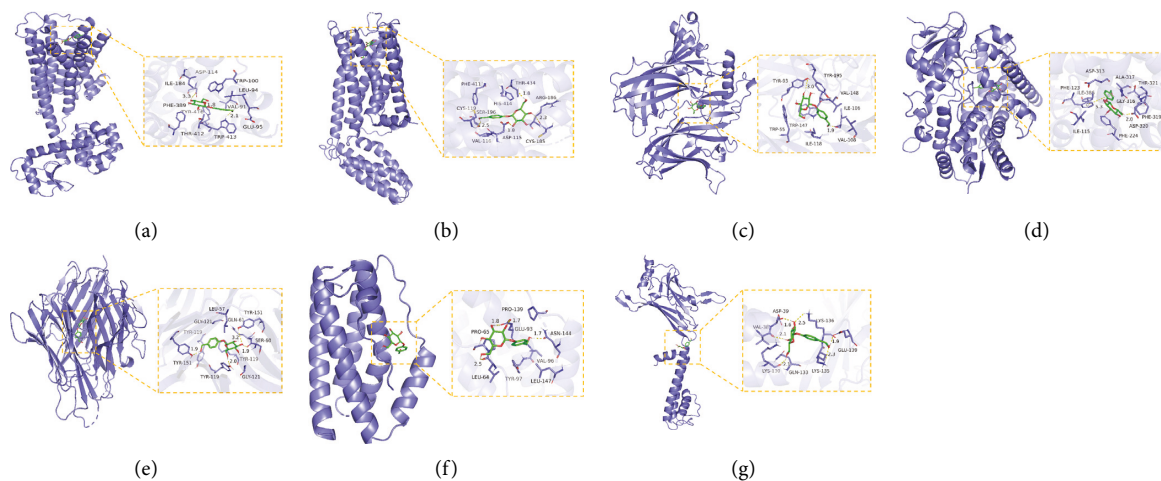


FIGURE 6: Docking model of gastrodin with seven important targets. (a) DRD2 and gastrodin; (b) DRD4 and gastrodin; (c) CHRNA3 and gastrodin; (d) CYP1A1 and gastrodin; (e) TNF and gastrodin; (f) IL6 and gastrodin; (g) KCNJ3 and gastrodin.

critical drug metabolic enzymes capable of catalyzing phase I reactions of drugs [51]. AMP, atomoxetine, and tricyclic antidepressants, commonly used in ADHD treatment, are metabolized by CYP1A2 [52], but their relationship with CYP1A1 has not been reported. Our results suggested that gastrodin might down-regulate CYP1A1 expression. It was speculated that a beneficial interaction existed between the CYP450-metabolized therapeutic drugs for ADHD and gastrodin. Specifically, gastrodin might reduce the metabolic

rate of these drugs *in vivo* by inhibiting CYP1A1 activity, thereby improving their efficacy. TNF and IL6 are well-known important cytokines of inflammation and immune response. Excess inflammatory cytokines could influence the turnover of monoamine neurotransmitters and induce various neuropsychiatric disorders [53]. Inflammation has been implicated as a trigger of ADHD [54], and gastrodin has been proved to have anti-inflammatory pharmacological effects, which can alleviate cognitive impairment by

lessening TNF- α and IL-6 levels [18]. KCNJ3, also termed GIRK1 or Kir3.1, is extensively expressed in the central nervous system and binds to three other potassium channel proteins (i.e., KCNJ6/GIRK2, KCNJ9/GIRK3, and KCNJ5/GIRK4) to form the G protein-gated inwardly rectifying potassium (GIRK) channel [55, 56]. The GIRK channel can bind to DA D2-like receptors, resulting in neuron self-inhibition and reduced DA release [57]. This is relevant to the pathogenesis of many neuropsychiatric disorders, such as ADHD, schizophrenia, and epilepsy [58]. GIRK channel blockers could prevent drug-induced hyperactivity in mice [59]. In our study, gastrodin might down-regulate KCNJ3 expression, implying that inhibition of the GIRK channel through KCNJ3 might be a main mechanism of gastrodin during ADHD treatment.

Subsequently, further functional analysis was conducted on the potential targets of gastrodin in ADHD treatment. As shown in Figure 4, these targets mainly participated in the biological process of DA transport and the molecular function of postsynaptic neurotransmitter receptor activity, mainly located at excitatory synapses. The KEGG pathway enrichment analysis results highlighted that the neuroactive ligand-receptor interaction, cholinergic synapse, and dopaminergic synapse were the main pathways for the gastrodin therapeutic effect (Figure 5). According to the results obtained in this study, the important targets and pathways of gastrodin in ADHD treatment were closely related to DA receptor activity, nAChR activity, drug interaction, inflammatory response, GIRK channel, and neurotransmitter transmission. Therefore, the specific mechanisms of gastrodin in ADHD treatment could be concluded from the following aspects: (1) Above all, gastrodin might promote the release and transport of DA by enhancing the function of DA receptors, as well as inhibiting proinflammatory cytokines and GIRK channel. (2) Gastrodin elevated the function of the central cholinergic system by acting on nAChR. (3) Gastrodin might reduce the metabolic rate of CYP450-metabolized therapeutic drugs for ADHD, and the combination of gastrodin with these drugs might have a synergistic effect.

Our study also has some limitations. First of all, the sample size in the gastrodin intervention group was poor in dataset GSE85871, which took MCF7 cells as the object to analyze the gene expression of different TCM ingredients. The results would definitely vary if different human cells and tissues were used for research. Second, the FC value of gastrodin targets supplemented by the four drug databases could not be obtained, and the exact effects of gastrodin on the predicted targets and pathways need further experimental verification. Finally, distinguishment was not made between the ADHD subtypes. In accordance with the Diagnostic and Statistical Manual of Mental Disorders, 5th edition (DSM-5), ADHD could be classified as hyperactive/impulsive type, inattentive type, and combined type [60], which presented diverse clinical manifestations and pathogenesis [61]. In the future, based on the results of this study, the effective mechanisms of gastrodin in ADHD treatment will be first verified. Then, detailed clinical and experimental research programs are expected to be designed to observe the effects of gastrodin on different subtypes of ADHD.

5. Conclusions

In conclusion, according to bioinformatics and network pharmacology studies, the main targets of gastrodin for ADHD treatment might be DRD2, DRD4, CHRNA3, CYP1A1, TNF, IL6, and KCNJ3, which were preliminarily verified by molecular docking. Gastrodin might exert an anti-ADHD effect by enhancing the function of the dopaminergic system and central cholinergic system, inhibiting the inflammatory response and GIRK channel, and exerting a synergistic effect with other drugs on ADHD. Among them, gastrodin might promote the release and transport of DA through various mechanisms, which deserves the most attention. Gastrodin should be considered a multitarget drug for ADHD treatment. Taken together, the present study is expected to provide important information to further complement the pharmacological effects of gastrodin and the clinical ADHD treatment.

Data Availability

The data supporting the conclusions of this article are included within the article.

Conflicts of Interest

The authors have no conflicts of interest to declare.

Authors' Contributions

Zhe Song performed methodology and wrote the manuscript. Guangzhi Luo and Chengen Han provided the related softwares and platforms. Guangyuan Jia contributed to data curation. Baoqing Zhang conceived the study and revised the manuscript. All the authors have read and approved the final manuscript.

Supplementary Materials

Supplementary Table 1: the 460 DEGs in GSE85871. Supplementary Table 2: the known targets of gastrodin in four drug databases. Supplementary Table 3: 584 gastrodin-related drug targets. Supplementary Table 4: the ADHD-related disease genes. (*Supplementary Materials*)

References

- [1] A. Thapar and M. Cooper, "Attention deficit hyperactivity disorder," *The Lancet*, vol. 387, no. 10024, pp. 1240–1250, 2016.
- [2] R. Thomas, S. Sanders, J. Doust, E. Beller, and P. Glasziou, "Prevalence of attention-deficit/hyperactivity disorder: a systematic review and meta-analysis," *Pediatrics*, vol. 135, no. 4, pp. 994–1001, 2015.
- [3] P. Song, M. Zha, Q. Yang, Y. Zhang, X. Li, and I. Rudan, "The prevalence of adult attention-deficit hyperactivity disorder: a global systematic review and meta-analysis," *Journal of Global Health*, vol. 11, Article ID 04009, 2021.
- [4] M. Chatterjee, S. Saha, S. Shom, S. Sinha, and K. Mukhopadhyay, "Adhesion G protein-coupled receptor L3 gene variants: statistically significant association observed in

- the male Indo-caucasoid Attention deficit hyperactivity disorder probands,” *Molecular Biology Reports*, vol. 48, no. 4, pp. 3213–3222, 2021.
- [5] K. Sayal, V. Prasad, D. Daley, T. Ford, and D. Coghill, “ADHD in children and young people: prevalence, care pathways, and service provision,” *The Lancet Psychiatry*, vol. 5, no. 2, pp. 175–186, 2018.
 - [6] A. A. J. Verlaet, B. Ceulemans, H. Verhelst et al., “Effect of pycnogenol® on attention-deficit hyperactivity disorder (ADHD): study protocol for a randomised controlled trial,” *Trials*, vol. 18, no. 1, p. 145, 2017.
 - [7] M. Seyedi, F. Gholami, M. Samadi et al., “The effect of vitamin D3 supplementation on serum BDNF, dopamine, and serotonin in children with attention-deficit/hyperactivity disorder,” *CNS & Neurological Disorders—Drug Targets*, vol. 18, no. 6, pp. 496–501, 2019.
 - [8] J. M. Swanson, M. Kinsbourne, J. Nigg et al., “Etiologic subtypes of attention-deficit/hyperactivity disorder: brain imaging, molecular genetic and environmental factors and the dopamine hypothesis,” *Neuropsychology Review*, vol. 17, no. 1, pp. 39–59, 2007.
 - [9] T. P. Shellenberg, W. W. Stoops, J. A. Lile, and C. R. Rush, “An update on the clinical pharmacology of methylphenidate: therapeutic efficacy, abuse potential and future considerations,” *Expert Review of Clinical Pharmacology*, vol. 13, no. 8, pp. 825–833, 2020.
 - [10] J. R. Young, A. Yanagihara, R. Dew, and S. H. Kollins, “Pharmacotherapy for preschool children with attention deficit hyperactivity disorder (ADHD): current status and future directions,” *CNS Drugs*, vol. 35, no. 4, pp. 403–424, 2021.
 - [11] C. Ching, G. D. Eslick, and A. S. Poulton, “Evaluation of methylphenidate safety and maximum-dose titration rationale in attention-deficit/hyperactivity disorder: a meta-analysis,” *JAMA Pediatrics*, vol. 173, no. 7, pp. 630–639, 2019.
 - [12] O. J. Storebø, N. Pedersen, E. Ramstad et al., “Methylphenidate for attention deficit hyperactivity disorder (ADHD) in children and adolescents - assessment of adverse events in non-randomised studies,” *The Cochrane Database of Systematic Reviews*, vol. 5, no. 5, Article ID C, 2018.
 - [13] Z. Yang, Q. Zhang, L. Yu, J. Zhu, Y. Cao, and X. Gao, “The signaling pathways and targets of traditional Chinese medicine and natural medicine in triple-negative breast cancer,” *Journal of Ethnopharmacology*, vol. 264, Article ID 113249, 2021.
 - [14] C. Tang, Y. Ye, Y. Feng, and R. J. Quinn, “TCM, brain function and drug space,” *Natural Product Reports*, vol. 33, no. 1, pp. 6–25, 2016.
 - [15] S. Bae, S. Park, and D. H. Han, “A mixed herbal extract as an adjunctive therapy for attention deficit hyperactivity disorder: a randomized placebo-controlled trial,” *Integrative Medicine Research*, vol. 10, no. 3, Article ID 100714, 2021.
 - [16] Y. Bai, H. Yin, H. Bi, Y. Zhuang, T. Liu, and Y. Ma, “De novo biosynthesis of gastrodin in *Escherichia coli*,” *Metabolic Engineering*, vol. 35, pp. 138–147, 2016.
 - [17] X. Wang, S. Yan, A. Wang, Y. Li, and F. Zhang, “Gastrodin ameliorates memory deficits in 3,3'-iminodipropionitrile-induced rats: possible involvement of dopaminergic system,” *Neurochemical Research*, vol. 39, no. 8, pp. 1458–1466, 2014.
 - [18] X. Wang, L. Chen, Y. Xu et al., “Gastrodin alleviates peri-operative neurocognitive dysfunction of aged mice by suppressing neuroinflammation,” *European Journal of Pharmacology*, vol. 892, Article ID 173734, 2021.
 - [19] X. L. Wang, G. H. Xing, B. Hong et al., “Gastrodin prevents motor deficits and oxidative stress in the MPTP mouse model of Parkinson’s disease: involvement of ERK1/2-Nrf2 signaling pathway,” *Life Sciences*, vol. 114, no. 2, pp. 77–85, 2014.
 - [20] Z. Peng, H. Wang, R. Zhang et al., “Gastrodin ameliorates anxiety-like behaviors and inhibits IL-1beta level and p38 MAPK phosphorylation of hippocampus in the rat model of posttraumatic stress disorder,” *Physiological Research*, vol. 62, no. 5, pp. 537–545, 2013.
 - [21] J. Yan, Z. Yang, N. Zhao, Z. Li, and X. Cao, “Gastrodin protects dopaminergic neurons via insulin-like pathway in a Parkinson’s disease model,” *BMC Neuroscience*, vol. 20, no. 1, p. 31, 2019.
 - [22] Z. Cai, J. Huang, H. Luo et al., “Role of glucose transporters in the intestinal absorption of gastrodin, a highly water-soluble drug with good oral bioavailability,” *Journal of Drug Targeting*, vol. 21, no. 6, pp. 574–580, 2013.
 - [23] Y. Lai, R. Wang, W. Li et al., “Clinical and economic analysis of gastrodin injection for dizziness or vertigo: a retrospective cohort study based on electronic health records in China,” *Chinese Medicine*, vol. 17, no. 1, p. 6, 2022.
 - [24] X. Wang, Z. Y. Wang, J. H. Zheng, and S. Li, “TCM network pharmacology: a new trend towards combining computational, experimental and clinical approaches,” *Chinese Journal of Natural Medicines*, vol. 19, no. 1, pp. 1–11, 2021.
 - [25] G. Yu, W. Wang, X. Wang et al., “Network pharmacology-based strategy to investigate pharmacological mechanisms of Zuojinwan for treatment of gastritis,” *BMC Complementary and Alternative Medicine*, vol. 18, no. 1, p. 292, 2018.
 - [26] M. Chu, T. Gao, X. Zhang et al., “Elucidation of potential targets of San-Miao-San in the treatment of osteoarthritis based on network pharmacology and molecular docking analysis,” *Evidence-Based Complementary and Alternative Medicine*, vol. 2022, Article ID 7663212, 13 pages, 2022.
 - [27] W. Dan, J. Liu, X. Guo, B. Zhang, Y. Qu, and Q. He, “Study on medication rules of traditional Chinese medicine against antineoplastic drug-induced cardiotoxicity based on network pharmacology and data mining,” *Evidence-Based Complementary and Alternative Medicine*, vol. 2020, Article ID 7498525, 15 pages, 2020.
 - [28] S. V. Faraone, J. Biederman, and E. Mick, “The age-dependent decline of attention deficit hyperactivity disorder: a meta-analysis of follow-up studies,” *Psychological Medicine*, vol. 36, no. 2, pp. 159–165, 2006.
 - [29] V. Simon, P. Czobor, S. Bálint, Á. Mészáros, and I. Bitter, “Prevalence and correlates of adult attention-deficit hyperactivity disorder: meta-analysis,” *British Journal of Psychiatry*, vol. 194, no. 3, pp. 204–211, 2009.
 - [30] W. Retz, Y. Ginsberg, D. Turner et al., “Attention-deficit/hyperactivity disorder (ADHD), antisociality and delinquent behavior over the lifespan,” *Neuroscience & Biobehavioral Reviews*, vol. 120, pp. 236–248, 2021.
 - [31] A. Gbessemehlan, J. Arsandaux, M. Orri et al., “Perceived stress partially accounts for the association between attention deficit hyperactivity disorder (ADHD) symptoms and suicidal ideation among students,” *Psychiatry Research*, vol. 291, Article ID 113284, 2020.
 - [32] P. Jennum, L. H. Hastrup, R. Ibsen, J. Kjellberg, and E. Simonsen, “Welfare consequences for people diagnosed with attention deficit hyperactivity disorder (ADHD): a matched nationwide study in Denmark,” *European Neuropsychopharmacology*, vol. 37, pp. 29–38, 2020.

- [33] V. Rahi and P. Kumar, "Animal models of attention-deficit hyperactivity disorder (ADHD)," *International Journal of Developmental Neuroscience*, vol. 81, no. 2, pp. 107–124, 2021.
- [34] X. Ye, Y. Wang, J. Zhao et al., "Identification and characterization of key chemical constituents in processed *Gastrodia elata* using UHPLC-MS/MS and chemometric methods," *Journal of Analytical Methods in Chemistry*, vol. 2019, Article ID 4396201, 10 pages, 2019.
- [35] J. C. Martel and S. Gatti McArthur, "Dopamine receptor subtypes, physiology and pharmacology: new ligands and concepts in schizophrenia," *Frontiers in Pharmacology*, vol. 11, p. 1003, 2020.
- [36] M. Li, L. Zhou, X. Sun et al., "Dopamine, a co-regulatory component, bridges the central nervous system and the immune system," *Biomedicine & Pharmacotherapy*, vol. 145, Article ID 112458, 2022.
- [37] C. Liu, P. Goel, and P. S. Kaeser, "Spatial and temporal scales of dopamine transmission," *Nature Reviews Neuroscience*, vol. 22, no. 6, pp. 345–358, 2021.
- [38] T. A. Hegvik, K. Waløen, S. K. Pandey, S. V. Faraone, J. Haavik, and T. Zayats, "Druggable genome in attention deficit/hyperactivity disorder and its co-morbid conditions. New avenues for treatment," *Molecular Psychiatry*, vol. 26, no. 8, pp. 4004–4015, 2021.
- [39] M. Zhou, H. Rebholz, C. Brocia et al., "Forebrain over-expression of CK1 δ leads to down-regulation of dopamine receptors and altered locomotor activity reminiscent of ADHD," *Proceedings of the National Academy of Sciences*, vol. 107, no. 9, pp. 4401–4406, 2010.
- [40] J. W. Buckholtz, M. T. Treadway, R. L. Cowan et al., "Dopaminergic network differences in human impulsivity," *Science*, vol. 329, no. 5991, p. 532, 2010.
- [41] F. ElBaz Mohamed, T. M. Kamal, S. S. Zahra, M. A. H. Khfagy, and A. M. Youssef, "Dopamine D4 receptor gene polymorphism in a sample of Egyptian children with attention-deficit hyperactivity disorder (ADHD)," *Journal of Child Neurology*, vol. 32, no. 2, pp. 188–193, 2017.
- [42] S. Cortese, "The neurobiology and genetics of attention-deficit/hyperactivity disorder (ADHD): what every clinician should know," *European Journal of Paediatric Neurology*, vol. 16, no. 5, pp. 422–433, 2012.
- [43] G. Tripp and J. R. Wickens, "Neurobiology of ADHD," *Neuropharmacology*, vol. 57, no. 7-8, pp. 579–589, 2009.
- [44] K. E. Browman, P. Curzon, J. B. Pan et al., "A-412997, a selective dopamine D4 agonist, improves cognitive performance in rats," *Pharmacology Biochemistry and Behavior*, vol. 82, no. 1, pp. 148–155, 2005.
- [45] M. L. Woolley, K. A. Waters, C. Reavill et al., "Selective dopamine D4 receptor agonist (A-412997) improves cognitive performance and stimulates motor activity without influencing reward-related behaviour in rat," *Behavioural Pharmacology*, vol. 19, no. 8, pp. 765–776, 2008.
- [46] A. Hayward, L. Adamson, and J. C. Neill, "Partial agonism at the $\alpha 7$ nicotinic acetylcholine receptor improves attention, impulsive action and vigilance in low attentive rats," *European Neuropsychopharmacology*, vol. 27, no. 4, pp. 325–335, 2017.
- [47] A. S. Potter, G. Dunbar, E. Mazzulla, D. Hosford, and P. A. Newhouse, "AZD3480, a novel nicotinic receptor agonist, for the treatment of attention-deficit/hyperactivity disorder in adults," *Biological Psychiatry*, vol. 75, no. 3, pp. 207–214, 2014.
- [48] C. Fleisher and J. McGough, "Sofinicine: a novel nicotinic acetylcholine receptor agonist in the treatment of attention-deficit/hyperactivity disorder," *Expert Opinion on Investigational Drugs*, vol. 23, no. 8, pp. 1157–1163, 2014.
- [49] A. Childress and F. R. Sallee, "Pozanicline for the treatment of attention-deficit/hyperactivity disorder," *Expert Opinion on Investigational Drugs*, vol. 23, no. 11, pp. 1585–1593, 2014.
- [50] Y. M. Abd-Elhakim, G. G. Moustafa, N. I. El-Sharkawy, M. M. A. Hussein, M. H. Ghoneim, and M. M. El Deib, "The ameliorative effect of curcumin on hepatic CYP1A1 and CYP1A2 genes dysregulation and hepatorenal damage induced by fenitrothion oral intoxication in male rats," *Pesticide Biochemistry and Physiology*, vol. 179, Article ID 104959, 2021.
- [51] G. Magliocco, A. Thomas, J. Desmeules, and Y. Daali, "Phenotyping of human CYP450 enzymes by endobiotics: current knowledge and methodological approaches," *Clinical Pharmacokinetics*, vol. 58, no. 11, pp. 1373–1391, 2019.
- [52] A. Sharma and J. Couture, "A review of the pathophysiology, etiology, and treatment of attention-deficit hyperactivity disorder (ADHD)," *Annals of Pharmacotherapy*, vol. 48, no. 2, pp. 209–225, 2014.
- [53] J. P. C. Chang, K. P. Su, V. Mondelli, and C. M. Pariante, "Cortisol and inflammatory biomarker levels in youths with attention deficit hyperactivity disorder (ADHD): evidence from a systematic review with meta-analysis," *Translational Psychiatry*, vol. 11, no. 1, p. 430, 2021.
- [54] A. Önder, Ö. Gizli Çoban, and A. Sürer Adanır, "Elevated neutrophil-to-lymphocyte ratio in children and adolescents with attention-deficit/hyperactivity disorder," *International Journal of Psychiatry in Clinical Practice*, vol. 25, no. 1, pp. 43–48, 2021.
- [55] C. L. Marker, M. Stoffel, and K. Wickman, "Spinal G-protein-gated K $^{+}$ channels formed by GIRK1 and GIRK2 subunits modulate thermal nociception and contribute to morphine analgesia," *Journal of Neuroscience*, vol. 24, no. 11, pp. 2806–2812, 2004.
- [56] K. Yamada, Y. Iwayama, T. Toyota et al., "Association study of the KCNJ3 gene as a susceptibility candidate for schizophrenia in the Chinese population," *Human Genetics*, vol. 131, no. 3, pp. 443–451, 2012.
- [57] D. Jeremic, I. Sanchez-Rodriguez, L. Jimenez-Diaz, and J. D. Navarro-Lopez, "Therapeutic potential of targeting G protein-gated inwardly rectifying potassium (GIRK) channels in the central nervous system," *Pharmacology & Therapeutics*, vol. 223, Article ID 107808, 2021.
- [58] S. Djebbari, G. Iborra-Lázaro, S. Temprano-Carazo et al., "G-protein-gated inwardly rectifying potassium (Kir3/GIRK) channels govern synaptic plasticity that supports hippocampal-dependent cognitive functions in male mice," *The Journal of Neuroscience*, vol. 41, no. 33, pp. 7086–7102, 2021.
- [59] F. Soeda, Y. Fujieda, M. Kinoshita, T. Shirasaki, and K. Takahama, "Centrally acting non-narcotic antitussives prevent hyperactivity in mice: involvement of GIRK channels," *Pharmacology, Biochemistry, and Behavior*, vol. 144, pp. 26–32, 2016.
- [60] J. Tarver, D. Daley, and K. Sayal, "Attention-deficit hyperactivity disorder (ADHD): an updated review of the essential facts," *Child: Care, Health and Development*, vol. 40, no. 6, pp. 762–774, 2014.
- [61] V. Salvi, G. Migliarese, V. Venturi et al., "ADHD in adults: clinical subtypes and associated characteristics," *Rivista di Psichiatria*, vol. 54, no. 2, pp. 84–89, 2019.

Research Article

The Inhibitory Effect of Polyphenon 60 from Green Tea on Melanin and Tyrosinase in Zebrafish and A375 Human Melanoma Cells

Mehar Ali Kazi,¹ Reshma Sahito,² Qamar Abbas,³ Sana Ullah,⁴ Abdul Majid,⁵ Abdul Rehman Phull ,^{6,7} Md. Mominur Rahman ,⁸ and Song Ja Kim ⁷

¹Institute of Biochemistry, University of Sindh, Jamshoro 76080, Pakistan

²Department of Zoology, University of Sindh, Jamshoro 76080, Pakistan

³Department of Biology, College of Science, University of Bahrain, Sakhir 32038, Bahrain

⁴Department of Agro-Environmental Sciences, Kyushu University, Fukuoka, Japan

⁵Department of Biochemistry, Shah Abdul Latif University, Khairpur, Pakistan

⁶Department of Food Science and Biotechnology, Gachon University, Gyeonggi-do 13120, Republic of Korea

⁷Department of Biology, Kongju National University, Gongju, Chungnam 32588, Republic of Korea

⁸Department of Pharmacy, Faculty of Allied Health Sciences, Daffodil International University, Dhaka 1207, Bangladesh

Correspondence should be addressed to Abdul Rehman Phull; ab.rehman111@yahoo.com, Md. Mominur Rahman; mominur.ph@diu.edu.bd, and Song Ja Kim; ksj85@kongju.ac.kr

Received 23 May 2022; Revised 22 July 2022; Accepted 12 August 2022; Published 2 September 2022

Academic Editor: Christos Tsagkaris

Copyright © 2022 Mehar Ali Kazi et al. This is an open access article distributed under the Creative Commons Attribution License, which permits unrestricted use, distribution, and reproduction in any medium, provided the original work is properly cited.

Polyphenon 60 (PP60) from green tea has long been used as an antioxidant, anticancer, antimicrobial, and antimutagenic. *Aim of the Study.* To investigate tyrosinase inhibition-related kinetic mechanism and antimelanogenesis potential of PP60. *Materials and Methods.* The effect of PP60 on melanin and tyrosinase was evaluated in A375 melanoma cells and zebrafish embryos. The melanoma cells were treated with 20, 40, and 60 $\mu\text{g}/\text{mL}$ of PP60, and tyrosinase expression was induced by using L-DOPA. The western blot method was used for the evaluation of tyrosinase expression. Cell lysates were prepared from treated and untreated cells for cellular tyrosinase and melanin quantification. Furthermore, zebrafish embryos were treated with 20, 40, and 60 $\mu\text{g}/\text{mL}$ of PP60 and reference drug kojic acid for determination of depigmentation and melanin quantification. *In vitro* assays were also performed to examine the impact of PP60 on mushroom tyrosinase activity. To determine cytotoxicity, MTT was used against melanoma cell line A375. *Results.* PP60 showed good tyrosinase inhibitory activity with an IC_{50} value of $0.697 \pm 0.021 \mu\text{g}/\text{mL}$ as compared to kojic acid a reference drug with an IC_{50} value of $2.486 \pm 0.085 \mu\text{g}/\text{mL}$. Kinetic analysis revealed its mixed type of inhibition against mushroom tyrosinase. In addition, western blot analysis showed that at 60 $\mu\text{g}/\text{mL}$ dose of PP60 significantly reduced L-DOPA-induced tyrosinase expression in melanoma cells. PP60 significantly inhibits the cellular tyrosinase ($p < 0.05$) and reduces the melanin ($p < 0.05$) contents of melanoma cells. Furthermore, PP60 was found to be very potent in significantly reducing the zebrafish embryos' pigmentation ($p < 0.05$) and melanin ($p < 0.05$) content at the dose of 60 $\mu\text{g}/\text{mL}$. *Conclusions.* Our results demonstrate that PP60 has a strong potency to reduce pigmentation. It may be useful for the cosmetic industries to develop skin whitening agents with minimal toxic effects.

1. Introduction

In addition to protecting the skin from radiation, melanin is also accountable for the color of the skin, eyes, and hair [1]. In Human skin melasma, senile lentiginos, freckles, birthmarks, ephelides, nevus, and pigmented acne scars are developed due to the accumulation of excess amount of

melanin [2]. In melanocytes, the tyrosinase enzyme regulates the creation of melanin. Melanocytes reside in the epidermis (basal layer) [3].

Tyrosinase inhibitors are important in the fight against excessive melanin synthesis since it is the principal enzyme involved in speeding up the process of melanin synthesis [4]. On the other hand, because free radicals may also promote

melanin synthesis, different natural and synthetic antioxidant systems can scavenge such radicals that might regulate excessive melanin formation [5, 6].

Membrane-bound copper-containing glycoprotein, tyrosinase governs the two reactions, which are most essential in the formation of melanin, the monophenol to o-diphenols of ortho hydroxylation and the o-quinones corresponding oxidation. The Melanin (eumelanin and pheomelanin) production pathway in melanosomes has two steps. The first step of melanogenesis starts with tyrosine oxidation to dopaquinone catalyzed by tyrosinase, this first step is rate-limiting, and all other reactions proceed spontaneously at optimum pH. After dopaquinone formation by tyrosinase, the compound is converted to dopa and dopachrome through auto-oxidation [7].

The enzyme tyrosinase is found in fungi, plants, and mammals in abundance [8]. Melanin is a pigment that affects the color of the skin based on its type, quantity, and distribution in keratinocytes. Melanogenesis is initiated by the hydrolysis of L-tyrosine to L-dihydroxyphenylalanine (L-DOPA) followed by oxidation to DOPA quinone [9]. These reactions are catalyzed by tyrosinase. Subsequently, after a series of oxidation-reduction reactions, melanin is synthesized [10]. Tyrosinase thus plays a significant role in melanogenesis and it is a very likely target of the skin pigmentation studies performed globally [10].

Literature has reported tyrosinase as the most significant and crucial contributor to the deterioration and short half-life of fruits and vegetables during the postharvest period [11]. As a result, tyrosinase inhibitors have been of great interest to several researchers.

Natural products of herbal origin have been gaining interest among scientists in recent years for their disease prevention and health promotive roles [12–15]. Polyphenols are a class of bioactive chemicals found in fruits, vegetables, and tea [16, 17]. Tea contains a wide range of substances, particularly polyphenols, and several studies have demonstrated that these substances lower the risk of a number of illnesses. In terms of natural polyphenols, green tea extract is the most abundant source [18, 19]. Polyphenols in green tea have been extensively studied for their potential benefits, such as antibacterial, antimutagenic, and anticancer properties [20]. To the best of our knowledge, the inhibitory action of polyphenon 60 (PP60) from green tea on melanin synthesis has not been described hitherto. In the present work, PP60 in green tea has been shown to suppress melanogenesis both in the A375 melanoma cells and zebrafish embryos.

2. Material and Methods

2.1. Antityrosinase Activity Assay. The antityrosinase activity against mushroom tyrosinase (Sigma Chemical, USA) was conducted as described before [21]. Each microplate a well-contained reaction mixture comprised of tyrosinase (30 U/mL), phosphate buffer (20 mM, pH 6.8), and PP60 sample. The test plate was incubated at 25°C for 10 min. After preincubation, 20 μ L of L-DOPA (0.85 mM, Sigma Chemicals, USA) was poured into every well and incubated further

for 20 min at similar conditions. With the help of an optimal tunable microplate reader (Sunnyvale, CA, USA), the dopachrome absorbance was measured at 475 nm. The phosphate buffer and kojic acid were used as a negative and positive control, respectively. The potential of PP60 inhibition was stated as the percentage of inhibition in activity. Whereas IC₅₀ was calculated as the amount of PP60 required to produce 50% inhibition in enzyme activity. All the concentrations were tested thrice. With the GraphPad prism, the IC₅₀ values were calculated. The following equation was used to compute the tyrosinase inhibition %:

$$\text{Tyrosinase inhibition (\%)} = \left[\frac{B - S}{B} \right] \times 100. \quad (1)$$

In the above, the *B* is for the blank, and *S* is for the absorbance of sample.

2.2. Kinetics of Tyrosinase Inhibition. PP60 activity for tyrosinase inhibition was studied in a series of tests. PP60 concentrations were 0, 25, 5, 1, and 2 μ g/mL. L-DOPA concentrations ranged from 0.0625 to 2 mM. The method was similar to the mushroom tyrosinase inhibition test methodology. The starting linear component of optical density was evaluated up to five minutes following enzyme addition at 30 s intervals. Lineweaver–Burk plots were used to determine the enzyme's inhibition type. To estimate the EI dissociation constant, 1/*V* was determined, whereas to determine the ESI dissociation constant, intercept against inhibitor concentrations was used.

2.3. Human A375 Melanoma Cell Culture. The cells (A375 melanoma cell) were provided by the Korean Cell Line Bank (KCLB) and cultured in DMEM with 10% heat-inactivated FBS (fetal bovine serum), 50 μ g/mL (streptomycin), and 50 μ /ml (penicillin). Incubation in a humidified CO₂ incubator (95% O₂, 5% CO₂) at 37°C was done with cells seeded at a concentration of 2 \times 10⁵ per ml in cell culture dishes (35 mm) for Western blotting and 96-well plates for MTT cell viability assays. After two days, the medium was refreshed, and the same protocol was followed for cell culturing until 70–75% confluence was achieved. Similarly, in a new medium, cells were allowed to develop to 70–75% confluence.

2.4. Cell Viability Assay. MTT test was used for cell viability assessment. The A375 cells were seeded in 96-well plates and treated to varying doses (0–70 μ g/mL) of PP60 for 24 hours at 37°C under CO₂. Afterward, ten microliters of MTT reagent (0.5 μ g/mL) were added to each well for four hours to create purple formazan crystals. Once the formazan crystals were formed, 100 μ L of MTT reagent 2 (Solubilization buffer; 10% SDS with 0.01 N HCl and DMSO solution) was added, followed by overnight incubation in a CO₂ incubator. At last, optical density at 595 nm was measured with an OPTIMax microplate reader (Sunnyvale, CA, USA). The experiment was performed three times.

2.5. Western Blotting. A375-melanoma cells were mixed for 24 hours with 20, 40, or 60 $\mu\text{g}/\text{mL}$ PP60 with or without 50 mM L-DOPA to induce tyrosinase expression. The cells were rinsed with cold 1X PBS twice, harvested and protein was extracted with radioimmunoprecipitation assay buffer (50 mM tris HCl, 150 mM NaCl, pH 7.4, 0.1% SDS, and 1% Nonidet P-40) along with protease and phosphatase inhibitors. An 8% SDS-polyacrylamide gel was used to separate equal amounts of proteins. The size-fragmented proteins were carefully transferred to nitrocellulose membranes and labeled for 3 minutes. They were then rinsed with 1X Tris-buffered saline/tween-20 (TBST-20) for 5 minutes and blocked for 1 hour in blocking buffer and 5% nonfat dried skim milk in TBST-20. After three 1 X TBST washes (30 min), upon incubation with primary antibodies for 24 hours at 4°C, membranes were rinsed and incubated for 3 hours with a 1 : 2000 dilution of horseradish peroxidase-conjugated secondary antibody followed by a second experiment the next day. In addition, the membranes were then rinsed thrice with 1X TBST and developed using a chemiluminescence kit (DOGEN, Seoul, Korea). The ImageJ program measured resolved bands for Windows (version 1.46r; NIH, USA). The protein GAPDH was used as a load check.

2.6. Cellular Tyrosinase Activity Assay. Cellular tyrosinase activity assay was performed by adopting the repeating approach [22]. The A375 cells were maintained and grown at the concentration of 1×10^4 cells in 35 mm culture dishes. Then, cells were exposed to PP60 (20, 40, and 60 $\mu\text{g}/\text{mL}$) and L-DOPA (50 mM) for 72 hours. The cells were washed twice with PBS and lysed using radioimmunoprecipitation assay buffer. The collected supernatants were incubated afterward at 37°C with 5 μL of L-DOPA substrate solution for 1 hour. The tyrosinase activity of PP60 was measured through a well-plate reader (OPTIMax Tunable, Sunnyvale, CA, USA).

2.7. Assay of Melanin Contents on Melanoma Cells. The repeated approach of Lee et al., [22] was used to assess melanoma melanin content. The A375 cells were grown at the concentration of 1×10^4 cells in 35 mm cell culture dishes. The impact of PP60 on melanin content was studied in cells by exposing to 0 to 60 $\mu\text{g}/\text{mL}$ of PP60 for 72 hours. After the predetermined treatment of PP60, the cells were harvested and collected in PCR tubes at the speed of 1000 rpm for 10 minutes. Afterward, the pellet was dissolved in a solution of 1 N NaOH for 90 minutes at 60°C. A microplate reader measured the absorbance of the supernatant at 450 nm (OPTIMax Tunable, Sunnyvale, CA, USA).

2.8. The In Vivo Zebrafish Assay of Depigmentation. The *in vivo* depigmentation approach in zebrafish was conducted through a previously reported slightly modified method [23].

2.8.1. Zebrafish Husbandry. The animals were obtained from a commercial vendor and acclimatized for a month at $28 \pm 2^\circ\text{C}$ with a photoperiod of 14 h light and 10 h dark.

Fresh brine shrimp larvae and dry food were provided twice a day. The fish were kept alive through chemico-biological, mechanical filtration, and aeration. Induced spawning was produced in the presence of light in the morning. All procedures were performed according to the principles of laboratory animal care (NIH publication 85-23, revised 1985), and Kongju National University's Institutional Review Board approved the study (IRB number 2011-2). The collection of embryos took 30 minutes.

2.8.2. PP60 Treatment and Phenotype-Based Evaluation. In 200 μL of E3 medium (Sodium chloride 5 mM, KCl 0.17 mM, CaCl_2 0.33 mM, Magnesium sulfate 0.33 mM), 2-3 synchronized embryos were pipetted per well into 96-well plates. After fertilization, they were exposed to the E3 medium for 9 to 72 hours, totaling 63 hours. Kojic acid was used as a positive control. With the stereomicroscope (SMZ745T, Nikon, Japan), anesthesia was administered to embryos with dechorionated cell bodies using tricaine methanesulfonate (150 mg/L) solution (Sigma, Chemicals, USA). ImageJ software was used to measure pixels (National Health Institution of USA).

2.9. Identification of Melanin Contents from Zebrafish. The approach of and Baek et al. [1, 24] over *in vivo* depigmentation of zebrafish embryos was used in this study. The total synchronized 20 embryos were mixed with 20, 40, and 60 $\mu\text{g}/\text{mL}$ of PP60, and the reference medication was 3 mL of kojic acid in E3 medium. In tricaine MS-222 solution, the embryos were anesthetized at 72 hours post fertilization. After anesthesia, the embryos were washed thrice in an E3 medium. Additionally, both untreated and treated embryo eyes were removed. A homogenized embryo extract (pellet) was then prepared via centrifugation and homogenization. Analyzing the absorbance at 405 nm in comparison to a synthetic melanin standard curve allowed us to determine the melanin content. All experiments were performed in triplicate.

2.10. Statistical Analysis. With the Statistical Package for Social Sciences (SPSS version 16.0 Inc. Chicago, Illinois, USA), data were analyzed by one-way analysis of variance (ANOVA). A posthoc Tukey-Kramer test was used when the normality test failed the Ranks test. The value difference, $p < 0.05$ was considered statistically significant.

3. Results and Discussion

Skin pigmentation is an ever-vibrant field of research around the globe and the multimillion-dollar cosmetic industry has undergone a tremendous surge in its research and development sector. This has led to a staggering rise in the variety of skin products available in the market [9, 25]. There has been a great interest in the use of plant extracts and compounds isolated from natural sources including secondary metabolites, i.e., polyphenols to investigate new bioactive compounds targeting melanin production [26]. Tyrosinase

enzyme along with TRP-1 and 2 proteins are the key players in the melanogenesis pathway and these can be easy targets for drug candidates affecting pigmentation. The suppression of this enzyme and the proteins is a highly effective way to decrease melanin synthesis [27].

3.1. Antityrosinase Activity Assay. The antityrosinase inhibitory potential of PP60 was evaluated using an *in vitro* assay. For the determination IC_{50} value, different doses of PP60 ranging from 0 to 10 $\mu\text{g}/\text{mL}$ were used in the experiment. According to the results, PP60 possessed a very competitive inhibition counter to that of mushroom tyrosinase exhibiting an IC_{50} value of $0.697 \pm 0.021 \mu\text{g}/\text{mL}$ compared to kojic acid with an IC_{50} value of $2.486 \pm 0.085 \mu\text{g}/\text{mL}$. The larger quantity of catechin in PP60 reported by Jung et al. [28] showed the therapeutic benefit of PP60 on acne, it may be due to the participation of catechins in tyrosinase inhibition. Tyrosinase catalyzes the conversion of tyrosine to L-DOPA which finally converts to DOPA quinone. Thus, most skin-lightening treatments block tyrosinase to reduce melanogenesis. The antioxidative ability of tea polyphenols has been partially credited with the potential health advantages linked with tea drinking. Green tea has recently been linked to improved overall antioxidative status and protection against oxidative damage in humans when ingested as part of a balanced, regulated diet [1].

3.2. Kinetic Study. The manner of PP60 inhibition against mushroom tyrosinase was studied kinetically (Table 1). By measuring EI and ESI constants, PP60 was tested for its ability to inhibit the free enzyme and the enzyme-substrate complex. Figure 1 shows the Lineweaver–Burk plot of $1/V$ versus $1/[\text{L-DOPA}]$ at various PP60 concentrations, which exhibits a succession of straight lines (A). PP60 intersected the second quadrant in Figure 1(a). In the rising PP60 concentrations, the decrease of V_{max} occurred with the increase of K_m . PP60 inhibits tyrosinase in two ways: by competitively creating enzyme inhibitor complexes and noncompetitively interrupting enzyme-substrate inhibitor complexes. Secondary slope vs. PP60 concentration plots indicated EI dissociation constants K_i Figure 1(b), whereas secondary intercept versus PP60 concentration plots gave ESI dissociation constants K_i' Figures 1(b) and 1(c). The smaller the K_i than K_i' indicated better enzyme-PP60 binding and so favored competitive over noncompetitive mechanisms (Table 1).

3.3. Cellular Viability Results of PP60. The cellular viability (MTT assay) was performed for the detection of the cellular toxicity of PP60 targeting A375 cells. The A375 melanoma cells were evaluated for 24 h with different concentrations (0–70 $\mu\text{g}/\text{mL}$). The results confirmed the noncytotoxicity of PP60 compared to those of control (Figure 2). However, an insignificant decrease in cell viability was demonstrated by PP60 in a concentration dependent manner as shown in Figure 2. The cells with no treatment of PP60 were supposed to be 100% viable.

3.4. PP60 Decreases the Expression of the Enzyme Tyrosinase. In western blots, tyrosinase enzyme expression was assessed. PP60 was applied to A375 melanoma cells at 0, 20, 40, and 60 $\mu\text{g}/\text{mL}$ to examine how it affects tyrosinase activity. Tyrosinase expression was induced with L-DOPA. Results showed the significant induction of tyrosinase expression (4.39 fold, $p < 0.001$) in L-DOPA treated cells (Figure 3) compared to normal control. Most significant ($p < 0.001$) inhibition of tyrosinase expression occurred at the dose of 60 $\mu\text{g}/\text{mL}$ in comparison to L-DOPA enhanced expression, while moderate significant ($p < 0.05$) reduction of tyrosinase expressions were found at the 20 and 40 $\mu\text{g}/\text{mL}$ (Figures 3(a) and 3(b)). Inhibiting melanin formation has two basic modes of action. First, it suppresses the tyrosinase enzyme activity *in vitro*, and then it reduces tyrosinase protein levels in cells. Hydroxyquinone, arbutin, and kojic acid are examples of the first technique [29]. However, many medications work by blocking tyrosinase expression in cells [30]. However, our data indicated that PP60 inhibits both expressions of tyrosinase in L-DOPA-induced cells and *in vitro* enzyme activity against mushroom tyrosinase.

3.5. Results of PP60 Effect on Cellular Tyrosinase from A375 Melanoma Cells. The PP60 effect on the activity of cellular tyrosinase was analyzed; the lysates of the cells were prepared from the A375 melanoma cells, mixed for 72 h with 20, 40, and 60 $\mu\text{g}/\text{mL}$ of PP60 and 50 μM of L-DOPA. The results showed the significant downregulation of cellular tyrosinase at the concentration of 60 $\mu\text{g}/\text{mL}$ PP60 compared to control and L-DOPA exposed cells. The above results together with these results (Figure 4.) consistent with that PP60 have both modes of inhibition of tyrosinase indirect *in vitro* and in cells.

3.6. Melanin Content from Melanoma Cells. In the Mammalian skins, melanin contributes a pivotal role in color determination. The effects of PP60 as well as L-DOPA and varying concentration ranges of PP60, on melanin, were examined in the melanoma cells. For the 3 days of treatment with 50 μM of L-DOPA, a significant ($p < 0.05$, Figure 5) increase was determined. PP60 decreased the melanin contents significantly as the concentration of PP60 increased; also, the prominent decrease was investigated at 60 $\mu\text{g}/\text{mL}$ compared to L-DOPA treated with the control cells. As Figure 5 indicates that melanin content from melanoma cells matched with the tyrosinase inhibitory activities of 60 $\mu\text{g}/\text{mL}$ of PP60, it might be melanin downregulation due to the inhibition of tyrosinase. The melanin activity of the 95% tea ethanolic extracts was higher *in vitro*. This occurrence might be explained by the extract's increased concentration of antioxidant chemicals, including natural plant polyphenols. [31].

3.7. PP60 Reduces the Melanogenesis in Zebrafish Embryos. It is very important to study zebrafish as a vertebrate model for its similar gene sequence to humans [32]. Because of these similar and beneficial gene sequences, through *in vivo*

TABLE I: The kinetic parameters of the L-DOPA activity of mushroom tyrosinase, in the presence of different concentrations of PP60.

Dose ($\mu\text{g/mL}$)	V_{max} ($\Delta\text{A/Sec}$)	K_m inhibition (mM) type	K_i ($\mu\text{g/mL}$)	K_i' ($\mu\text{g/mL}$)
0.00	4.891×10^{-6}	0.043		
0.25	4.848×10^{-6}	0.161		
0.5	3.727×10^{-6}	0.181 mixed	1.125	11.35
1.0	3.599×10^{-6}	0.204		
2.0	3.333×10^{-6}	0.235		

V_{max} , K_m , and K_i are equal to reaction velocity, Michaelis–Menten constant, and El dissociation constant, respectively.

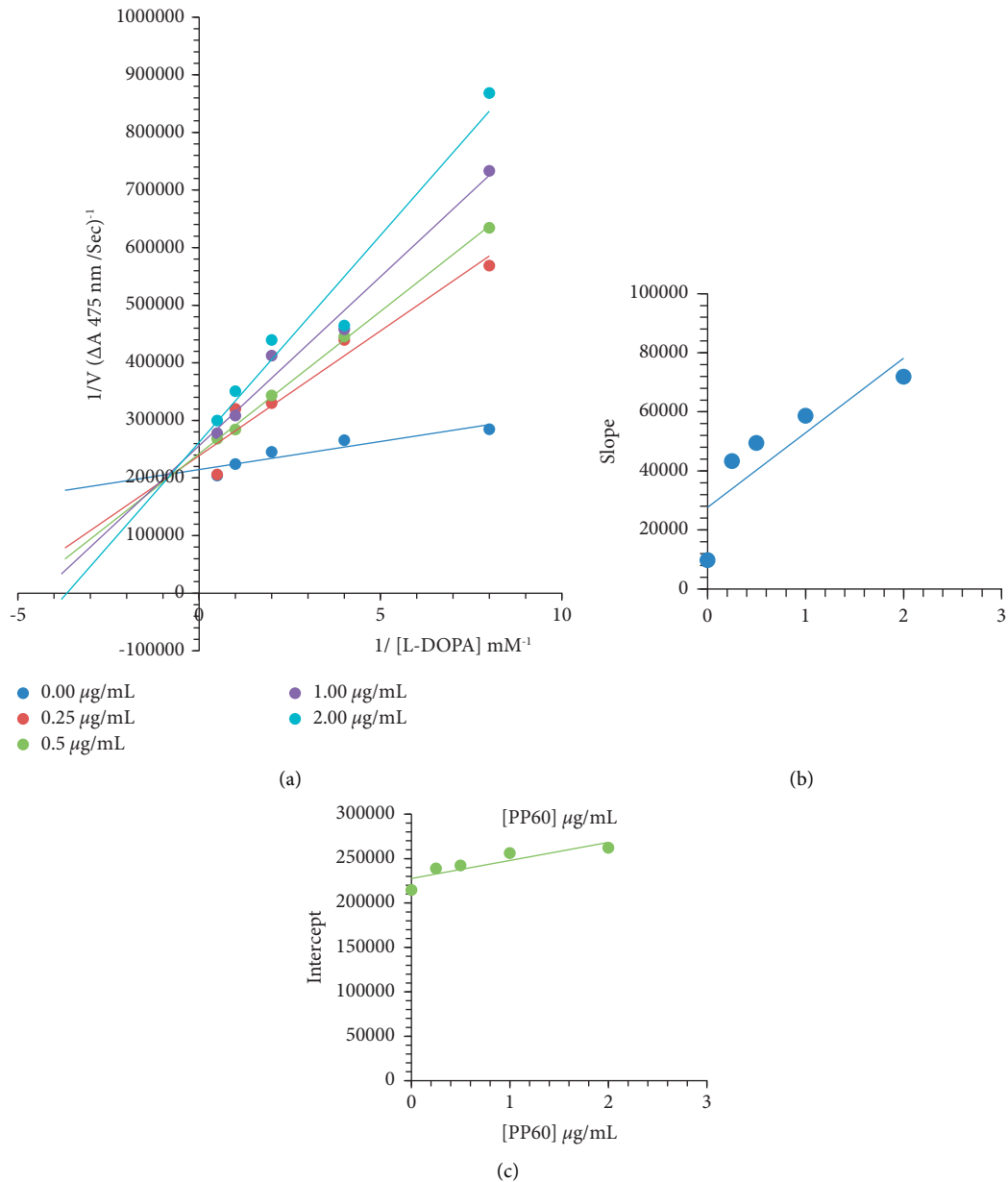


FIGURE 1: A plot of the Lineweaver–Burk plot for tyrosinase inhibition of PP60. (a) Accordingly, the concentrations of PP60 were 0, 0.25, 0.5, 1.0, and 2.0 $\mu\text{g/mL}$. The L-DOPA concentrations of the subjects were, respectively, 0.0625, 0.125, 0.25, 0.5, 1, and 2 mM. The insets (b) and (c) are plots of slopes and of vertical intercepts versus various doses of PP60 to evaluate inhibition constants. Using the least square fit with linear least squares, the lines were drawn.

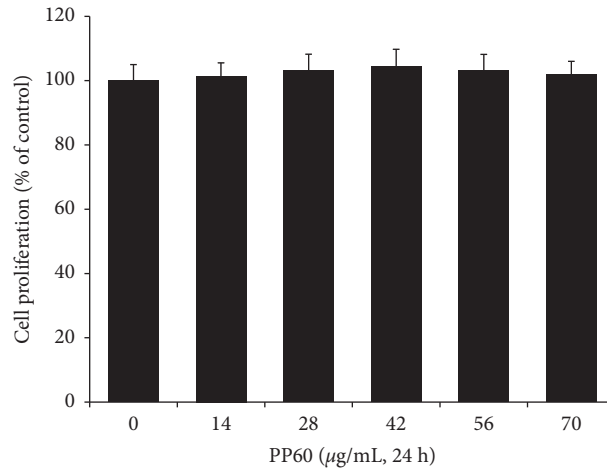


FIGURE 2: The cell viability of PP60 was evaluated by treating A375 melanoma cells for 24 hours with various concentrations and examining cytotoxicity using the viability assay kit. All of the results and values are represented as the average of triplicate experiments with standard deviation.

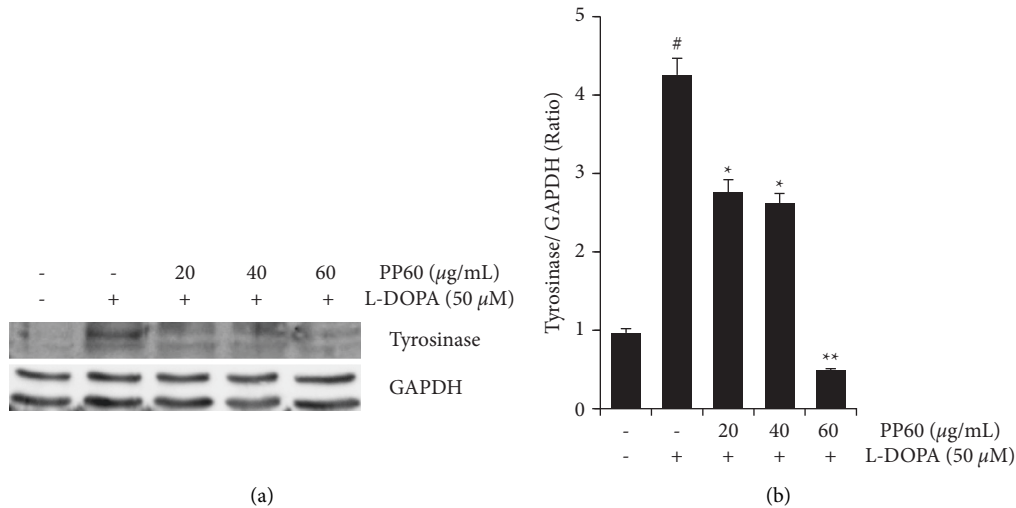


FIGURE 3: The protein expression of the enzyme tyrosinase was analyzed in comparison with GAPDH on the A375 melanoma cell line. The cells (a, b) were targeted to different L-DOPA concentrations with and without (20, 40, and 60 g/mL) of PP60 for 24 hours. From the western blot analysis, the appearance of tyrosinase was clarified with the help of GAPDH as a loading control. The differences were considered significant at the level of # $p < 0.001$ for L-DOPA induced in comparison to normal control and * $p < 0.05$, ** $p < 0.001$ PP60 inhibited tyrosinase expressions in comparison to L-DOPA induced.

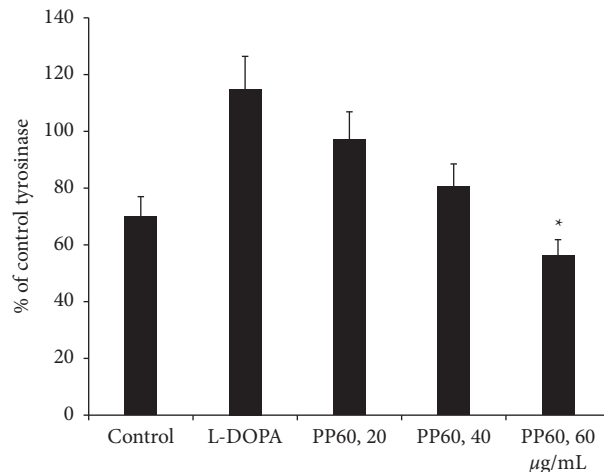


FIGURE 4: The PP60 was evaluated against the cellular tyrosinase. The cells of A375 of melanoma were evaluated with ranges of concentration from 20, 40, and 60 µg/mL of PP60 along with 50 mM L-DOPA for tyrosinase induction. * $p < 0.05$; values expressed as a % control.

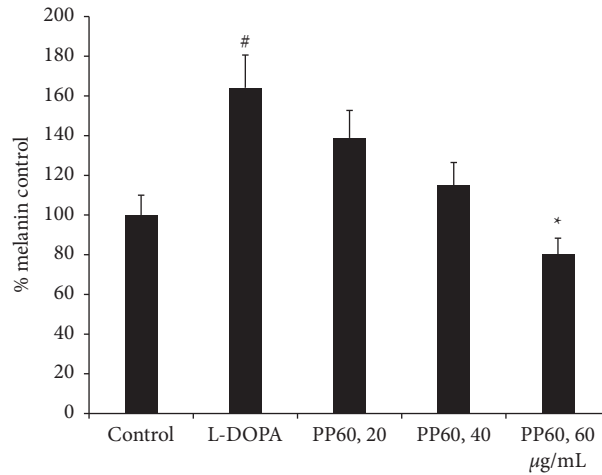


FIGURE 5: PP60 effect against melanin assay was studied. PP60 was added in varying concentrations to A375 melanoma cells, 20, 40, and 60 $\mu\text{g/mL}$. Percentage values are shown as % control. # Showed significantly higher melanin compared to control ($p < 0.01$), while * representing PP60 mediated reduction in melanin compared to L-DOPA group ($p < 0.05$).

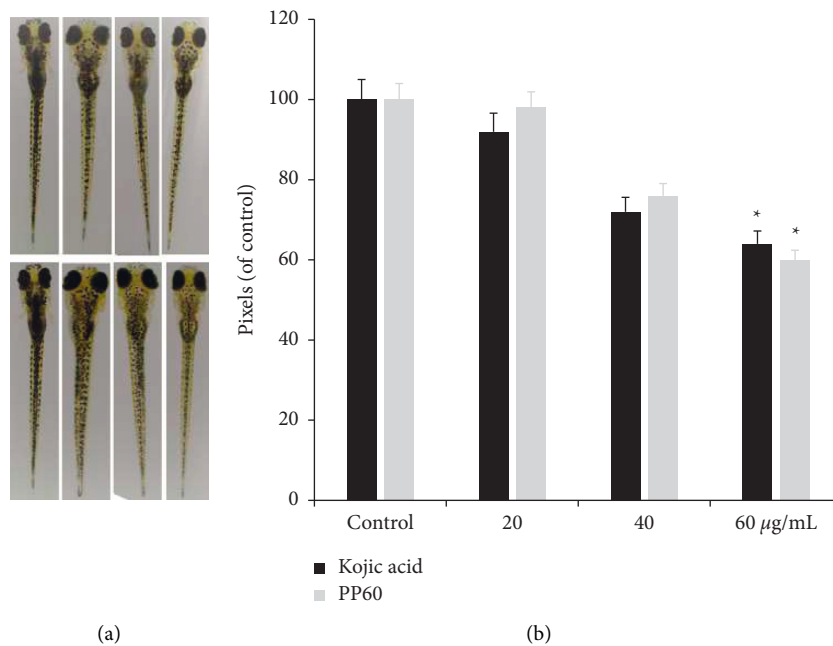


FIGURE 6: The depigmentation effect of PP60 on zebrafish. Positive control, kojic acid, and embryos treated with sample PP60 at 20, 40, and 60 $\mu\text{g/mL}$. (a) Representative picture of the pigmentation levels of zebrafish treated with PP60 and kojic acid. (b) Pixel comparison of PP60's and koji acid's depigmenting effect at the level of $*p < 0.05$.

assays of zebrafish embryos, we determined the potency of PP60's depigmentation ability. The inhibition effects of PP60 on zebrafish pigmentation were studied using PP60 at different concentrations (20, 40, and 60 $\mu\text{g/mL}$) as well as kojic acid at the same concentration as the positive control. Figure 6(a) shows a significant decrease in pigment level among zebrafish ($p < 0.05$) while Figure 6(b) shows a reduction of 36% in pigmentation with 60 $\mu\text{g/mL}$ kojic acid (positive control). Phenolic compounds are well-known for their wide array of biological functions [33, 34] and antioxidant polyphenols in green tea are well-known for quenching free radicals [35]. Reactive oxygen species (ROS)

scavenging and interfacing with melanogenic regulators have been shown to have antimelanoma properties in the literature [22].

3.8. Effect of PP60 on Zebrafish Melanin Contents. The content of melanin was determined from zebrafish embryos. There is a significant reduction of melanin occurs ($p < 0.05$) when 60 $\mu\text{g/mL}$ of PP60 is added to the Zebrafish embryos compared to control kojic acid (a reference drug). Melanin contents moderately decreased in the kojic acid-treated embryos, while PP60 decreased the melanin more than the

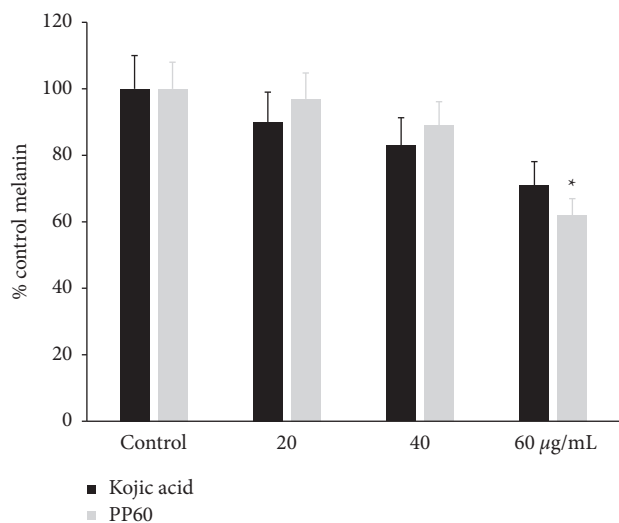


FIGURE 7: The PP60 and its effect on melanin contents were measured using embryos of the zebrafish. The positive control kojic acid together with the embryos of the zebrafish was evaluated with 20, 40, and 60 $\mu\text{g/mL}$ of PP60. Percentages of control are presented. * $p < 0.05$.

kojic acid (Figure 7). As early as 28 hpf, the first zebrafish larval melanocytes begin to develop, and by 60 hpf, 460 postmitotic melanocytes are contributing to the formation of the pigment pattern [36]. There is a strong correlation between the decrease in melanin concentration and the loss of dendritic morphology [37].

4. Conclusions

The current study demonstrated that PP60 possesses a remarkable capacity to inhibit tyrosinase activity both competitively and noncompetitively. Moreover, PP60 also inhibited melanin synthesis in melanoma cell lines as well as in zebrafish embryos. At a concentration of 60 $\mu\text{g/mL}$, PP60 caused a significant decrease in melanin synthesis in the melanoma cells as well as inhibition of tyrosinase activity. The results were further confirmed by the findings of western blot analysis. The tyrosinase inhibition and, subsequently, the pigmentation lowering activity of PP60 was assessed in vitro followed by in vivo examination. The toxicity profile of PP60 was also evaluated, and the results of cell viability revealed no cytotoxicity against A375 melanoma cells and the zebrafish. This further confirmed the selective action of PP60 and adds sustenance to the possibility of developing minimally cytotoxic antimelanogenic drugs.

Data Availability

The data used to support the findings of this study are available from the corresponding author upon request.

Conflicts of Interest

The authors declare no conflicts of interest.

Acknowledgments

This project was supported by National Research Foundation (2020R111A3B306969912).

References

- [1] S. H. Baek and S. H. Lee, "Sesamol decreases melanin biosynthesis in melanocyte cells and zebrafish: possible involvement of MITF via the intracellular cAMP and p38/JNK signalling pathways," *Experimental Dermatology*, vol. 24, no. 10, pp. 761–766, 2015.
- [2] R. K. Tripathi, V. J. Hearing, K. Urabe, P. Aroca, and R. A. Spritz, "Mutational mapping of the catalytic activities of human tyrosinase," *Journal of Biological Chemistry*, vol. 267, no. 33, pp. 23707–23712, 1992.
- [3] S. Parvez, M. Kang, H. S. Chung et al., "Survey and mechanism of skin depigmenting and lightening agents," *Phytotherapy Research*, vol. 20, no. 11, pp. 921–934, 2006.
- [4] S. Ullah, Y. C. Chung, and C.-G. Hyun, "Induction of melanogenesis by fosfomycin in B16F10 cells through the upregulation of P-JNK and P-p38 signaling pathways," *Antibiotics*, vol. 9, no. 4, p. 172, 2020.
- [5] Y.-J. Liu, J.-L. Lyu, Y.-H. Kuo, C.-Y. Chiu, K.-C. Wen, and H.-M. Chiang, "The anti-melanogenesis effect of 3, 4-dihydroxybenzalacetone through downregulation of melanosome maturation and transportation in B16F10 and human epidermal melanocytes," *International Journal of Molecular Sciences*, vol. 22, no. 6, p. 2823, 2021.
- [6] M. Ahmed, A. R. Phul, I. U. Haq et al., "Antioxidant, anticancer and antibacterial potential of Zakhm-e-hayat rhizomes crude extract and fractions," *Pakistan Journal of Pharmaceutical Sciences*, vol. 29, no. 3, pp. 895–902, 2016.
- [7] Z. Ashraf, M. Rafiq, S.-Y. Seo, K. S. Kwon, M. M. Babar, and N. S. Sadaf Zaidi, "Kinetic and in silico studies of novel hydroxy-based thymol analogues as inhibitors of mushroom tyrosinase," *European Journal of Medicinal Chemistry*, vol. 98, pp. 203–211, 2015.
- [8] S.-Y. Seo, V. K. Sharma, and N. Sharma, "Mushroom tyrosinase: recent prospects," *Journal of Agricultural and Food Chemistry*, vol. 51, no. 10, pp. 2837–2853, 2003.
- [9] Q. Abbas, H. Raza, M. Hassan, A. R. Phull, S. J. Kim, and S. Y. Seo, "Acetazolamide inhibits the level of tyrosinase and melanin: an enzyme kinetic, in vitro, in vivo, and in silico studies," *Chemistry and Biodiversity*, vol. 14, no. 9, p. 375, Article ID e1700117, 2017.
- [10] M. N. Masum, K. Yamauchi, and T. Mitsunaga, "Tyrosinase inhibitors from natural and synthetic sources as skin-lightening agents," *Reviews in Agricultural Science*, vol. 7, no. 0, pp. 41–58, 2019.
- [11] S. Ullah, J. Akter, S. J. Kim et al., "The tyrosinase-inhibitory effects of 2-phenyl-1, 4-naphthoquinone analogs: importance of the (E)- β -phenyl- α , β -unsaturated carbonyl scaffold of an endomethylene type," *Medicinal Chemistry Research*, vol. 28, no. 1, pp. 95–103, 2019.
- [12] R. Sharma, P. Bedarkar, D. Timalisina, A. Chaudhary, and P. K. Prajapati, "Bhavana, an ayurvedic pharmaceutical method and a versatile drug delivery platform to prepare potentiated micro-nano-sized drugs: core concept and its current relevance," *Bioinorganic Chemistry and Applications*, vol. 2022, Article ID 1685393, 15 pages, 2022.
- [13] R. Sharma, P. Kakodkar, A. Kabra, and P. K. Prajapati, "Golden ager Chyawanprash with meager evidential base from human clinical trials," *Evidence-Based Complementary*

- and Alternative Medicine*, vol. 2022, Article ID 9106415, 6 pages, 2022.
- [14] R. Sharma and N. Martins, "Telomeres, DNA damage and ageing: potential leads from ayurvedic rasayana (Anti-Ageing) drugs," *Journal of Clinical Medicine*, vol. 9, no. 8, p. 2544, 2020.
- [15] R. Sharma and P. K. Prajapati, "Predictive, preventive and personalized medicine: leads from ayurvedic concept of Prakriti (human constitution)," *Current Pharmacology Reports*, vol. 6, pp. 441–450, 2020.
- [16] T. Mann, W. Gerwat, J. Batzer et al., "Inhibition of human tyrosinase requires molecular motifs distinctively different from mushroom tyrosinase," *Journal of Investigative Dermatology*, vol. 138, no. 7, pp. 1601–1608, 2018.
- [17] Q. Abbas, M. Saleem, A. R. Phull et al., "Green synthesis of silver nanoparticles using *Bidens frondosa* extract and their tyrosinase activity," *Iranian Journal of Pharmaceutical Research*, vol. 16, no. 2, pp. 763–770, 2017.
- [18] B. Frei and J. V. Higdon, "Antioxidant activity of tea polyphenols in vivo: evidence from animal studies," *Journal of Nutrition*, vol. 133, no. 10, pp. 3275S–3284S, 2003.
- [19] S. Ullah and C.-G. Hyun, "Evaluation of total flavonoid, total phenolic contents, and antioxidant activity of strychnobiflavone," *Indonesian Journal of Chemistry*, vol. 20, no. 3, pp. 716–721, 2019.
- [20] D. Shah, M. Gandhi, A. Kumar, N. Cruz-Martins, R. Sharma, and S. Nair, "Current insights into epigenetics, noncoding RNA interactome and clinical pharmacokinetics of dietary polyphenols in cancer chemoprevention," *Critical Reviews in Food Science and Nutrition*, vol. 26, pp. 1–37, 2021.
- [21] M. Rafiq, Y. Nazir, Z. Ashraf et al., "Synthesis, computational studies, tyrosinase inhibitory kinetics and antimelanogenic activity of hydroxy substituted 2-[(4-acetylphenyl) amino]-2-oxoethyl derivatives," *Journal of Enzyme Inhibition and Medicinal Chemistry*, vol. 34, no. 1, pp. 1562–1572, 2019.
- [22] J. Lee, S. Lee, B. Lee, K. Roh, D. Park, and E. Jung, "Development of tyrosinase promoter-based fluorescent assay for screening of anti-melanogenic agents," *Biological and Pharmaceutical Bulletin*, vol. 38, pp. b15–00305, 2015.
- [23] W.-C. Chen, T.-S. Tseng, N.-W. Hsiao et al., "Discovery of highly potent tyrosinase inhibitor, TI, with significant anti-melanogenesis ability by zebrafish in vivo assay and computational molecular modeling," *Scientific Reports*, vol. 5, no. 1, pp. 7995–7998, 2015.
- [24] K.-D. Hsu, H.-J. Chen, C.-S. Wang et al., "Extract of *Ganoderma formosanum* mycelium as a highly potent tyrosinase inhibitor," *Scientific Reports*, vol. 6, no. 1, pp. 32854–32859, 2016.
- [25] F. B. Pimentel, R. C. Alves, F. Rodrigues, and M. B. Oliveira, "Macroalgae-derived ingredients for cosmetic industry—an update," *Cosmetics*, vol. 5, no. 1, 2017.
- [26] Y. Qi, J. Liu, Y. Liu et al., "Polyphenol oxidase plays a critical role in melanin formation in the fruit skin of persimmon (*Diospyros kaki* cv "Heishi")," *Food Chemistry*, vol. 330, Article ID 127253, 2020.
- [27] S. Zolghadri, A. Bahrami, M. T. Hassan Khan et al., "A comprehensive review on tyrosinase inhibitors," *Journal of Enzyme Inhibition and Medicinal Chemistry*, vol. 34, no. 1, pp. 279–309, 2019.
- [28] M. K. Jung, S. Ha, J.-a. Son et al., "Polyphenon-60 displays a therapeutic effect on acne by suppression of TLR2 and IL-8 expression via down-regulating the ERK1/2 pathway," *Archives of Dermatological Research*, vol. 304, no. 8, pp. 655–663, 2012.
- [29] M.-J. Oh, M. Abdul Hamid, S. Ngadiran, Y.-K. Seo, M. R. Sarmidi, and C. S. Park, "Ficus deltoidea (Mas cotek) extract exerted anti-melanogenic activity by preventing tyrosinase activity in vitro and by suppressing tyrosinase gene expression in B16F1 melanoma cells," *Archives of Dermatological Research*, vol. 303, no. 3, pp. 161–170, 2011.
- [30] S.-Y. Chung, Y.-K. Seo, J.-M. Park et al., "Fermented rice bran downregulates MITF expression and leads to inhibition of α -MSH-induced melanogenesis in B16F1 melanoma," *Bio-science, Biotechnology, and Biochemistry*, vol. 73, no. 8, pp. 1704–1710, 2009.
- [31] Y. Luo, J. Wang, S. Li et al., "Discovery and identification of potential anti-melanogenic active constituents of *Bletilla striata* by zebrafish model and molecular docking," *BMC Complementary Medicine and Therapies*, vol. 22, no. 1, pp. 9–14, 2022.
- [32] M. B. Veldman and S. Lin, "Zebrafish as a developmental model organism for pediatric research," *Pediatric Research*, vol. 64, no. 5, pp. 470–476, 2008.
- [33] R. Sharma, N. Garg, D. Verma et al., "Indian medicinal plants as drug leads in neurodegenerative disorders," *Nutraceuticals in Brain Health and Beyond*, vol. 1, pp. 31–45, 2021.
- [34] R. Sharma, A. Kabra, M. M. Rao, and P. K. Prajapati, "Herbal and holistic solutions for neurodegenerative and depressive disorders: leads from ayurveda," *Current Pharmaceutical Design*, vol. 24, no. 22, pp. 2597–2608, 2018.
- [35] J. D. Lambert and R. J. Elias, "The antioxidant and pro-oxidant activities of green tea polyphenols: a role in cancer prevention," *Archives of Biochemistry and Biophysics*, vol. 501, no. 1, pp. 65–72, 2010.
- [36] T.-J. Wang, J. An, X.-H. Chen, Q.-D. Deng, and L. Yang, "Assessment of *Cuscuta chinensis* seeds effect on melanogenesis: comparison of water and ethanol fractions in vitro and in vivo," *Journal of Ethnopharmacology*, vol. 154, no. 1, pp. 240–248, 2014.
- [37] H. M. Wang, C. Y. Chen, and Z. H. Wen, "Identifying melanogenesis inhibitors from *Cinnamomum subavenium* with in vitro and in vivo screening systems by targeting the human tyrosinase," *Experimental Dermatology*, vol. 20, no. 3, pp. 242–248, 2011.

Research Article

***Tridax procumbens* Ameliorates Streptozotocin-Induced Diabetic Neuropathy in Rats via Modulating Angiogenic, Inflammatory, and Oxidative Pathways**

Munish Kakkar,¹ Tapan Behl²,² Celia Vargas-De-La Cruz,^{3,4} Hafiz A. Makeen⁵,⁵ Mohammed Albratty,⁶ Hassan A. Alhazmi^{6,7},^{6,7} Abdulkarim M. Meraya⁸,⁸ Ghadeer M. Albadrani,⁹ and Mohamed M. Abdel-Daim^{10,11}

¹Chitkara College of Pharmacy, Chitkara University, Rajpura, Punjab, India

²School of Health Sciences & Technology, University of Petroleum and Energy Studies, Bidholi 248007, Dehradun, Uttarakhand, India

³Department of Pharmacology, Bromatology and Toxicology, Faculty of Pharmacy and Biochemistry, Universidad Nacional Mayor de San Marcos, Lima, Peru

⁴E-Health Research Center, Universidad de Ciencias y Humanidades, Lima, Peru

⁵Pharmacy Practice Research Unit, Clinical Pharmacy Department, College of Pharmacy, Jazan University, Jazan, Saudi Arabia

⁶Department of Pharmaceutical Chemistry and Pharmacognosy, College of Pharmacy, Jazan University, Jazan, Saudi Arabia

⁷Substance Abuse and Toxicology Research Center, Jazan University, Jazan, Saudi Arabia

⁸Department of Pharmacy Practice, Faculty of Pharmacy, Jazan University, P.O. Box 114-45124, Jazan, Saudi Arabia

⁹Department of Biology, College of Science, Princess Nourah bint Abdulrahman University, P.O. Box 84428, Riyadh 11671, Saudi Arabia

¹⁰Department of Pharmaceutical Sciences, Pharmacy Program, Batterjee Medical College, P.O. Box 6231, Jeddah 21442, Saudi Arabia

¹¹Pharmacology Department, Faculty of Veterinary Medicine, Suez Canal University, Ismailia 41522, Egypt

Correspondence should be addressed to Tapan Behl; tapanbehl31@gmail.com

Received 14 June 2022; Accepted 8 July 2022; Published 31 August 2022

Academic Editor: Rupesh K. Gautam

Copyright © 2022 Munish Kakkar et al. This is an open access article distributed under the Creative Commons Attribution License, which permits unrestricted use, distribution, and reproduction in any medium, provided the original work is properly cited.

Tridax procumbens (TP) is a traditional Indian therapeutic plant and was evaluated for its blood glucose lowering abilities, as well as for its ability to curb diabetic neuropathy (DN). Administering 45 mg/kg body weight of streptozotocin (STZ) intraperitoneally for four weeks, DN was induced in Wistar rats. After the rats' tails were clipped, the blood glucose levels were measured. Body weight and urine volume were also assessed. Oxidative stress makers such as superoxide dismutase (SOD), thiobarbituric acid reactive substances (TBARS), catalase (CAT), inflammatory cytokines for instance tumor necrosis factor (TNF)- α , and interleukin (IL)-1 β were estimated. Further, protein kinase C (PKC- β) and vascular endothelial growth factor (VEGF) were also estimated as angiogenic markers. Behavioral parameters were also evaluated by using cold allodynia using acetone test, hot allodynia using Eddy's hot plate, grip strength test using Rota rod, and hyperalgesia test using Tail flick technique. The statistical assessment of findings was done employing one-way (ANOVA) analysis of variance, and subsequently Turkey as *post hoc* with GraphPad Prism software package. The ingestion of TP for 1 month in DN rats stemmed in a substantial decline in blood glucose concentrations matched to nontreated rats with DN. There had been a considerable improvement in DN as evident from the finding from biochemical markers. The serum level of antioxidant defense enzymes was significantly increased, while the activities of TBARS had been substantially reduced in the TP treated rats with DN. TP averted DN-triggered surge levels of TNF- α and IL-6 in the serum. Further, PKC- β and VEGF concentrations had been also reduced by the treatment TP. The findings of this research demonstrated that the restorative impact of TP on DN rats might be linked to the anti-inflammatory and antioxidative antiangiogenic retorts.

1. Introduction

The condition of peripheral neuropathy is extremely complex and prevalent. In the general population, approximately 8% of individuals have peripheral neuropathy, which rises to 15 percent in individuals older than 40 years [1]. Prediabetes and type 2 diabetes (T2D) are the utmost common roots of peripheral neuropathy in the Europe and US. The majority of diabetic patients, together with those with type-1 diabetes (T1D), progress to neuropathy at some point in their lives. The incidence of prediabetes and type-2 diabetes is increasing worldwide, especially in countries that consume more western foods. As more people of America progress to prediabetes and T2D, the number of those with neuropathy will double. Currently, more than twenty million American people have diabetic neuropathy as a result of prediabetes, T1D, or T2D [2]. There are also 316 million people worldwide, who suffer from prediabetes, and 387 million who suffer from diabetes, respectively, and despite a lack of exact figures, the figures suggest that at least 200 million of those with diabetes suffer from neuropathy.

Multiple forms of peripheral nervous system (PNS) harm can be caused by diabetes. A stocking-glove neuropathy is the most common type of nerve damage. This condition has, therefore, become synonymous with diabetic neuropathy (DN). The pattern of injury is similar in those possessing prediabetic conditions, auxiliary to the notion that damage of nerve from diabetes has been related to blood sugar levels ranging from normal to hyperglycemic [3]. A primary characteristic of DN is disordered sensory processing in the feet, which can lead to positive and negative symptoms, including tingling, pain, and tingling sensations (paraesthesia), as well as numbness; discomfort caused by a loss of sensory function may cause pain once touched (allodynia) the feet and increased hyperalgesia (pain sensitivity). Symptoms of motor nerve dysfunction seem far along in the progression of the disease and typically manifest as distal weakness of the toes, calves, and ankles. There is currently no explanation as to where axons-sensory is susceptible to conditions of diabetes more than axons-motor. Over time, lower extremity sensation, as well as motor weakness, led to falls, numb, and insensitive feet.

The only modifiable treatment for DN is improving lifestyle and controlling diabetes, despite decades of research. Based on a review from Cochrane database, which reviewed all the retrieved and available clinical trials, hard glucose control appears to lower the occurrence of diabetic neuropathy in patients with T1D but has very little or no outcome on patients with T2D despite having improved glucose control for more than 10 years [4]. Callaghan et al. suggested that it is not one disease, but two, with alike clinical exhibitions. Clearly, the mechanisms underlying DN differ between T2D and T1D, and this difference is informative. For the last two decades, diabetes mellitus pathogenesis has been studied using glucose and the T1D rat as a

model despite this paradox. All United States trials targeting an intervention to alter the progressive nature of DN have botched. Large pharmaceutical companies are now walking away from the disease due to a lack of basic understanding. This causes a high burden on society, but the individual costs are even greater, owing to the ache and helplessness to work laterally with deprived quality of life (QWL) each patient suffers. As a consequence of the enormity of the issue, both at an individual and societal level, mechanisms need to be understood, and early diagnosis to prevent poor patient outcomes is required [5].

It has become more urgent than ever to explore novel ways for treating diabetes and preventing its onset while reducing the side effects of other conventional medications. Despite the fact that conventional therapies are effective and satisfactory, but there is an increasing number of side effects associated with them, developing newfangled medicines sourced from natural sources with lesser adverse effects and similar effectiveness as conventional medicines is urgently needed [6–9]. The popularity of plants is based on their effectiveness, ease of accessibility, low cost, and relative lack of harmful effects. For instance, *Bacopa monnieri* contains compounds that enhance memory, *Curcuma longa* has anti-inflammatory properties, *Momordica charantia* is hypoglycemic, etc. These have shown their respective therapeutic properties without side effects. According to recent reports, WHO strongly recommends Artemisinin and its derivatives from *Artemisia annua* as a treatment for malaria caused by *Plasmodium falciparum*, since synthetic antimalarials alone are ineffective [10]. Similarly, a flavonoid isolated from milk thistle, that is, *Silybum marianum*, has been granted approval as drug for treating various liver disorders in Germany and western countries [10].

Tridax procumbens extracts were found to hold anti-inflammatory, analgesic, and antidiabetic functionalities in animal models. Preclinical studies have indicated that acute and subacute administration of *Tridax procumbens* to diabetic (induced by alloxan) rats reduced fasting glucose levels in blood, but not those of control rats without diabetes. In rats loaded with cholesterol (1 g/100 g body weight), *Tridax procumbens* also reduced blood levels of total cholesterol (TC), LDL, VLDL, and triglycerides levels, along with atherogenic index, and atherogenic coefficient [11]. The effectiveness of *Tridax procumbens* in controlling blood glucose and lowering cardiovascular risk in diabetics has not been studied in clinical studies. There has been as well a paucity of evidence concerning the molecular mechanisms that underlie the anti-inflammatory and antihyperglycemic activities of *Tridax procumbens*. In this study, *Tridax procumbens* was evaluated for its blood glucose lowering abilities as well as for its ability to curb diabetic neuropathy. The body weight, urine volume, and glycated hemoglobin were also assessed. Behavioral parameters were also assessed using various *in vivo* models using rats. Further, the resolution of this current investigation was to explore possible mechanisms for antihyperglycemic, anti-inflammatory, angiogenic, and antioxidant effects *in vivo* using various biochemical marker estimations.

2. Materials and Methods

2.1. The Plant and the Extracts. *Tridax procumbens* whole plant was collected from National Institute of Pharmaceutical Education and Research (NIPER), Mohali, Punjab. The collection has been done during the months of August and September. The voucher specimen was deposited and was stored in a publicly available herbarium of the institute with reference number NIP-H-290. A mechanical grinder was used to chop and pulverize the plant parts after being shade dried. After powdering the crude extract (1 kg), ether was used to defat it. For comprehensive removal of fatty ingredients, this step was repeated three times. The samples were then subjected to a series of fractionations using increasingly polarized organic solvents: methanol, petroleum ether, and ethyl acetate. After comprehensive extraction of the crude drug, the four extracts were received, and under condensed pressure, the extracts were concentrated. Four concentrated extracts of *Tridax procumbens* (TP) were obtained (yield 0.65%, 0.65%, 0.65%, and 0.65% w/w when calculated with respect to the starting dried plant material). After that, the final extracts were cooled to 4°C before use.

2.2. Animals. Adult male and female Wistar rats (weighing 100–250 g) were employed for this experimentation. The rats were arranged from the animal facility, Chitkara College of Pharmacy, Chitkara University, Punjab. Polypropylene cages have been used for housing the animals (atmosphere controlled at 23 ± 1°C temperature together with a light and dark cycle of 12 h). An acclimatization period of one week preceded the experiment for all animals. In addition to a standard pellet diet, the rats had unrestricted approach to drinking water. By protocol reference number IAEC/CCP/21/02/PR-010, the study protocols have been permitted by the IAEC. During the study, the rats were taken care of and used in compliance with the standards prescribed by Committee for the Purpose of Control and Supervision of Experiments on Animals (CPCSEA), India.

2.3. Chemicals and Drugs. Streptozotocin (STZ) and Gabapentin have been bought from Sigma-Aldrich (St. Louis, USA). All other drugs and chemicals used in the study were of standard quality and of analytical grade, which includes Citric acid (Fisher Scientific), Trisodium citrate (Fisher Scientific), Sodium dihydrogen phosphate (HiMedia Laboratories Pvt. Ltd.), Disodium hydrogen phosphate (HiMedia Laboratories Pvt. Ltd.), Pentobarbital (Kamron Laboratories Ltd., Gujarat, India), Xylazine (Troikaa Pharmaceuticals Ltd.), Ketamine (Troikaa Pharmaceuticals Ltd.), Disodium-EDTA (Fisher Scientific), Isophane insulin injection IP (huminsulin® 30/70) (Eli Lilly and Company Pvt. Ltd, India), Tropicamide eye drops (Sunways (I.) P. Ltd, Mumbai, India), and formaldehyde (Qualigens Fine Chemicals, Mumbai, India). The various standard ELISA as well as other biochemical kits used included Rat Glycated Hemoglobin (KINESISDx), Rat IL-1 β (KRISHGEN Biosystems), Rat TNF- α (KRISHGEN Biosystems), Rat VEGF ELISA (KRISHGEN Biosystems), Rat PKC- β ELISA

(KINESISDx), Rat Lipid Peroxide (LPO) ELISA (KINESISDx), Superoxide Dismutase (SOD) Colorimetric Activity Kit (ARBOR assays), and Catalase Colorimetric Activity Kit (ARBOR assays).

2.4. Diabetes Induction. By injecting streptozotocin (STZ) at an intraperitoneal dosage of 45 mg/kg (prepared in 0.1 M citrate buffer at a pH of 4.5) into Wistar rats fasted overnight, diabetes was induced. Blood levels of glucose were analyzed initially at 0 time and 48 hours later following the injection of vehicle or streptozotocin. The diabetic animals were considered to be included in the experiment if their blood glucose levels exceeded 300 mg/dl. From the literature study, in order to decrease the mortality in diabetic rats, 1 unit of huminsulin was administered if the blood glucose levels are greater than 450–500 mg/dl, and if they are greater than 600 mg/dl rats, 2 units of huminsulin via subcutaneous route was administered [12].

2.5. Design of Experiment. Forty-eight (48) rats had been grouped into eight groupings at random. In group I (Normal control), rats were given saline orally, group II comprised of diabetes rats representing the diabetic group known as diabetic control group, in group III (*Tridax procumbens* per se group), normal rats were given *Tridax procumbens* daily for 28 days, and group IV was Gabapentin-treated diabetic rats who received daily Gabapentin (50 mg/kg, p.o); min before administration. The Gabapentin dose has been selected, referring to an earlier published literature. The experimental design and grouping of animals are summarized as follows:

- (i) Group I: Normal control.
- (ii) Group II: Positive control (Diabetic).
- (iii) Group III: TP per se group.
- (iv) Group IV: Gabapentin (50 mg/kg body weight).
- (v) Group V: TP 250 mg/kg.
- (vi) Group VI: TP 375 mg/kg.
- (vii) Group VII: TP 500 mg/kg.
- (viii) Group VIII: Standard drug (Gabapentin) + TP 500 mg/kg

2.6. General Parameters. During the progression of the study, overnight fasted rats were engaged for blood collection initially at week 0 and thereafter at 48 hrs, 1st week, 2nd week, and 3rd week in each group. The tails of the rats were pricked with a syringe, and blood glucose was measured using an electronic glucometer and glucose test strips [13]. During the 4th week of observation, a blood sample varying from 0.5 ml to 1 ml was stored from the retroorbital technique for the estimation of glycated hemoglobin (HbA_{1c}) [13]. Before starting the study (baseline value), and 48 hours after STZ administration, the bodyweight was noted. Furthermore, bodyweight of control, diabetic rats, and treated rats was determined from week 1 to week 4 [13].

After acclimatization for a day, we collected the urine samples from animals in individual urine collection cages. From day 0 onward, urine samples were collected from the control, diabetic control, and treatment groups every week to establish baseline data [13].

2.7. Biochemical Estimation. In the next step, all rats were decapitated, and both sciatic nerves were carefully excised and rinsed in ice-cold saline. All sciatic nerve samples collected were homogenized in buffer of phosphate & put at a temperature of -80°C for subsequent investigation and estimations of various biochemical markers including catalase (CAT), thiobarbituric acid reactive substances (TBARS), superoxide dismutase (SOD), interleukin- 1β (IL- 1β), tumor necrosis factor- α (TNF- α), and protein kinase C (PKC- β) and vascular endothelial growth factor (VEGF).

2.7.1. Angiogenic and Inflammatory Parameters. By employing Enzyme Linked-Immuno-Sorbent Assay (ELISA), VEGF levels and PKC activity were determined. ELISA kits were employed to estimate the IL- 1β & TNF- α levels as previously described in a previous article [14].

2.7.2. Oxidative Stress Parameters. The amount of thiobarbituric acid reactive substances (TBARS) was estimated using the previously described method. A previously described method was used to determine the catalase levels in sciatic nerve homogenate [15]. As was done previously, an earlier method for measuring SOD was also used to appraise levels of SOD [16].

2.8. Behavioral Experiments

2.8.1. Cold Allodynia Using Acetone Test. The mid-plantar region of the hind leg of every group of Wistar rats was gently rubbed with acetone drops ($50\ \mu\text{L}$). There were nociceptive pain responses seen in the form of paw licking, rubbing, shaking, and even withdrawal of food in response to cold stimuli. After application of acetone, a digital stopwatch was used to measure the response time (1 minute). Both paws were sampled three times for each reading, and the mean value was considered [17].

2.8.2. Hot Allodynia Using Eddy's Hot Plate. The nociceptive response to TP is estimated through this method [18]. The animals were placed on hot plate, which were put at a constant 55°C temperature for the duration of experiment. As a feedback response as thermal hyperalgesia, paw licking and jumping were taken with the help of digital stopwatches and considered as positive reactions to heat. The animals that exceeded the cutoff time were removed from the hot plate until baseline values were achieved.

2.8.3. Grip Strength Test Using Rota Rod. An accelerating rotarod apparatus was used to assess rats' motor coordination (Ugo Basile, Italy, Model 7750) [19]. Before the experiment, rats

were skilled for three consecutive days at a static speed of 20 to 25 rpm (five minutes each day). During the test day, rats were placed contrary to the rotating rod, which began at 4 rotations per minute (rpm) and accelerated gradually up to 20–25 rpm. A decrease in muscle grip indicates relaxation of muscles. An index of muscle relaxation is taken from the variance in drop off time from the rotating rotarod between groups.

2.8.4. Hyperalgesia Using Tail Flick. In this method, the withdrawal of the tail from the heat is taken as an endpoint [20]. In order to prevent damage to the tail using a hot plate at 55°C , 10–12 sec was observed to be cut off. Animals that do not withdraw their tails within 3–5 seconds are rejected from the study. The reaction time was noted after the drug/TP had been administered at 5, 15, 30, and 60 minutes.

2.9. Statistical Assessment. Each of the data points has been expressed as a mean + SD. An ANOVA was conducted as a one-way test, followed by a Tukey-Kramer test, which were conducted as *post hoc* tests based on $p < 0.05$ statistical differences between groups. GraphPad Prism software was used in this study (version 7, GraphPad Software, San Diego, USA).

3. Results

3.1. General Parameters

3.1.1. Influence of TP on Blood Glucose, Body Weight, HbA_{1c} and Urine Volume. Diabetes results in a significant weight loss to 158.73 ± 1.54 ($p < 0.01$) and a steady statistically significant exponential elevation in blood glucose levels as well as urine volume by approximately 565.22 ± 4.72 ($p < 0.01$) and 80.56 ± 1.27 ($p < 0.01$), and correspondingly, in assessment with normal rats (Table 1). Diabetic rats administered with TP (250, 375, and 500 mg/kg) and standard treatment Gabapentin exhibited substantial decline in the blood glucose levels along with the urine volume as well as upsurge in the bodyweight in treatment rats as equated with diabetic rats. Additionally, the combination treatment of highest dose of TP 500 mg/kg with the standard drug, Gabapentin, produced an additive effect in the decreasing the levels of blood glucose levels but produced nonsignificant differences in the urine volume and bodyweight (Tables 2 and 3). Upon completion of the study, the HbA_{1c} levels were estimated for all study groups. A steady, statistically considerable raise in HbA_{1c} amount was seen in diabetic rats. Diabetic Wistar rats administered with TP (250, 375, and 500 mg/kg) and standard Gabapentin showed momentous decrease in HbA_{1c} level. Additionally, the combination treatment of highest dose of TP 500 mg/kg with the standard drug, Gabapentin, produced nonsignificant differences in HbA_{1c} concentration as equated to typical and normal Wistar rats (Table 4).

3.2. Angiogenic Parameters

3.2.1. Effect of TP on Sciatic VEGF Levels and PKC- β Activity. Angiogenesis is designated as de novo formation of newer blood vessels followed by growth. The role of angiogenesis

TABLE 1: Impact of TP on blood level of glucose throughout antidiabetic study model (postgeneration of diabetes).

	Normal control	Disease control	TP per se	Standard (Gabapentin)	T.P. 250 mg	T.P. 375 mg	T.P. 500 mg	T.P. 500 mg + Gabapentin
Week 0	225.72 ± 2.51	229.22 ± 4.82	223.26 ± 5.26	220.23 ± 5.24	221.33 ± 4.33	227.75 ± 1.51	211.24 ± 2.61	230.15 ± 4.81
Week 1	234.51 ± 2.51	211.33 ± 1.73	196.26 ± 3.15	205.21 ± 3.13	185.43 ± 2.73 ⁺	187.33 ± 8.52 ^{*,†}	190.05 ± 4.47 ^{*,††,a}	202.23 ± 4.51 ^{*,††,a}
Week 2	229.25 ± 3.16	183.43 ± 1.9	189.6 ± 5.61	187.56 ± 5.6	182.18 ± 3.71	191.85 ± 8.31 [*]	197.32 ± 2.81 ^{*,††,a}	203.61 ± 3.42 ^{*,††,aa,b}
Week 3	245.72 ± 0.71	173.88 ± 1.01	191.54 ± 6.14	170.51 ± 6.11 ^{**}	176.23 ± 4.13 ⁺	194.25 ± 7.71 ^{**}	204.23 ± 6.62 ^{*,††,a}	224.23 ± 5.3 ^{*,††,aa,b}
Week 4	257.16 ± 1.84	158.73 ± 1.54 [#]	201.36 ± 5.22	167.33 ± 5.24	164.24 ± 3.11 ^{##,†}	178.83 ± 6.7 ^{##,*,†}	212.72 ± 5.14 ^{#,*,††,a}	256.03 ± 4.64 ^{††,aa,b}

TABLE 2: Impact of TP on the body weight.

	Normal control	Diabetic control	Gabapentin 50 mg/kg	T.P. 250 mg	T.P. 375 mg	T.P. 500 mg	T.P. 500 mg/kg + Gabapentin
0 Week	91.65 ± 2.84	97.60 ± 3.22	99.09 ± 2.11	100.14 ± 2.51	97.93 ± 1.74	97.36 ± 3.64	96.17 ± 2.84
48 hours	93.28 ± 2.66	524.59 ± 3.51	554.13 ± 2.73	552.64 ± 2.61	547.94 ± 10.34	549.94 ± 3.24	545.56 ± 7.64
Week 1	94.73 ± 1.75	542.92 ± 2.56	515.16 ± 1.84***	529.53 ± 2.81***,+	511.74 ± 5.44***,+	497.53 ± 3.74***,+,aa	485.25 ± 6.28***,+,aa,bb
Week 2	93.27 ± 2.25	551.35 ± 3.12	490.12 ± 2.55**	501.37 ± 2.71**	487.25 ± 6.44***,+a	480.46 ± 3.86***,+,aa	415.74 ± 4.84***,+,aa,bb
Week 3	92.29 ± 2.37	554.82 ± 3.13	455.36 ± 1.94**	477.86 ± 2.81***,+	457.67 ± 5.24***,+aa	430.84 ± 3.64***,+,aa	370.73 ± 4.55***,+,aa,bb
Week 4	90.92 ± 1.18	565.22 ± 4.72###	418.61 ± 1.58###****	420.64 ± 2.71###****,+	397.67 ± 5.75###****,+aa	381.18 ± 3.27###****,+,aa	304.41 ± 4.55***,+,aa,bb

TABLE 3: Impact of TP on the volume of urine postinduction of diabetes in Wistar albino rats.

	Normal control	Diabetic control	Standard (Gabapentin)	T.P. 250 mg/kg	T.P. 375 mg/kg	T.P. 500 mg/kg	T.P. 500 mg/kg + Gabapentin
0 Week	13.61 ± 0.23	12.96 ± 0.37	14.39 ± 0.26	13.76 ± 0.24	14.66 ± 0.17	14.84 ± 0.36	13.16 ± 0.38
Week 1	13.78 ± 0.38	54.23 ± 1.33	49.47 ± 1.22**	64.2 ± 0.44**,+ ⁺	61.29 ± 2.76**,+ ⁺	56.16 ± 0.91**,+ ^a	47.78 ± 2.85**,+ ^a
Week 2	14.03 ± 0.48	71.53 ± 1.52	46.58 ± 0.51**	56.44 ± 0.65**,+ ⁺	54.21 ± 0.87**,+ ^a	50.22 ± 0.47**,+ ^a	41.25 ± 0.69**,+ ^{aa}
Week 3	14.06 ± 0.46	74.47 ± 1.34	43.36 ± 0.47**	54.24 ± 0.44**,+ ⁺	51.58 ± 0.34**,+ ^a	44.14 ± 0.33**,+ ^a	35.84 ± 0.58**,+ ^{aa}
Week 4	15.75 ± 0.46	80.56 ± 1.27 ^{###}	39.23 ± 0.47 ^{##,***}	56.35 ± 0.37 ^{###,***,+}	47.17 ± 0.21 ^{##,***,a}	36.85 ± 0.32 ^{#,***,a}	27.68 ± 0.32 ^{#,***,+^{aa},b}

TABLE 4: Effect of TP on the glycated hemoglobin (HbA1c) levels postinduction of diabetes in Wistar albino rats at week 4.

Groups	Glycated haemoglobin (HbA1c)
Normal control	3.55 ± 0.49
Disease control	6.30 ± 0.33 ^{##}
TP per se	3.53 ± 0.39 ^{**}
Standard (Gabapentin)	3.57 ± 0.38 ^{**}
TP 250 mg	5.57 ± 0.19 ^{##,***,aa}
TP 375 mg	4.45 ± 0.19 ^{##,***,a,b}
TP 500 mg	3.72 ± 0.27 ^{**^{bb,c}}
TP 500 mg + Gabapentin	3.55 ± 0.16 ^{**^{bb,c}}

has been available in the literature in development of diabetes related complications of nephropathy. Angiogenic indicators were assessed to be high; namely, PKC- β and VEGF were augmented in serum STZ-post administration. PKC- β is an essential marker in determining angiogenesis. VEGF initiation is thought to occur as a result of PKC- β activation under tumorigenesis, according to the outdated view or ischemic conditions that additionally enhance endothelial cells angiogenesis via a paracrine mechanism. Following STZ administration, PKC- β levels increased in the serum of Wistar rats, which led to the development of diabetes. Administration of TP 250, 375, and 500 mg/kg and standard Gabapentin showed noteworthy diminution in PKC- β levels. Additionally, the combination treatment of highest dose of TP 500 mg/kg with the standard drug, Gabapentin, produced nonsignificant differences in PKC- β levels in maintaining the level of PKC- β to the levels found in normal rats (Table 5).

VEGF is a potent biological marker entity employed in appraisal of degree of angiogenesis. From the available literature, it can be deduced that the increase in the levels of VEGF is associated in the rat model of diabetes caused by the administration of STZ. TP (250, 375, and 500 mg/kg) administration and standard treatment Gabapentin displayed substantial decrease in the levels of VEGF. Additionally, the combination treatment of highest dose of TP 500 mg/kg with the standard drug, Gabapentin, produced nonsignificant differences in maintaining the level of VEGF to the levels found in normal Wister rats (Table 5).

3.3. Inflammatory Parameters

3.3.1. Effect of TP on Sciatic Levels of IL-1 β and TNF- α . The concentrations of IL-1 β and TNF- α were augmented in serum of rat after administration of STZ as toxicant. Diabetic Wistar rats treated with TP (250, 375, and 500 mg/kg)

accompanied by the standard drug Gabapentin meaningfully drained the levels of mediators of inflammatory cascade such as TNF- α and IL-1 β to normal. The IL-1 β levels as proinflammatory cytokine are exceptionally high in circumstances of diabetes associated complications. Administration of TP (250, 375, and 500 mg/kg) and standard treatment Gabapentin displayed a noteworthy decrease in the levels of VEGF. Additionally, in the combination treatment of highest dose of TP 500 mg/kg with the standard drug, Gabapentin, produced nonsignificant differences in maintaining the IL-1 β level to the levels found in normal (Table 5).

There are several biomarkers for describing the tissue inflammation grade, including TNF- α as the most common one. From the literature evidence, it has been found that the levels of TNF- α significantly increase in animal model of diabetes administered with STZ. In the research, TP administration at mg/kg basis (250, 375, and 500) and standard Gabapentin showed a noteworthy decrease in the TNF- α levels. Additionally, the combination treatment of highest dose of TP 500 mg/kg with the standard drug, Gabapentin, produced nonsignificant differences in maintaining the level of TNF- α to the levels found in normal rats (Table 5).

3.4. Assessment of Oxidative Stress Parameters

3.4.1. Effect of TP on Sciatic TBARS, CAT, and SOD. The TBARS levels in all groups were measured after four weeks of treatment. The TBARS levels in diabetic controls have significantly increased (8.02 ± 1.20 U/mg protein). Compared to the untreated groups, the TP administered rats experienced a noteworthy reduction in levels as 6.78 ± 0.46, 6.06 ± 0.31, 4.99 ± 0.24, and 4.57 ± 0.28 U/mg protein for TP 250, 375, and 500 mg/kg and Gabapentin + TP 500 mg/kg, respectively (Table 6).

Sciatic nerve homogenates from diabetic control rats were found to have a significant reduction in SOD (1.44 ± 0.39 U/mg protein) compared to normal rats (4.14 ± 0.37 U/mg protein). In disparity, rats in the TP administered group had higher levels of SOD—2.33 ± 0.43, 2.80 ± 0.05, 3.49 ± 0.15, and 3.83 ± 0.25 U/mg protein in Group TP 250, 375, and 500 mg/kg and TP 500 mg/kg + Gabapentin, respectively (Table 6). In rats treated with TP and Gabapentin, these have shown significant and dose-dependent effects.

In diabetic control group, CAT levels had been considerably diminished in the sciatic nerve homogenate (1.32 ± 0.29 U/mg of protein) when equated to the normal animals (3.33 ± 0.45 U/mg of protein). A noteworthy

TABLE 5: Impact of TP on endogenous angiogenic and inflammatory biomarkers in rats.

Groups	PKC (ng/ml)	VEGF (pg/ml)	IL-1 β (pg/ml)	TNF- α (pg/ml)
Normal control	21.80 \pm 1.9	5.670 \pm 0.26	23.16 \pm 1.21	2.04 \pm 0.23
Disease control	76.73 \pm 4.81 ^{###}	11.69 \pm 0.73 ^{###}	47.85 \pm 4.31 ^{##}	5.70 \pm 0.52 ^{###}
Standard (Gabapentin)	22.87 \pm 1.97 ^{***}	6.710 \pm 0.84 ^{***}	24.09 \pm 1.73 ^{**}	2.59 \pm 0.31 ^{**}
TP per se	22.03 \pm 1.42 ^{***}	5.902 \pm 0.47 ^{***}	26.26 \pm 1.88 ^{**}	2.39 \pm 0.25 ^{**}
TP 250 mg	36.46 \pm 1.97 ^{#,*,a}	8.970 \pm 0.52 ^{#,aaa}	35.40 \pm 2.06 ^{#,aa}	3.76 \pm 0.71 ^{#,a}
TP 375 mg	31.46 \pm 1.97 ^{#,*,a,b}	8.193 \pm 0.28 ^{#,*,aa,b}	31.61 \pm 1.38 ^{#,*,aa,b}	3.29 \pm 0.28 ^{#,*,b}
TP 500 mg	25.94 \pm 2.16 ^{***,bb,c}	7.165 \pm 0.51 ^{**,b,c}	24.93 \pm 1.46 ^{**,bb,c}	2.53 \pm 0.24 ^{**,b}
TP 500 mg + gabapentin	24.01 \pm 1.56 ^{***,bb,c}	6.877 \pm 0.12 ^{**,bb,cc}	23.24 \pm 0.84 ^{**,bb,c}	2.19 \pm 0.12 ^{**,b,c}

TABLE 6: Impact of TP on endogenous oxidative stress biomarkers in rats.

Groups	TBARS (U/mg protein)	Catalase (U/mg protein)	SOD (U/mg protein)
Normal control	3.98 \pm 0.42	3.33 \pm 0.45	4.14 \pm 0.37
Disease control	8.02 \pm 1.20 ^{###}	1.32 \pm 0.29 ^{##}	1.44 \pm 0.39 ^{###}
Standard (Gabapentin)	4.94 \pm 0.39 ^{**}	2.51 \pm 0.13 ^{**}	3.60 \pm 0.53 ^{**}
TP per se	5.27 \pm 0.31	2.83 \pm 0.25	3.76 \pm 0.29
TP 250 mg	6.78 \pm 0.46 ^{#,*,aa}	1.66 \pm 0.20 ^{#,aa}	2.33 \pm 0.43 ^{#,*,aa}
TP 375 mg	6.06 \pm 0.31 ^{#,*,a}	1.91 \pm 0.11 ^{#,*,a}	2.80 \pm 0.05 ^{#,*,a}
TP 500 mg	4.99 \pm 0.24 ^{**,b,c}	2.48 \pm 0.21 ^{**,bb,c}	3.49 \pm 0.15 ^{**,b}
TP 500 mg + Gabapentin	4.57 \pm 0.28 ^{**,bb,cc}	2.70 \pm 0.19 ^{**,bb,cc}	3.83 \pm 0.25 ^{**,bb,c}

upsurge in CAT levels has been detected in TP treated rats—1.66 \pm 0.20, 1.91 \pm 0.11, 2.48 \pm 0.21 and 2.70 \pm 0.19 U/mg protein in Group TP 250, 375, and 500 mg/kg and TP 500 mg/kg + Gabapentin, respectively (Table 6). TP and Gabapentin were shown to produce significant and dose-dependent effects in rats.

3.5. Behavioral Experiments

3.5.1. Cold Allodynia Using Acetone Test. Table 7 showed the results. Group TP 250, 375, and 500 mg/kg and TP 500 mg/kg + Gabapentin have recorded average readings of 5.12 \pm 0.57, 4.73 \pm 1.09, 4.67 \pm 0.18, and 4.45 \pm 0.77, respectively, in cold hyperalgesia results equated to week 4 (** p < 0.01). As the diabetes-induced group recorded delayed responses to hyperalgesia, in the diabetic group, longer responses were observed.

3.5.2. Hot Allodynia in Hot Plate Technique (Eddy's Hot Plate). TP treated rats (250, 375, and 500 mg/kg) and TP 500 mg/kg + Gabapentin have revealed a mean reaction latency of 6.28 \pm 0.65, 5.14 \pm 1.23, 4.88 \pm 0.23, and 4.56 \pm 0.78, respectively, on 4th week (Table 8). In equation to the results from the diabetic group during 4th week, the results were suggestively different (** p < 0.01).

3.5.3. Grip Strength Test Using Rota Rod. Neuromuscular coordination logged an augmentation of 96.93 \pm 2.62, 106.88 \pm 3.03, 116.75 \pm 3.26, and 124.65 \pm 3.72 for Group TP 250, 375, and 500 mg/kg and TP 500 mg/kg + Gabapentin, respectively (Table 9). In comparison to diabetes control rats, the outcomes from fourth week of experimentation were quite significant. When comparing all the treated groups to the diabetic control groups, all the outcomes had a

noteworthy p < 0.01 value. The healing and protective effects of TP and Gabapentin were, therefore, highlighted.

3.5.4. Hyperalgesia Using Tail Flick. The hyperalgesia retorts of rats treated with TP 250, 375, and 500 mg/kg and TP 500 mg/kg + Gabapentin have improved to 5.98 \pm 1.62, 6.28 \pm 1.82, 6.39 \pm 1.74, and 6.44 \pm 1.68, correspondingly on assessment from 4th week findings (Table 10). The findings were significant (p < 0.01).

4. Discussion

As of now, no treatment schedule other than belligerent and strict glycemic control has proven effective at halting diabetic neuropathy. Recent studies have demonstrated the effectiveness of natural products and their derivative bioactive phytoconstituents against diabetes in animal models and humans. In the study presented here, TP was investigated to determine whether it had protective effects in contrast to experimentally induced diabetic neuropathy (DN) in diabetic animals, building on earlier studies. STZ administration was linked with significant upsurges in blood glucose and concentration of HbA_{1c} in the present investigation, which is reliable and allied with preceding conclusions reported earlier. As an eminent cytotoxin of β -cell of pancreatic tissue, STZ diminishes the insulin secretory functionalities and elevates blood levels of glucose by increasing cellular oxidative stress [21, 22].

Diabetic rats also lost weight due to diabetes. A decrease in insulin levels may be causing the accumulation of amino acids as a result of increased tissue protein turnover for metabolic energy. The treatment with TP resulted in diminution of weight loss, blood sugar, and HbA_{1c} levels. Due to its use as a gauge of glycemic control, HbA_{1c} is habitually associated with diabetes complications over time [23]. Many

TABLE 7: Impact of TP on Cold hyperalgesia: acetone drop test in Wistar albino rats.

	0 Week	1 Week	2 Week	3 Week	4 Week
Normal control	4.4 ± 0.22	4.43 ± 0.05	4.63 ± 1.21	4.61 ± 1.72	4.53 ± 0.62
Disease control	4.18 ± 0.83	5.95 ± 1.02	6.86 ± 1.27	7.85 ± 1.62	9.75 ± 1.22 ^{##}
Standard (Gabapentin)	4.63 ± 1.02	5.43 ± 1.1*	5.13 ± 1.32**	4.83 ± 1.17**	4.4 ± 1.15***
TP 250 mg/kg	4.33 ± 0.85	5.93 ± 1.04 ^a	5.6 ± 1.05***,a	5.18 ± 0.98***,a	5.12 ± 0.57 ^{##,***,aa}
TP 375 mg/kg	4.53 ± 0.71	5.89 ± 1.08 ^a	5.69 ± 0.98***,aa	5.23 ± 1.11***,a	4.73 ± 1.09 ^{##,***,a}
TP 500 mg/kg	4.73 ± 1.06	5.58 ± 0.99*,a	5.34 ± 1.03***,a	5.08 ± 1.01**	4.67 ± 0.18**
TP 500 mg + Gabapentin	4.69 ± 0.86	5.47 ± 1.02*,bb	5.14 ± 1.01*,bb	5.03 ± 0.87***,b	4.45 ± 0.77***,bb

TABLE 8: Impact of TP on Thermal Hyperalgesia: Eddy's hot plate test to assess diabetic neuropathy in Wistar albino rats.

	0 Week	1 Week	2 Week	3 Week	4 Week
Normal control	4.29 ± 0.21	4.43 ± 0.051	4.63 ± 1.22	4.64 ± 1.82	4.45 ± 0.51
Disease control	4.5 ± 0.51	5.99 ± 1.71	6.68 ± 1.14	7.69 ± 1.81	9.73 ± 1.52 ^{##}
Standard (Gabapentin)	4.92 ± 1.1	5.53 ± 1.01*	5.16 ± 2.51**	4.99 ± 1.01**	4.63 ± 1.52***
TP 250 mg/kg	4.92 ± 1.11	5.96 ± 1.63 ^a	6.63 ± 1.61***,a	6.36 ± 0.51***,a	6.28 ± 0.65 ^{##,***,aa}
TP 375 mg/kg	4.82 ± 1.73	5.96 ± 1.61*,a	5.74 ± 2.09***,aa	5.34 ± 1.81***,a	5.14 ± 1.23 ^{##,***,a}
TP 500 mg/kg	4.88 ± 1.51	5.54 ± 0.5	5.38 ± 1.76***,a	5.11 ± 1.56**	4.88 ± 0.23**
TP 500 mg + Gabapentin	4.94 ± 1.71	5.45 ± 1.34*,bb	5.22 ± 1.21*,bb	5.12 ± 0.92***,b	4.56 ± 0.78***,bb

TABLE 9: Impact of TP on Grip strength: Rota rod test to assess muscle grip strength to evaluate DPN in Wistar rats.

	0 Week	1 Week	2 Week	3 Week	4 Week
Normal control	133.21 ± 2.32	137.32 ± 2.62	133.85 ± 3.32	139.73 ± 3.92	138.25 ± 3.42
Disease control	133.51 ± 2.41	79.88 ± 4.71 [#]	63.55 ± 2.14 ^{##}	46.45 ± 2.94 ^{##}	36.58 ± 2.41 [#]
Standard (Gabapentin)	135.85 ± 3.12	85.35 ± 1.14*	94.1 ± 2.39**	109.95 ± 3.23**	123.38 ± 2.63***
TP 250 mg/kg	138.85 ± 2.65	86.75 ± 2.65 ^a	80.65 ± 2.23***,a	85.25 ± 3.3***,a	96.93 ± 2.62 ^{##,***,aa}
TP 375 mg/kg	138.73 ± 1.39	84.8 ± 2.61*,a	90.72 ± 3.11***,aa	90.15 ± 2.8***,a	106.88 ± 3.03 ^{##,***,a}
TP 500 mg/kg	136.75 ± 2.71	91.55 ± 3.52	96.32 ± 3.91***,a	99.09 ± 2.78**	116.75 ± 3.26**
TP 500 mg + Gabapentin	137.81 ± 2.91	85.45 ± 3.29*,bb	93.15 ± 4.32*,bb	108.01 ± 4.18***,b	124.65 ± 3.72***,bb

TABLE 10: Impact of TP on the thermal hyperalgesia in tail flick technique to appraise the neuropathic pain in Wistar rats.

	0 Week	1 Week	2 Week	3 Week	4 Week
Normal control	6.29 ± 0.21	6.49 ± 1.33	5.91 ± 1.24	5.69 ± 0.99	6.55 ± 1.42
Disease control	6.56 ± 2.51	5.35 ± 1.35 [#]	4.44 ± 1.25 ^{##}	4.01 ± 1.92 ^{##}	3.31 ± 1.52 [#]
Standard (Gabapentin)	6.51 ± 1.05	5.48 ± 1.1*	5.64 ± 1.51**	5.91 ± 1.11**	6.42 ± 1.41***
TP 250 mg/kg	6.46 ± 1.08	5.38 ± 1.63 ^a	5.45 ± 1.11***,a	5.64 ± 1.53***,a	5.98 ± 1.62 ^{##,***,aa}
TP 375 mg/kg	6.67 ± 1.21	5.41 ± 1.76*,a	5.56 ± 1.39***,aa	5.71 ± 2.09***,a	6.28 ± 1.82 ^{##,***,a}
TP 500 mg/kg	6.36 ± 1.51	5.42 ± 1.43	5.68 ± 1.86***,a	5.83 ± 1.68**	6.39 ± 1.74**
TP 500 mg + Gabapentin	6.59 ± 1.51	5.58 ± 1.55*,b	5.69 ± 1.82*,b	5.89 ± 1.42***,b	6.44 ± 1.68***,b

in vivo and *in vitro* studies demonstrated antihyperglycemic properties of TP [24, 25]. Many mechanisms, including improved insulin discharge and insulin sensitivity, augmented uptake of glucose, and α -glucosidase activity inhibition may underlie TP antihyperglycemic actions. Aside from amending key enzymes responsible for glucose homeostasis in liver, TP might also be attributed to decrease glucose production [25]. There is no doubt that prolonged hyperglycemia contributes to deterioration of the nociceptive edge, a reduction of sensory-motor nerve conduction velocity (NCV), and several manifestations of conjured-pain, including cold allodynia, hot allodynia, grip weakness, and hyperalgesia [26].

The neurobehavioral tests performed in the present study designated that STZ injections caused impaired sensory function based on cold allodynia, hot allodynia, grip

strength, and hyperalgesia. However, TP amended sensory aberrations and confirmed significant antinociceptive properties, as evidenced by a decline in paw withdrawal threshold and paw withdrawal latency, as well as a reduction in fall and tail flicking time. As a matter of fact, the results also indicated that TP demonstrated potentiation of the antinociceptive effects of Gabapentin as well. In contrast, while TP treatment altered and ameliorated hyperglycemia and partly reduced and inverted neuropathic pain, the combination of TP and Gabapentin exhibited greater reversal of DN development, suggesting the involvement of other mechanisms besides reducing the elevated glucose levels. The increased reactive nitrogen/oxygen species, oxidative stress, and free radicals, generated by metabolic and vascular insults, contributed to progressive damage and dysfunction of nerve fibers in DN. Neuropathy is generally

known to be caused by the excess excitability of the afferent nociceptors and the central neurons present in diabetic peripheral nerve impairment consequently of oxidative stress [27]. The polyol pathway may be responsible for increased NADPH consumption in diabetes, while mitochondrial superoxide production, PKC activation, and glucose autooxidation may also contribute to oxidative stress [28, 29]. Moreover, previous reports have revealed that patients with DN have impaired antioxidant defenses [30, 31]. Therefore, antioxidants may assist in treating DN by reducing oxidative stress. TP treatment diminished protein carbonylation, as well as lipid peroxidation, and increased antioxidant actions in the present study. DN may be caused by oxidative damage to the myelinated structure of nerves, which predominantly consists of lipids [31].

TP has been demonstrated to be a powerful scavenger of free radicals, antioxidants, and enzymes (free radical generating) inhibitor. The phenolic and flavonoid phyto-components present in this plant extract might be accredited to its capability for scavenging free radicals due to its structural characteristics. The phytoconstituents in TP possessed phenolic nuclei as well as structures with unsaturated side chains, which eases the ability to generate a phenoxy radical owing to stabilization by resonance of the molecules [32].

Oxidative stress is a significant factor in DN progression, and it is primarily caused by the oxidation of monosaccharides and proteins [33]. The findings of the present investigation presented an extraordinary elevation of TBARS as biomarker of peroxidation of lipid, in the sciatic nerve homogenate of diabetic Wistar rats. Two endogenous antioxidants, SOD and Catalase (CAT), are considered early defenses against free radicals and ROS or RNS. The current research found that SOD and CAT levels in the sciatic homogenate of diabetic rats had been substantially reduced. An imperative antioxidant enzyme that contributes to decomposition of free radicals is the endogenous defense mechanisms, amongst which are antioxidant enzymes (SOD and CAT). Nonetheless, SOD protects biological tissues and environment from extremely responsive superoxide anions (O_2^-) by transforming them into hydrogen peroxide (H_2O_2), and hyperglycemia reduces SOD action in the homogenate of sciatic nerve of Wistar rats due to nonenzymatic glycosylation [29]. These data are in treaty with findings from this present study, in which diminished SOD and CAT activity were observed in diabetic rats homogenized isolated sciatic nerves. Contrary to this, CAT is crucial in catalyzing the decomposition of harmful H_2O_2 to O_2 and H_2O . CAT activation is decreased in diabetes, which decreases cellular defense and makes tissues further vulnerable to free radicals. By inhibiting the enzyme activity in diabetic rats, we also found a connection between DN and oxidative stress. Thus, the simultaneous reduction in endogenous antioxidant defenses system renders sciatic nerves more susceptible to hyperglycemia provoked oxidative stress.

An upsurge in the activity of PKC- β and levels of VEGF was observed in this current study in diabetic rats induced with STZ. Hyperglycemia causes impaired nerve conduction due to the possible impairment of the PKC- β /HuR/VEGF

pathway and increased activity of PKC- β and VEGF. A substantial upsurge in this enzyme activity was found in diabetic rats' sciatic nerves and erythrocytes [34, 35]. Furthermore, the creation and excretion of VEGF have been described to increase in experimental models of DN. Previous reports have found that exogenous VEGF can improve diabetic patient outcomes, and neuronal survival and maintenance are reliant on these factors. Antioxidant effects of VEGF may be a result of Bcl-2 upregulation, phosphor Akt pathway activation, stimulation of mTOR signaling, and increased activity of endogenous enzymes responsible for scavenging of free radicals [36]. The TP treatment significantly decreased PKC- β activity, and there was a decrease in DN and behavioral parameters among STZ-induced diabetic rats with higher VEGF levels in nerve homogenate. This investigation demonstrated that TP reversed elevations in TNF- α and IL-1 β levels. In reality, cytokines of proinflammatory kind, for instance IL-1 β and TNF- α , have been proven to perform a noteworthy part in the pathophysiology of neurodegeneration and transmission of pain in diabetic patient [37]. Furthermore, the activity of IL-1 β and TNF- α is upregulated in dorsal root ganglion region as well as peripheral nerves under hyperglycemic conditions [38]. Treatment with TP had revealed to avert biochemical and functional deficits of peripheral nerves in diabetic animals, as indicated by estimated biomarker levels. The anti-hyperuricemia, antioxidant, and antibacterial activity [39], anti-inflammatory and antiapoptotic actions [40], and antiosteoporotic activity of TP had been well recognized in several disease models. According to previous studies, TP inhibits the expression of proinflammatory cytokines by constricting NF- κ B signaling and NLRP3 inflammasome activity [40]. This present investigation demonstrated that TP enhanced functionality of peripheral nerves in diabetic rats through improved control of glycemic status, suppression of neuroinflammation, oxidative stress, and inhibition of hallmark biomarkers. Despite this, the combination therapy improved nociception and nerve conduction velocities by modulating the angiogenic, inflammatory, and oxidative stress markers more than the individual therapies and may prove advantageous when treating diabetic patients with peripheral neuropathy.

5. Conclusion

Based on the findings, *Tridax procumbens* (TP) offered a novel and promising complementary approach to the treatment of diabetes, bringing potential benefits to diabetes neuropathy management. Human subjects can be included in future studies in order to determine what dose of TP extract provides the best control of blood glucose besides optimum management of diabetic neuropathy. TP extract alone for mechanistic studies would validate current findings and allow for detailed phytochemical screening and fractionation for bioactivity-guided assays. In order to determine TP effect on glucose uptake in skeletal muscle cells, independent of insulin signaling, more research is needed. Moreover, future studies can be designed to investigate in more detail the phytochemical composition of the present

extract. Clinical trials need to be designed to study the observed therapeutic effect of the plant in relevant human population. The present investigation provided evidence that TP could be beneficial in managing diabetes through improved peripheral nervous health as well as neuroprotective effect, while offering a mechanistic explanation for the traditionally attributed antidiabetic and anti-inflammatory actions.

Data Availability

The data used or analyzed during the study are available from the corresponding authors.

Ethical Approval

This study was approved by the Institutional Animal Ethics Committee (IAEC) under the protocol No. IAEC/CCP/21/02/PR-010.

Conflicts of Interest

The authors declare that they have no conflicts of interest.

Acknowledgments

This research was supported by Princess Nourah bint Abdulrahman University Researchers Supporting Project number (PNURSP2022R30), Princess Nourah bint Abdulrahman University, Riyadh, Saudi Arabia.

References

- [1] M. M. Engelgau, L. S. Geiss, J. B. Saaddine et al., "The evolving diabetes burden in the United States," *Annals of Internal Medicine*, vol. 140, no. 11, pp. 945–950, 2004.
- [2] A. Menke, S. Casagrande, L. Geiss, and C. C. Cowie, "Prevalence of and trends in diabetes among adults in the United States, 1988–2012," *JAMA*, vol. 314, no. 10, pp. 1021–1029, 2015.
- [3] R. Lee, T. Y. Wong, and C. Sabanayagam, "Epidemiology of diabetic retinopathy, diabetic macular edema and related vision loss," *Eye and Vision*, vol. 2, pp. 17–25, 2015.
- [4] D. Anderson and D. W. Zochodne, "Current ideas on the treatment of diabetic neuropathies," *Expert Review of Endocrinology and Metabolism*, vol. 11, no. 2, pp. 187–195, 2016.
- [5] K. M. Chan, T. Gordon, D. W. Zochodne, and H. A. Power, "Improving peripheral nerve regeneration: from molecular mechanisms to potential therapeutic targets," *Experimental Neurology*, vol. 261, pp. 826–835, 2014.
- [6] S. S. U. Hassan, I. Muhammad, S. Q. Abbas et al., "Stress driven discovery of natural products from actinobacteria with anti-oxidant and cytotoxic activities including docking and ADMET properties," *International Journal of Molecular Sciences*, vol. 22, no. 21, Article ID 11432, 2021.
- [7] M. Majid, A. Farhan, M. I. Asad et al., "An extensive pharmacological evaluation of new anti-cancer triterpenoid (nummularic acid) from *Ipomoea batatas* through in vitro, In Silico, and In Vivo Studies," *Molecules*, vol. 27, 2022.
- [8] I. Muhammad, W. Luo, R. M. Shoaib et al., "Guaiane-type sesquiterpenoids from *Cinnamomum migao* H. W. Li: and their anti-inflammatory activities," *Phytochemistry*, vol. 190, Article ID 112850, 2021.
- [9] S. Shams Ul Hassan, H. Z. Jin, T. Abu-Izneid, A. Rauf, M. Ishaq, and H. A. R. Suleria, "Stress-driven discovery in the natural products: a gateway towards new drugs," *Biomedicine & Pharmacotherapy*, vol. 109, pp. 459–467, 2019.
- [10] T. Sen and S. K. Samanta, "Medicinal plants, human health and biodiversity: a broad review," *Advances in Biochemical Engineering*, vol. 147, pp. 59–110, 2015.
- [11] C. J. Ikwuchi and C. C. Ikwuchi, "Alteration of plasma lipid profile and atherogenic indices of cholesterol loaded rats by *Tridax procumbens* Linn: implications for the management of obesity and cardiovascular diseases," *Biokemistri*, vol. 21, no. 2, pp. 95–99, 2010.
- [12] K. Kohzaki, A. J. Vingrys, and B. V. Bui, "Early inner retinal dysfunction in streptozotocin-induced diabetic rats," *Investigative Ophthalmology & Visual Science*, vol. 49, no. 8, pp. 3595–3604, 2008.
- [13] A. J. King, "The use of animal models in diabetes research," *British Journal of Pharmacology*, vol. 166, no. 3, pp. 877–894, 2012.
- [14] K. R. Patil, U. B. Mahajan, B. S. Unger et al., "Animal models of inflammation for screening of anti-inflammatory drugs: implications for the discovery and development of phytopharmaceuticals," *International Journal of Molecular Sciences*, vol. 20, no. 18, p. 4367, 2019.
- [15] B. Chance and A. Maehly, "The Assay of Catalases and Peroxidases," *Methods of Biochemical Analysis*, vol. 1, 1955.
- [16] H. P. Misra and I. Fridovich, "The role of superoxide anion in the autoxidation of epinephrine and a simple assay for superoxide dismutase," *Journal of Biological Chemistry*, vol. 247, no. 10, pp. 3170–3175, 1972.
- [17] A. Nozad, N. Hamidi, and M. Amani, "The role of glutamate transporter-1 in firing activity of locus coeruleus neurons and nociception in rats," *Experimental Brain Research*, vol. 239, no. 4, pp. 1287–1294, 2021.
- [18] J. R. Deuis, K. Yin, M. A. Cooper, K. Schroder, and I. Vetter, "Role of the NLRP3 inflammasome in a model of acute burn-induced pain," *Burns*, vol. 43, no. 2, pp. 304–309, 2017.
- [19] M. Lundblad, E. Vaudano, and M. A. Cenci, "Cellular and behavioural effects of the adenosine A2a receptor antagonist KW-6002 in a rat model of l-DOPA-induced dyskinesia," *Journal of Neurochemistry*, vol. 84, no. 6, pp. 1398–1410, 2003.
- [20] M. Shimoyama, N. Shimoyama, C. E. Inturrisi, and K. J. Elliott, "Gabapentin enhances the antinociceptive effects of spinal morphine in the rat tail-flick test," *Pain*, vol. 72, no. 3, pp. 375–382, 1997.
- [21] J.-Y. Cherng and M.-F. Shih, "Improving glycogenesis in Streptozocin (STZ) diabetic mice after administration of green algae *Chlorella*," *Life Sciences*, vol. 78, no. 11, pp. 1181–1186, 2006.
- [22] M. Wei, L. Ong, M. T. Smith et al., "The streptozotocin-diabetic rat as a model of the chronic complications of human diabetes," *Heart Lung & Circulation*, vol. 12, no. 1, pp. 44–50, 2003.
- [23] A. Zaidi, S. P. Singh, S. T. Raza, and F. Mahdi, "Role of HBA1C in the diagnosis of patients with diabetes mellitus," *Era's Journal of Medical Research*, vol. 6, no. 2, pp. 78–83, 2019.
- [24] H. Pareek, S. Sharma, B. S. Khajja, K. Jain, and G. C. Jain, "Evaluation of hypoglycemic and anti-hyperglycemic potential of *Tridax procumbens* (Linn.)," *BMC Complementary and Alternative Medicine*, vol. 9, no. 1, p. 48, 2009.

- [25] R. R. Petchi, S. Parasuraman, and C. Vijaya, "Antidiabetic and antihyperlipidemic effects of an ethanolic extract of the whole plant of *Tridax procumbens* (Linn.) in streptozotocin-induced diabetic rats," *Journal of Basic and Clinical Pharmacy*, vol. 4, pp. 88–92, 2013.
- [26] N. E. Cameron and M. A. Cotter, "Effects of antioxidants on nerve and vascular dysfunction in experimental diabetes," *Diabetes Research and Clinical Practice*, vol. 45, pp. 137–146, 1999.
- [27] S. Dewanjee, S. Das, A. K. Das et al., "Molecular mechanism of diabetic neuropathy and its pharmacotherapeutic targets," *European Journal of Pharmacology*, vol. 833, pp. 472–523, 2018.
- [28] L. Piconi, L. Quagliaro, and A. Ceriello, "Oxidative Stress in Diabetes," *Clinical Chemistry and Laboratory Medicine*, vol. 41, 2003.
- [29] H. Yang, X. Jin, C. W. Kei Lam, and S.-K. Yan, "Oxidative stress and diabetes mellitus," *Clinical Chemistry and Laboratory Medicine*, vol. 49, no. 11, pp. 1773–1782, 2011.
- [30] B. Lipinski, "Pathophysiology of oxidative stress in diabetes mellitus," *Journal of Diabetes and Its Complications*, vol. 15, no. 4, pp. 203–210, 2001.
- [31] D. Pitocco, M. Tesauro, R. Alessandro, G. Ghirlanda, and C. Cardillo, "Oxidative stress in diabetes: implications for vascular and other complications," *International Journal of Molecular Sciences*, vol. 14, no. 11, pp. 21525–21550, 2013.
- [32] C. Ikewuchi J, C. Ikewuchi C, and M. Igboh Ngoz, "Chemical profile of *Tridax procumbens* linn," *Pakistan Journal of Nutrition*, vol. 8, no. 5, pp. 548–550, 2009.
- [33] S. de M Bandeira, L. J. S. Da Fonseca, G. da S Guedes, L. A. Rabelo, M. O. Goulart, and S. M. L. Vasconcelos, "Oxidative stress as an underlying contributor in the development of chronic complications in diabetes mellitus," *International Journal of Molecular Sciences*, vol. 14, no. 2, pp. 3265–3284, 2013.
- [34] M. Amadio, C. Bucolo, G. M. Leggio, F. Drago, S. Govoni, and A. Pascale, "The PKC β /HuR/VEGF pathway in diabetic retinopathy," *Biochemical Pharmacology*, vol. 80, no. 8, pp. 1230–1237, 2010.
- [35] T. Rajchgot, S. C. Thomas, J.-C. Wang et al., "Neurons and microglia," *A Sickly-Sweet Duo in Diabetic Pain Neuropathy*, vol. 13, 2019.
- [36] B. P. Tsai, J. Jimenez, S. Lim et al., "A novel Bcr-Abl-mTOR-eIF4A axis regulates IRES-mediated translation of LEF-1," *Open biology*, vol. 4, no. 11, Article ID 140180, 2014.
- [37] S. Ahshin-Majd, S. Zamani, T. Kiamari, Z. Kiasalari, T. Baluchnejadmojarad, and M. Roghani, "Carnosine ameliorates cognitive deficits in streptozotocin-induced diabetic rats: possible involved mechanisms," *Peptides*, vol. 86, pp. 102–111, 2016.
- [38] N. F. Abdelkader, S. M. Ibrahim, P. E. Moustafa, and M. A. Elbaset, "Inosine mitigated diabetic peripheral neuropathy via modulating GLO1/AGEs/RAGE/NF- κ B/Nrf2 and TGF- β /PKC/TRPV1 signaling pathways," *Biomedicine & Pharmacotherapy*, vol. 145, Article ID 112395, 2022.
- [39] Y. Andriana, T. D. Xuan, T. N. Quy, T. N. Minh, T. M. Van, and T. D. Viet, "Antihyperuricemia, antioxidant, and antibacterial activities of *Tridax procumbens* L," *Foods*, vol. 8, no. 1, 2019.
- [40] V. M. Berlin Grace, S. Viswanathan, D. David Wilson et al., "Significant action of *Tridax procumbens* L. leaf extract on reducing the TNF- α and COX-2 gene expressions in induced inflammation site in Swiss albino mice," *Inflammopharmacology*, vol. 28, no. 4, pp. 929–938, 2020.

Research Article

The Effects of Er Xian Decoction Combined with Baduanjin Exercise on Bone Mineral Density, Lower Limb Balance Function, and Mental Health in Women with Postmenopausal Osteoporosis: A Randomized Controlled Trial

Keqiang Li ¹, Hongli Yu,¹ Xiaojun Lin,² Yuying Su,³ Lifeng Gao,⁴ Minjia Song,⁵ Hongying Fan,⁶ Daniel Krokosz,¹ Huixin Yang,⁵ and Mariusz Lipowski ¹

¹Gdansk University of Physical Education and Sport, Gdańsk, Poland

²School of Public Health and Management, Wenzhou Medical University, Wenzhou, China

³Physical Education College, Bohai University, Jinzhou, China

⁴Henan Province Hospital of Traditional Chinese Medicine, Zhengzhou, China

⁵Harbin University of Physical Education, Harbin, China

⁶School of Psychology, Beijing Sport University, Beijing, China

Correspondence should be addressed to Mariusz Lipowski; mariusz.lipowski@awf.gda.pl

Received 31 March 2022; Revised 20 May 2022; Accepted 21 May 2022; Published 30 June 2022

Academic Editor: Rajeev K. Singla

Copyright © 2022 Keqiang Li et al. This is an open access article distributed under the Creative Commons Attribution License, which permits unrestricted use, distribution, and reproduction in any medium, provided the original work is properly cited.

Background. Postmenopausal osteoporosis (PMOP) is a common disease in older women that can severely jeopardize their health. Previous studies have demonstrated the effect of Er xian decoction (EXD) or Baduanjin exercise (BE) on PMOP. However, reports on the effect of EXD combined with BE on PMOP are limited. This study aimed to investigate the impact of EXD combined with BE on bone mineral density (BMD), lower limb balance, and mental health in women with PMOP. **Methods.** A 1:1:1 simple randomization technique was employed. Fifty participants with postmenopausal osteoporosis were allocated to three groups: the EXD group (EXD = 15); the BE group (BE = 18); and the combined group (EXD + BE = 17). After both 8 weeks and 16 weeks of intervention treatment, participants improved significantly with respect to BMD and the one-leg standing test (OLST), Berg balance scale (BBS), timed up and go (TUG) test, self-anxiety scale (SAS), and self-rating depression scale (SDS). The results were used to compare the effect of the intervention on BMD, lower limb balance function, and mental health in patients with PMOP. **Results.** Compared to the EXD and BE groups, the EXD + BE group showed the strongest effects on BMD, lower limb balance function, and mental health ($p < 0.01$). A correlation between BMD and lower limb balance and mental health was noted in the EXD + BE group. The change in mental health (SAS score) was correlated with BMD (femoral neck) improvement. **Conclusions.** The present study demonstrates that EXD combined with BE (EXD + BE) may have a therapeutic advantage over both monotherapies for treating BMD, lower limb balance function, and mental health in patients with PMOP. The feasibility of the approach for a large-scale RCT was also confirmed. Er xian decoction combined with Baduanjin exercise (EXD + BE) might offer a viable treatment alternative for participants with postmenopausal osteoporosis given its promising effects in disease control and treatment, with good efficacy and safety profiles.

1. Introduction

Osteoporosis is a systemic, multifactorial disease that causes morbidity and mortality in the elderly and is increasing in prevalence worldwide [1]. Many factors contribute to

osteoporosis, such as estrogen deficiency, genetics, nutritional deficiencies, chronic diseases, and aging. Postmenopausal osteoporosis (PMOP) symptoms are mainly characterized by a decrease in bone mineral density (BMD) and changes in biochemical indicators of bone metabolism

[2], which affect the stability of the lower limbs and increase the risk of fracture. Meanwhile, the decrease in BMD, bone loss, and increased fracture risk has a strong negative impact on the mental health of postmenopausal women with osteoporosis [3–8]. Western medicine is still the primary treatment for women with PMOP. However, the long-term use of Western medicine still cannot completely cure the disease. Moreover, most Western drugs are expensive, have adverse side effects, and damage the patient's body. Examples of such medications include bisphosphonates, tibolone, calcitonin, and parathyroid hormone (PTH) therapy [9–11]. Many animal studies and clinical experiments have proved that traditional Chinese medicine has a significant effect on the prevention and treatment of postmenopausal osteoporosis (PMOP) and has fewer side effects on the body than chemically synthesized medicines [12]. Therefore, the treatment of PMOP with traditional Chinese medicine will be examined in this paper.

Er xian decoction (EXD) is a multi-herb formula composed of six herbs, namely, *Rhizome curculiginis*, *Herba epimedii*, *Radix Morinda officinalis*, *Rhizome anemarrhenae*, *Cortex Phellodendron*, and *Radix Angelica sinensis*. It has several biological and pharmacological effects [13]. It has long been used to treat osteoporosis, perimenopausal syndrome, and age-related diseases in elderly patients [14–16].

EXD can improve BMD [17], promote endocrine activity and provide antioxidants [13], and treat menopause-related symptoms [18, 19]. Moreover, studies have reported that EXD is effective and safe in reducing the frequency and severity of hot flashes and improving menopausal symptoms in perimenopausal women in Hong Kong [18]. EXD showed neuroprotective effects on corticosterone-injured PC12 cells in vitro and improved depression-like behavior in mice [20]. In OVX rats, atrophy of the uterus and reduction of BMD were suppressed by treatment with EXD (*Herba epimedii*) [17]. Additionally, studies have reported that EXD can stimulate the secretion of T from Leydig cells, P from luteal cells, and E2 from granulosa cells [15].

The effectiveness of Baduanjin as an exercise intervention has been recognized in many international studies [21]. It consists of eight independent, simple, subtle, and smooth movements and is a form of qigong. BE, an important means of Chinese traditional rehabilitation therapy [21], can improve patients' blood microcirculation, transport blood calcium to the bone, promote calcium absorption, promote bone mineral salt deposition, promote and increase the proliferation and activity of bone cells, delay bone loss with age, and increase BMD [22]. Although the potential effectiveness of each movement may be different, the overall Baduanjin exercise (BE) has been demonstrated to improve physical and psychological health [23, 24]. One study has reported that a 12-week BE program significantly prevents bone loss in middle-aged women [23]. In addition, clinical observation shows that BE improves balance and fall risk in patients with senile osteoporosis [25]. Finally, a comprehensive review shows that BE facilitates improvements in psychological health and may be a suitable choice for interventions [24]. Although several studies have

demonstrated a stimulatory effect of exercise on bone tissue, it is not recommended as a substitute for medical treatment.

Few published studies have investigated the effects of combination therapy using physical exercise and drugs to treat osteoporosis. Therefore, this study aims to evaluate the effect of EXD combined with BE on patients with PMOP. After 8 weeks and 16 weeks of intervention, measurements were performed to investigate the impact of the different treatments on the BMD, lower limb balance function, and mental health of study participants.

2. Methods and Materials

2.1. Study Design and Participants

2.1.1. Experimental Design. This study enrolled 57 participants. Seven participants dropped out after the first screening for personal reasons unrelated to the study. Two had a scheduling conflict, two did not give a reason, and three could not perform the exercises. The remaining 50 eligible subjects were enrolled and randomly assigned to the BE group (BE, $n=18$), EXD group (EXD, $n=15$), and combined group (BE + EXD, $n=17$). All participants completed their intervention (Figure 1).

2.1.2. Participants. From September 2021 to February 2022, 57 older citizens from six villages were randomly selected from the Lingxi Township of Wenzhou City, Zhejiang Province, China. The participants were between 50 and 70 years old, and they were required to have lived in the selected villages for more than six months in the past year. The participants completed a questionnaire survey that included the inclusion and exclusion criteria. After the screening, two participants left with no reason provided, two left the study due to scheduling conflicts, and three were excluded because their physical conditions were unsuitable. Finally, a total of 50 participants qualified for the study.

2.2. Diagnostic Criteria for Subject Recruitment

2.2.1. Inclusion Criteria. The inclusion criteria were as follows: women are aged from 50 to 79 years old and have been in natural menopause for more than one year; the BMD T score of the lumbar spine (L2–L4) or femoral shaft is -2.5 or less; the anatomical structure of the lumbar spine is suitable for dual-energy X-ray bone density measurement, and there is no severe scoliosis, trauma, or sequelae related to bones or surgery; the participant is in good health and can move outdoors for at least 30 minutes every day; the participant can understand the research process, is willing to participate in a treatment trial, and signed the informed consent form.

2.2.2. Exclusion Criteria. The exclusion criteria were as follows: the participant suffers from other severe somatic diseases or dysfunctions; the participant is unable to stand stably in place for 30 minutes; the participant has taken other anti-osteoporosis drugs (desquamate, estrogen, raloxifene)

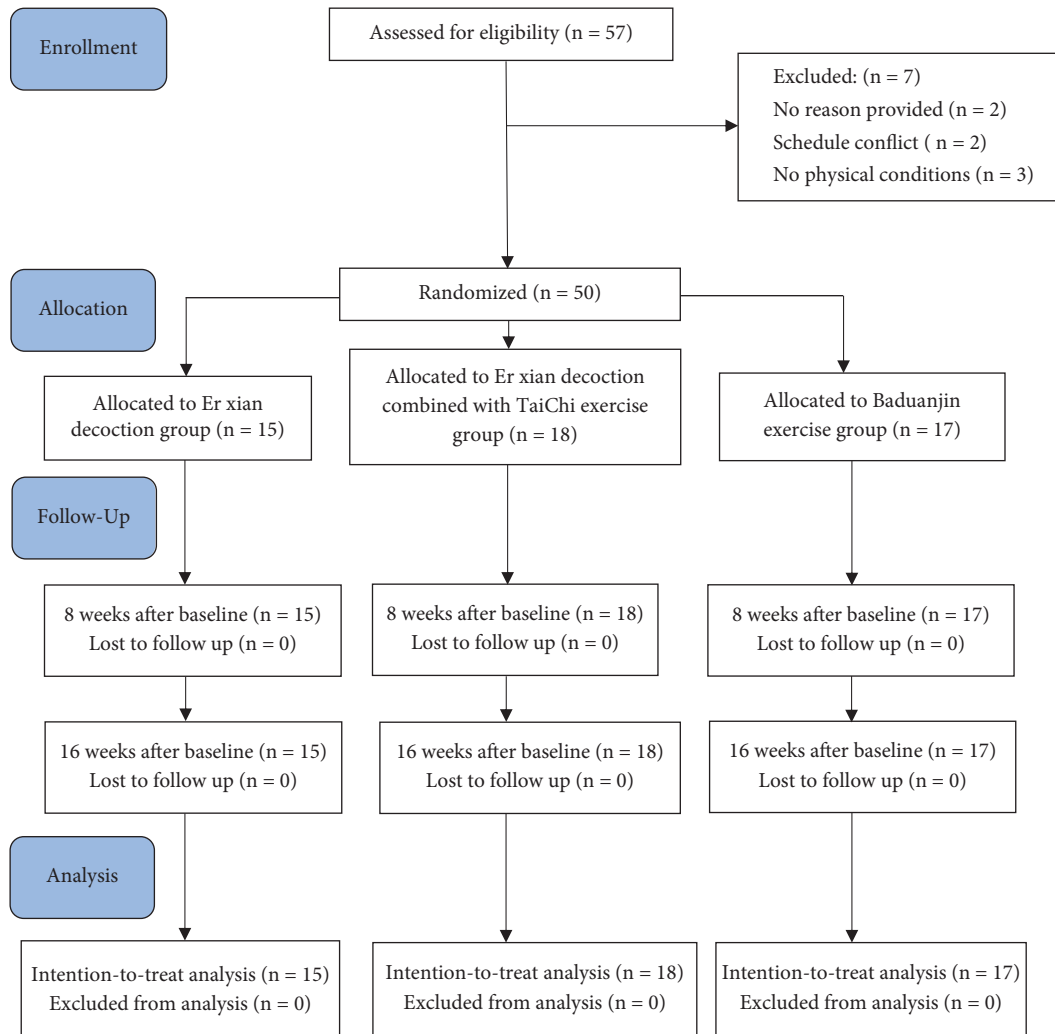


FIGURE 1: Study flow diagram of the progress through the phases of the experiment.

orally less than three months before entering the group; the participant suffers from mental illness or cognitive dysfunction.

2.3. Randomization and Allocation. Fifty participants who fulfilled the eligibility criteria were randomly allocated to three intervention-based groups: the BE group (BE, $n = 18$), EXD group (EXD, $n = 15$), or combined group (BE + EXD, $n = 17$). To ensure blinding, an independent researcher who was not a part of this study performed the randomized allocation. A 1:1:1 simple randomization technique was employed. A unique, random, computer-generated code was assigned to each participant via SPSS (version 26.0, Armonk, New York, USA). The allocation was concealed in sealed, opaque envelopes that were provided to researchers before applying the assigned interventions. All study personnel and participants were blinded to the treatment assignment for the duration of the trial. The experimental intervention times for the three groups were 8 weeks and 16 weeks.

2.4. Intervention. Calcium carbonate D3 tablets (Caltrate), a health supplement, can positively affect bone density. These primary drugs were given to all participants, who were asked to take two tablets once a day for 16 weeks (calcium carbonate D3 tablets (Caltrate); approval number: Sinopharm Zhunzi H10950029; manufacturer: Wyeth Pharmaceutical Co., Ltd.; specification: 600 mg).

2.4.1. Baduanjin Exercise Group (BE; $n = 17$). The participants in this group performed BE for 8 weeks and 16 weeks and continued to use their primary drugs. In the first week, they were guided by a professional Baduanjin coach. Then, they began a formal 15-week BE intervention period after mastering the moving and breathing methods. During this intervention period, the participants exercised independently. Each week, they performed the BE movements no fewer than five times, for a total duration of 45 minutes per session [26]. They prepared for exercises for 5 minutes

before practice, and they practiced once a day. Follow-up was performed every two weeks by the coach who adjusted the exercise intensity according to the specific situation of the participants.

2.4.2. Er Xian Decoction Group (EXD; $n = 15$). Participants in this group continued to use their primary drugs and also took EXD. The medicinal components of EXD are as follows: *Rhizoma curculiginis* (15 g), *Herba epimedii* (15 g), *Radix Angelica sinensis* (10 g), *Cortex Phellodendri* (10 g), *Rhizoma anemarrhenae* (10 g), and *Radix Morinda officinalis* (10 g) [27]. The medicine was mixed with 800 ml water, decocted to 150 ml, and taken once daily. The participants consumed the EXD for 16 weeks [28].

2.4.3. Combined Group (BE + EXD; $n = 18$). In addition to consuming primary drugs and EXD, the participants in this group performed the BE for 8 weeks and 16 weeks. In the first week, they were guided by a professional Baduanjin coach and then began a formal 15-week intervention period of BEs after mastering the moving and breathing methods. During this intervention period, the participants exercised independently and performed the BE no fewer than five times per week for a total duration of 45 minutes per session [26]. They prepared for the exercises for 5 minutes before practice and practiced once a day. Follow-up was performed every two weeks by the coach who adjusted the exercise intensity appropriately according to the specific situation of each participant.

2.5. Measurements

2.5.1. Bone Mineral Density (BMD). A dual-energy X-ray absorptiometry (DEXA) scan is a valid and reliable tool for measuring BMD (Prodigy-GE Healthcare, Chicago, IL, USA) [29]. During a DEXA scan, participants lay supine on an open X-ray table. The participants were asked to keep still during the scan as the large scanning arm passed over their bodies. A trained radiologist scanned each participant's hip and spine regions for approximately 20 minutes. Using the information from the DEXA scans, the participants were classified into the normal bone mass density (score between -1 and 0 or higher), osteopenia (between -1.1 and -2.4), and osteoporosis (a score of -2.5 or less) [30]. We also calculated the Z-score, which compares the obtained bone density to the age-matched normal average bone and is often helpful in cases of severe osteoporosis [30, 31].

2.5.2. One-Leg Standing Test (OLST). An OLST was used to assess static balance. The participants were asked to close their eyes, stand on their preferred leg, lift the other leg to an approximately 90° angle at the knee, keep their arms by their sides, and maintain balance without using any assistive device. The test was completed when the stance foot shifted or when the lifted foot was replaced on the ground (whichever occurred first). Each participant had three attempts for each leg. The standing duration (in seconds) was

recorded for each attempt, and the best (longest) score was selected for analysis [32]. Cronbach's α value of this test is 0.69.

2.5.3. Berg Balance Scale (BBS). The BBS includes 14 items: standing up from a sitting position; standing without support; sitting position without a backrest, but landing with both feet or putting them on a stool; sitting down from a standing position; transferring; closing eyes without support; standing with both feet together without support; stretching upper limbs and moving forward in standing position; picking up articles from the ground in a standing position; turning to look back in a standing position; turning 360 degrees; putting one foot on a step or stool in a standing position without support; and standing without support with one foot in front. The scoring standard of each item was from 0 to 4, and the total score was from 0 to 56. This range is divided into five grades: zero, poor, fair, good, and normal [33]. Cronbach's α value of this test is 0.77.

2.5.4. Timed Up and Go (TUG) Test. In the TUG test, participants sat on a straight-back chair (the chair's seat height is about 45 cm), wearing the shoes they usually wear, and then leaned against the back of the chair with their hands crossed at their chest. After the "start" instruction, the subjects immediately stood up from the chair, walked forward for 3 meters at their normal walking gait, and turned around after passing the 3-meter marker. Then, they walked back to the chair and sat down, returning to the starting position. The participants could not receive any help during the test [34]. The time was recorded (in seconds) with a stopwatch. Before the formal test, the subjects could practice once or twice to ensure that they understood the whole test process. The formal test was conducted three times, and the average value was taken. The scoring criteria are as follows: If completion time is <10 seconds, the subject can conduct free movement. If completion time is <20 seconds, the subject can move independently. If completion time is 20–29 seconds, the subject's activity is unstable, and there is a high risk of falling. If completion time is >30 seconds, there is an obstacle to activity. Cronbach's α value of this test is 0.71.

2.5.5. Self-Anxiety Scale (SAS). The SAS is used to evaluate the subjective feelings of anxiety in patients and can be used as a self-assessment tool for the clinical understanding of anxiety symptoms [35]. It consists of 20 items, and the frequency of symptoms defined by the items is evaluated according to the following scales: 1–4.1 means "given the other items, 'never or rarely' would be more natural than 'no or few'"; 2 means "sometimes"; 3 means "most of the time"; and 4 means "always." The scores of items 5, 9, 13, 17, and 19 must be calculated in reverse, and the rest can be calculated in sequence. The scores of the 20 items are added to get the rough score, and the rough score is multiplied by 1.25 to obtain the standard score. The critical standard of anxiety assessment in China is 50 points, and a score of 50 points or

more indicates anxiety. Cronbach's α value of this measure is 0.62.

2.5.6. Self-Rating Depression Scale (SDS). SDS is a short-term self-rating scale compiled by Zung in 1965 [36]. It is easy to implement and can effectively reflect the symptoms of depression, together with their severity and changes. The scale consists of 20 declarative sentences and corresponding question items. Each item is equivalent to a related symptom, which is graded according to four levels: 1 is "never or rarely," 2 is "sometimes," 3 is "most of the time," and 4 is "always." Ten of the 20 items (items 2, 5, 6, 11, 12, 14, 16, 17, 18, and 20) are scored in reverse order. The scores of the 20 items are summed to obtain the rough score, and the rough score is multiplied by 1.25 to obtain the standard score. Cronbach's α value of this test is 0.85.

2.6. Sample Size. The sample size was determined based on our pilot study using $G * Power$ 3 [37]. An a priori, repeated-measure ANOVA indicated that a total sample size of 50 was needed to achieve 95% power to detect the interaction effect size of 0.21 at a 0.05 level of significance. A total sample size of 57 participants was enrolled in the study.

2.7. Statistical Analyses. Statistical analysis was performed using SPSS (version 26.0, Armonk, New York, USA). The Shapiro–Wilk tests were performed to determine the normality of the data distribution. Normally distributed data were expressed as means with SDs, and Student's t -test was used to compare between-group differences. Non-normally distributed data were presented using the median (P25, P75), and the Mann–Whitney U test was used. The baseline characteristics between comparison groups were analyzed using the chi-square (χ^2) test or Fisher's exact test for categorical variables described as frequencies (percentages). We used the paired t -test to compare the differences within the group at baseline and at 8 and 16 weeks. An ANOVA with repeated measurements with post hoc tests was used to compare the differences between different groups, as this technique is more appropriate for examining the effect of the combined treatment on BMD, lower limb balance function, and mental health of patients with PMOP. Statistical significance was defined as $p < 0.05$, and $p < 0.01$ was the standard of high statistical significance. The correlation analysis was used to analyze the correlation between lower limb balance, changes in mental health, and BMD improvement.

3. Results

3.1. Descriptive Statistics of Sociodemographic Information of the Three Groups. The study included 50 participants with PMOP, and the largest employment group was farmers (42%). Married participants comprised 84% of the sample. No significant differences were noted among the three groups in terms of social demographic data, including age, occupation, BMI, duration of menopause, duration of

PMOP, and marital status. Table 1 shows the demographic data.

3.2. BMD in Three Groups at Baseline, 8 Weeks, and 16 Weeks. Before the intervention, there was no significant difference between the three groups in the BMD of the lumbar spine (L2–4) and femoral neck ($p > 0.05$). After both 8 weeks and 16 weeks of intervention, the BMD of the lumbar spine and femoral neck in the EXD + BE and EXD groups was higher than that at the baseline ($p < 0.05$). Furthermore, the BMD of the lumbar spine and femoral neck was higher in the EXD + BE group than in the BE group ($p < 0.05$). The BMD of the lumbar spine and femoral neck in the EXD + BE group was higher than that in the EXD group ($p < 0.01$; Table 2 and Figure 2).

3.3. OLST, BBS, and TUG in Three Groups at Baseline, 8 Weeks, and 16 Weeks. Before the intervention, there was no significant difference in the OLST, BBS, and TUG scores between the three groups ($p > 0.05$). After 8 weeks and 16 weeks of intervention, the OLST, BBS, and TUG scores in the EXD + BE and BE groups were higher than those at the baseline ($p < 0.05$). The OLST, BBS, and TUG scores in the EXD + BE group were higher than those in the BE group ($p < 0.05$). Meanwhile, the OLST, BBS, and TUG scores in the EXD + BE group were higher than those in the EXD group ($p < 0.01$; Table 3 and Figure 3).

3.4. Mental Health in Three Groups at Baseline, 8 Weeks, and 16 Weeks. Before the intervention, there was no significant difference between the three groups in SAS and SDS ($p > 0.05$). After 8 weeks and 16 weeks of intervention, the SAS and SDS scores in the EXD + BE, BE, and EXD groups were higher than those at the baseline ($p < 0.05$). The SAS and SDS scores in the EXD + BE group were higher than those in the BE and the EXD groups ($p < 0.05$; Table 4 and Figure 4).

3.5. Correlation between Changes in Mental Health, Lower Limb Balance Function, and Improvement of BMD. After 8 weeks and 16 weeks of intervention, the BMD, lower limb balance, and mental health of participants in all three groups improved. We used correlation analysis to analyze the correlation between lower limb balance, changes in mental health, and BMD improvement. The results (Table 5 and Figure 5) show a significant positive correlation between lower limb balance (BBS) and BMD improvement (LS L2–4; $r = 0.359$, $p < 0.05$). Moreover, the results show a significant negative correlation between lower limb balance (TUG) and BMD improvement (LS L2–4; $r = 0.521$, $p < 0.01$). However, there is no significant correlation between BMD and OLST. In addition, the change in mental health (SAS) was negatively correlated with BMD (FN) improvement ($r = -0.576$, $p < 0.01$). However, there is no significant correlation between BMD and mental health (SDS).

TABLE 1: Demographic data.

Variable		EXD (<i>n</i> = 15)	BE (<i>n</i> = 17)	EXD + BE (<i>n</i> = 18)	<i>p</i>
Age (years)		56.41 ± 1.68	57.02 ± 1.64	57.31 ± 1.48	0.317
Employment status	Worker	4 (26.6%)	5 (29.4%)	5 (27.8%)	0.578
	Manager	0	2 (11.8%)	0	
	Farmer	6 (40%)	7 (41.2%)	8 (44.4%)	
	Other	5 (33.4%)	3 (17.6%)	5 (27.8%)	
BMI (kg/m ²)		24.36 ± 2.03	24.48 ± 2.09	24.54 ± 1.99	0.486
Duration of menopause (years)		6.44 ± 1.81	6.51 ± 1.23	6.23 ± 2.21	0.37
Duration of PMOP (years)		4.66 ± 1.61	4.47 ± 1.24	4.31 ± 1.43	0.547
Marital status	Married	13 (86.7%)	14 (82.4%)	15 (83.3%)	0.942
	Other	2 (13.3%)	3 (17.6%)	3 (16.7%)	

TABLE 2: Changes in BMD in the three groups at baseline, 8 weeks, and 16 weeks (g/cm³, *x* ± *s*), *n* = 50.

Variable by group	No.	Mean (SE)			From baseline to 16 weeks, mean (95% CI)	
		Baseline	8 wk	16 wk	Within-group change	Between-group difference change
Lumbar spine L2-4 (g/cm³)						
EXD	15	0.73 ± 0.01	0.78 ± 0.03	0.82 ± 0.02	0.09 (0.07 to 0.1) ^a	NA
BE	17	0.72 ± 0.02	0.67 ± 0.01	0.76 ± 0.01	0.04 (0.03 to 0.05)	NA
EXD + BE	18	0.75 ± 0.01	0.87 ± 0.01	0.98 ± 0.01	0.23 (0.22 to 0.24) ^a	NA
EXD vs. BE	NA	NA	NA	NA	NA	0.06 (0.05 to 0.07)
EXD vs. EXD + BE	NA	NA	NA	NA	NA	-0.15 (-0.16 to -0.14) ^a
BE vs. EXD + BE	NA	NA	NA	NA	NA	-0.22 (-0.23 to -0.21) ^a
Femoral neck (g/cm³)						
EXD	15	0.75 ± 0.01	0.81 ± 0.01	0.85 ± 0.01	0.1 (0.09 to 0.11) ^a	NA
BE	17	0.75 ± 0.01	0.77 ± 0.01	0.75 ± 0.01	0 (-0.01 to 0)	NA
EXD + BE	18	0.73 ± 0.01	0.87 ± 0.01	0.97 ± 0.01	0.24 (0.23 to 0.25) ^b	NA
EXD vs. BE	NA	NA	NA	NA	NA	0.1 (-0.09 to 0.11) ^a
EXD vs. EXD + BE	NA	NA	NA	NA	NA	-0.11 (-0.12 to -0.1) ^a
BE vs. EXD + BE	NA	NA	NA	NA	NA	-0.21 (-0.22 to -0.2) ^a

Note. BE: BE group; EXD: EXD group; EXD + BE: EXD combined with BE; LS: lumbar spine L2-4; FN: femoral neck; NA: not applicable. a: *p* < 0.05, b: *p* < 0.01.

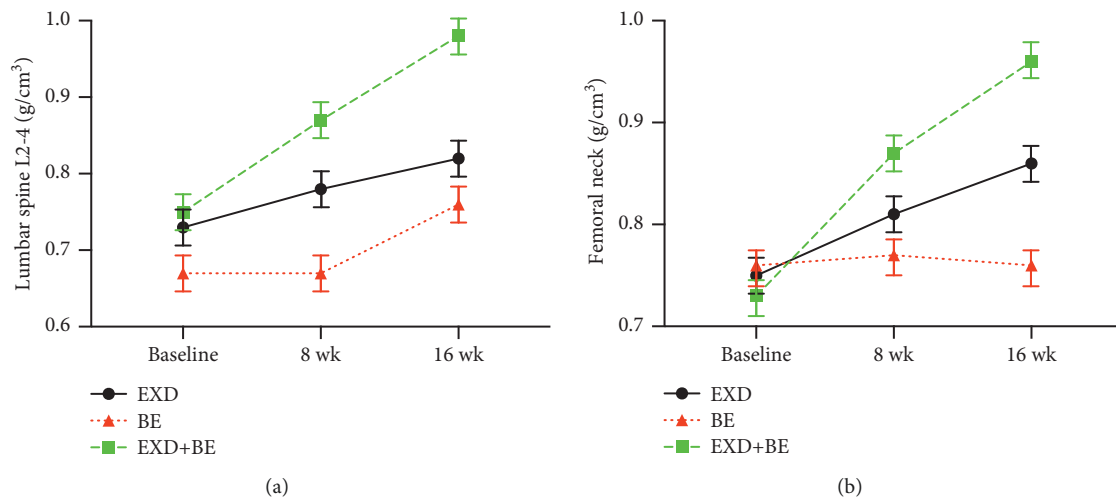


FIGURE 2: Changes in BMD in the three groups at baseline, 8 weeks, and 16 weeks.

TABLE 3: Changes in OLST, BBS, and TUG in the three groups at baseline, 8 weeks, and 16 weeks ($x \pm s$), $n = 50$.

Variable by group	No.	Mean (SE)			From baseline to 16 wk, mean (95% CI)	
		Baseline	8 wk	16 wk	Within-group change	Between-group difference change
Left leg balance (eyes closed), s						
EXD	15	3.74 ± 0.17	4.11 ± 0.15	4.83 ± 0.18	1.09 (0.956 to 1.22) ^a	NA
BE	17	3.66 ± 0.22	8.76 ± 0.25	8.82 ± 0.18	5.16 (5 to 5.31) ^b	NA
EXD + BE	18	3.81 ± 0.17	9.12 ± 0.13	9.21 ± 0.17	5.4 (5.26 to 5.53) ^b	NA
EXD vs. BE	NA	NA	NA	NA	NA	-3.98 (-4.11 to -3.85) ^b
EXD vs. EXD + BE	NA	NA	NA	NA	NA	-4.38 (-4.51 to -4.25) ^b
BE vs. EXD + BE	NA	NA	NA	NA	NA	-0.39 (-0.52 to -0.27)
Right leg balance (eyes closed), s						
EXD	15	3.55 ± 0.07	3.54 ± 0.06	3.66 ± 0.19	0.11 (-0.02 to 0.24)	NA
BE	17	3.74 ± 0.15	7.71 ± 0.18	7.23 ± 0.18	3.48 (3.36 to 3.61) ^b	NA
EXD + BE	18	3.88 ± 0.22	7.21 ± 0.18	7.30 ± 0.19	3.41 (3.26 to 3.57) ^b	NA
EXD vs. BE	NA	NA	NA	NA	NA	-3.56 (-3.7 to -3.42) ^b
EXD vs. EXD + BE	NA	NA	NA	NA	NA	-3.63 (-3.77 to -3.5) ^b
BE vs. EXD + BE	NA	NA	NA	NA	NA	-0.07 (-0.2 to 0.05)
TUG, s						
EXD	15	7.33 ± 0.18	7.31 ± 0.16	7.53 ± 0.24	0.19 (-0.01 to 0.38)	NA
BE	17	7.48 ± 0.23	7.28 ± 0.17	7.14 ± 0.18	-0.34 (-0.49 to -0.19) ^a	NA
EXD + BE	18	7.23 ± 0.14	6.67 ± 0.16	6.54 ± 0.19	-0.68 (-0.77 to -0.59) ^b	NA
EXD vs. BE	NA	NA	NA	NA	NA	0.38 (0.24 to 0.52)
EXD vs. EXD + BE	NA	NA	NA	NA	NA	0.98 (0.85 to 1.12) ^c
BE vs. EXD + BE	NA	NA	NA	NA	NA	0.6 (0.47 to 0.73) ^b
BBS						
EXD	15	38.36 ± 2.08	36.33 ± 1.15	39.24 ± 1.38	0.87 (-0.43 to 2.18)	NA
BE	17	38.33 ± 1.57	39.33 ± 1.78	41.39 ± 2.16	3.06 (1.78 to 4.33) ^a	NA
EXD + BE	18	39.31 ± 1.26	44.27 ± 1.58	45.23 ± 1.02	5.92 (5.12 to 6.72) ^b	NA
EXD vs. BE	NA	NA	NA	NA	NA	-2.15 (-3.29 to -1.01) ^a
EXD vs. EXD + BE	NA	NA	NA	NA	NA	-5.99 (-7.11 to -4.86) ^c
BE vs. EXD + BE	NA	NA	NA	NA	NA	-3.84 (-4.92 to -2.75) ^b

Note. BE: BE group; EXD: EXD group; EXD + BE: EXD combined with BE; OLST: one-leg standing test; BBS: Berg balance scale test score; TUG: timed up and go test; NA: not applicable. a: $p < 0.05$, b: $p < 0.01$, c: $p < 0.001$.

4. Discussion

This study aimed to evaluate the effectiveness of the combination of EXD and BE on the BMD, lower limb balance function, and mental health of patients with PMOP. The research reflected the practical need to find a harmless, non-pharmaceutical intervention with minimal side effects, and the results support the feasibility and acceptability of EXD combined with BE in clinical trials. Our main finding is the significant increase of BMD in patients with PMOP in the EXD + BE group. In contrast, no significant improvement was observed in the EXD group or the BE group. Furthermore, participants in the EXD + BE group also showed a simultaneous improvement in lower limb balance function and mental health. In addition, these changes in lower limb balance function and mental health are significantly correlated with the improvement of BMD. The participants had no adverse reactions during the intervention, and all the participants were satisfied with the intervention program.

4.1. The Effects of EXD Combined with BE on BMD in Women with PMOP. One of our most remarkable findings is that the overall effect of the EXD + BE intervention on BMD is significantly higher than that of the BE or EXD groups. This is notable given that most studies, including both population

and experimental studies, have confirmed that EXD or exercise can improve BMD [12, 14, 23, 38–42].

In addition to medication, exercise can improve BMD. Exercise has attracted much clinical attention because of its convenience, affordability, and safety, and it has been recommended by many guidelines for the prevention and treatment of osteoporosis [43, 44]. It has been proven that exercise can effectively intervene in the symptoms of PMOP [45–48].

The effect of exercise on estrogen levels may explain its therapeutic effect. Estrogen deficiency and bone resorption of osteoclasts are important causes of PMOP. Moreover, estrogen plays a very important role in the mechanism of female bone metabolism. Studies have shown that exercise can promote a slight increase in estrogen concentration [45]. Estrogen inhibits the secretion of thyroid hormone, which, in turn, reduces bone absorption, promotes the secretion of calcitonin, and reduces bone resorption. Estrogen receptors secrete factors that can effectively improve the proliferation of osteoblasts and promote bone-transforming growth factor β . Furthermore, the production of bone collagen molecules indirectly reduces the activity of osteoblasts, increases kidney 25-hydroxyl α -hydroxylase activity, and increases the production of 1, 25-(OH) 2D3 to increase the calcium absorption rate of the small intestine [48].

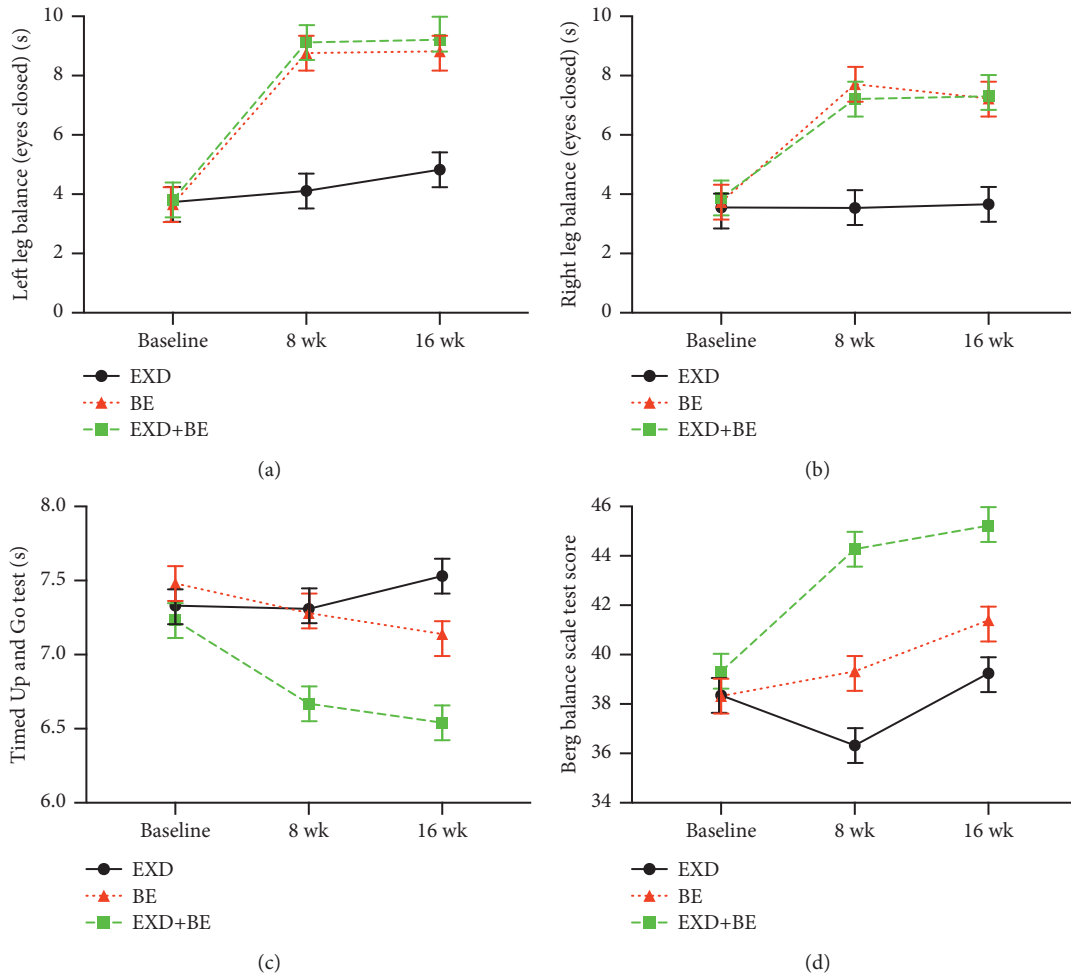


FIGURE 3: Changes in OLST, BBS, and TUG in the three groups at baseline, 8 weeks, and 16 weeks.

TABLE 4: Change in mental health (SDS, SAS) in the three groups at baseline, 8 weeks, and 16 weeks ($n = 50$).

Variable by group	No.	Mean (SE)			From baseline to 16 weeks, mean (95% CI)	
		Baseline	8 weeks	16 weeks	Within-group change	Between-group difference change
SDS						
EXD	15	51.22 ± 1.74	49.63 ± 1.72	47.07 ± 2.19	-4.14 (-5.33 to -2.95) ^b	NA
BE	17	50.03 ± 1.85	49.51 ± 1.38	47.06 ± 1.81	-2.96 (-4.45 to -1.47) ^a	NA
EXD + BE	18	50.71 ± 2.04	47.53 ± 2.01	46.06 ± 2.26	-4.64 (-6.13 to -3.16) ^b	NA
EXD vs. BE	NA	NA	NA	NA	NA	0.01 (-1.48 to 1.5)
EXD vs. EXD + BE	NA	NA	NA	NA	NA	1.01 (-0.46 to 2.49) ^a
BE vs. EXD + BE	NA	NA	NA	NA	NA	1 (-0.42 to 2.43) ^a
SAS						
EXD	15	53.45 ± 1.94	51.39 ± 2.11	50.55 ± 2.06	-2.89 (-4.67 to -1.12) ^a	NA
BE	17	50.84 ± 1.83	49.83 ± 1.82	46.65 ± 2.28	-4.18 (-5.38 to -2.98) ^b	NA
EXD + BE	18	53.37 ± 1.83	49.58 ± 1.31	46.02 ± 1.23	-7.34 (-8.56 to -6.13) ^c	NA
EXD vs. BE	NA	NA	NA	NA	NA	3.89 (2.54 to 5.24) ^b
EXD vs. EXD + BE	NA	NA	NA	NA	NA	4.52 (3.19 to 5.86) ^b
BE vs. EXD + BE	NA	NA	NA	NA	NA	0.63 (-0.65 to 1.92)

Note. BE: BE group; EXD: EXD group; EXD + BE: EXD combined with BE; SAS: self-anxiety scale; SDS: self-rating depression scales; NA: not applicable. a: $p < 0.05$, b: $p < 0.01$, c: $p < 0.001$.

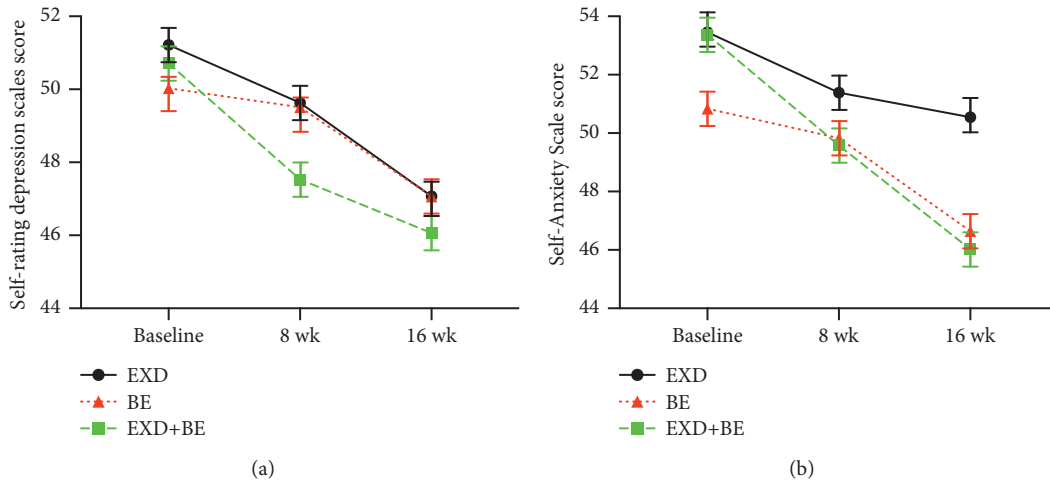


FIGURE 4: Change in mental health (SDS, SAS) in the three groups at baseline, 8 weeks, and 16 weeks.

TABLE 5: Correlations between changes in lower limb balance, mental health, and BMD.

Variable	BBS	TUG	OLST	SAS	SDS
LS L2-4	0.359 ^a	-0.521 ^b	-0.041	0.353	0.063
FN	-0.089	0.096	0.116	-0.576 ^b	-0.266

Note. The data in the table are the correlation coefficient (r). a: $p < 0.05$; b: $p < 0.01$. LSL2-4: lumbar spine L2-4; FN: femoral neck; OLST: one-leg standing test; BBS: Berg balance scale test score; TUG: timed up and go; SAS: self-anxiety scale; SDS: self-rating depression scales.

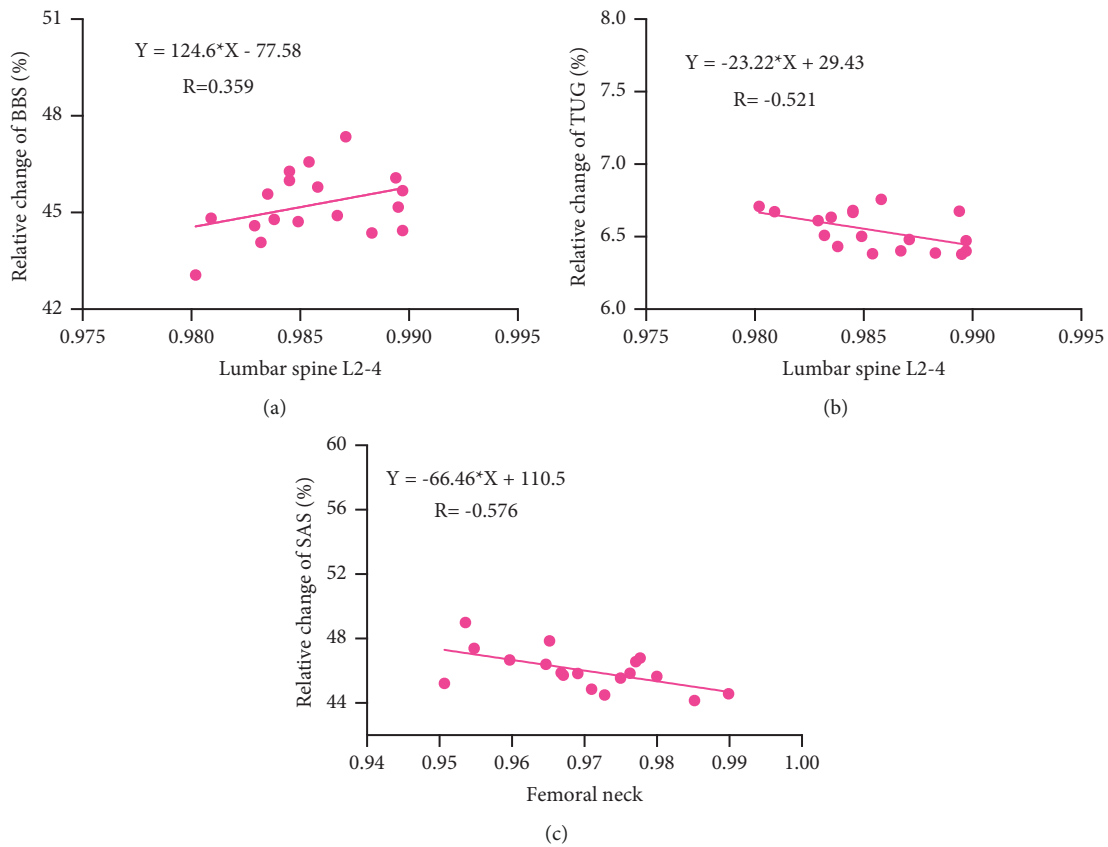


FIGURE 5: Correlations between changes in lower limb balance, mental health, and BMD.

Meanwhile, BE can fully stretch the muscles of the spine, neck, waist, and hip; increase the flexibility of neck and waist movement and muscle strength; and stimulate the bone cells of corresponding segments to strengthen tendons and bones.

We found that combining EXD with BE (EXD + BE) had more advantageous effects on the prevention of bone loss and the improvement of BMD in patients with PMOP than either intervention on its own. However, this study shows only that exercise combined with medicine may have a therapeutic advantage over each monotherapy in improving BMD; the detailed mechanism is not completely clear as to whether this is merely an additive benefit or whether there is some synergistic effect between the two mechanisms. At present, there is no literature about the mechanism by which EXD combined with BE improves BMD. Thus, a longer-term trial would be required to evaluate the effects of EXD combined with BE on BMD.

4.2. The Effects of EXD Combined with BE on Lower Limb Balance Function and Mental Health in Women with PMOP. Our study also demonstrated that the participants in the EXD + BE group showed significant improvement in lower limb balance. The present study supports previous studies showing the improvement of lower limb balance function from EXD and BE [17, 21, 40, 49–51]. In addition, there is a significant positive correlation between lower limb balance (BBS test score) and BMD improvement (lumbar spine L2–4; $r=0.402$, $p<0.05$). Meanwhile, we observed a significant negative correlation between lower limb balance (TUG test score) and BMD improvement (femoral neck; $r=0.661$, $p<0.01$). However, there was no significant correlation between BMD and lower limb balance (OLST). These findings were consistent with results reported in other studies [52, 53].

Second, we observed significant improvements in mental health from EXD combined with BE. These improvements are related to improving BMD in patients with PMOP, and this result is consistent with the research of other scholars [13, 54–59]. In addition, the change in mental health (self-anxiety score) was negatively correlated with BMD improvement (lumbar spine L2–4; $r=-0.625$, $p<0.01$). However, we observed no significant correlation between BMD and mental health (self-rating depression score). These findings are in line with other studies [60].

In summary, positive effects of EXD combined with BE were observed on lower limb balance and mental health in women with PMOP, but the detailed mechanisms need further study.

5. Limitations of the Study

This study has several limitations. First, the study has a small sample size for exercise intervention research. As a result, its reference value for new clinical intervention methods is limited.

Second, our study did not add clinical data for auxiliary measurement, which led to an increase in the deviation of the research results. The patients with PMOP in the EXD + BE group experienced interference and influence on indexes related to the investigation, especially on mental health. This is due to an increase in group communication and the Hawthorne effect.

Finally, as this study lacks a follow-up process after the intervention, it cannot determine whether EXD combined with BE will maintain the influence on BMD in the long term. At present, there is no more intensive study on the combination of EXD and BE, and the mechanism of the influence remains unclear.

6. Conclusion

The 16-week intervention of EXD combined with BE improved the BMD of patients with PMOP, especially the density of the lumbar spine (L2–4) and femoral neck. We also found that EXD combined with BE can improve balance and mental health in patients with PMOP. In addition, our study shows that BE is an effective, safe, and helpful exercise that can improve the physical and mental health of women with PMOP. In the future, research should focus on interventions involving combinations of non-pharmaceutical treatments or the lowest dose of drugs that can provide health benefits to different groups.

Data Availability

The data used to support the findings of this study are available from the corresponding author upon request.

Conflicts of Interest

The authors declare that they have no conflicts of interest.

Authors' Contributions

Keqiang Li, Hongli Yu, Xiaojun Lin, Yuying Su, Lifeng Gao, Minjia Song, and Mariusz Lipowski contributed to methodology. Keqiang Li, Hongli Yu, Mariusz Lipowski, and Xiaojun Lin worked on software, validation, and resources. Keqiang Li, Hongli Yu, Lifeng Gao, and Daniel Krokosz carried out formal analysis. Keqiang Li, Mariusz Lipowski, Huixin Yang, and Xiaojun Lin conducted investigation. Keqiang Li, Hongli Yu, Mariusz Lipowski, Lifeng Gao, Daniel Krokosz, Xiaojun Lin, and Huixin Yang performed data curation. Keqiang Li, Xiaojun Lin, and Hongli Yu prepared the original draft. Keqiang Li, Xiaojun Lin, and Mariusz Lipowski revised and edited the manuscript. Keqiang Li and Xiaojun Lin helped with visualization. Keqiang Li, Mariusz Lipowski, Lifeng Gao, Daniel Krokosz, Xiaojun Lin, and Huixin Yang were responsible for project administration. Keqiang Li and Mariusz Lipowski participated in funding acquisition. All authors were involved in

conceptualization and supervision and read and approved the final version of the manuscript.

References

- [1] J. Y. Reginster and N. Burlet, "Osteoporosis: a still increasing prevalence," *Bone*, vol. 38, pp. S4–S9, 2006.
- [2] R. Pacifici, "Estrogen, cytokines, and pathogenesis of postmenopausal osteoporosis," *Journal of Bone and Mineral Research*, vol. 11, no. 8, pp. 1043–1051, 2009.
- [3] H. B. Erez, A. Weller, N. Vaisman, and S. Kreitler, "The relationship of depression, anxiety and stress with low bone mineral density in post-menopausal women," *Arch Osteoporos*, vol. 7, pp. 247–255, 2012.
- [4] D. Michelson, C. Stratakis, L. Hill et al., "Bone mineral density in women with depression," *New England Journal of Medicine*, vol. 335, no. 16, pp. 1176–1181, 1996.
- [5] B. Jahelka, T. Dorner, R. Terkula, M. Quittan, H. Broll, and L. Erlacher, "Health-related quality of life in patients with osteopenia or osteoporosis with and without fractures in a geriatric rehabilitation department," *Wiener Medizinische Wochenschrift*, vol. 159, no. 9–10, pp. 235–240, 2009.
- [6] D. T. Gold, "The nonskeletal consequences of osteoporotic fractures. psychologic and social outcomes," *Rheumatic Disease Clinics of North America*, vol. 27, no. 1, pp. 255–262, 2001.
- [7] D. Gold, "Physical and psychosocial consequences of osteoporotic vertebral fracture (Part 2). identifying and managing the non-skeletal consequences of osteoporosis," *Advances in Osteoporotic Fracture Management*, vol. 1, no. 3, pp. 74–79, 2002.
- [8] A. Seven, B. Yuksel, G. Yavuz, M. Polat, B. Unlu, and N. Keskin, "The evaluation of hormonal and psychological parameters that affect bone mineral density in postmenopausal women," *European Review for Medical and Pharmacological Sciences*, vol. 20, 2016.
- [9] P. D. Delmas, "Treatment of postmenopausal osteoporosis," *The Lancet*, vol. 359, no. 9322, pp. 2018–2026, 2002.
- [10] P. Barrionuevo, E. Kapoor, N. Asi et al., "Efficacy of pharmacological therapies for the prevention of fractures in postmenopausal women: a network meta-analysis," *Journal of Clinical Endocrinology & Metabolism*, vol. 104, no. 5, pp. 1623–1630, 2019.
- [11] R. Eastell, C. J. Rosen, D. M. Black, A. M. Cheung, M. H. Murad, and D. Shoback, "Pharmacological management of osteoporosis in postmenopausal women: an endocrine society * clinical practice guideline," *Journal of Clinical Endocrinology & Metabolism*, vol. 104, no. 5, pp. 1595–1622, 2019.
- [12] E. Mukwaya, F. Xu, M. S. Wong, and Y. Zhang, "Chinese herbal medicine for bone health," *Pharmaceutical Biology*, vol. 52, no. 9, pp. 1223–1228, 2014.
- [13] S. C. W. Sze, Y. Tong, Y. B. Zhang et al., "A novel mechanism: Erxian decoction, a Chinese medicine formula, for relieving menopausal syndrome," *Journal of Ethnopharmacology*, vol. 123, no. 1, pp. 27–33, 2009.
- [14] C. Wang, Z. Zhang, and J. Ma, "Treatment of 50 cases of osteoporosis with Er-Xian decoction," *Shan Xi Zhong Yi*, vol. 19, pp. 205–206, 1998.
- [15] Q. Liu, J. R. Shi, Y. Yang, Z. Q. Fang, S. H. Liang, and R. X. Guo, "Effects on secretory function of rat gonad by Erxian decoction and its disassembled prescriptions," *Zhongguo Zhong Yao Za Zhi = Zhongguo Zhongyao Zazhi = China Journal of Chinese Materia Medica*, vol. 30, no. 13, pp. 1023–1026, 2005.
- [16] X. H. Shen, Z. Q. Fang, and D. X. Wu, "Effect of Er-xian decoction and its disassembled prescription on enzyme activities and their gene expression of antioxidant enzymes in aging rat," *Zhongguo Zhong Xi Yi Jie He Za Zhi Zhongguo Zhongxiyi Jiehe Zazhi = Chinese Journal of Integrated Traditional and Western Medicine*, vol. 15, no. 11, pp. 672–674, 1995.
- [17] H. Nian, L. P. Qin, Q. Y. Zhang, H. C. Zheng, Y. Yu, and B. K. Huang, "Antiosteoporotic activity of Er-Xian decoction, a traditional Chinese herbal formula, in ovariectomized rats," *Journal of Ethnopharmacology*, vol. 108, no. 1, pp. 96–102, 2006.
- [18] S. F. Fu, Y. Q. Zhao, M. Ren et al., "A randomized, double-blind, placebo-controlled trial of Chinese herbal medicine granules for the treatment of menopausal symptoms by stages," *Menopause*, vol. 23, no. 3, pp. 311–323, 2016.
- [19] L. L. D. Zhong, Y. Tong, G. W. K. Tang et al., "A randomized, double-blind, controlled trial of a Chinese herbal formula (Er-Xian decoction) for menopausal symptoms in Hong Kong perimenopausal women," *Menopause*, vol. 20, no. 7, pp. 767–776, 2013.
- [20] L. Zhang, Y. Yang, L. Di, J. L. Li, and N. Li, "Er-xian decoction, a famous Chinese medicine formula, antagonizes corticosterone-induced injury in PC12 cells, and improves depression-like behaviours in mice," *Pharmaceutical Biology*, vol. 58, no. 1, pp. 498–509, 2020.
- [21] C. Wang, J. Liang, Y. Si, Z. Li, and A. Lu, "The effectiveness of traditional Chinese medicine-based exercise on physical performance, balance and muscle strength among older adults: a systematic review with meta-analysis," *Aging Clinical and Experimental Research*, vol. 34, no. 4, pp. 725–740, 2022.
- [22] K. L. Hertel and M. G. Trahiotis, "Exercise in the prevention and treatment of osteoporosis: the role of physical therapy and nursing," *Nursing Clinics of North America*, vol. 36, no. 3, pp. 441–453, 2001.
- [23] H. H. Chen, M. L. Yeh, and F. Y. Lee, "The effects of Baduanjin Qigong in the prevention of bone loss for middle-aged women," *The American Journal of Chinese Medicine*, vol. 34, no. 5, pp. 741–747, 2006.
- [24] F. K. Cheng, "Effects of Baduanjin on mental health: a comprehensive review," *Journal of Bodywork and Movement Therapies*, vol. 19, no. 1, pp. 138–149, 2015.
- [25] Z. F. Li Qd, Y. J. Zhang, R. Peng, J. Li, W. Chen, and H. Xu, "Clinical observation on eight-section brocade in improving balance ability and fall risk of senile osteoporosis," *Western Journal of Traditional Chinese Medicine*, vol. 9, pp. 62–65, 2019.
- [26] M. Li, Q. Fang, J. Li et al., "The effect of Chinese traditional exercise-Baduanjin on physical and psychological well-being of college students: a randomized controlled trial," *PLoS One*, vol. 10, no. 7, Article ID e0130544, 2015.
- [27] M. Zhenglai, *Practical Dictionary of Pharmacology of Traditional Chinese Medicine Formulae*, Jiangsu Press of Scientific Technology, Wuxi Shi, China, 1989.
- [28] N. Wu, "The efficacy of Erxian decoction on menopausal osteoporosis in 60 women," *Yun-Nan Journal of Traditional Chinese Medicine*, vol. 27, no. 6, p. 18, 2006.
- [29] A. E. Smith-Ryan, M. G. Mock, E. D. Ryan, G. R. Gerstner, E. T. Trexler, and K. R. Hirsch, "Validity and reliability of a 4-compartment body composition model using dual energy X-ray absorptiometry-derived body volume," *Clinical Nutrition*, vol. 36, no. 3, pp. 825–830, 2017.

- [30] J. A. Kanis and J. A. Kanis, "Assessment of fracture risk and its application to screening for postmenopausal osteoporosis: synopsis of a WHO report. WHO study group," *Osteoporosis International: A Journal Established as Result of Cooperation Between the European Foundation for Osteoporosis and the National Osteoporosis Foundation of the USA*, vol. 4, no. 6, pp. 368–381, 1994.
- [31] G. M. Blake and I. Fogelman, "The role of DXA bone density scans in the diagnosis and treatment of osteoporosis," *Postgraduate Medical Journal*, vol. 83, no. 982, pp. 509–517, 2007.
- [32] T. Michikawa, Y. Nishiwaki, T. Takebayashi, and Y. Toyama, "One-leg standing test for elderly populations," *Journal of Orthopaedic Science: Official Journal of the Japanese Orthopaedic Association*, vol. 14, no. 5, pp. 675–685, 2009.
- [33] K. O. Berg, S. L. Wood-Dauphinee, J. I. Williams, and B. Maki, "Measuring balance in the elderly: validation of an instrument," *Canadian Journal of Public Health*, vol. 83, no. Suppl 2, pp. S7–S11, 1992.
- [34] D. Podsiadlo and S. Richardson, "The timed "up & go": a test of basic functional mobility for frail elderly persons," *Journal of the American Geriatrics Society*, vol. 39, no. 2, pp. 142–148, 1991.
- [35] W. W. Zung, "A rating instrument for anxiety disorders," *Psychosomatics*, vol. 12, no. 6, pp. 371–379, 1971.
- [36] W. W. K. Zung, "A self-rating depression scale," *Archives of General Psychiatry*, vol. 12, p. 63, 1965.
- [37] F. Faul, E. Erdfelder, A.-G. Lang, and A. G. Buchner, "G*Power 3: a flexible statistical power analysis program for the social, behavioral, and biomedical sciences," *Behavior Research Methods*, vol. 39, no. 2, pp. 175–191, 2007.
- [38] J. Y. Li, Y. S. Jia, L. M. Chai et al., "Effects of Chinese herbal formula Erxian decoction for treating osteoporosis: a systematic review," *Clinical Interventions in Aging*, vol. 12, pp. 45–53, 2017.
- [39] S. Liu, J. Huang, J. Wang et al., "Er-xian decoction stimulates osteoblastic differentiation of bone mesenchymal stem cells in ovariectomized mice and its gene profile analysis," *Stem Cells International*, vol. 2016, Article ID 4079210, 10 pages, 2016.
- [40] J. Zou, F. Lin, and L. Zhang, "Effect of long time taijiquan training on bone density and balance function in postmenopause women," *Chinese Rehabilitation Theory and Practice*, vol. 1, 2011.
- [41] Y.-J. Li, X.-R. Niu, and S. Hu, "Efficacy evaluation of different forms of traditional Chinese health-preservation exercises for osteoporosis: a network meta-analysis," *Journal of Acupuncture and Tuina Science*, vol. 19, no. 4, pp. 258–270, 2021.
- [42] L. Ruanyingdi, "Effect of healthy Qigong on the related indicators of bone metabolism and serum NO, NOS in postmenopausal women," Master thesis, Shenyang Sport University, Shenyang, China, 2011.
- [43] J. A. Kanis, C. Cooper, R. Rizzoli, and J. Y. Reginster, "Executive summary of European guidance for the diagnosis and management of osteoporosis in postmenopausal women," *Aging Clinical and Experimental Research*, vol. 31, no. 1, pp. 15–17, 2019.
- [44] P. Makras, A. D. Anastasilakis, G. Antypas et al., "The 2018 Guidelines for the diagnosis and treatment of osteoporosis in Greece," *Arch Osteoporos*, vol. 14, no. 1, p. 39, 2019.
- [45] D. Saintier, V. Khanine, B. Uzan, H. K. Ea, M. C. de Vernejoul, and M. E. Cohen-Solal, "Estradiol inhibits adhesion and promotes apoptosis in murine osteoclasts in vitro," *The Journal of Steroid Biochemistry and Molecular Biology*, vol. 99, no. 4-5, pp. 165–173, 2006.
- [46] W. T. S. J. He, "Tai Ji Chuan and the sub-cattle progress of primary osteoporosis," *Chinese Journal of Osteoporosis*, vol. 14, no. 8, pp. 587–600, 2008.
- [47] Y. Q. J. X. Shen, "Effects of exercise on bone mineral density of children and adolescents," *Journal of Wuhan Institute of Physical Education*, vol. 38, no. 5, pp. 55–57, 2004.
- [48] J. C. Gallagher, B. L. Riggs, J. Eisman, A. Hamstra, S. B. Arnaud, and H. F. DeLuca, "Intestinal calcium absorption and serum vitamin D metabolites in normal subjects and osteoporotic patients: effect of age and dietary calcium," *Journal of Clinical Investigation*, vol. 64, no. 3, pp. 729–736, 1979.
- [49] T. Tian, Y. Cai, J. Zhou et al., "Effect of eight-section brocade on bone mineral density in middle age and elderly people: protocol for a systematic review and meta-analysis of randomised controlled trials," *Medicine (Baltimore)*, vol. 99, no. 1, Article ID e18549, 2020.
- [50] L. Qin, T. Han, Q. Zhang et al., "Antiosteoporotic chemical constituents from Er-Xian decoction, a traditional Chinese herbal formula," *Journal of Ethnopharmacology*, vol. 118, no. 2, pp. 271–279, 2008.
- [51] L. Zhu, W. Wu, M. Chen et al., "Corrigendum to "effects of nonpharmacological interventions on balance function in patients with osteoporosis or osteopenia: a network meta-analysis of randomized controlled trials," *Evidence-Based Complementary and Alternative Medicine*, vol. 2021, Article ID 9892786, 1 page, 2021.
- [52] B. A. M. Larsson, L. Johansson, D. Mellstrom et al., "One leg standing time predicts fracture risk in older women independent of clinical risk factors and BMD," *Osteoporosis International*, vol. 33, pp. 185–194, 2021.
- [53] L. H. Fan Lu, X. Chen, and X. Zhu, "Correlation between bone mineral density and balance function in the elderly Chinese," *Journal of Osteoporosis and Bone Mineral Salt Diseases*, vol. 7, no. 4, pp. 298–307, 2014.
- [54] I. Acimovic, "The influence of health qigong on the subjectively expressed psychophysical state of patients with rheumatoid arthritis, rheum, osteoporosis, osteopenia," *Chinese Medicine and Culture*, vol. 1, no. 3, p. 150, 2018.
- [55] J. Zhou, Y. Yu, B. Cao et al., "Characteristic of clinical studies on Baduanjin during 2000-2019: a comprehensive review," *Evidence-Based Complementary and Alternative Medicine*, vol. 2020, Article ID 4783915, 9 pages, 2020.
- [56] L. Jing, Y. Jin, X. Zhang, F. Wang, Y. Song, and F. Xing, "The effect of Baduanjin Qigong combined with CBT on physical fitness and psychological health of elderly housebound," *Medicine (Baltimore)*, vol. 97, no. 51, Article ID e13654, 2018.
- [57] J. S. M. Chan, R. T. H. Ho, K. F. Chung et al., "Qigong exercise alleviates fatigue, anxiety, and depressive symptoms, improves sleep quality, and shortens sleep latency in persons with chronic fatigue syndrome-like illness," *Evidence-Based Complementary and Alternative Medicine*, vol. 2014, Article ID 106048, 10 pages, 2014.

- [58] C.-W. Wang, C. H. Chan, R. T. Ho, J. S. Chan, S.-M. Ng, and C. L. Chan, "Managing stress and anxiety through Qigong exercise in healthy adults: a systematic review and meta-analysis of randomized controlled trials," *BMC Complementary and Alternative Medicine*, vol. 14, no. 1, p. 8, 2014.
- [59] H. Y. Chen, T. W. Kao, J. W. Huang, T. J. Tsai, and K. D. Wu, "Treatment of menopausal symptoms with Er-xian decoction: a systematic review," *Clinical Nephrology*, vol. 70, no. 3, pp. 233–239, 2008.
- [60] F. Yang, Y. Liu, S. Chen et al., "A GABAergic neural circuit in the ventromedial hypothalamus mediates chronic stress-induced bone loss," *The Journal of Clinical Investigation*, vol. 130, no. 12, pp. 6539–6554, 2020.

Research Article

Elucidating the Neuroprotective Effect of *Tecoma stans* Leaf Extract in STZ-Induced Diabetic Neuropathy

Amit Gupta,¹ Tapan Behl ,¹ Aayush Sehgal,¹ Sukhbir Singh,¹ Neelam Sharma,¹ Shivam Yadav,² Khalid Anwer,³ Celia Vargas-De-La Cruz,^{4,5} Sridevi Chigurupati,^{6,7} Abdullah Farasani,^{8,9} and Saurabh Bhatia^{10,11}

¹Chitkara College of Pharmacy, Chitkara University, Rajpura, Punjab, India

²Yashraj Institute of Pharmacy, Lucknow, Uttar Pradesh, India

³Department of Pharmaceutics, College of Pharmacy, Prince Sattam Bin Abdulaziz University, Alkharj, Saudi Arabia

⁴Department of Pharmacology, Bromatology and Toxicology, Faculty of Pharmacy and Biochemistry, Universidad Nacional Mayor de San Marcos, Lima, Peru

⁵E-Health Research Center, Universidad de Ciencias y Humanidades, Lima, Peru

⁶Department of Medicinal Chemistry and Pharmacognosy, College of Pharmacy, Qassim University, Buraidah 52571, Saudi Arabia

⁷Department of Biotechnology, Saveetha College of Engineering, Saveetha Institute of Medical and Technical sciences, Saveetha University, Saveetha Nagar, Thandalam, Chennai 602105, India

⁸Biomedical Research Unit, Medical Research Center, Jazan University, Jazan, Saudi Arabia

⁹Department of Medical Laboratory Technology, College of Applied Medical Sciences, Jazan University, Jazan, Saudi Arabia

¹⁰Natural & Medical Sciences Research Centre, University of Nizwa, Birkat Al Mauz, Nizwa, Oman

¹¹School of Health Science, University of Petroleum and Energy Studies, Dehradun, Uttarakhand, India

Correspondence should be addressed to Tapan Behl; tapanbehl31@gmail.com

Received 27 May 2022; Accepted 10 June 2022; Published 26 June 2022

Academic Editor: Rajeev K. Singla

Copyright © 2022 Amit Gupta et al. This is an open access article distributed under the Creative Commons Attribution License, which permits unrestricted use, distribution, and reproduction in any medium, provided the original work is properly cited.

Background. Diabetes is considered one of the most encyclopedic metabolic disorders owing to an alarming rise in the number of patients, which is increasing at an exponential rate. With the current therapeutics, which only aims to provide symptomatic and momentary relief, the scientists are shifting gears to explore alternative therapies which not only can target diabetes but can also help in limiting the progression of diabetic complications including diabetic neuropathy (DN). **Methods.** *Tecoma stans* leaf methanolic extract was prepared using the Soxhlet method. A streptozotocin (STZ; 45 mg/kg)-induced diabetic animal model was used and treatment with oral dosing of *T. stans* leaf extract at the different doses of 200 mg/kg, 300 mg/kg, and highest dose, i.e., 400 mg/kg, was initiated on day 3 after STZ administration. The pharmacological response for general and biochemical (angiogenic, inflammatory, and oxidative) parameters and behavioral parameters were compared using Gabapentin as a standard drug with the results from the test drug. **Results.** Parameters associated with the pathogenesis of diabetic neuropathy were evaluated. For general parameters, different doses of *T. stans* extract (TSE) on blood sugar showed significant effects as compared to the diabetic group. Also, the results from biochemical analysis and behavioral parameters showed significant positive effects in line with general parameters. The combination therapy of TSE at 400 mg/kg with a standard drug produced nonsignificant effects in comparison with the normal group. **Conclusion.** The leaves of *T. stans* possess antidiabetic effects along with promising effects in the management of DN by producing significant effects by exhibiting antioxidative, antiangiogenic, and anti-inflammatory properties, which are prognostic markers for DN, and thus, *T. stans* can be considered as an emerging therapeutic option for DN.

1. Introduction

Diabetes mellitus is nowadays considered one of the “lifestyle” disorders, and over centuries, various species of plants are considered a fundamental resource of potent hypoglycaemic agents [1]. In developing nations, specifically, medicinal agents are utilized to treat DM to overcome the cost burden of conventional medications on the population [2]. Since decades, plants and their byproducts have been used as a major source of medicines due to their therapeutic potential. In recent times, treating diseases including DM utilizing medicinal plant agents is suggested as these plants possess numerous phytoconstituents, namely, glycosides, alkaloids, saponins, flavonoids, carotenoids, and terpenoids, which show hypoglycaemic activity [3]. In one of the recent studies, it was postulated that the synergistic effect of biologically active constituents such as glucosinolates, lignans, polyphenols, coumarins, and carotenoids leads to the major beneficial characteristics of every plant matrix and this signifies the initial step for understanding its beneficial actions and biological activities [4]. The hypoglycaemic actions which result after treatment with plant extracts are generally ascribed to their capability to increase the pancreatic gland tissue performance, which is achieved by decreasing the intestinal absorption of sugar or by enhancing insulin hormone secretions [5].

There is an array of literature available, which describes the potential of natural products derived from plant origin, which have the potential to become the drug of choice in various metabolic disorders. These products, when used as monotherapy or in combination with current allopathic drugs, were shown to decrease the therapeutic dose, however achieving the same pharmacological effects [6]. The least adverse effects, low cost, and easy availability make these plant-based formulations the major option among all the available treatments, specifically in rural regions [7]. On the other hand, numerous plants are rich resources of bioactive agents that are free from detrimental adverse effects and exhibit excellent pharmacological actions [8, 9].

Various studies carried out over the past few decades confirm the therapeutic potential of various herbal plants in the management of diabetes and diabetes-associated complications [10]. From these plants, promising results are also obtained from *T. stans*, which is considered a drug of choice in Mexico for the management of diabetes. From the available evidence in the published literature, the tremendous potential of *T. stans* in the management of various disorders can be easily deduced due to the presence of an array of active phytoconstituents. This was evident from the literature that *T. stans* possesses multiple pharmacological properties which include anticancer, cardioprotective, wound-healing, anti-inflammatory, neuroprotective, antimicrobial, and various other pathological properties, which are involved directly and indirectly in the pathogenesis of various metabolic disorders [10]. Multiple studies in the past had revealed several other uses of different extracts of *T. stans* apart from its antidiabetic properties. Studies till date reported anticancer activity in vivo and in vitro of methanolic extracts of *T. stans* flowers [11], antinociceptive

and anti-inflammatory potential of flower extract *T. stans* [12], antioxidant and cytotoxic activity of *T. stans* leaves [13] along with antidiabetic effects on STZ induced diabetic rats.

An array of in vitro and in vivo studies had been conducted in the past few decades, which had confirmed the tremendous antidiabetic potential of *T. stans*. The available literature and studies confirm that the plant leaves, flowers, hardwood, and whole plant can be used to procure active pharmaceutical ingredients, which can elicit therapeutic properties. The antidiabetic effects were mainly mediated by the presence of alkaloids, flavonoids, and glycosides, which have been shown to decrease fasting glycemic levels, an area under the glucose tolerance curve [14]. These active constituents can also decrease plasma cholesterol levels and can exhibit antifungal effects, antimicrobial effects, and even hepatoprotective effects [15]. In addition, the methanolic extract of *T. stans* is known to possess activities that includes intestinal α -glucosidase inhibition, decreasing hypoglycaemic peaks, and even affecting postprandial antidiabetic effects [16]. These effects are not only limited to the management of diabetes but can also help in reducing triglyceride levels including cholesterol without any changes in blood fasting glucose levels and is also associated with the management of various pathological conditions [17].

It has been already confirmed from various research that *T. stans* leaf extract contains the monoterpenoid alkaloids such as tecostanine and tecomine, saponins, and flavonoids, which have a hypoglycaemic effect and exert varied effects in multiple pathological conditions. However, no study has been carried out and is available in the literature to explore the effect of *T. stans* in diabetic neuropathy. Hence, through the undertaken study, we tried to explore the effect of *T. stans* on diabetic neuropathy, which is the most common complication associated with diabetes [18].

2. Materials and Methods

2.1. Plant Material. Fresh leaves of *T. stans* were collected from Jaswant Green Nursery, Punjab, India. The leaves were authenticated by the National Institute of Pharmaceutical Education and Research (NIPER), Mohali, Punjab, with reference number NIP-H-286. The voucher specimen was deposited and was stored in a publicly available herbarium of the institute.

2.2. Extract Preparation. The leaves were collected (5.0 kg), washed thoroughly with tap water, and dried. They were coarsely powdered (4–6 mm) with simultaneous removal of ground material (1.3 kg) with methanol solution (60%, 1:10 ratio, w/v) at 60°C for 30 min. This was followed by their extraction with a Soxhlet apparatus using 60 g of dried coarse powder with 300 ml of methanol for 6–8 h at room temperature to prepare the methanolic extract. The remaining drug was dried to remove the methanol followed by maceration of the dried powder with distilled water for 48 h. Later, marc was pressed, and the extract was collected. The volume was further concentrated using a rotary vacuum evaporator at a temperature not exceeding 60°C for 30–40

minutes at 500 mm of Hg until it formed a paste which was further dried till it was converted to powder and stored at 40°C in a well-closed container for further analysis [19].

2.3. Chemical Used. All the chemicals used in the study were collected from the store of Chitkara College of Pharmacy, Chitkara University, and of analytical grade manufactured by Loba Chemie. The standard drug, Gabapentin, was a benevolent gift sample from Magbro Healthcare Pvt. Ltd., Solan, India. The biochemical kits were obtained from allied scientific products.

2.4. Animals. This study involves the in vivo evaluation of *T. stans* in Wistar rats (200–250 gm), irrespective of their sex. These animals were approved by Institutional Animal Ethic Committee (IAEC) from Chitkara College of Pharmacy, Chitkara University, Punjab. The animals were kept in controlled conditions as per the standard procedures having adequate humidity and ventilation with proper lighting. The room temperature was maintained at $23 \pm 1^\circ\text{C}$. The care of these animals was undertaken as per the guidance obtained from the committee for the purpose of control and supervision of experimental animals (CDCSEA), and the research protocol was submitted to the IAEC under the protocol no. IAEC/CCP/21/02/PR-007.

Diabetes in these animals was induced using STZ with a single administration of intraperitoneal (i.p.) streptozotocin (STZ) injection (dose of 45 mg/kg) in 0.1 M citrate buffer having a pH value of 4.5 in overnight fasted Wistar rats [20]. The preparation of citrate buffer having a pH value of 4.5 was carried out by adding 25.5 ml of 0.1 M citric acid solution (19.2 g/1000 ml distilled water) and 24.5 ml of 0.1 M sodium citrate dehydrate ($\text{C}_6\text{H}_9\text{Na}_3\text{O}_9$) in 29.4 g/1000 ml of distilled water, and after that, pH was confirmed using a pH meter [21]. Blood glucose levels were estimated prior to induction of diabetes and 48 hours after STZ injection. Blood glucose levels in all experimental groups were estimated with a glucometer along with glucose test strips. Animals with more than 300 mg/dl blood glucose values were considered diseased (diabetic control) and were considered part of this present study [22]. The experimental animals were randomly assigned to the following groups and were marked accordingly:

- (i) Group 1: normal control
- (ii) Group 2: diabetic control
- (iii) Group 3: *T. stans* per se
- (iv) Group 4: Gabapentin (50 mg/kg body weight)-treated group
- (v) Group 5: *T. stans* extract 200 mg/kg-treated group
- (vi) Group 6: *T. stans* extract 300 mg/kg-treated group
- (vii) Group 7: *T. stans* extract 400 mg/kg-treated group
- (viii) Group 8: *T. stans* extract 400 mg/kg + Gabapentin-treated group

All these groups were analyzed for confirmation of STZ-induced diabetes by general parameter estimation of blood

glucose levels, biweekly, and increased level of blood glucose and subsequent mortality were controlled by administration of huminsulin (1 unit of huminsulin if blood glucose is greater than 500 mg/dl and 2 units if value was greater than 600 mg/dl). Also, the biochemical parameters for the confirmation of angiogenesis, oxidation, and inflammation were analyzed using ELISA kits. These tests were further backed with the behavioral parameters, which were further analyzed to monitor the effect of test and standard drugs in STZ-induced diabetic neuropathy and associated secondary complications.

2.5. Statistical Analysis. For statistical analysis, one-way and two-way ANOVA using GraphPad PRISM version 9.0 was used and the interpretation was carried out as mean \pm SD ($n = 6$). The results involved the post hoc use of Tukey–Kramer’s multiple comparisons. The level of statistical significance was expressed at $p < 0.05$, $p < 0.01$, and $p < 0.001$.

3. Results

The dried coarse powdered leaves were subjected to continuous hot extraction by using methanol as the solvent. From extraction of leaves of *T. stans* by the continuous hot percolation method using methanol, the average yield was 11.6% w/w. Furthermore, 3 different doses were prepared to determine the activity of methanolic extract of *T. stans* leaves at different doses of 200 mg/kg, 300 mg/kg, and 400 mg/kg. Its activity was determined by analyzing general parameters like changes in blood glucose levels. These results from the test drugs were then compared with those using a standard drug, which included Gabapentin. From the literature evidence, it can be concluded that the standard drug exhibits a statistically significant effect in maintaining these physical parameters in comparison with the disease control group [23–25]; however, the effects of Gabapentin in regulating the blood glucose is limited. The experimental rats administered with *T. stans* extract also showed statistically significant results in terms of effectiveness and improvements against the disease control group. Also, using the highest dose in combination with the standard drugs either produced additive effects, or nonsignificant results were seen in comparison to the normal rats.

3.1. General Parameters. The study includes an estimation of general parameters, which are required for the confirmation of diabetes in the present study. A general confirmatory test, which includes blood glucose, was done, which confirmed that diabetes was induced in the experimental Wistar rats, which were further evaluated for diabetes-related complications of neuropathy. Diabetic neuropathy was further evaluated using biochemical and behavioral parameters.

3.1.1. Estimation of Blood Glucose Levels. The activity of methanolic extract of *T. stans* leaves at different doses of 200 mg/kg, 300 mg/kg, and 400 mg/kg was determined by analyzing general parameters like increase/decrease in blood

glucose levels. These results from the test drugs were then compared to those using a standard drug, which included Gabapentin. The results from this experiment concluded that experimental rats administered with *T. stans* extract also showed statistically significant results in terms of effectiveness and improvements against the disease control group but were not able to achieve normal glycemic levels as compared to normal rats as shown in Figure 1. However, using the highest dose, i.e., 400 mg/kg, in combination with the standard drug produced nonsignificant results that were seen in comparison to the standard treatment alone. This confirms the dose saturation observed at the dose of 400 mg/kg when used as a combination therapy.

3.2. Determination of Angiogenic Parameters. Angiogenesis is purported as de novo synthesis of new blood vessels. From the published literature, angiogenesis has been considered one of the primary triggers, which is involved in the pathogenesis of diabetes-related complications of neuropathy [26]. The main factors responsible for the pathogenesis resulting in abnormal/excessive formation of new blood vessels are mediated by downstream mediators, vascular endothelial growth factor (VEGF) and protein kinase C (PKC), which were augmented in the serum postadministration of STZ [27]. Diabetic rats administered with *T. stans* extract of 200 mg/kg, 300 mg/kg, and the highest dose, i.e., 400 mg/kg, along with the standard treatment Gabapentin showed a significant decrease in the levels of angiogenic markers to the normalization levels in a dose-dependent manner.

3.2.1. Estimation of PKC- β Levels. From the published literature, it is evident that protein kinase C (PKC) is considered a crucial marker in determining angiogenesis. Postadministration of STZ in Wistar rats results in increased levels of PKC, which is involved in the pathogenesis of diabetes and associated complications [28]. Administration of *T. stans* extracts at 200 mg/kg, 300 mg/kg, and the highest dose, i.e., 400 mg/kg, along with the standard treatment Gabapentin showed a significant decrease in the levels of PKC in comparison to the disease control group. In addition, in the combination treatment of the highest dose of *T. stans*, i.e., 400 mg/kg with the standard drug, Gabapentin, produced nonsignificant differences in PKC- β levels in maintaining the level of PKC- β to the levels found in normal rats as shown in Figure 2.

3.2.2. Estimation of VEGF Levels. VEGF is a potent biomarker and is considered a parameter for the determination of angiogenesis. From the available literature, it can be deduced that an increase in levels of VEGF is associated in the animal model of diabetes induced by the administration of STZ [29]. Administration of *T. stans* extract at 200 mg/kg, 300 mg/kg, and the highest dose, i.e., 400 mg/kg, along with the standard treatment Gabapentin showed a significant decrease in the levels of VEGF in comparison to the disease control group [30]. In addition, the combination treatment of the highest dose of *T. stans*, i.e., 400 mg/kg with the

standard drug, Gabapentin, produced nonsignificant differences in maintaining the level of VEGF to the levels found in normal rats as shown in Figure 3.

3.3. Determination of Inflammatory Parameters. The levels of tumor necrosis factor alpha (TNF- α) and interleukin 1 beta (IL-1 β) were augmented in the serum of rats after administration of STZ. Diabetic Wistar rats treated with *T. stans* extract at different doses of 200 mg/kg, 300 mg/kg, and the highest dose, i.e., 400 mg/kg along with the standard treatment Gabapentin significantly drained the levels of inflammatory mediators such as IL-1 β and TNF- α to the levels found in the normal rats.

3.3.1. Estimation of IL- β Levels. The levels of proinflammatory cytokines (IL-1 β) are exceptionally high in conditions of diabetes-associated complications [31, 32]. Administration of *T. stans* extracts at 200 mg/kg, 300 mg/kg, and the highest dose, i.e., 400 mg/kg, along with the standard treatment Gabapentin showed a significant decrease in the levels of VEGF in comparison to the disease control group. In addition, in the combination treatment of the highest dose of *T. stans*, i.e., 400 mg/kg with the standard drug, Gabapentin, produced nonsignificant differences in maintaining the level of IL-1 β to the levels found in normal rats as shown in Figure 4.

3.3.2. Estimation of TNF- α Levels. TNF- α is a common biomarker that depicts the extent of inflammation in any tissue. From the literature evidence, it has been found that the levels of TNF- α significantly increase in an animal model of diabetes administered with STZ. In this study, administration of *T. stans* extracts at 200 mg/kg, 300 mg/kg, and the highest dose, i.e., 400 mg/kg, along with the standard treatment Gabapentin showed a significant decrease in the levels of TNF- α in comparison to the disease control group [33]. In addition, the combination treatment of the highest dose of *T. stans* extract, i.e., 400 mg/kg, with the standard drug, Gabapentin, produced nonsignificant differences in maintaining the level of TNF- α to the levels found in normal rats as shown in Figure 5.

Data are expressed as mean \pm SD ($n=6$). Data were statistically analyzed using one-way ANOVA followed by Tukey-Kramer's multiple comparison test at $p < 0.05$, $p < 0.01$, and $p < 0.001$. The values are expressed as [#] $p < 0.05$ and ^{##} $p < 0.01$ compared with the normal control group; * $p < 0.05$ and ** $p < 0.01$ compared with the diabetic control group; ^a $p < 0.05$ compared with standard treatment Gabapentin; ^b $p < 0.05$ compared with TSE 200 mg/kg; and ^c $p < 0.05$ compared with TSE 300 mg/kg.

3.4. Determination of Oxidation Parameters. In this study, the antioxidant parameters were also measured using ELISA kits. From the literature evidence, it was confirmed that an increase in the activity of the malondialdehyde (MDA) enzyme was predominant in the diabetic animal models after treatment of STZ injection with a simultaneous decrease in catalase and superoxide dismutase (SOD) activity [34, 35]. In

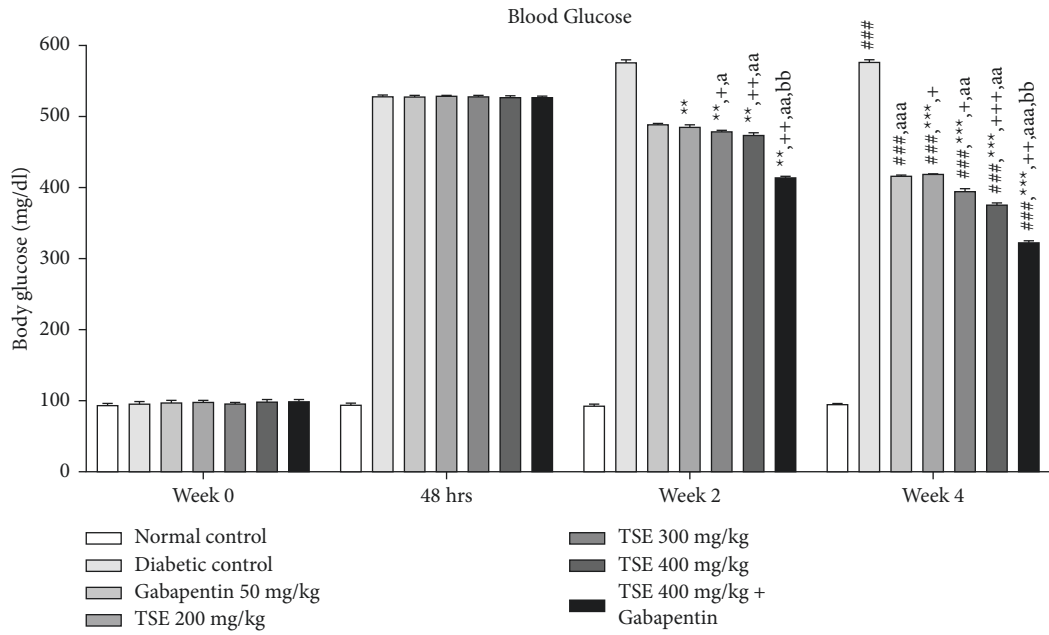


FIGURE 1: Effect of *T. stans* extract on blood glucose levels. Data are expressed as mean \pm SD ($n = 6$). Data were statistically analyzed using two-way ANOVA followed by Tukey–Kramer’s multiple comparison test at $p < 0.05$, $p < 0.01$, and $p < 0.001$. The values were expressed as $^{\#}p < 0.05$, $^{\#\#}p < 0.01$, and $^{\#\#\#}p < 0.001$ vs. normal control group at the 4th week; $^*p < 0.05$, $^{**}p < 0.01$, and $^{***}p < 0.001$ vs. diabetic control group; $^+p < 0.05$, $^{++}p < 0.01$, and $^{+++}p < 0.001$ vs. standard treatment with Gabapentin; $^ap < 0.05$ and $^{aa}p < 0.01$ vs. TSE 200 mg/kg; and $^bp < 0.05$ and $^{bb}p < 0.01$ vs. TSE 300 mg/kg.

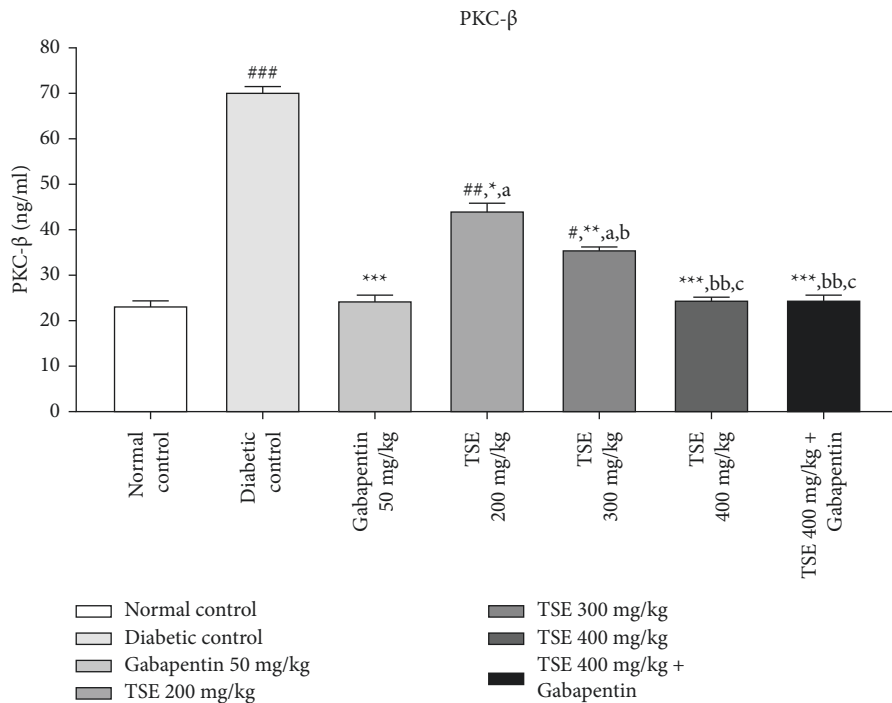


FIGURE 2: Estimation of PKC- β levels after completion of the study protocol. Data are expressed as mean \pm SD ($n = 6$). Data were statistically analyzed using one-way ANOVA followed by Tukey–Kramer’s multiple comparison test at $p < 0.05$, $p < 0.01$, and $p < 0.001$. The values are expressed as $^{\#}p < 0.05$, $^{\#\#}p < 0.01$, and $^{\#\#\#}p < 0.001$ compared with the normal control group; $^*p < 0.05$, $^{**}p < 0.01$, and $^{***}p < 0.001$ compared with the diabetic control group; $^ap < 0.05$ compared with standard treatment Gabapentin; $^bp < 0.05$ and $^{bb}p < 0.01$ compared with TSE 200 mg/kg; and $^cp < 0.05$ compared with TSE 300 mg/kg.

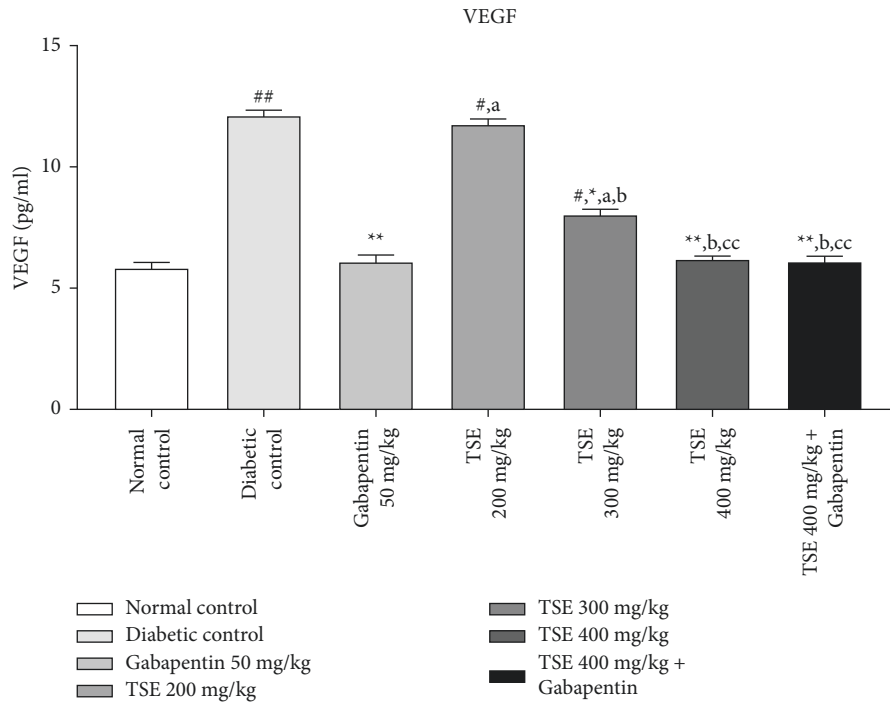


FIGURE 3: Estimation of VEGF levels after completion of the study protocol. Data are expressed as mean \pm SD ($n = 6$). Data were statistically analyzed using one-way ANOVA followed by Tukey–Kramer’s multiple comparison test at $p < 0.05$, $p < 0.01$, and $p < 0.001$. The values are expressed as $^{\#}p < 0.05$ and $^{\#\#}p < 0.01$ compared with the normal control group; $^*p < 0.05$ and $^{**}p < 0.01$ compared with the diabetic control group; $^ap < 0.05$ compared with standard treatment Gabapentin; $^bp < 0.01$ compared with TSE 200 mg/kg; and $^cp < 0.05$ and $^{cc}p < 0.01$ compared with TSE 300 mg/kg.

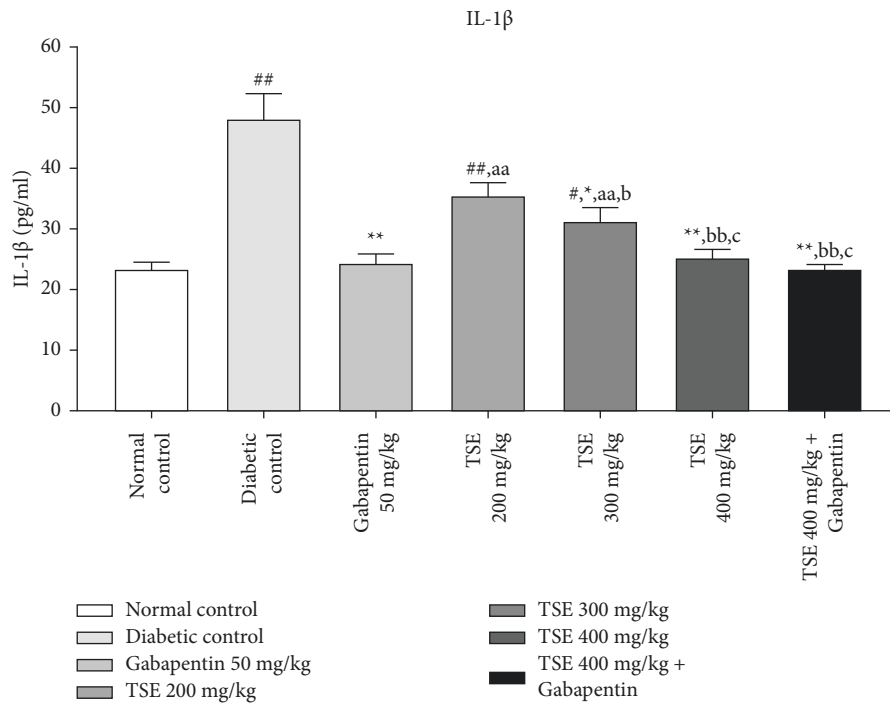


FIGURE 4: Estimation of IL- β levels after completion of the study protocol. Data are expressed as mean \pm SD ($n = 6$). Data were statistically analyzed using one-way ANOVA followed by Tukey–Kramer’s multiple comparison test at $p < 0.05$, $p < 0.01$, and $p < 0.001$. The values are expressed as $^{\#}p < 0.05$ and $^{\#\#}p < 0.01$ compared with the normal control group; $^*p < 0.05$ and $^{**}p < 0.01$ compared with the diabetic control group; $^ap < 0.05$ and $^{aa}p < 0.01$ compared with standard treatment, Gabapentin; $^bp < 0.05$ and $^{bb}p < 0.01$ compared with TSE 200 mg/kg; and $^cp < 0.05$ compared with TSE 300 mg/kg.

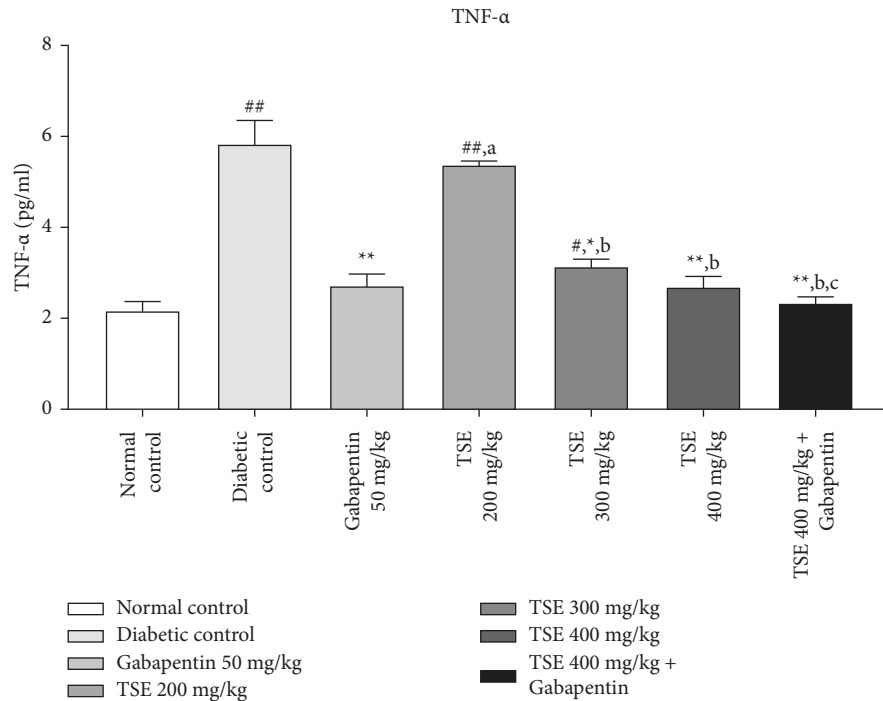


FIGURE 5: Estimation of TNF- α levels after completion of the study protocol.

this study, administration of *T. stans* extract at 200 mg/kg, 300 mg/kg, and 400 mg/kg and standard treatment Gabapentin significantly altered the antioxidant enzymes to the levels found in the normal rats.

3.4.1. Estimation of Catalase Levels. From the published literature, it is evident that the level of catalase dropped extensively in the disease control animal group and is responsible for decreasing antioxidant activity. Administration of *T. stans* extract at different doses of 200 mg/kg, 300 mg/kg, and the highest dose, i.e., 400 mg/kg, along with the standard treatment Gabapentin in disease control animals showed a statistically significant escalation in the levels of catalase in comparison against disease control [36]. The combination produced statistically nonsignificant effects vs. Gabapentin as shown in Figure 6.

3.4.2. Estimation of SOD Levels. STZ-injected rats depicted a momentous downfall in SOD levels implicating conditions with severe oxidative stress. Administration of *T. stans* extract at 200 mg/kg, 300 mg/kg, and the highest dose, i.e., 400 mg/kg, along with the standard treatment Gabapentin in diabetic rats significantly upregulated the elevation of SOD against the disease control group [36]. The combination produced nonsignificant results vs. Gabapentin-treated group as shown in Figure 7.

3.4.3. Estimation of TBARS Levels. It has been seen from the literature evidence that administration of STZ leads to the substantial increase in the level of serum MDA, which is considered to be a marker for severe oxidative stress.

Administration of *T. stans* extract at 200 mg/kg, 300 mg/kg, and the highest dose, i.e., 400 mg/kg, along with the standard treatment Gabapentin was shown to significantly decrease the level of MDA in the treatment group in comparison to the disease control group [37]. The combination produced statistically nonsignificant results in comparison to Gabapentin as shown in Figure 8.

3.5. Determination of Behavioural Parameters

3.5.1. Cold Allodynia Using the Acetone Test. In this experiment, acetone drops (50 μ L) were applied gently to the midplantar surface of the hind paw of Wistar rats for all groups. Reaction in the form of paw licking, rubbing, or shaking movement of the hind paw and even food withdrawal was recorded as a means of nociceptive pain response to the cold stimuli. The response time was noted with a digital stopwatch (1 min duration) after the application of acetone. For each reading, both paws were sampled 3 times and the mean was calculated. The results are depicted in Table 1.

3.5.2. Hot Allodynia Using Eddy's Hot Plate. This method involves the estimation of the nociceptive response of methanolic extract of *T. stans*. Each animal from all groups was placed on a hot plate, which was maintained at a constant temperature of 55°C. The reaction in the form of paw licking or jumping was taken with the help of a digital stopwatch and considered a positive response to the hot stimuli, and these responses were considered as a feedback response as thermal hyperalgesia. The animals exceeding the cutoff time were removed from the hot plate till baseline values were achieved. The results are depicted in Table 2.

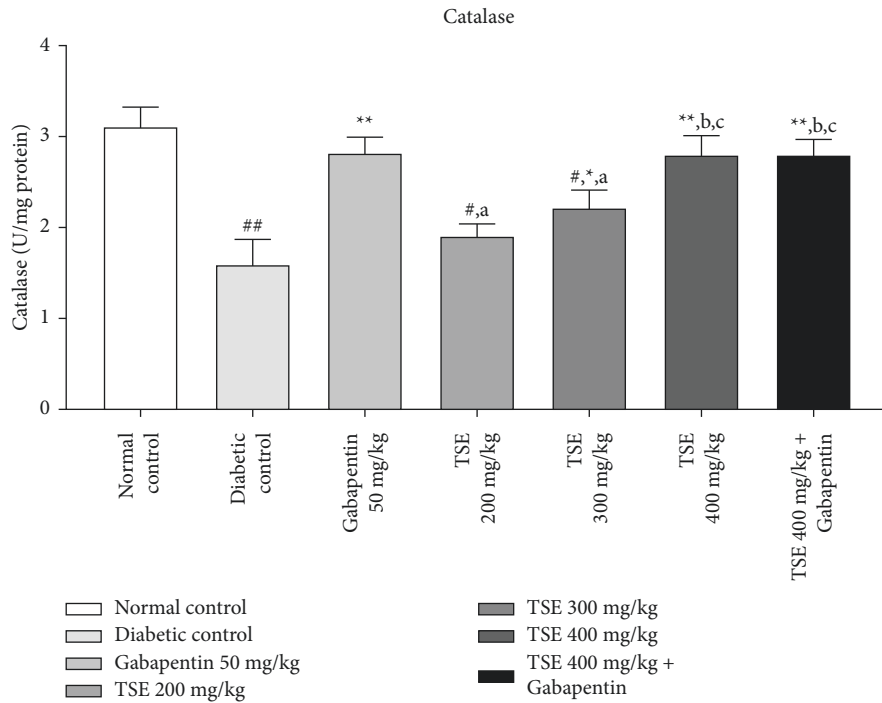


FIGURE 6: Estimation of catalase level after completion of the study protocol. Data are expressed as mean \pm SD ($n = 6$). Data were statistically analyzed using one-way ANOVA followed by Tukey–Kramer’s multiple comparison test at $p < 0.05$, $p < 0.01$, and $p < 0.001$. The values are expressed as $^{\#}p < 0.05$ and $^{\#\#}p < 0.01$ compared with the normal control group; $^*p < 0.05$ and $^{**}p < 0.01$ compared with the diabetic control group; $^ap < 0.05$ compared with standard treatment, Gabapentin; $^bp < 0.05$ compared with TSE 200 mg/kg; and $^cp < 0.05$ compared with TSE 300 mg/kg.

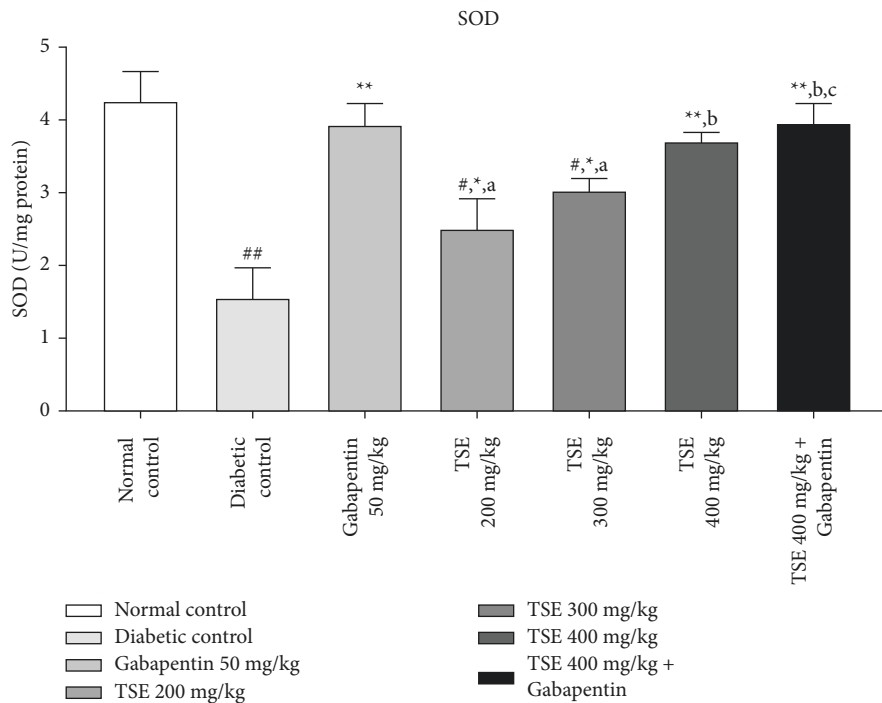


FIGURE 7: Estimation of SOD levels after completion of the study protocol. Data are expressed as mean \pm SD ($n = 6$). Data were statistically analyzed using one-way ANOVA followed by Tukey–Kramer’s multiple comparison test at $p < 0.05$, $p < 0.01$, and $p < 0.001$. The values are expressed as $^{\#}p < 0.05$ and $^{\#\#}p < 0.01$ compared with the normal control group; $^*p < 0.05$ and $^{**}p < 0.01$ compared with the diabetic control group; $^ap < 0.05$ compared with standard treatment, Gabapentin; $^bp < 0.05$ compared with TSE 200 mg/kg; and $^cp < 0.05$ compared with TSE 300 mg/kg.

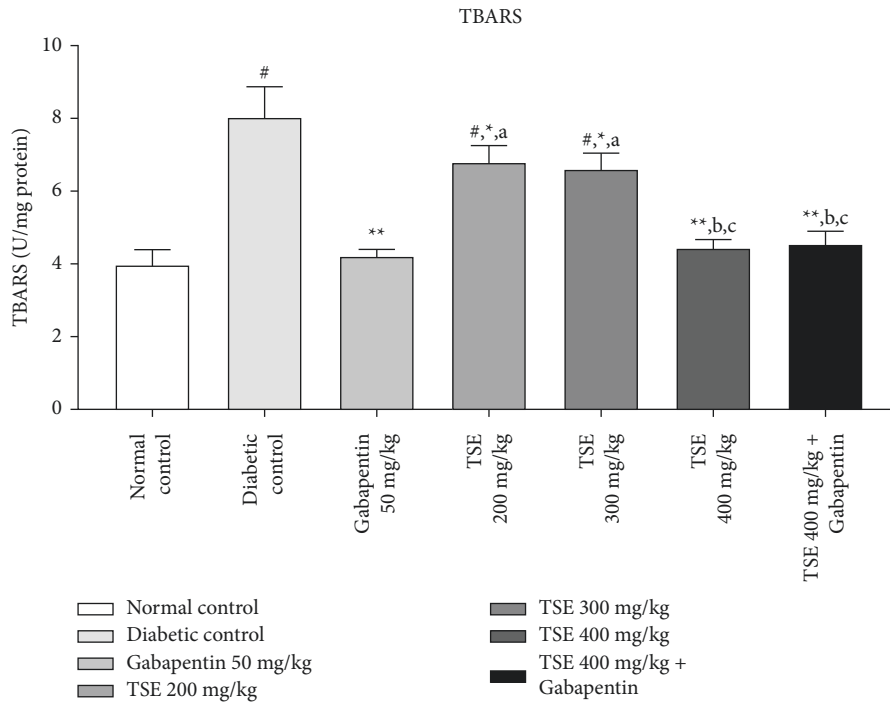


FIGURE 8: Estimation of TBARS levels after completion of the study protocol. Data are expressed as mean ± SD (n = 6). Data were statistically analyzed using one-way ANOVA followed by Tukey–Kramer’s multiple comparison test at p < 0.05, p < 0.01, and p < 0.001. The values are expressed as #p < 0.05 and ##p < 0.01 compared with the normal control group; *p < 0.05 and **p < 0.01 compared with the diabetic control group; ^ap < 0.05 compared with standard treatment, Gabapentin; ^bp < 0.05 compared with TSE 200 mg/kg; and ^cp < 0.05 compared with TSE 300 mg/kg.

TABLE 1: Effect of *Tecoma stans* extract on cold allodynia.

	Normal Control	Diabetic Control	Gabapentin 50 mg/kg	TSE 200 mg/kg	TSE 300 mg/kg	TSE 400 mg/kg	TSE 400 mg/kg + Gabapentin
0 Week	4.42 ± 0.21	4.21 ± 0.51	4.65 ± 1.22	4.35 ± 0.51	4.55 ± 0.51	4.75 ± 1.6	4.71 ± 1.8
Week 1	4.45 ± 0.51	5.98 ± 1.82	5.45 ± 1.12 *	5.95 ± 1.74 +	5.91 ± 1.5 +	5.60 ± 0.40 **,+	5.49 ± 1.25 *
Week 2	4.65 ± 1.22	6.89 ± 1.25	5.15 ± 5.62**	5.62 ± 1.72 **,+	5.71 ± 0.30 **,+	5.36 ± 1.87 **,+	5.16 ± 1.30 *
Week 3	4.63 ± 1.82	7.88 ± 1.92	4.85 ± 6.12**	5.20 ± 0.41 **,+	5.25 ± 1.7 **,+	5.10 ± 1.67 **	5.05 ± 1.32 **
Week 4	4.55 ± 0.51	9.78 ± 1.52##	4.42 ± 1.52***	4.93 ± 0.51##,***,+	4.83 ± 1.12##,***,+	4.69 ± 0.14 **	4.47 ± 0.68 **

Data are expressed as mean ± SD (n = 6). Data were statistically analyzed using two-way ANOVA followed by Tukey–Kramer’s multiple comparison test at p < 0.05, p < 0.01, and p < 0.001. The values are expressed as #p < 0.05 and ##p < 0.01 compared with the normal control group at the 4th week; *p < 0.05, **p < 0.01, and ***p < 0.001 compared with the diabetic control group; +p < 0.05, ++p < 0.01, and +++p < 0.001 compared with standard treatment Gabapentin.

TABLE 2: Effect of *Tecoma stans* extract on thermal hyperalgesia.

	Normal Control	Diabetic Control	Gabapentin 50 mg/kg	TSE 200 mg/kg	TSE 300 mg/kg	TSE 400 mg/kg	TSE 400 mg/kg + Gabapentin
0 Week	4.21 ± 0.21	4.51 ± 0.51	4.83 ± 1.2	4.85 ± 1.22	4.73 ± 1.82	4.75 ± 1.6	4.81 ± 1.8
Week 1	4.32 ± 0.51	5.88 ± 1.82	5.42 ± 1.12	5.75 ± 1.74 +	5.85 ± 1.5 +	5.43 ± 0.40	5.34 ± 1.25 *,aa
Week 2	4.55 ± 1.22	6.59 ± 1.25	5.05 ± 2.62**	5.72 ± 1.72 **,+	5.69 ± 2.30 **,+	5.29 ± 1.87 **,+	5.11 ± 1.30 **,aa
Week 3	4.53 ± 1.82	7.58 ± 1.92	4.95 ± 3.12**	5.25 ± 0.41 **,+	5.23 ± 1.7 **,+	5.09 ± 1.67 **	5.01 ± 1.32 **,a
Week 4	4.35 ± 0.51	9.58 ± 1.52##	4.48 ± 1.52 ***	4.92 ± 0.51##,***,+	4.88 ± 1.12##,***,+	4.75 ± 0.14#,***	4.45 ± 0.68 **,aa

Data are expressed as mean ± SD (n = 6). Data were statistically analyzed using two-way ANOVA followed by Tukey–Kramer’s multiple comparison test at p < 0.05, p < 0.01, and p < 0.001. The values are expressed as #p < 0.05 and ##p < 0.01 compared with the normal control group at the 4th week; *p < 0.05, **p < 0.01, and ***p < 0.001 compared with the diabetic control group; +p < 0.05, ++p < 0.01, and +++p < 0.001 compared with standard treatment Gabapentin; and ^ap < 0.05 and ^{aa}p < 0.01 compared with TSE 200 mg/kg.

3.5.3. Grip Strength Test Using Rotarod. This test is used to estimate the muscle strength by gripping the rotarod, and falling-off time is noted. Since this method involves the principle of analyzing muscle strength,

muscle relaxation is noted in the animal models of diabetic neuropathy. For this experiment, a fixed speed of 20 to 25 rpm is maintained. The results are depicted in Table 3.

TABLE 3: Effect of *Tecoma stans* extract on the grip strength test.

	Normal Control	Diabetic Control	Gabapentin 50 mg/kg	TSE 200 mg/kg	TSE 300 mg/kg	TSE 400 mg/kg	TSE 400 mg/kg + Gabapentin
0 Week	124.21 ± 2.21	124.51 ± 2.51	123.85 ± 3.22	128.85 ± 2.76	126.73 ± 1282	124.75 ± 2.6	127.81 ± 2.8
Week 1	125.32 ± 2.51	69.88 ± 4.82	75.35 ± 1.12*	74.75 ± 2.74	73.85 ± 2.52 ⁺	79.55 ± 4.40 ^{*,+}	74.50 ± 4.25 [*]
Week 2	123.85 ± 3.22	52.59 ± 2.25	83.05 ± 5.62**	70.72 ± 4.12 ^{***,+}	79.69 ± 3.30 ^{***,++}	85.29 ± 4.87 ^{***,a}	82.11 ± 5.30 ^{*,aa}
Week 3	129.73 ± 3.82	35.58 ± 4.92	99.95 ± 6.12**	75.25 ± 3.41 ^{***,++}	80.15 ± .2.71 ^{***,++}	89.09 ± 2.67 ^{**,aa}	98.01 ± 4.32 ^{***,aa}
Week 4	128.25 ± 3.51	23.58 ± 3.52 ^{##}	114.38 ± 2.52 ^{***}	84.93 ± 4.51 ^{##,***,+++}	94.88 ± 3.12 ^{##,***,+}	104.75 ± 3.14 ^{#,***,aa}	116.45 ± 3.68 ^{**,aaa}

Data are expressed as mean ± SD ($n = 6$). Data were statistically analyzed using two-way ANOVA followed by Tukey–Kramer's multiple comparison test at $p < 0.05$, $p < 0.01$, and $p < 0.001$. The values are expressed as ^{*} $p < 0.05$ and ^{##} $p < 0.01$ compared with the normal control group at 4th week; ^{*} $p < 0.05$, ^{**} $p < 0.01$, and ^{***} $p < 0.001$ compared with the diabetic control group; ⁺ $p < 0.05$, ⁺⁺ $p < 0.01$, and ⁺⁺⁺ $p < 0.001$ compared with standard treatment Gabapentin; ^a $p < 0.05$ and ^{aa} $p < 0.01$ compared with TSE 200 mg/kg.

3.5.4. Hyperalgesia Using Tail Flick. This method involves hyperalgesia induced by heat and involves withdrawal of Wistar rat tail, which is considered an endpoint. Following the protocol, any animal which fails to withdraw its tail within 5 seconds is rejected from the experiment. After the administration of the test drug and standard drug, the reaction time was noted after 30 minutes. The results are depicted in Table 4.

4. Discussion

From the literature survey, it was concluded that *T. stans* has shown promising results and beneficial effects in the treatment of diabetes and management of associated hyperglycemia [10]. The effects were not only limited to management of glucose levels but also have shown promising results as antioxidants. *T. stans* flowers, its leaves, and the complete plant have been used by various scientists in the management of various metabolic disorders due to their antioxidant activity and radical scavenging activity, which are also associated with decreasing blood glucose levels. These effects are mainly mediated by the presence of various chemical constituents including monoterpenoid alkaloids (specifically tecostanine and tecomanine), phenolics compounds (sinapic acids, o-coumaric, vanillic, caffeic, and chlorogenic), p-sitosterol, triterpenoids (α -amyrin, oleanolic, and ursolic acids), and lapachol [10]. The combined effects of these might prove beneficial in the management of various metabolic disorders.

In this study, we hypothesize that *T. stans* leaves could help in the management of diabetes-associated complications of neuropathy. Hence, this study was undertaken to explore the potential of *T. stans* extract in the management of diabetic-associated complications of neuropathy. Also, we evaluated the modulation of glycemetic, angiogenic, inflammatory, and oxidative pathways in the pathogenesis of diabetic neuropathy. The methanolic extract of *T. stans* was used based on the literature findings, as most of the active constituents which includes complex indole alkaloids were found to be more soluble in the methanolic extract.

Pathogens act as a trigger to activate phagocytes which ultimately results in the activation of the immune complex leading to the generation of highly toxic reactive oxygen species (RoS), which are responsible for the ingestion of pathogens. It has been seen that NADPH oxidase mediates increased consumption of oxygen, which is required for the production of superoxide radicals and ultimately results in the oxidative burst [38]. From the literature studies and the available data, various oxidants such as nitric oxide radical, hydrogen peroxide, and peroxynitrite radicals are responsible for the induction of oxidative stress in the case of diabetic neuropathy [39]. These agents serve as a trigger for the generation of oxidative stress in various animal models as well. The peroxidation byproducts of lipids are used for the estimation of RoS [40]. Also, the polyunsaturated fatty acids are peroxidized by MDA which acts as a stabilizing agent in the cellular membrane. In conditions of inflammation, the level of MDA is found to be significantly increased. This condition holds true for the animal model of diabetic neuropathy as well.

Wistar rats with STZ-induced diabetes were employed as an experimental model where the study was capped as 28 days for the development of diabetic neuropathy. The study had ten groups with six rats in each. Gabapentin (10 mg/kg) was used as a standard antidiabetic drug in the treatment of diabetic neuropathy. As evident from the literature, Gabapentin exhibits its effect as an antioxidant and anti-inflammatory agent, the combined effect of which resulted in decreased blood glucose levels; however, it may not be sufficient in comparison to the standard care of treatment for diabetes mellitus alone [41].

Methanolic extract of *T. stans* leaves at different concentrations of 200 mg/kg, 300 mg/kg, and 400 mg/kg was employed as a test drug, and the effects were compared with the standard care of treatment with Gabapentin in diabetic neuropathy. For the general parameters, blood glucose was estimated weekly for a period of 4 weeks. Thereafter, animals were sacrificed after the 4th week and the blood was collected via cardiac puncture. Various biomarkers for oxidative stress, angiogenesis, and inflammation were evaluated using ELISA kits.

TABLE 4: Effect of *Tecoma stans* extract on thermal hyperalgesia using tail flick.

	Normal Control	Diabetic Control	Gabapentin 50 mg/kg	TSE 200 mg/kg	TSE 300 mg/kg	TSE 400 mg/kg	TSE 400 mg/kg + Gabapentin
0 Week	7.21 ± 0.21	7.51 ± 2.51	7.34 ± 1.05	7.40 ± 1.08	7.61 ± 1.21	7.32 ± 1.51	7.52 ± 1.51
Week 1	7.32 ± 1.51	6.48 ± 4.82	6.35 ± 1.12	6.25 ± 2.74	6.30 ± 2.5	6.32 ± 4.40	6.50 ± 4.25
Week 2	6.85 ± 1.22	5.59 ± 2.25	6.55 ± 1.62*	6.36 ± 4.12**,+	6.40 ± 3.30 **,+	6.59 ± 4.87 **,a	6.57 ± 5.30 **,aa
Week 3	6.73 ± 0.82	5.08 ± 4.92	6.95 ± 1.12**	6.59 ± 3.41**,+	6.64 ± .2.7 **,+	6.89 ± 2.67 **,a	6.91 ± 4.32**,aa
Week 4	7.25 ± 1.51	4.58 ± 3.52##	7.09 ± 2.52***	6.73 ± 4.51##,***	6.88 ± 3.12#,***,+	6.95 ± 3.14 ***,a	7.03 ± 3.68**,aa

Data are expressed as mean ± SD ($n = 6$). Data were statistically analyzed using two-way ANOVA followed by Tukey–Kramer’s multiple comparison test at $p < 0.05$, $p < 0.01$, and $p < 0.001$. The values are expressed as # $p < 0.05$ and ## $p < 0.01$ compared with the normal control group at the 4th week; * $p < 0.05$, ** $p < 0.01$, and *** $p < 0.001$ compared with the diabetic control group; + $p < 0.05$, ++ $p < 0.01$, and +++ $p < 0.001$ compared with standard treatment Gabapentin; and ^a $p < 0.05$ and ^{aa} $p < 0.01$ compared with TSE 200 mg/kg.

T. stans at various doses (200, 300, and 400 mg/kg) in lieu of its antioxidant effects significantly demolished the levels of MDA and was found to be responsible to safeguard the structural integrity of the cellular membranes. Also, the levels of biomarkers including catalase and SOD which were decreased significantly in disease control groups were embarked with normalization following the treatment of *T. stans* extract. To establish the decreased pain threshold as determined by increased flinching in the formalin test and decreased withdrawal latency in hot plate and tail flick tests, which is a known secondary complication of DN, behavioral parameters which included hot and cold hyperalgesia along with tail flick were analyzed. Similarly, the rotarod test was employed to assess the effect of treatment on motor coordination. Non-significant differences were seen for TSE at 300 and 400 mg/kg when compared with the standard treatment. Also, the combination therapy brings similar results in line with the standard treatment of Gabapentin. Thus, it may be concluded based on the findings and available literature that the pharmacological activity possessed by the *T. stans* is mainly attributed to the presence of alkaloids, flavonoids, and glycosides, which act as an active pharmaceutical ingredient for these therapeutic mechanisms showing antioxidant, antiangiogenic and anti-inflammatory properties.

5. Conclusion

T. stans methanolic extract has provided promising results as an antioxidant, antiangiogenic, and anti-inflammatory mainly at 300 mg/kg and 400 mg/kg doses, an activity in line with the standard drug Gabapentin. Moreover, the methanolic extract of *T. stans* has shown tremendous potential as an immune-modulating agent and was found to significantly affect the levels of inflammatory cytokines which included TNF- α as an IL-1 β .

The herbal drugs appear to prevent oxidative stress-mediated damage by altering the responses of endogenous enzymes of antioxidant, thereby highlighting beneficial effects. The concentrations of thiobarbituric acid reactive substances (TBARS) were lowered on treatment, while the activity of catalase and SOD was increased. The concentrations of angiogenic parameters VEGF and PKC were also lowered in treated animal groups as compared to control groups indicating the beneficial effect of the herbal extract in attenuating angiogenesis mediated diabetes-associated neuropathy. Similarly, promising results were obtained from

behavioral parameters, where TSE (300 and 400 mg/kg) produced nonsignificant differences when compared with the standard treatment, depicting its antihyperalgesia and effect of motor coordination.

Therefore, the study evidently signifies the effective role of methanolic extract of *T. stans* in the management of neuropathy by acting as antioxidant, antiangiogenic, and anti-inflammatory agents and thus further research will warrant the ethnomedicinal use of this plant in the management of diabetic neuropathy.

Data Availability

The data used or analyzed during the study are available from the corresponding author.

Ethical Approval

This study was approved by the Institutional Animal Ethics Committee (IAEC) under protocol no. IAEC/CCP/21/02/PR-007.

Conflicts of Interest

The authors declare no conflicts of interest.

References



- [1] V. A. Chaddha, A. S. Kushwah, and V. A. Shrivastava, “An importance of herbal drugs as anti-diarrheal: a review,” *International Journal of Research in Applied, Natural and Social Sciences*, vol. 1, no. 7, pp. 25–28, 2013.
- [2] R. Sharma and P. K. Prajapati, “Diet and lifestyle guidelines for diabetes: evidence based ayurvedic perspective,” *Romanian Journal of Diabetes Nutrition and Metabolic Diseases*, vol. 21, no. 4, pp. 335–346, 2014.
- [3] M. Anand and R. Basavaraju, “A review on phytochemistry and pharmacological uses of *Tecoma stans* (L.) Juss. ex Kunth,” *Journal of Ethnopharmacology*, vol. 265, Article ID 113270, 2021.
- [4] A. Durazzo, “Study approach of antioxidant properties in foods: update and considerations,” *Foods*, vol. 6, no. 3, p. 17, 2017.
- [5] P. V. Röder, B. Wu, Y. Liu, and W. Han, “Pancreatic regulation of glucose homeostasis,” *Experimental and Molecular Medicine*, vol. 48, no. 3, p. E219, 2016.
- [6] F. Blanc, *From Chasing Violations to Managing Risks: Origins, Challenges and Evolutions in Regulatory Inspections*, Edward Elgar Publishing, Cheltenham, UK, 2018.

- [7] T. S. Bansode and B. K. Salalkar, "Phytotherapy: herbal medicine in the management of Diabetes mellitus," *Plant Science Today*, vol. 4, no. 4, pp. 161–165, 2017.
- [8] M. Majid, A. Farhan, M. I. Asad et al., "An extensive pharmacological evaluation of new anti-cancer triterpenoid (nummularic acid) from *Ipomoea batatas* through in vitro, in silico, and in vivo studies," *Molecules*, vol. 27, no. 8, p. 2474, 2022.
- [9] A. V. David, A. Anand David, R. Arulmoli, and S. Parasuraman, "Overviews of biological importance of quercetin: a bioactive flavonoid," *Pharmacognosy Reviews*, vol. 10, no. 20, p. 84, 2016.
- [10] A. Gupta and T. Behl, "Proposed mechanism of *Tecoma stans* in diabetes-associated complications," *The Natural Products Journal*, vol. 11, no. 2, pp. 127–139, 2021.
- [11] S. Kameshwaran, V. Suresh, G. Arunachalam, SK. Kanthlal, and M. Mohanraj, "In vitro and in vivo anticancer activity of methanolic extract of *Tecoma stans* flowers," *International Research Journal of Pharmacy*, vol. 3, no. 3, pp. 246–251, 2012.
- [12] S. Kameshwaran, V. Suresh, G. Arunachalam, P. R. Frank, and V. Manikandan, "Evaluation of antinociceptive and anti-inflammatory potential of flower extract *Tecoma stans*," *Indian Journal of Pharmacology*, vol. 44, no. 4, p. 543, 2012.
- [13] K. Pallavi, B. Vishnavi, P. K. Mamatha, and A. Amruthapriyanka, "Phytochemical investigation and antimicrobial activity of *Tecoma stans*," *World Journal of Pharmaceutical Research*, vol. 3, no. 2, pp. 70–72, 2014.
- [14] S. B. Gaikwad, G. Krishna Mohan, and M. S. Rani, "Phytochemicals for diabetes management," *Pharmaceutical Crops*, vol. 5, no. 1, pp. 11–28, 2014.
- [15] L. Aguilar-Santamaría, G. Ramírez, P. Nicasio, C. Alegría-Reyes, and A. Herrera-Arellano, "Antidiabetic activities of *Tecoma stans* (L.) juss. Ex kunth," *Journal of Ethnopharmacology*, vol. 124, no. 2, pp. 284–288, 2009.
- [16] G. Ramirez, A. Zamilpa, M. Zavala, J. Perez, D. Morales, and J. Tortoriello, "Chrysoeriol and other polyphenols from *Tecoma stans* with lipase inhibitory activity," *Journal of Ethnopharmacology*, vol. 185, pp. 1–8, 2016.
- [17] A. J. Alonso-Castro, R. Zapata-Bustos, J. Romo-Yañez, P. Camarillo-Ledesma, M. Gómez-Sánchez, and L. A. Salazar-Olivo, "The antidiabetic plants *Tecoma stans* (L.) Juss. ex Kunth (Bignoniaceae) and *Teucrium cubense* Jacq (Lamiaceae) induce the incorporation of glucose in insulin-sensitive and insulin-resistant murine and human adipocytes," *Journal of Ethnopharmacology*, vol. 127, no. 1, pp. 1–6, 2010.
- [18] M. Lozoya-Meckes and V. Mellado-Campos, "Is the *Tecoma stans* infusion an antidiabetic remedy?" *Journal of Ethnopharmacology*, vol. 14, no. 1, pp. 1–9, 1985.
- [19] S. Raju, S. Kavimani, V. Uma Maheshwara rao, K. Sreeramulu Reddy, and G. Vasanth Kumar, "Floral extract of *Tecoma stans*: a potent inhibitor of gentamicin-induced nephrotoxicity in vivo," *Asian Pacific journal of tropical medicine*, vol. 4, no. 9, pp. 680–685, 2011.
- [20] C. Sankaranarayanan and L. Pari, "Thymoquinone ameliorates chemical induced oxidative stress and β -cell damage in experimental hyperglycemic rats," *Chemico-Biological Interactions*, vol. 190, no. 2–3, pp. 148–154, 2011.
- [21] C. A. Krome, *Studies on the Suitability of Jatropha Curcas Kernel Meal as an Alternative Protein Source in Diets for Carp (Cyprinus carpio) and Tilapia (Oreochromis niloticus)*, University of Stirling, Stirling, UK, 2014.
- [22] M. A. Abeleh, Z. B. Ismail, K. R. Alzaben et al., "Induction of diabetes mellitus in rats using intraperitoneal streptozotocin: a comparison between 2 strains of rats," *European Journal of Scientific Research*, vol. 32, no. 3, pp. 398–402, 2009.
- [23] K. G. Abdel-Wahhab, E. M. Daoud, A. El Gendy, H. H. Mourad, F. A. Mannaa, and M. M. Saber, "Efficiencies of low-level laser therapy (LLL) and gabapentin in the management of peripheral neuropathy: diabetic neuropathy," *Applied Biochemistry and Biotechnology*, vol. 186, no. 1, pp. 161–173, 2018.
- [24] H. F. Miranda, F. Sierralta, V. Jorquera, P. Poblete, J. C. Prieto, and V. Noriega, "Antinociceptive interaction of gabapentin with minocycline in murine diabetic neuropathy," *Inflammopharmacology*, vol. 25, no. 1, pp. 91–97, 2017.
- [25] M. F. Mahomoodally, D. Lobine, M. C. N. Picot-Allain, N. Sadeer, S. Jugreet, and G. Zengin, "Conventional and non-conventional targets of natural products in the management of diabetes mellitus and associated complications," *Current Medicinal Chemistry*, vol. 28, no. 23, pp. 4638–4669, 2021.
- [26] C. Oses, B. Olivares, M. Ezquer et al., "Preconditioning of adipose tissue-derived mesenchymal stem cells with deferroxamine increases the production of pro-angiogenic, neuroprotective and anti-inflammatory factors: potential application in the treatment of diabetic neuropathy," *PLoS One*, vol. 12, no. 5, Article ID e0178011, 2017.
- [27] C. M. O. Volpe, P. H. Villar-Delfino, P. M. F. Dos Anjos, and J. A. Nogueira-Machado, "Cellular death, reactive oxygen species (ROS) and diabetic complications," *Cell Death & Disease*, vol. 9, no. 2, p. 119, 2018.
- [28] T. T. Wan, X. F. Li, Y. M. Sun, Y. B. Li, and Y. Su, "Recent advances in understanding the biochemical and molecular mechanism of diabetic retinopathy," *Biomedicine & Pharmacotherapy*, vol. 74, pp. 145–147, 2015.
- [29] R. P. Hulse, N. Beazley-Long, N. Ved et al., "Vascular endothelial growth factor-A165b prevents diabetic neuropathic pain and sensory neuronal degeneration," *Clinical Science*, vol. 129, no. 8, pp. 741–756, 2015.
- [30] V. Königs, S. Pierre, M. Schicht et al., "GPR40 activation abolishes diabetes-induced painful neuropathy by suppressing VEGF-A expression," *Diabetes*, vol. 71, 2022.
- [31] S. S. Qi, M. L. Shao, Z. Sun et al., "Lycopene ameliorates diabetic osteoporosis via anti-inflammatory, anti-oxidation, and increasing Osteoprotegerin/RANKL expression ratio," *Journal of Functional Foods*, vol. 83, Article ID 104539, 2021.
- [32] Y. Zhao, L. Zhang, Y. Qiao et al., "Heme oxygenase-1 prevents cardiac dysfunction in streptozotocin-diabetic mice by reducing inflammation, oxidative stress, apoptosis and enhancing autophagy," *PLoS One*, vol. 8, no. 9, Article ID e75927, 2013.
- [33] C. D. Anfuso, M. Olivieri, A. Fidilio et al., "Gabapentin attenuates ocular inflammation: in vitro and in vivo studies," *Frontiers in Pharmacology*, vol. 8, p. 173, 2017.
- [34] S. O. Adewole, E. A. Caxton-Martins, and J. A. O. Ojewole, "Protective effect of quercetin on the morphology of pancreatic β -cells of streptozotocin-treated diabetic rats," *African Journal of Traditional, Complementary and Alternative Medicines: AJTCAM*, vol. 4, no. 1, pp. 64–74, 2006.
- [35] T. Baluchnejadmojarad, Z. Kiasalari, S. Afshin-Majd, Z. Ghasemi, and M. Roghani, "S-allyl cysteine ameliorates cognitive deficits in streptozotocin-diabetic rats via suppression of oxidative stress, inflammation, and acetylcholinesterase," *European Journal of Pharmacology*, vol. 794, pp. 69–76, 2017.
- [36] H. Yosri, E. Said, W. F. Elkashef, and N. M. Gameil, "Modulatory role of gabapentin against ovalbumin-induced asthma, bronchial and airway inflammation in mice,"

- Environmental Toxicology and Pharmacology*, vol. 64, pp. 18–25, 2018.
- [37] L. Singh, A. Kaur, S. Garg, A. P. Singh, and R. Bhatti, “Protective effect of esculetin, natural coumarin in mice model of fibromyalgia: targeting pro-inflammatory cytokines and MAO-A,” *Neurochemical Research*, vol. 45, no. 10, pp. 2364–2374, 2020.
- [38] E. A. Bordt and B. M. Polster, “NADPH oxidase-and mitochondria-derived reactive oxygen species in proinflammatory microglial activation: a bipartisan affair?” *Free Radical Biology and Medicine*, vol. 76, pp. 34–46, 2014.
- [39] A. B. Oyenih, A. O. Ayeleso, E. Mukwevho, and B. Masola, “Antioxidant strategies in the management of diabetic neuropathy,” *BioMed Research International*, vol. 2015, Article ID 515042, 15 pages, 2015.
- [40] N. Ahuja, H. P. Singh, D. R. Batish, and R. K. Kohli, “Eugenol-inhibited root growth in *Avena fatua* involves ROS-mediated oxidative damage,” *Pesticide Biochemistry and Physiology*, vol. 118, pp. 64–70, 2015.
- [41] J. Andres, J. N. Clements, and D. Salmieri, “A possible case of gabapentin-induced mild hyperglycemia,” *Journal of Pharmacy Technology*, vol. 30, no. 4, pp. 140–144, 2014.

Research Article

Neurobehavioral and Biochemical Evidences in Support of Protective Effect of Marrubiin (Furan Labdane Diterpene) from *Marrubium vulgare* Linn. and Its Extracts after Traumatic Brain Injury in Experimental Mice

Nidhi,¹ Govind Singh,¹ Rekha Valecha,² Govind Shukla,³ Deepak Kaushik,¹ Mohammad Akhlaquer Rahman,⁴ Rupesh K. Gautam,⁵ Kumud Madan,⁶ Vineet Mittal ,¹ and Rajeev K. Singla ^{7,8}

¹Department of Pharmaceutical Sciences, Maharshi Dayanand University, Rohtak 124001, India

²Department of Pharmacy, Delhi Skill and Entrepreneurship University, New Delhi 110065, India

³University College of Ayurveda, Dr. S. R. Rajasthan Ayurveda University, Jodhpur 342304, India

⁴Department of Pharmaceutics and Industrial Pharmacy, College of Pharmacy, Taif University, P.O. Box 11099, Taif 21944, Saudi Arabia

⁵Department of Pharmacology, MM School of Pharmacy, MM University, Sadopur-Ambala 134007, India

⁶Lloyd Institute of Management and Technology (Pharm.), Greater Noida, India

⁷Institutes for Systems Genetics, Frontiers Science Center for Disease-Related Molecular Network, West China Hospital, Sichuan University, Chengdu 610041, Sichuan, China

⁸Global Research and Publishing Foundation, New Delhi 110059, India

Correspondence should be addressed to Vineet Mittal; dr.vineet123@rediffmail.com and Rajeev K. Singla; rajeevsingla26@gmail.com

Received 31 March 2022; Revised 27 April 2022; Accepted 6 May 2022; Published 24 May 2022

Academic Editor: Abraham Wall Medrano

Copyright © 2022 Nidhi et al. This is an open access article distributed under the Creative Commons Attribution License, which permits unrestricted use, distribution, and reproduction in any medium, provided the original work is properly cited.

Traumatic brain injuries due to sudden accidents cause major physical and mental health problems and are one of the main reasons behind the mortality and disability of patients. Research on alternate natural sources could be a boon for the rehabilitation of poor TBI patients. The literature indicates the *Marrubium vulgare* Linn. and its secondary metabolite marrubiin (furan labdane diterpene) possess various pharmacological properties such as vasorelaxant, calcium channel blocker, antioxidant, and anti-edematogenic activities. Hence, in the present research, both marrubiin and hydroalcoholic extracts of the plant were evaluated for their neuroprotective effect after TBI. The neurological severity score and oxidative stress parameters are significantly altered by the test samples. Moreover, the neurotransmitter analysis indicated a significant change in GABA and glutamate. The histopathological study also supported the observed results. The improved neuroprotective potential of the extract could be attributed to the presence of a large number of secondary metabolites including marrubiin.

1. Introduction

Injuries are a major public health problem today. Traumatic brain injury (TBI) is defined as damage to the brain resulting from an external mechanical force, such as that caused by rapid acceleration or deceleration, blast waves,

crush, or impact, and can lead to temporary or permanent impairment of cognitive, physical, and psychosocial functions [1–3]. TBIs in India have been increasing significantly due to rapid motorization, industrialization, migration, and changing value systems of Indian society. Also, the Centre for Disease Control and Prevention

estimated that the incidence of TBI affects a large number of the population worldwide. Apart from instantaneous deaths, the suffering and poor quality of life among survivors is a living testimony to the impact of TBIs. The total volume of TBI in India is unknown, but estimates suggest that there are more than a million trauma-related deaths in India per year, of which 50% are TBI-related [4, 5]. It involves a complex cascade of changes including pathological, metabolic, and gene-related changes which not only include cell damage but also contribute to the activation of inflammatory cytokines (IL-6, TNF- α), increase in intracellular calcium regulation, oxidative stress, and mitochondrial dysfunction that contributes to neurodegeneration. Other pathological changes as part of secondary injury include the neurological deficit, activation of microglial cells, disruption of the blood-brain barrier, cerebral edema, intestinal damage, and abnormal nitrite, glutamate, and calcium level [6–8]. The study of the literature indicated that there is not any particular treatment strategy for TBI and research on new compounds or plant metabolites is highly required to improve the quality of life [9]. Enough pieces of evidence are present in the literature which could prove the phytochemicals/extracts to be effective and protective in TBI. A huge number of herbal extracts or plant actives are also reported to possess a significant role in neuroprotection, reduction of inflammation, and management of oxidative stress [10–14].

The *Marrubium* genus (Family: Lamiaceae) has nearly thirty plant species and is indigenous to Europe and Asian countries. Among various species, *Marrubium vulgare* L. is a perennial herb commonly known as “white horehound” in different regions of Europe [15]. The hydroalcoholic extract of selected medicinal herbs was reported to possess significant pharmacological properties by inhibiting the action of neurotransmitters such as acetylcholine, prostaglandin E, histamine, and bradykinin [16–19]. The various secondary metabolites of different categories such as marrubiin (diterpene), arenarioside, acteoside, forsythoside B, and ballotetroside (phenylpropanoids esters) have been isolated and identified from the plant extracts [20–24]. The pharmacological potential of marrubiin as anti-inflammatory, vasorelaxant, antioxidant, and calcium channel (L-type) blocker has been well established [25]. The other diterpenes present in the plant extract like marrubinic acid and marubienol also exhibited analgesic and antiedematogenic activities [23]. Moreover, the various phenylpropanoid esters of the herb showed significant anti-inflammatory potential due to the inhibition of the cyclooxygenase-2 (COX-2) enzyme [22].

On the basis of a literature study, the hydroalcoholic extract of *Marrubium vulgare* L. and marrubiin, a potential and well-tolerated diterpene (LD₅₀ 370 mg/kg) of the herb, are selected to evaluate their protective effect against TBI in experimental mice. Further, the research work is also extended to evaluate the possible synergistic protective effect of plant active (marrubiin)/extract with some selected marketed drugs like lixisenatide (L), nimodipine (N), acamprosate (A), and celecoxib (C) (Figure 1) [12, 26, 27].

2. Results and Discussion

The selected medicinal plant, *Marrubium vulgare* L., and its active constituent, marrubiin, are reported to possess numerous pharmacological properties such as vasorelaxant, antioxidant, antihypertensive, antispasmodic, anti-inflammatory, antiedematogenic, and antidiabetic properties [17, 25]. Hence, in the present study, the plant active and hydroalcoholic extract of the herb is explored for its neuroprotective potential against TBI. Moreover, the selected dose of plant extract/active is also investigated for protective action in combination with some marketed drugs like lixisenatide, celecoxib, nimodipine, and acamprosate.

The powdered sample of the plant was extracted by cold maceration method and a dark brown extract was obtained with a percentage yield of $8.5 \pm 1.2\%$ (w/w). The extract was also analyzed by HPTLC for marrubiin concentration and was calculated to be present in $7.1 \pm 0.8\%$ (w/w) concentration. On the basis of literature and the result of extract analysis, two doses of the extract, 700 mg/kg and 1400 mg/kg, were selected for the present experimental protocol. The Swiss albino mice were used to study the neuroprotective effect of the herb and its active principle along with selected marketed drugs. TBI was induced in the animals of different groups, except control, by the weight drop method.

2.1. Assessment of Neurological Severity Score. After TBI, the assessment of NSS reflects the rough magnitude of motor and cognitive deficiency such as difficulty in memory, attention deficits, and decrease in concentration in affected animals. Early assessment of NSS is a simple and reliable method to evaluate the motor ability and cognitive skills in injured rodents. Numbers of tasks were performed to check the NSS like straight walk, exit circle, grip strength, startle reflex, beam walk, and round stick balance. NSS of 5–7 indicated moderate injury in the experimental animals of negative control (group 2) [28–30]. The NSS of animals from different groups was presented in Figure 2.

The interpretation of data confirmed that plant extracts at 1400 mg/kg significantly altered the score in the treated group as compared to the –ve control after the 7th day of treatment protocol ($p < 0.05$). Further, this extract in combination with selected marketed drugs (Group 8) significantly reduced the severity score even after the 4th and 7th days of treatment ($p < 0.01$). The assessment of NSS gives a fair idea about the neuroprotective effect of plant extract alone and in combination with marketed drugs. Further, the motor coordination, mobility, and memory potential in trauma-affected animals were evaluated by performance in the open field, rotarod, and plus-maze activities.

2.1.1. Open Field Performance Analysis. On the 7th day of the experimental protocol, the mobility/locomotor performance in various animals was further analyzed by open field and rotarod performance analysis. In this test, the number of lines crossed by mice from different groups was counted for at least 5 minutes and presented graphically in Figure 3(a). Results confirmed that the trauma significantly ($p < 0.001$)

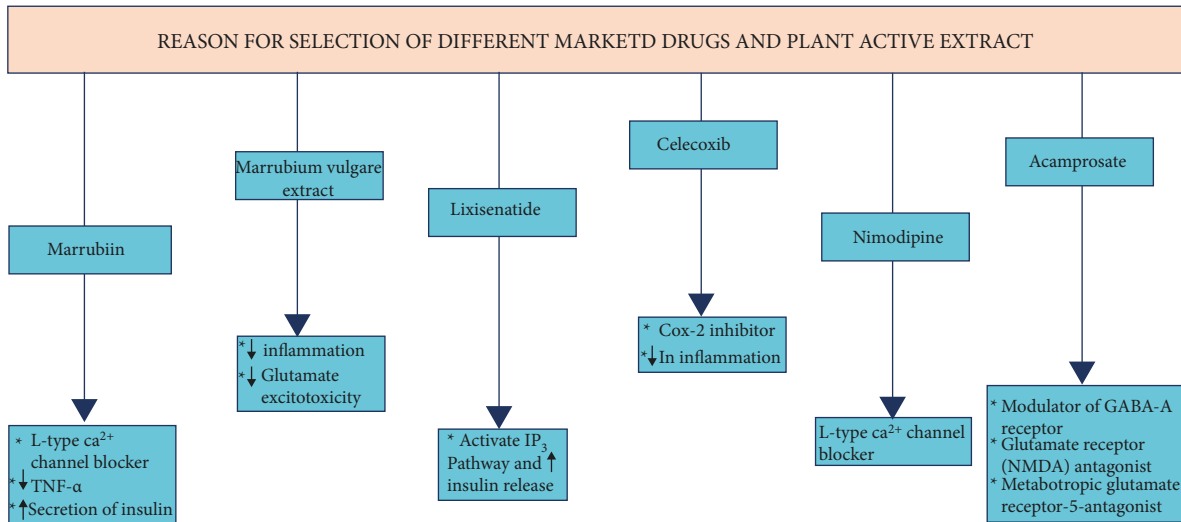


FIGURE 1: Pharmacological rationale for the selection of various test samples (plant active/extract) and marketed drugs for the present study.

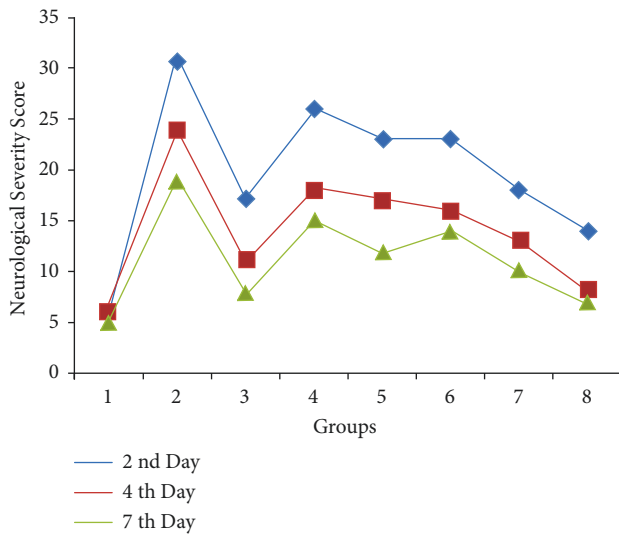


FIGURE 2: Change in the neurological severity score on different days of experimental study (2nd, 4th, and 7th day).

reduced the number of lines crossed by mice (77 ± 6.4) as compared to the control group (160 ± 12.4). Further, the animals treated with plant extract (1400 mg/kg) enhanced their mobility ($p < 0.05$) which was further improved significantly when this extract was supplemented with marketed drugs ($p < 0.01$).

2.1.2. Rotarod Performance Analysis. Motor coordination in the experimental animals was further investigated by analysis of rotarod performance. In this experiment, the falling latency of animals of various groups from a rotating rod (25 rpm) for five minutes was observed and noted (Figure 3(b)). Falling latency in the control group (43 ± 2.510) was significantly ($p < 0.01$) reduced in the TBI-affected group (7.6 ± 1.631). Delay in falls was also altered in animals treated with marrubiin at different doses but the change was not significant as compared to the affected group

($p > 0.05$). Moreover, the extract of the selected medicinal plant at a higher dose significantly enhanced the falling latency of experimental animals ($p < 0.01$). The significance of the result was further improved when the selected dose (1400 mg/kg) of the extract was administered along with all marketed drugs ($p < 0.001$).

2.1.3. Elevated Plus Maze Study. TBI can also cause the short-term loss in memory of the animals under the protocol. A simple apparatus such as an elevated plus maze could be employed to evaluate the cognitive function in different groups. On the seventh day of the experiment, the number of entries in the closed arm of the elevated plus maze was recorded for a minimum of 5 minutes (Figure 3(c)). Loss in memory potential of injured mice was indicated by the significant reduction ($p < 0.001$) in the number of entries (1.6 ± 0.32) as compared to the control group (12 ± 1.1). Treatment with plant extracts/active constituents and different drugs altered the memory deficit induced by the TBI. But the improvement in impaired memory function was significant in animals fed with plant extract at high doses ($p < 0.01$). Further, the synergistic neuroprotective effect was exhibited by rodents on giving the extract along with selected commercial drugs.

2.1.4. Estimation of Biochemical Parameters. The concentration of various endogenous oxidative stress parameters (GSH, MDA, Catalase) was determined and was indicated in Figure 4. TBI significantly reduced the GSH concentration as compared to the control group ($p < 0.001$) whereas the level of malondialdehyde and catalase increased significantly ($p < 0.01$) (Figure 5). Further, the results suggested that the plant extract alone in higher concentration and along with the marketed drugs significantly altered the oxidative stress parameters ($p < 0.05$ and $p < 0.01$, respectively). Moreover, the total protein content in the test samples was determined and concentration was found to be significantly altered in treated groups (Figure 6). Also, the nitric oxide (NO)

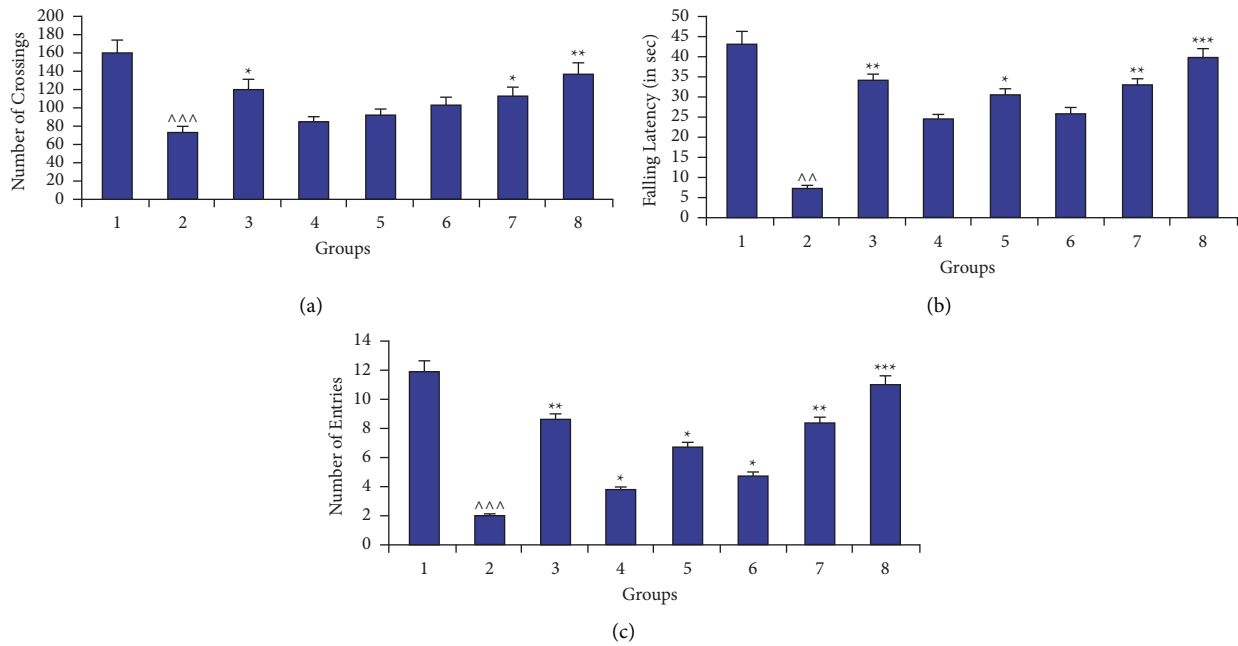


FIGURE 3: Effect of different neurobehavioral tests: (a) open field, (b) rotarod, and (c) elevated plus maze in different groups (1: control; 2: (-ve) control (TBI); 3: marketed drugs (L + C + N + A); 4, 5: marrubiin (50,100 mg/kg); 6, 7: *M. vulgare* extract (700,1400 mg/kg); 8: *M. vulgare* extract (1400 mg/kg) + marketed drugs) (^ $p < 0.05$; ^^ $p < 0.01$; ^^^ $p < 0.001$ as compared to the control group; * $p < 0.05$; ** $p < 0.01$; *** $p < 0.001$ as compared to the -ve control).

concentration was altered by test groups but the change was significant with the marrubiin (50 mg/kg) and plant extract at a higher dose ($p < 0.05$).

2.1.5. Neurotransmitters (GABA and Glutamate) Analysis. The concentration of inhibitory (GABA) and excitatory (Glutamate) neurotransmitters was modulated significantly ($p < 0.001$) in the animals suffering from traumatic brain injury (Figure 6). Treatment with test drugs (extract and plant active) at different doses enhanced the GABA concentration but the change was insignificant ($p > 0.05$) with a low dose of marrubiin and plant extract. But a higher dose of the extract ($p < 0.01$) and active constituent ($p < 0.05$) of the herb displayed a significant change in the quantity of GABA. Further, the glutamate analysis confirmed the significant reduction ($p < 0.01$) in its level on treatment with *Marrubium vulgare* extract at an elevated dose (1400 mg/kg). Also, there is a synergistic alteration in the effect produced by herbal extract in combination with marketed drugs ($p < 0.001$).

2.1.6. Histopathological Study. On the 8th day of the experimental protocol, the histopathological changes in the cerebral cortex of brain sections from the animals of different treated groups were observed. The nuclei (pink stain) and cytoplasm (violet color) could be easily differentiated in the neuronal cell of brain tissue. The intact neuronal cell from the samples of different treated groups was depicted as a black arrow in the photographs, but when there is no clear

distinction between cytoplasm and nuclei, then it was displayed as a red arrow in the section pictures (Figure 7).

Trauma due to accidents, blasts, and falls is the most prevalent cause of injury to the brain [31]. TBI not only causes the mortality of individuals but also produced a large number of short- and long-term consequences to brain functions. According to an estimate, TBI contributes to more than 30% of all injury-related deaths in the USA, and about half of the survivors (43%) faced significant chronic disabilities due to the nonavailability of clinically effective treatment protocol [32, 33]. After the TBI, there occur different primary and secondary pathological signaling cascades. The effect due to primary insult cannot be treated but can be prevented whereas the functional impairment and chronic disability of neurons after secondary injury because of oxidative stress, excitotoxicity, inflammation, and mitochondrial dysfunction could be targeted for the improvement of patient life after injury [8, 34].

The selected medicinal plant *Marrubium vulgare* L. and marrubiin (plant active) were investigated for neuroprotective effects after TBI. After TBI, the assessment of NSS reflects the rough magnitude of motor and cognitive deficiency such as difficulty in memory, attention deficits, and decrease in concentration in affected animals. Improvement in the motor ability and cognitive skills of injured rodents was exhibited by the various test groups especially the plant extract in a higher dose and its combination with marketed drugs. The literature revealed that marrubiin itself and the plant extract are potent calcium channel blockers and the significantly altered functional ability of mice might be due

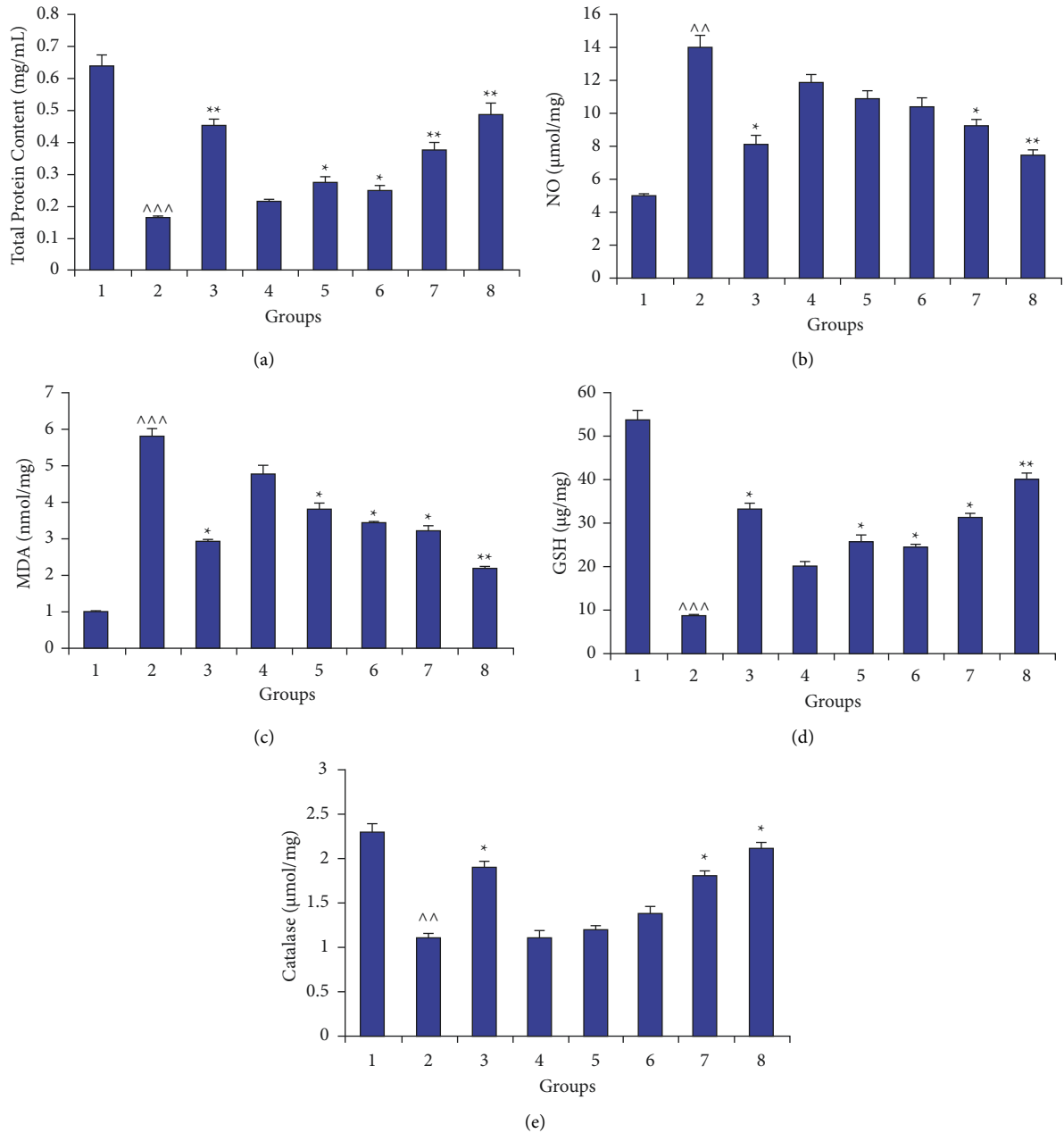


FIGURE 4: Evaluation of various biochemical (oxidative stress) parameters: (a) total protein content, (b) nitric oxide, (c) malondialdehyde (MDA), (d) glutathione (GSH), and (e) catalase, in different groups (1: control; 2: (-ve) control (TBI); 3: marketed drugs (L + C + N + A); 4, 5: marrubiin (50,100 mg/kg); 6, 7: *M. vulgare* extract (700,1400 mg/kg); 8: *M. vulgare* extract (1400 mg/kg) + marketed drugs; [^] $p < 0.05$; ^{^^} $p < 0.01$; ^{^^^} $p < 0.001$ as compared to the control group; ^{*} $p < 0.05$; ^{**} $p < 0.01$; ^{***} $p < 0.001$ as compared to the -ve control).

to this action [16, 35]. Also, the scientists had proved that the calcium channel blockers not only improved the behavioral deficits but also prevent the disruption in spatial memory of experimental animals [36, 37].

Moreover, sudden trauma to the brain triggers the different signaling pathways in astrocytes and neurons that lead to the upregulation of calcium and downregulation of endothelial nitric oxide synthase (eNOS). It further enhanced the concentration of reactive oxidative species (ROS) and leads to mitochondrial dysfunction and apoptosis [38, 39]. It has also been reported that NO, which is a unique

molecule, causes cytotoxicity due to enhanced oxidative stress, and the plant extract significantly altered the various stress parameters along with the NO to exert the neuro-protective effect in the injured animals [40]. The observed results could be attributed to the blockage of Cav 1.2 and Cav 1.3 (L-type) postsynaptic calcium channels localized in the soma, spines, and shaft of dendrites which further help in the downregulation of enhanced calcium inflow and decrease the ROS production which could help in the restoration of the mitochondrial respiratory chain and its integrity [16, 35, 37]. In past, the treatment with plant extract was also

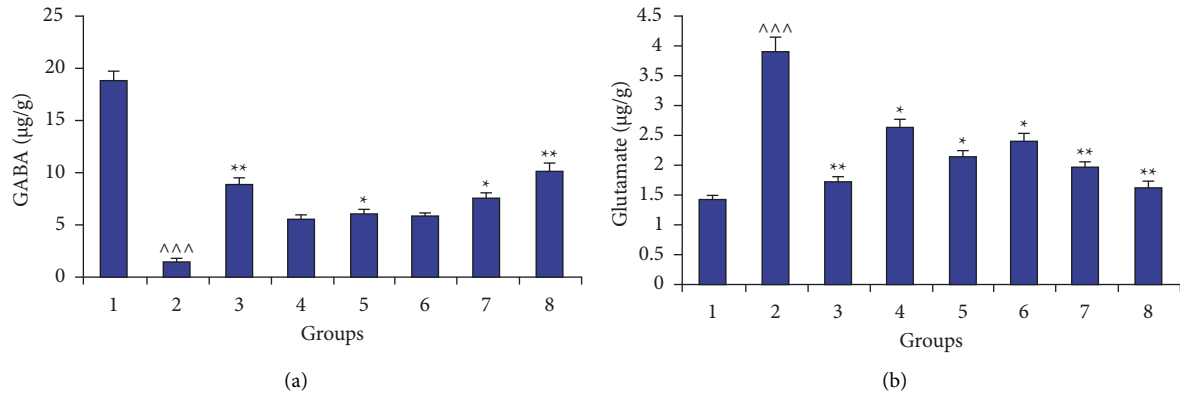


FIGURE 5: Neurotransmitter: (a) GABA (inhibitory) and (b) glutamate (excitatory) analysis in different groups (1: control; 2: (-ve) control (TBI); 3: marketed drugs (L + C + N + A); 4, 5: marrubiin (50,100 mg/kg); 6, 7: *M. vulgare* extract (700,1400 mg kg); 8: *M. vulgare* extract (1400 mg/kg) + marketed drugs; ^ $p < 0.05$; ^^ $p < 0.01$; ^^ $p < 0.001$ as compared to the control group; * $p < 0.05$; ** $p < 0.01$; *** $p < 0.001$ as compared to the -ve control).

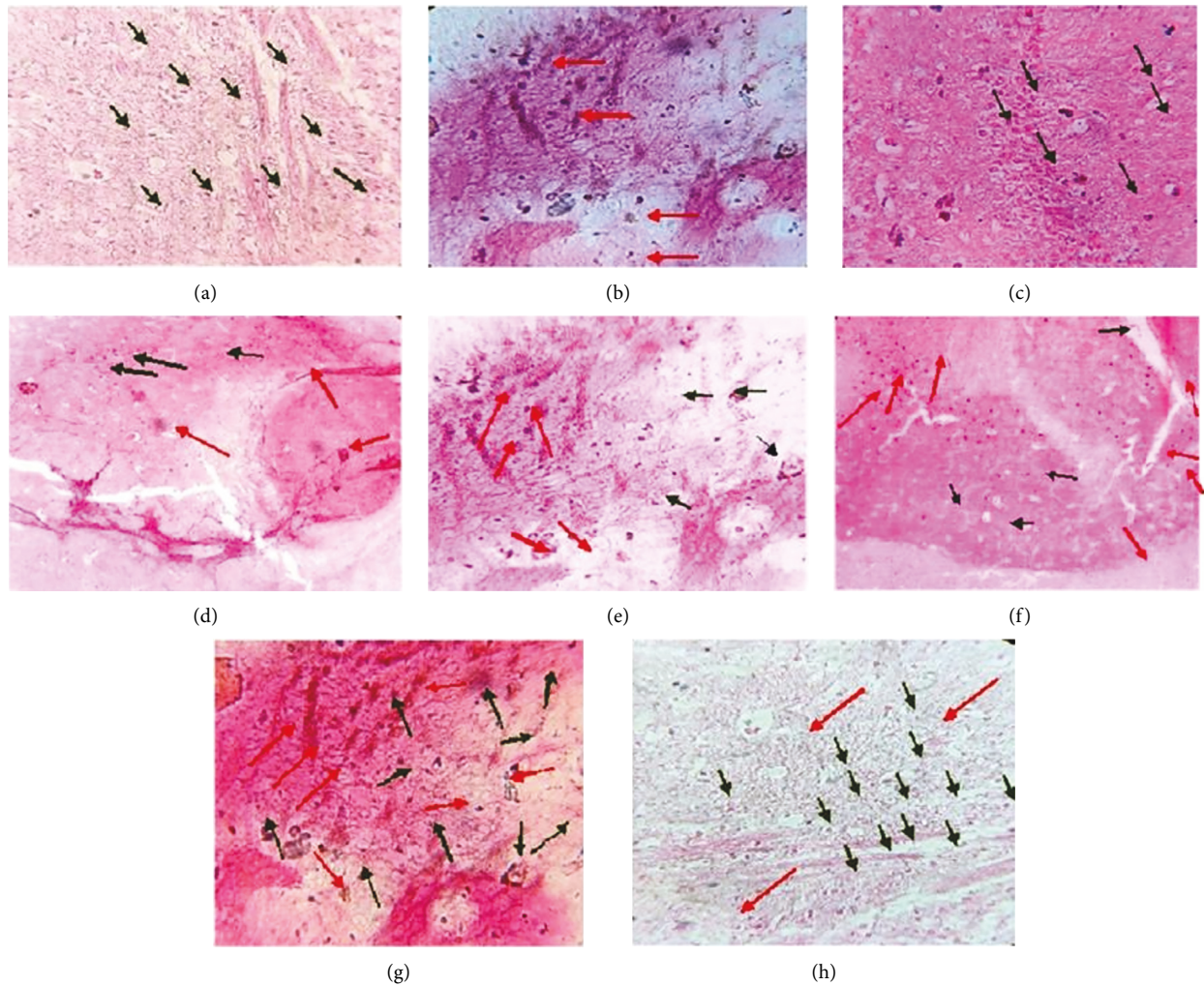


FIGURE 6: Photomicrographs of brain sections of experimental animals from different groups (a) control; (b) (-ve) control (TBI); (c) marketed drugs (L + C + N + A); (d, e) marrubiin (50,100 mg/kg); (f, g) *M. vulgare* extract (700,1400 mg kg); (h) *M. vulgare* extract (1400 mg/kg) + marketed drugs depicting intact neuron by black arrow and nonintact cells by red arrow.

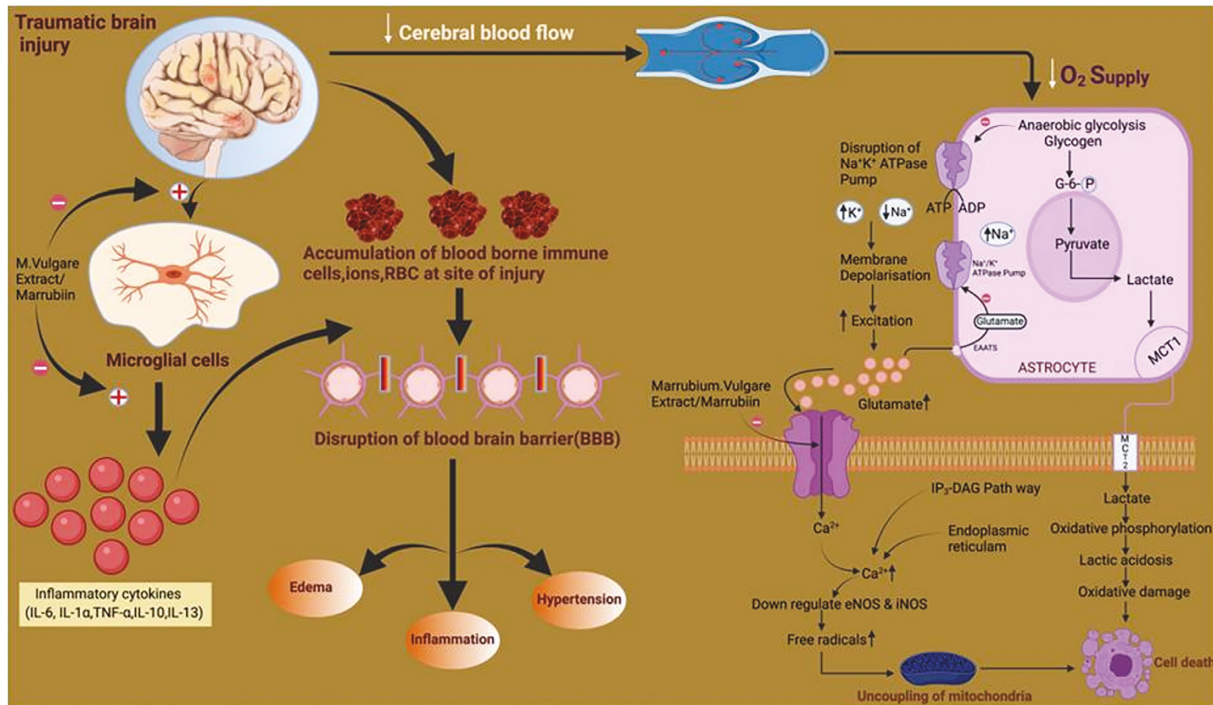


FIGURE 7: Proposed site of action of *Marrubium vulgare* extract/marrubiin to bring out the protective effect after TBI.

postulated to reduce the microglial activation which could be another reason for better neuroprotective action by affecting the inflammatory cascade after TBI [18, 41, 42].

The results of the neurotransmitters analysis indicated that there is a significant alteration in GABA (\downarrow) and glutamate levels (\uparrow) after the injury. These findings match with previous investigations which enhanced the glutamate level and excitotoxicity induced signaling cascades which resulted in neurodegeneration [43]. Also, it has been postulated that the imbalance between these neurotransmitters leads to neurodegeneration in the brain [44–46]. But treatment with *Marrubium vulgare* extract and marrubiin significantly modulates their concentration in a positive manner. The neuroprotective effect of the test samples implies that excitotoxicity due to enhanced glutamate was reduced and the balance between GABA and glutamate was improved to bring out this action. Further, the calcium channel blockers, especially of L-type, were reported to reduce the necrosis in glutamate toxicity; therefore, the present results could be attributed to the inhibition of voltage-gated cation (Ca^{2+}) channels by plant active and extract [16, 35, 47]. Also, the vasospasm is the obvious feature in a significant number of traumatic cases and vasorelaxant action of the plant active/extract could further enhance the recovery in the victims after injury [33, 48]. Moreover, the photomicrographs of the histopathology of brain sections further confirmed the neuroprotective nature of plant extract at a higher dose and its combination with selected marketed/commercial drugs.

The present findings indicated that recovery after the injury was more significant with the herb extract as compared to plant active alone. Such results could be due to the presence of pharmacologically important secondary

metabolites including marrubiin, in the plant extract. Marrubiin was reported to block the L-type calcium channels and thus bring out the vasorelaxant and anti-excitotoxicity effect of herb. Also, the inhibition of these cation channels could reduce the activation of resident microglial cells and thus lessen the release of pro-inflammatory cytokines (IL-1 α , IL-6) [18, 41, 42]. Further, the previous investigations established that the different phytochemicals such as renarioside, acteoside, forsythoside B, and ballotetroside as phenylpropanoid esters present in the extract can inhibit the cyclooxygenase-2 (COX-2) enzymes and thus are responsible for the anti-inflammatory action of herb (C) [21, 24, 49]. Moreover, the hydroalcoholic extract was also reported to reduce the spasm induced by acetylcholine and oxytocin at experimental conditions [50]. In addition, oxidative stress was considered to be as one of significant parameters in inducing the secondary effects after TBI [51]. The level of GSH was reduced whereas the MDA and catalase concentration enhanced significantly after the injury in experimental animals. Treatment with the plant extract at higher dose significantly altered the oxidative stress parameters. The antioxidant potential of the herbal extract could be due to the presence of total phenolic and flavonoid content in addition to marrubiin which could also be a possible reason behind the fast recovery of injured animals [17, 52–54]. Finally, TBI also reported to induce the oedema in the brain which is mainly responsible for the significant number of mortality in the head injury cases and the selected plant extract/marrubiin also possess the anti-oedematogenic properties [23, 55]. Hence, the improved neuroprotective effect of the selected medicinal plant could also be attributed to the antioedematogenic potential along

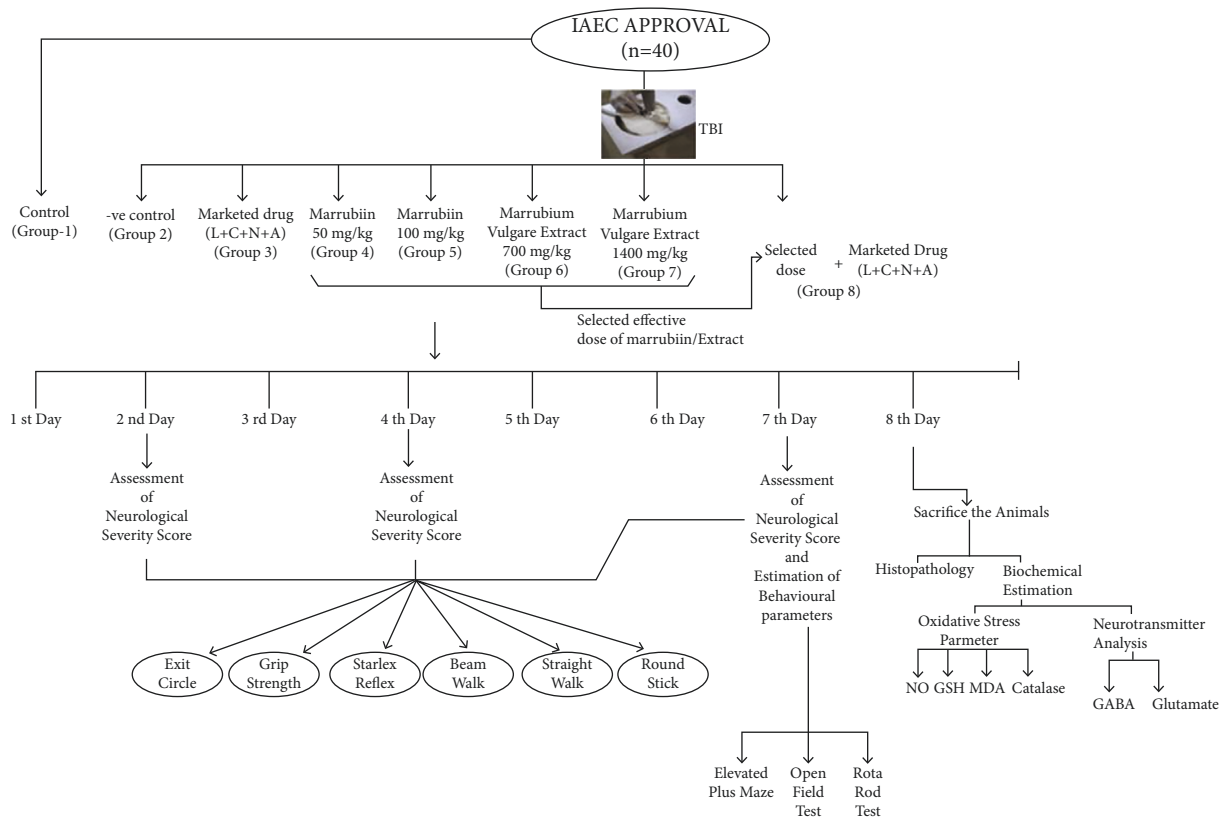


FIGURE 8: Detailed experimental protocol for the present study.

with other discussed properties. On the basis of the above discussion, the proposed site of action of plant extract/active to bring out the protective effect in the pathological cascade of TBI is depicted in Figure 7.

3. Materials and Methods

3.1. Plant Sample and Reagents. The selected herb, *Marrubium vulgare* L., was collected from the local district of Nainital, Uttarakhand, and identified by a botanist. A voucher specimen was also kept in the laboratory of the department for future reference. All the procured chemicals and reagents were of analytical grade. The plant active, marrubiin, was purchased from the reliable commercial source, Extrasynthese (France).

3.2. Extraction of Plant Sample and Analysis. The collected sample of the whole plant was thoroughly washed in running tap water and shade dried. The dried herb was powdered, sieved (60–80), and extracted with hydroalcoholic solvent (50%) by the cold maceration method. The powdered sample (100 g) was kept in a round bottom flask with solvent (1 : 15) at room temperature for 10 days with occasional stirring. The extract obtained was concentrated, lyophilized, and stored at low temperature in an airtight container till further study. Also, the qualitative and quantitative analysis of the extract for the marrubiin concentration was performed using a validated HPTLC protocol which was previously developed in our laboratory [56, 57].

3.3. Animals. For the present research, the swiss albino mice (25–30 g) were procured from the disease-free small animal house of Lala Lajpat Rai University of Veterinary and Animal Sciences (LLRUVAS), Hisar, India. The animals were housed in the group of five ($n = 5$) in polypropylene cages ($29 \times 22 \times 14$ cm) lined with proper bedding. They were acclimatized as per the standard CPCSEA guidelines for at least two weeks under natural light/dark cycle at $25 \pm 2^\circ\text{C}$. During this period, they have free access to standard rodent feed and water *ad libitum*.

3.4. Experimental Protocol and Induction of Traumatic Brain Injury. TBI is followed by not only the immediate primary effects but also some cellular, genomic, and biochemical changes termed the secondary insult. These effects could last up to some minutes to some days [58]. Hence, the experimental protocol should be kept for seven days to effectively evaluate the protective effect of the selected plant active/extract against secondary insult after TBI. Prior to the commencement of experiments, the research protocol was duly approved by the institutional animal ethical committee (1767/RE/S/14/CPCSEA/CAH/153–165, dated-17/12/18), MDU, Rohtak. After the specified time period (15 days) of acclimatization of experimental animals, they were divided into twelve groups ($n = 5$). The detailed experimental protocol is illustrated in Figure 8. The TBI was induced in the animals of all groups except the first group (control) by the standard weight-drop method. Animals were placed in a closed chamber and anesthesia was induced with 4%

isoflurane. After 5–7 minutes, the mouse was removed from the closed chamber and placed on the open circuit with 2% isoflurane maintenance. The reflexes were checked by pressing the hind paw and observing the eye movements. In the absence of reflexes, the mouse was placed on the foaming bed, and a midline incision was given over the head of mice and exposed the skull. The metallic disc was fixed over the exposed skull and placed properly under the metallic pipe (1 m long). After that, 66 g weight (spherical brass ball) was dropped through the upper end of the pipe to induce closed head injury. After brain trauma, the scalp was sutured, neosporin powder (GlaxoSmithKline Pharmaceuticals Ltd., Bangalore, India) was applied over the scalp, and the mouse was returned to their cage for recovery [59]. The test drugs/extracts were given to animals of different groups as per the protocol for seven days. The neurological severity score for each group was calculated after 24 hrs, 4th day, and 7th day, and behavioral parameters were studied on the 7th day of the experimental study. On the next day, the animals were sacrificed by cervical dislocation and used for histological and biochemical study.

3.5. Neurobehavioral Study. Immediate after the TBI, the pathological cascade is initiated and it reflects through impairment in motor coordination, balance, and locomotor dysfunction of animals. Also, due to impact, there could be a loss of memory in experimental mice. The magnitude of these parameters could be assessed as per the following protocols.

3.5.1. Assessment of Neurological Severity Score. The neurological severity score (NSS) roughly determines the magnitude of loss in motor and locomotor function. The various tasks like exit circle, beam walk, round stick, straight walk, startle reflex, and grip strength after 24 hrs (2nd day), 4th day, and 7th day of injury were performed to calculate it. One point was given for non/delayed performance and zero points for the completion of tasks. All the tasks were carried out as per the standard procedures. Briefly, in the exit circle, the mice were placed in the center of the circle and the time taken to exit the circular instrument was monitored for three minutes. In beam walk, the animal was kept on the wooden beam on an elevated surface (60 cm). On the other end, a box (20 × 25 × 24 cm) with a 10 cm opening was placed. The time taken by the mice to reach the box was noted and compared with the control for the calculation of scores. For grip strength, the mice were held up by the tail, and their paws were touched by the anatomical forceps. If the mouse grips the forceps, 0 points were counted, and on failure or performance with very low intensity, 1 point was added. In the straight walk test, the mouse was placed on a clear surface and observed for the walking pattern. The impaired gait pattern and failure to actively explore environs by the animal are credited for 1 point and a normal walk earns nil. In the round stick balance test, the ability of mice to balance over a round stick (Φ 5 mm) for 10 seconds was evaluated. The alertness of the mice and response to the sound of a hand clap was evaluated in the startle reflex test [60].

3.5.2. Open Field Test. After the injury, the motor and exploratory behavior of mice can be evaluated by this simple test. In this, the mice were placed in the middle of the apparatus (70 × 70 × 25 cm) and the number of squares crossed by at least the anterior paw of animals was recorded for 5 min by visual inspection [61].

3.5.3. Rota Rod Test. The coordination in the motor skills can further be evaluated by this test. The ability of the animals to hold on to the accelerated rotating rod depicts the motor functions. In this test, the mice were placed on a rotating rod (5 rpm), and it was accelerated at a speed of 5 rpm every 40 seconds. The animals were kept on the rotating rod till the rod speed reached 25 rpm. The average latency in the fall of mice from the rod was noted for 5 minutes [62].

3.5.4. Elevated Plus Maze. The learning and memory potential of the drug in the experimental mice can be evaluated by the previously described methods. In this test, a wooden plus maze with open and closed arms was kept in an elevated place (25 cm from the floor). The mice were placed on the open arm of the elevated plus maze, and no entries in the closed arm and open arm were recorded for 5 min [63].

3.6. Analysis of Biochemical Parameters. On the eighth day of the experimental study, the whole brain of animals from each group was isolated and cleaned with ice-cold normal saline. The brain samples were homogenized with phosphate buffer (pH 7.4) and immediately centrifuged at 2500 rpm for 15 min. The homogenate was used to analyze the various biochemical parameters.

3.6.1. Total Protein Content. Alkaline copper solution 5 ml was added to 1 ml of brain tissue homogenate and allowed to stand for 10 minutes. Further, the 0.5 ml of diluted Folin's reagent (1:2) was added and mixed properly. After 30 minutes, the absorbance of the prepared solution was taken at 750 nm in a UV-Visible spectrophotometer. The total protein content was determined in mg/mL [64].

3.6.2. Estimation of Catalase. The catalase assay of the different samples was performed by the method described by Sinha et al., [65]. In this, the small portion of brain homogenate (0.1 mL) was mixed with 0.1 mL of phosphate buffer (0.01 M, pH 7.4) and 0.4 ml of distilled water. Further, the addition of 0.5 ml of H₂O₂ (2 M) initiated the reaction. The mixture was incubated for 1 min at room temperature and the reaction was ended by mixing 2 ml of potassium dichromate-acetic acid reagent. The solution was kept for 15 minutes in a boiling water bath. On cooling the solution, the green color appeared and the absorbance was taken at 570 nm in a UV-Visible spectrophotometer. The concentration of catalase was expressed as μ moles/mg of protein [66].

3.6.3. Estimation of Malondialdehyde (MDA). Malondialdehyde is an indicator of lipid peroxidation and was estimated as previously described [67]. The supernatant of tissue homogenate was mixed with various reagents like acetic acid (1.5 ml, 20%), thiobarbituric acid (1.5 ml, 0.8%), and sodium dodecyl sulfate (0.2 ml, 8.1%). The mixture was heated at 100°C for 60 min and cooled. After cooling, 5 ml of n-butanol: pyridine (15 : 1 v/v) and distilled water (1 ml) were added with vigorous shaking. The solution was centrifuged at 4000 rpm for 10 min, and the separated organic layer was removed and absorbance was measured at 532 nm using a UV-Visible spectrophotometer (Shimadzu UV Spectrophotometer, UV-1800 Series, India). The amount of malondialdehyde present in the sample was expressed as nmol/mg protein.

3.6.4. Nitric Oxide (NO) Assay. The accumulation of nitrite was assayed spectrophotometrically using a Greiss reagent. The supernatant (100 μ l) was mixed with an equal volume of Greiss reagent and kept for 10 min at room temperature. The absorbance of the reaction mixture was measured at 540 nm against a blank solution (distilled water). The concentration of NO in the sample was calculated by plotting the standard curve of sodium nitrite (5–30 μ mol/ml) and was expressed as μ moles of NO/mg protein [68].

3.6.5. Measurement of Reduced Glutathione (GSH). The reduced glutathione content in the tissue homogenate was measured by the previously described method using a UV-Visible spectrophotometer. The processed sample was mixed with an equal volume of sulfosalicylic acid (5%) and then centrifuged at 2000 rpm at 4°C for 10 min to separate out the proteins. Take the supernatant and add phosphate buffer (2 mL, pH 8.4), 5,5'-dithiobis (2-nitrobenzoic acid, (0.5 mL), and distilled water (0.4 ml) thoroughly and take the absorbance at 412 nm. The concentration of GSH in the sample was determined using a standard curve prepared with reference GSH (5–25 μ g/ml) and expressed as μ g of GSH/mg protein [17, 69].

3.6.6. Estimation of GABA and Glutamate. The γ -aminobutyric acid (GABA) and glutamate concentration in the brain samples of various test groups were estimated using HPTLC. The spots of the test and standard samples were applied with the help of a Linomat 5 applicator (CAMAG, Switzerland) on precoated silica gel plates (20 \times 10 cm). The chromatogram was developed with n-butanol: glacial acetic acid: water (5:3:2) as a mobile phase. The plate was sprayed with ninhydrin (0.2%) and dried in an oven at 60–65°C for 3–4 minutes to visualize desired compounds. The developed plate was scanned at 482 nm and the area under the curve (AUC) of various components was quantitatively analyzed with the WINCAT software [70, 71].

3.7. Statistical Analysis. The statistical analysis of the data was performed by Prism Graph pad (version 9) software. The

data is represented as mean \pm SD (standard deviation) and the statistical significance of the data obtained in the various tests was carried out by the analysis of variance (ANOVA) followed by the Tukey test. The different significant level of data as compared to the control (group 1) or negative control (group 2) is also represented in bar diagrams and $p < 0.05$ is considered significant.

3.8. Histopathological Study. On the 8th day of the experimental study, the mice were sacrificed and some of the brain samples from each group were dissected for histopathological study. The tissue was fixed in Bouin's fixative for 72 h. After following all standard procedures, the tissues were embedded in wax blocks and trimming of tissue (7 μ m thickness) was done using a microtome. The tissue sections were stained with eosin and hematoxylin dyes and the counterstaining was done with Dibutylphthalate Polystyrene Xylene. The stained tissue sections were analyzed at 20 \times under a light microscope [72].

4. Conclusion

Increased incidences of the TBI posed a great challenge in terms of the physical, mental, economical, and social well-being of the victims. The secondary insult modulates not only the various neurobehavioral functions required for normal motor and cognitive functions but also induced the neurotoxic cascades due to enhanced oxidative stress and causes cell death and necrosis. Even the long back after the injury, the survivors of TBI, remained at the risk of inflammatory and immune-mediated pathological cascade leading to apoptosis and sudden death. The literature study revealed that along with the other alternatives, several herbal products (decoctions, pills, extracts) were also used for the management of TBI. The selected medicinal plant, *Marrubium vulgare* L., is traditionally used as a decoction in the Jammu and Kashmir region for many ailments. The results of the present study indicated that herb extract can also be used as neuroprotective after a traumatic head injury. Further, it is suggested that after establishing the role of the herb in the reduction of proinflammatory cytokines, the plant could be used for the faster recovery and rehabilitation of victims after TBI. Moreover, the financial burden of the secondary treatment cost for the poor patients with TBI could also be reduced by the use of such herbs.

Data Availability

The data related to the submitted manuscript could be readily available to the reader on request.

Ethical Approval

The present study was duly approved by the Institutional Animal Ethics Committee (IAEC), Maharshi Dayanand University, Rohtak, Haryana, India (1767/RE/S/14/CPCSEA/CAH/153–165, dated-17/12/18).

Conflicts of Interest

The authors declare no conflicts of interest for the present study.

Acknowledgments

The authors want to acknowledge the Director and technical staff of Central Instrumentation Laboratory and Central Animal House, Maharshi Dayanand University, Rohtak, for providing the necessary facilities to conduct the present research. This research received no external funding.

References






- [1] M. A. Flierl, P. F. Stahel, M. Kathryn, B. S. J. Morgan, W. R. Smith, and E. Shohami, "Mouse closed head injury model induced by a weight-drop device," *Nature Protocols*, vol. 4, no. 9, 2009.
- [2] A. I. R. Maas, N. Stocchetti, and B. Ross, "Moderate and severe traumatic brain injury in adults," *Lancet Neurology*, vol. 7, pp. 728–741, 2008.
- [3] M. Prins, T. Greco, D. Alexander, and C. C. Giza, "The pathophysiology of traumatic brain injury at a glance," *Disease Models & Mechanisms*, vol. 6, pp. 1307–1315, 2013.
- [4] A. I. R. Maas, "Traumatic brain injury in India: a big problem in need of data," *Neurology India*, vol. 65, no. 2, pp. 257–259, 2017.
- [5] N. Marklund, "Rodent models of traumatic brain injury: methods and challenges," *Methods in Molecular Biology*, vol. 1462, pp. 29–46, 2016.
- [6] I. Cernak, "Animal models of head trauma," *American Society for Experimental NeuroTherapeutics*, vol. 2, pp. 410–422, 2005.
- [7] O. Kalemci, H. E. Aydin, C. Kizmazoglu, I. Kaya, H. Yilmaz, and N. M. Arda, "Effects of quercetin and mannitol on erythropoietin levels in rats following acute severe traumatic brain injury," *Journal of Korean Neurosurgical Society*, vol. 60, no. 3, pp. 355–361, 2017.
- [8] A. F. Logsdon, B. P. Lucke-Wold, R. C. Turner, J. D. Huber, C. L. Rosen, and J. W. Simpkins, "Role of microvascular disruption in brain damage from traumatic brain injury," *Comprehensive Physiology*, vol. 5, no. 3, pp. 1147–1160, 2015.
- [9] A. Rana, S. Singh, R. Sharma, and A. Kumar, "Traumatic brain injury altered normal brain signaling pathways: implications for novel therapeutics approaches," *Current Neuropharmacology*, vol. 17, no. 7, pp. 614–629, 2019.
- [10] J. Gu, X. Zhang, Z. Fei et al., "Rhubarb extracts in treating complications of severe cerebral injury," *Chinese Medical Journal*, vol. 113, no. 6, pp. 529–531, 2000.
- [11] B. Y. Hu, X. J. Liu, Q. Ren et al., "Treatment with ginseng total saponins improves the neurorestoration of rat after traumatic brain injury," *Journal of Ethnopharmacology*, vol. 155, no. 2, pp. 1243–1255, 2014.
- [12] L. Li, X. Fan, X. T. Zhang et al., "The effects of Chinese medicines on CAMP/PKA signaling in central nervous system dysfunction," *Brain Research Bulletin*, vol. 132, pp. 109–117, 2017.
- [13] J. Matsumoto-Miyazaki, Y. Asano, S. Yonezawa et al., "Acupuncture increases the excitability of the cortico-spinal system in patients with chronic disorders of consciousness following traumatic brain injury," *Journal of Alternative & Complementary Medicine*, vol. 22, no. 11, pp. 887–894, 2016.
- [14] S. Saito, T. Kobayashi, T. Osawa, and S. Kato, "Effectiveness of Japanese herbal medicine yokukansan for alleviating psychiatric symptoms after traumatic brain injury," *Psychogeriatrics*, vol. 10, no. 1, pp. 45–48, 2010.
- [15] V. Mittal and A. Nanda, "The pharmacognostical evaluation of the *Marrubium vulgare* Linn collected from the pulwama district of Jammu and Kashmir state in India," *Journal of Chemical and Pharmaceutical Research*, vol. 8, pp. 7–15, 2016.
- [16] S. E. Bardai, N. Morel, W. Maurice et al., "The vasorelaxant activity of marrubenol and marrubiin from *Marrubium vulgare*," *Planta Medica*, vol. 69, no. 1, pp. 75–77, 2003.
- [17] A. Nanda and V. Mittal, "Design based ultrasound-assisted extraction of *Marrubium vulgare* linn and comparative evaluation of extracts for furan labdane diterpene (marrubiin) concentration and antihypertensive potential," *Current Bioactive Compounds*, vol. 16, no. 6, pp. 924–936, 2019.
- [18] V. Schlemper, A. Ribas, M. Nicolau, and V. Cechinel Filho, "Antispasmodic effects of hydroalcoholic extract of *Marrubium vulgare* on isolated tissues," *Phytomedicine*, vol. 3, no. 2, pp. 211–216, 1996.
- [19] M. M. d. Souza, R. A. P. d. Jesus, V. Cechinel-Filho, and V. Schlemper, "Analgesic profile of hydroalcoholic extract obtained from *Marrubium vulgare*," *Phytomedicine*, vol. 5, no. 2, pp. 103–107, 1998.
- [20] A. Boudjelal, C. Henchiri, L. Siracusa, M. Sari, and G. Ruberto, "Compositional analysis and in vivo anti-diabetic activity of wild algerian *Marrubium vulgare* L. infusion," *Fitoterapia*, vol. 83, no. 2, pp. 286–292, 2012.
- [21] M. A. M. Nawwar, A. M. D. El-mousallamy, H. H. Barakat, J. Buddrus, and M. Linscheid, "Flavonoid lactates from leaves of *Marrubium vulgare*," *Phytochemistry*, vol. 28, no. 11, pp. 3201–3206, 1989.
- [22] S. Sahpaz, T. Hennebelle, and F. Bailleul, "Marruboside, a new phenylethanoid glycoside from *Marrubium vulgare* L.," *Natural Product Letters*, vol. 16, no. 3, pp. 195–199, 2002.
- [23] H. K. Stulzer, M. P. Tagliari, J. A. Zampirolo, V. Cechinel-Filho, and V. Schlemper, "Antioedematogenic effect of marrubiin obtained from *Marrubium vulgare*," *Journal of Ethnopharmacology*, vol. 108, no. 3, pp. 379–384, 2006.
- [24] W. K. Zapp and Josef, "Accumulation of furanic labdane diterpenes in *Marrubium vulgare* and *leonurus cardiaca*," *Planta Medica*, vol. 64, no. 3, pp. 357–361, 1998.
- [25] O. K. Popoola, A. M. Elbagory, F. Ameer, and A. A. Hussein, "Marrubiin," *Molecules*, vol. 18, no. 8, pp. 9049–9060, 2013.
- [26] E.-S. E.-S. Alaa, S. S. Sokkar, M. E.-S. El-Sayad, E. S. Ramadan, and E. Y. Osman, "Celecoxib and omega-3 fatty acids alone and in combination with risperidone affect the behavior and brain biochemistry in amphetamine-induced model of schizophrenia," *Biomedicine & Pharmacotherapy*, vol. 82, pp. 425–431, 2016.
- [27] B. Mason and C. Heyser, "Acamprosate: a prototypic neuro-modulator in the treatment of alcohol dependence," *CNS & Neurological Disorders—Drug Targets*, vol. 9, no. 1, pp. 23–32, 2012.
- [28] C. Albert-Weissenberger, C. Várrallyay, F. Raslan, C. Kleinschnitz, and A. L. Sirén, "An experimental protocol for mimicking pathomechanisms of traumatic brain injury in mice," *Experimental & Translational Stroke Medicine*, vol. 4, no. 1, pp. 1–5, 2012.
- [29] G. Garjan, Tahereh, M. Sharifzadeh et al., "A novel traumatic brain injury model for induction of mild brain injury in rats," *Journal of Neuroscience Methods*, vol. 233, pp. 18–27, 2014.
- [30] I. Khalin, N. L. A. Jamari, N. B. A. Razak et al., "A mouse model of weight-drop closed head injury: emphasis on

- cognitive and neurological deficiency,” *Neural Regeneration Research*, vol. 11, no. 4, pp. 630–635, 2016.
- [31] V. E. Johnson, D. F. Meaney, D. K. Cullen, and D. H. Smith, “Animal models of traumatic brain injury,” *Handbook of Clinical Neurology*, vol. 127, pp. 115–128, 2015.
- [32] A. Jullienne, A. Obenaus, A. Ichkova, C. Savona-Baron, W. J. Pearce, and J. Badaut, “Chronic cerebrovascular dysfunction after traumatic brain injury,” *Journal of Neuroscience Research*, vol. 94, no. 7, pp. 609–622, 2016.
- [33] A. Salehi, J. H. Zhang, and A. Obenaus, “Response of the cerebral vasculature following traumatic brain injury,” *Journal of Cerebral Blood Flow and Metabolism*, vol. 37, no. 7, pp. 2320–2339, 2017.
- [34] D. Lozano, G. S. Gonzales-Portillo, S. Acosta et al., “Neuroinflammatory responses to traumatic brain injury,” *Neuropsychiatric Disease and Treatment*, vol. 11, pp. 97–106, 2015.
- [35] S. E. Bardai, B. Lyoussi, W. Maurice, and N. Morel, “Comparative study of the antihypertensive activity of marrubium vulgare and of the dihydropyridine calcium antagonist amlodipine in spontaneously hypertensive rat,” *Clinical and Experimental Hypertension*, vol. 26, no. 6, pp. 465–474, 2004.
- [36] A. Levy, R. M. Kong, M. J. Stillman et al., “Nimodipine improves spatial working memory and elevates hippocampal acetylcholine in young rats,” *Pharmacology, Biochemistry and Behavior*, vol. 39, no. 3, pp. 781–786, 1991.
- [37] K. Taya, Y. Watanabe, H. Kobayashi, and M. Fujiwara, “Nimodipine improves the disruption of spatial cognition induced by cerebral ischemia,” *Physiology & Behavior*, vol. 70, no. 1–2, pp. 19–25, 2000.
- [38] E. Radi, P. Formichi, C. Battisti, and A. Federico, “Apoptosis and oxidative stress in neurodegenerative diseases,” *Journal of Alzheimer’s Disease*, vol. 42, pp. S125–S152, 2014.
- [39] J. T. Weber, “Altered calcium signaling following traumatic brain injury,” *Frontiers in Pharmacology*, vol. 3, 2012.
- [40] H. Roman, J. C. Goodman, A. B. Valadka, and C. S. Robertson, “Role of nitric oxide in cerebral blood flow abnormalities after traumatic brain injury,” *Journal of Cerebral Blood Flow and Metabolism*, vol. 23, pp. 582–588, 2003.
- [41] P. M. Kanyonga, M. A. Faouzi, B. Meddah, E. M. Essassi, and Y. Cherrah, “Assessment of methanolic extract of *Marrubium vulgare* for anti-inflammatory, analgesic and anti-microbiologic activities,” *Journal of Chemical and Pharmaceutical Research*, vol. 3, no. 1, pp. 199–204, 2011.
- [42] C. Meyre-silva and V. Cechinel-filho, “A review of the chemical and pharmacological aspects of the genus *Marrubium*,” *Current Pharmaceutical Design*, vol. 16, pp. 3503–3518, 2010.
- [43] J.-h. Yi and A. S. Hazell, “Excitotoxic mechanisms and the role of astrocytic glutamate transporters in traumatic brain injury,” *Neurochemistry International*, vol. 48, pp. 394–403, 2006.
- [44] J. W. Blaszczuk and H. De Jesus-cortes, “Parkinson’s disease and neurodegeneration: GABA-collapse hypothesis,” *Frontiers in Neuroscience*, vol. 10, pp. 1–8, 2016.
- [45] V. S. Kokhan, K. Petr, A. Oleg, V. Belov, and M. V. Gulyaev, “Cortical glutamate/GABA imbalance after combined radiation exposure: relevance to human deep-space missions,” *Neuroscience*, vol. 416, pp. 295–308, 2019.
- [46] R. M. Guerriero, C. C. Giza, and R. Alexander, “Glutamate and GABA imbalance following traumatic brain injury,” *Current Neurology and Neuroscience Reports*, vol. 1, 2015.
- [47] K. Sendrowski, M. Rusak, P. Sobaniec et al., “Study of the protective effect of calcium channel blockers against neuronal damage induced by glutamate in cultured hippocampal neurons,” *Pharmacological Reports*, vol. 65, no. 3, pp. 730–736, 2013.
- [48] A. Nelson, P. A. Nyquist, R. Alexander, and S. A. Marshall, “Cerebral vasospasm in traumatic brain injury,” *Psychiatric Annals*, vol. 43, no. 7, pp. 328–330, 2013.
- [49] C. R. A. Y. Meyre-silva, V. Schlemper, F. Campos-buzzi, and V. Cechinel-filho, “Analgesic potential of marrubiin derivatives, a bioactive diterpene present in *Marrubium vulgare* (Lamiaceae),” *Il Farmaco*, vol. 60, 2005.
- [50] S. Lodhi, G. Prakash Vadnere, V. K. Sharma, and M. Rageeb Usman, “*Marrubium vulgare* L.: a review on phytochemical and pharmacological aspects,” *Journal of Intercultural Ethnopharmacology*, vol. 6, no. 4, pp. 429–452, 2017.
- [51] A. Rana, S. Singh, R. Deshmukh, and A. Kumar, “Pharmacological potential of tocopherol and doxycycline against traumatic brain injury-induced cognitive/motor impairment in rats,” *Brain Injury*, vol. 34, no. 8, pp. 1039–1050, 2020.
- [52] A.-O. Nadia, I. M. Abu-Reidah, R. Quirantes-Piné, K. Madani, and A. Segura-Carretero, “Phytochemical profiling, in vitro evaluation of total phenolic contents and antioxidant properties of *Marrubium vulgare* (horehound) leaves of plants growing in algeria,” *Industrial Crops and Products*, vol. 61, pp. 120–129, 2014.
- [53] T. Hatami, S. Ahmad Emami, S. S. Miraghaee, and M. Mojjarrab, “Total phenolic contents and antioxidant activities of different extracts and fractions from the aerial parts of *artemisia biennis* willd,” *Iranian Journal of Pharmaceutical Research*, vol. 13, no. 2, pp. 551–558, 2014.
- [54] A. Kadri, Z. Zarai, I. Ben Chobba et al., “Chemical composition and antioxidant activity of *Marrubium vulgare* L. essential oil from tunisia,” *African Journal of Biotechnology*, vol. 10, no. 19, pp. 3908–3914, 2011.
- [55] M. A. Abd-Elfattah Foda and A. Marmarou, “A new model of diffuse brain injury in rats. Part II: morphological characterization,” *Journal of Neurosurgery*, vol. 80, no. 2, pp. 301–313, 1994.
- [56] M. Vineet and A. Nanda, “Intensification of marrubiin concentration by optimization of microwave-assisted (low CO₂ yielding) extraction process for *Marrubium vulgare* using central composite design and antioxidant evaluation,” *Pharmaceutical Biology*, vol. 55, no. 1, pp. 1337–1347, 2017.
- [57] A. Nanda and V. Mittal, “Development of a novel, rapid and validated HPTLC protocol for the quantitative estimation of marrubiin from the extract of *Marrubium vulgare* linn,” *Journal of Advances in Medical and Pharmaceutical Sciences*, vol. 10, no. 3, pp. 1–8, 2016.
- [58] A. Kunz, U. Dirnagl, and P. Mergenthaler, “Acute pathophysiological processes after ischaemic and traumatic brain injury,” *Best Practice & Research Clinical Anaesthesiology*, vol. 24, no. 4, pp. 495–509, 2010.
- [59] A. Marmarou, M. A. Abd-Elfattah Foda, W. Van den Brink, J. Campbell, H. Kita, and K. Demetriadou, “A new model of diffuse brain injury in rats. Part I: pathophysiology and biomechanics,” *Journal of Neurosurgery*, vol. 80, no. 2, pp. 291–300, 1994.
- [60] J. Zhao, H. Chen, M. Zhang et al., “Early expression of serum neutrophil gelatinase-associated lipocalin (NGAL) is associated with neurological severity immediately after traumatic brain injury,” *Journal of the Neurological Sciences*, vol. 368, pp. 392–398, 2016.
- [61] E. Choleris, A. W. Thomas, M. Kavaliers, and F. S. Prato, “A detailed ethological analysis of the mouse open field test: effects of diazepam, chlordiazepoxide and an extremely low

- frequency pulsed magnetic field,” *Neuroscience & Biobehavioral Reviews*, vol. 25, no. 3, pp. 235–260, 2001.
- [62] J. Barot and B. Saxena, “Therapeutic effects of eugenol in a rat model of traumatic brain injury: a behavioral, biochemical, and histological study,” *Journal of Traditional and Complementary Medicine*, vol. 11, no. 4, pp. 318–327, 2021.
- [63] V. Mittal, S. K. Sharma, P. Jalwal, A. Hooda, and J. Mor, “Plumbago zeylanica roots: a potential source for improvement of learning and memory,” *International Journal of Pharma Bio Sciences*, vol. 1, no. 2, 2010.
- [64] O. H. Lowry, N. J. Rosebrough, A. L. Farr, and R. J. Randall, “Protein measurement with the folin phenol reagent,” *Journal of Biological Chemistry*, vol. 193, no. 1, pp. 265–275, 1951.
- [65] A. K. Sinha, “Colrimetric assay of catalase,” *Analytical Biochemistry*, vol. 47, pp. 389–394, 1972.
- [66] C. Govindasamy, K. S. Al-Numair, M. A. Alsaif, and K. P. Viswanathan, “Influence of 3-hydroxymethyl xylitol, a novel antidiabetic compound isolated from casearia esculenta (roxb.) root, on glycoprotein components in streptozotocin-diabetic rats,” *Journal of Asian Natural Products Research*, vol. 13, no. 8, pp. 700–706, 2011.
- [67] H. Ohkawa, N. Ohishi, and K. Yagi, “Assay for lipid peroxides in animal tissues by thiobarbituric acid reaction,” *Analytical Biochemistry*, vol. 95, no. 2, pp. 351–358, 1979.
- [68] L. C. Green, D. A. Wagner, J. Glogowski, L. Paul, J. S. W. Skipper, and S. R. Tannenbaum, “Analysis of nitrate, nitrite, and [15N] nitrate in biological fluids,” *Analytical Biochemistry*, vol. 126, no. 1, pp. 131–138, 1982.
- [69] G. L. Ellman, “Tissue sulfhydryl groups,” *Archives of Biochemistry and Biophysics*, vol. 82, no. 1, pp. 70–77, 1959.
- [70] J. S. Sancheti, M. F. Shaikh, P. F. Khatwani, S. R. Kulkarni, and S. Sathaye, “Development and validation of a HPTLC method for simultaneous estimation of L-glutamic acid and γ -aminobutyric acid in mice brain,” *Indian Journal of Pharmaceutical Sciences*, vol. 75, no. 6, pp. 716–721, 2013.
- [71] C. S. Babu, K. S. Kesavanarayanan, P. Kalaivani, V. Ranju, and M. Ramanathan, “A simple densitometric method for the quantification of inhibitory neurotransmitter gamma-aminobutyric acid (GABA) in rat brain tissue,” *Chromatography Research International*, vol. 2011, Article ID 732409, 5 pages, 2011.
- [72] A. Sivaraman, R. Sanchez-Salas, E. Barret et al., “Prostate histoscanning true targeting guided prostate biopsy: initial clinical experience,” *World Journal of Urology*, vol. 33, no. 10, pp. 1475–1479, 2015.

Research Article

In Vivo Anti-Inflammatory, Analgesic, Muscle Relaxant, and Sedative Activities of Extracts from *Syzygium cumini* (L.) Skeels in Mice

Abdur Rauf ¹, Yahya S. Al-Awthan ^{2,3}, Imtaiz Ali Khan,⁴ Naveed Muhammad,⁵ Syed Uzair Ali Shah,⁶ Omar Bahattab ², Mohammed A. Al-Duais,^{7,8} Rohit Sharma ⁹, and Md. Mominur Rahman ¹⁰

¹Department of Chemistry, University of Swabi, Swabi, Anbar 23430, Khyber Pakhtunkhwa (KP), Pakistan

²Department of Biology, Faculty of Science, University of Tabuk, Tabuk, Saudi Arabia

³Department of Biology, Faculty of Science, Ibb University, Ibb, Yemen

⁴Department of Entomology, University of Agriculture, Peshawar, Khyber Pakhtunkhwa (KP), Pakistan

⁵Department of Pharmacy, Abdul Wali Khan University, Mardan, Khyber Pakhtunkhwa (KP), Pakistan

⁶Department of Pharmacy, University of Swabi, Swabi, Anbar 23430, Khyber Pakhtunkhwa (KP), Pakistan

⁷Department of Biochemistry, Faculty of Science, University of Tabuk, Tabuk, Saudi Arabia

⁸Biochemistry Unit, Chemistry Department, Faculty of Science, Ibb University, Ibb, Yemen

⁹Department of Rasa Shastra & Bhaishajya Kalpana, Faculty of Ayurveda, Institute of Medical Sciences, Banaras Hindu University, Varanasi-221005, Uttar Pradesh, India

¹⁰Department of Pharmacy, Faculty of Allied Health Sciences, Daffodil International University, Dhaka 1207, Bangladesh

Correspondence should be addressed to Abdur Rauf; abdurrauf@uoswabi.edu.pk, Rohit Sharma; rohitsharma@bhu.ac.in, and Md. Mominur Rahman; mominur.ph@gmail.com

Received 30 January 2022; Revised 31 March 2022; Accepted 2 April 2022; Published 11 April 2022

Academic Editor: Christos Tsagkaris

Copyright © 2022 Abdur Rauf et al. This is an open access article distributed under the Creative Commons Attribution License, which permits unrestricted use, distribution, and reproduction in any medium, provided the original work is properly cited.

In the current study, the folklore medicine, *Syzygium cumini*, was experimentally evaluated for anti-inflammatory, analgesic, sedative, and muscle relaxant effects. The extract and fractions of *S. cumini* were found safe up to 1000 mg/kg with no mortality, except for slight sedation as a minor side effect. Both, the extract and various fractions of *S. cumini* demonstrated significant inhibition (86.34%) of carrageenan-induced inflammation in mice. Acetic acid induced writhes were attenuated ($p < 0.001$) by *S. cumini* in a dose-dependent manner, except for the *n*-hexane fraction. The maximum effect was observed at a dose of 500 mg/kg in mice. The maximum muscle relaxant effect of all tested samples was recorded at a dose of 500 mg/kg bodyweight, where the percent inhibition exhibited by dichloromethane fraction was 82.34%, followed by chloroform fractions (71.43%) and methanolic extract (70.91%). Our findings validate the folklore medicinal claims of *S. cumini*, as an analgesic and anti-inflammatory agent.

1. Introduction

Syzygium cumini L. (Myrtaceae), commonly known as jamun, jambolan, black plum, and jambolao, is widely distributed in India, Africa, South America, and Pakistan [1–3]. This genus is famous for its multimedicinal usage as an antidiabetic and laxative [3]. Various parts of *S. cumini* have been reported for the presence of diverse bioactive

natural compounds. *S. cumini* leaves are used for the treatment of constipation, dermatopathies, leucorrhea, diabetes, and gastropathies, and its bark is used as an anthelmintic, carminative, and astringent. Apart from its role in diabetes, *S. cumini* is also used as diuretic and astringent [4–6]. *S. cumini* has been documented for diverse pharmacological properties, such as anti-inflammatory, anti-hyperglycemic, antioxidant, antimicrobial, and

cardioprotective [7–11]. The crude extract of bark and its various fractions have been documented for excellent α -glucosidase, urease, and phosphodiesterase inhibitory potential [12]. Previous phytochemical investigations on *S. cumini* indicated the presence of various classes of bioactive compounds such as alkaloids, flavonoids, terpene, phenols, carbohydrates, saponins, and glycosides [12]. *S. cumini* leaves comprise of high level of flavonoids mainly myricetin, kaempferol, and quercetin. Other phytochemicals isolated from *S. cumini* include ferulic acid, ellagic acid, gallic acid, and chlorogenic acid [13–15]. Seed of *S. cumini* has been reported for the presence of α -terpineol, betulinic acid, eugenol, and other phenolic acids [16, 17]. The fruits are a rich source of anthocyanins such as delphinidin, cyaniding, and petudinine [17]. The stem of *S. cumini* is mainly composed phenolic acids, flavonoids, and terpenes [6, 16]. The major chemical constituents isolated from *S. cumini*, chlorogenic acid and delphinidin (Figure 1), might be involved in its various biological actions. Considering the multimedicinal usage of *S. cumini*, the current study was designed to evaluate its crude extracts and various fractions for in vivo anti-inflammatory, analgesic, muscle relaxation, and toxicological effects.

2. Materials and Methods

2.1. Plant Materials. The plant materials were collected in the month of July, 2020, from the local area of Anbar, Swabi, Khyber Pakhtunkhwa, Pakistan (GPS coordinates latitude 34°53'40.41"N, longitude 72°1'42.48"E). The plant specimen was identified and authenticated by Dr. Muhammad Ilyas, Department of Botany, University of Swabi, Swabi, Khyber Pakhtunkhwa, Pakistan. The specimen was tagged under voucher number UOS/Bot-103. The specimen was stored in the same department.

2.2. Preparation of Extract. *S. cumini* stem (10.76 kg) was washed with tap water to remove dust particles. The washed plant materials were dried under shade for 20 days. The dried plant material was ground with a grinding machine. The plant material was soaked in commercial grade methanol for 18 days until the extraction of polar and nonpolar compounds was almost complete. The methanolic extract was concentrated under low pressure and temperature to prevent the decomposition of heat-labile molecules. The dried methanolic extract (176.00 g) was subjected to fractionation using various solvents to obtain hexane (12.87 g), chloroform (37.66 g), dichloromethane (DCM) (42.32 g), and ethyl acetate (25.11 g) fractions. Commercial grade solvents were used for extractions and fractionations. The obtained fractions were dried and stored in the freezer for biological screening.

2.3. Animals. Healthy animals were purchased from Pakistan Council of Scientific and Industrial Research (PCSIR), Peshawar, and were maintained in the animal house of the Department of Pharmacy University of Swabi. The healthy mice of either sex were selected for in vivo pharmacological

activities. Mice were fed with standard laboratory food and water ad libitum. All the experimental procedures were approved from the Ethical Committee (UOS/Pharm11), Department of Pharmacy, University of Swabi, Khyber Pakhtunkhwa, Pakistan.

2.4. Toxicological Study. An acute toxicological study was done on healthy mice according to the published methods [18]. The animals of each group were treated either with distilled water or extract/fractions at dose of 100, 250, 500, and 1000 mg/kg animal bodyweight. Each animal was observed for 6 h for gross behavioral changes after the administration of dose and then checked for mortality after 24 h.

2.5. Anti-Inflammatory Activity. The carrageenan-induced paw edema model was practiced for the evaluation of the anti-inflammatory effect of all the tested samples following a standard procedure [19]. Animals were classified into various groups ($n = 6$): negative control (animals were treated with distilled water, 10 ml/kg, IP), positive control (animals were treated with diclofenac, 5 mg/kg, IP), and test groups (animals were treated with 25, 50, 100, 200, 250, and 500 mg/kg, PO with various extract and fractions). After 30 minutes of the treatments, each animal's subplanter of the hind paw was injected with 1% carrageenan solution. The induced edema (inflammation) was quantified through plethysmometer just after administration of carrageenan and then after 1 h, 2 h, 3 h, 4 h, and 5 h. The percent attenuation in edema was quantified using the following formula.

$$\% \text{ inhibition} = \frac{A - B}{A} \times 100, \quad (1)$$

where A and B represent the percent effect of negative control and tested group, respectively.

2.6. Analgesic Activity. The acetic acid-induced writhing test was used for evaluation of the antinociceptive effect of the extract and various fractions as per a previously reported method [20]. All the experimental healthy animals were fasted 2 h before the start of experiment. After 30 minutes of administration of distilled water (10 ml/kg), diclofenac (5 mg/kg), and extract/fractions (25, 50, 100, 200, 250, and 500 mg/kg), animals were treated with 1% acetic acid. After 5 min, the abdominal constrictions (writhes) were counted for 10 min. The attenuation in writhes during 10 minutes reflects the antinociceptive effect of the drugs.

2.7. Muscle Relaxation Activity. The crude extracts and various fractions were assessed for muscle relaxation potential by using the standard procedure [21].

2.7.1. Inclined Plane Model. The inclined plane was used in screening and contained two plywood boards, which are connected in such a way that one board is aligned from the base while the other at 60° from the base. All animals were

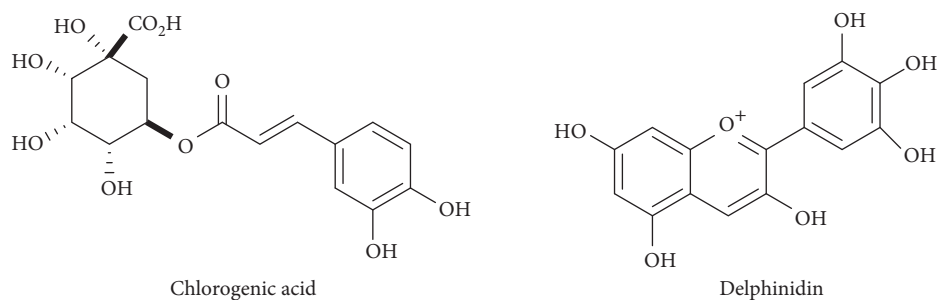


FIGURE 1: Chemical structures of major compounds isolated from *S. cumini*.

distributed into several groups, and each group composed six animals ($n=6$). Animals of every group were administered with distilled water (10 ml/kg), standard drug (diazepam, 1 mg/kg), and extract/fractions at 25, 50, 100, 200, 250, and 500 mg/kg. After the above administrations, animals were tested at 30 minutes, 60 minutes, and 90 minutes for the muscle coordination effect by allowing animals on the higher portion of the inclined plane for 30 seconds to hang or fall.

2.7.2. Traction Model. The traction model was designed using a metallic wire covered with rubbers. The wire was linked with each other with the help of a stand, around 60 cm above the lab bench. The animals were divided in groups, treated, and tested at regular intervals. After that, all animals were suspended with wire to hang.

2.8. Sedative Activity. The sedative effect of extract and all fractions was performed as per standard methods [18]. The animals were divided into different groups ($n=6$). The apparatus used in this screening comprised of an area of the white wood having 150 cm diameter bordered by stainless steel walls and was divided into nineteen squares by black lines. Then, the open-field apparatus was positioned inside of a light and sound attenuated room. Different groups of animals were fed with distilled water, diazepam, and extract/fractions as above. Thirty minutes after administration, all groups of animals were allowed to move from the center of the design box. The animals which crossed the maximum number of lines were recorded as “no sedation,” while animals with delayed movement were considered as “sedated.”

2.9. Statistical Analysis. The results have been displayed as mean \pm standard error of the mean (SEM), and statistical significance was tested using one-way ANOVA. GraphPad Prism was used for statistical analysis.

3. Results

3.1. Toxicological Profile. The acute toxicology profile is given in Table 1. There was no mortality observed in any extract or fraction treated groups, even at the highest administered dose (1000 mg/kg bodyweight) during 24 hours

of administration. However, at higher doses of various fractions, the locomotion was decreased, which is a determinant of sedative potential of the extract or fractions. The animals used for toxicity studies survived and did not exhibit any signs of delayed toxicity, even after 14 days observation.

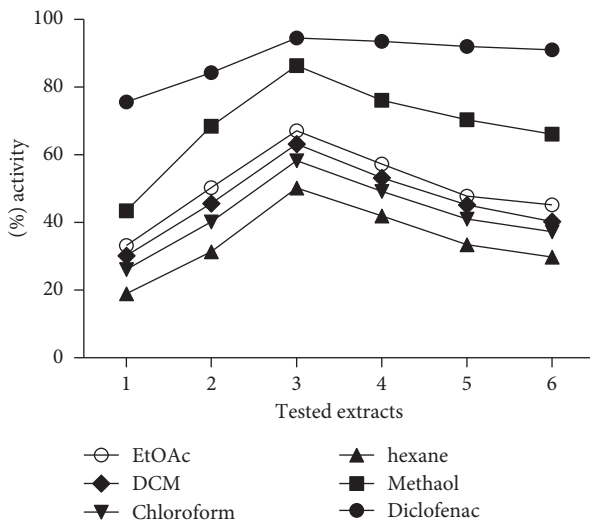
3.2. Anti-Inflammatory Effect. The percentage anti-inflammatory effect is shown in Figure 2. The maximum percent inhibition effect was observed at the third hour of experiment in both standard and test samples. Among test samples, the methanolic crude extract demonstrated maximum inhibition (86.11%) at the third hour of experiment compared to other fractions. The percent anti-inflammatory potential of ethyl acetate (67.09%), dichloromethane (63.23%), and chloroform fractions (59.25%) of *S. cumini* was also significant, with least activity of *n*-hexane fraction.

3.3. Analgesic Effect. The analgesic potential of extract and fractions at various doses is given in Table 2. The crude extract of *S. cumini* dose-dependently inhibited the number of writhes at 50 and 100 mg/kg ($p < 0.05$). This effect was further potentiated at a dose of 250 and 500 mg/kg bodyweight ($p < 0.001$). The chloroform, DCM, and ethyl acetate fractions exhibited comparatively similar effect as methanolic extract. However, the *n*-hexane fraction was devoid of any analgesic effect. The analgesic activity of test samples was compared to the standard drug, diclofenac (5 mg/kg).

3.4. Muscle Relaxant Effect. The muscle relaxant effect of *S. cumini* extract and various fractions is given in Table 3. In both the inclined plane and traction models, a uniform effect was observed. The effect was measured at 30, 60, and 90 minutes later after sample administration. A time and dose-dependent effect was seen with extract and various fractions except for *n*-hexane. The maximum muscle relaxant effect of all tested plant samples was recorded at a dose of 500 mg/kg bodyweight, where the percent inhibition for dichloromethane was maximum (82.34%), followed by chloroform fractions (71.43%), methanolic extract (70.91%), and ethyl acetate fraction (69.22%). The activity of all test samples was compared to the muscle relaxant effect produced by the standard drug diazepam (1 mg/kg bodyweight), which was considered 100%.

TABLE 1: Toxicological profile of crude extract and various fractions of *Syzygium cumini* in open-field screening.

Treatment	Doses (mg/kg)	Number of died animals/6	% mortality	Gross behavior changes
Normal saline	10 ml/kg	0/6	—	—
Methanolic extract	100	0/6	—	—
	250	0/6	—	—
	500	0/6	—	Inactive
	1000	0/6	—	Inactive
Hexane	100	0/6	—	—
	250	0/6	—	—
	500	0/6	—	—
	1000	0/6	—	—
Chloroform	100	0/6	—	—
	250	0/6	—	—
	500	0/6	—	Inactive
	1000	0/6	—	Inactive
DCM	100	0/6	—	—
	250	0/6	—	Inactive
	500	0/6	—	Inactive
	1000	0/6	—	Inactive
Ethyl acetate	100	0/6	—	—
	250	0/6	—	Inactive
	500	0/6	—	Inactive
	1000	0/6	—	Inactive

FIGURE 2: Anti-inflammatory screening of extract/fractions of *Syzygium cumini*.

3.5. Sedative Effects. The sedative effect of methanolic extract and fractions of *S. cumini* is given in Table 4. A significant ($p < 0.001$) sedation was noticed at higher doses (250 and 500 mg/kg) of the crude extract and various fractions of *S. cumini* except for *n*-hexane fraction. The tested samples were compared to the sedative effect produced by 0.5 mg/kg bodyweight of diazepam, which was the standard drug applied in this study.

4. Discussion

Natural products as therapeutic agents are the emerging, safe, and effective options in the modern era, especially in the developing world [22, 23]. Plant extracts as well as their

TABLE 2: Analgesic potential of crude extract and various fractions of *Syzygium cumini*.

Tested samples	Dose (mg/kg)	No. of writhes
Normal saline	10 mL/kg	61.098 ± 2.00
Diclofenac sodium	5	29.32 ± 2.20***
	25	44.09 ± 1.88
	50	39.34 ± 1.93*
	100	34.43 ± 2.19*
	250	29.98 ± 2.00***
Methanolic extract	500	25.09 ± 2.06***
	25	62.65 ± 2.65
	50	57.21 ± 2.12
	100	51.32 ± 2.08
	250	45.54 ± 1.90
<i>n</i> -Hexane	500	40.32 ± 1.87
	25	53.09 ± 2.12
	50	48.09 ± 3.01
	100	42.09 ± 2.98
	250	36.09 ± 2.06*
Chloroform	500	30.98 ± 2.43***
	25	41.34 ± 1.66
	50	35.66 ± 1.76*
	100	29.11 ± 2.09***
	250	23.09 ± 2.87***
DCM	500	18.34 ± 2.08***
	25	46.09 ± 1.56
	50	39.34 ± 1.32*
	100	33.98 ± 1.34*
	250	27.98 ± 1.34***
Ethyl acetate	500	22.87 ± 1.76***

* $P < 0.05$; ** $P < 0.01$, *** $P < 0.001$.

isolated constituents are gaining popularity as therapeutic agents, e.g., ivy leaf (antitussive) and silymarin (hepatoprotective). Considering the promising efficacy and

TABLE 3: Muscle relaxant effect of crude and various fractions of *S. cumini*.

Group	Dose (mg/ml)	Inclined plan model (%)			Traction screening (%)		
		30 min	60 min	90 min	30 min	60 min	90 min
Distilled water	10 mL/kg	0.0	0.0	0.0	0.0	0.0	0.0
Diazepam	1	100	100	100	100	100	100
Methanolic extract	25	35.65	44.23	53.09	34.80	43.00	52.36
	50	41.54	50.98	59.23	42.43	51.11	60.32
	100	45.21	54.87	63.12	44.21	53.87	64.04
	250	48.23	57.54	66.32	47.23	56.98	67.06
	500	52.00	61.23	70.91	51.87	60.08	69.98
<i>n</i> -Hexane	25	12.22	20.03	29.98	11.30	19.76	30.70
	50	16.17	25.66	33.54	17.00	26.23	34.09
	100	21.28	28.23	37.11	20.32	27.06	36.60
	250	24.98	33.43	41.09	23.37	30.32	40.09
	500	28.87	36.98	44.21	27.43	35.21	43.08
Chloroform	25	30.11	39.43	48.94	29.01	38.06	47.66
	50	36.32	45.77	54.76	35.88	44.98	53.56
	100	42.12	51.43	60.70	41.54	50.32	59.54
	250	47.43	56.32	65.83	46.43	55.32	64.76
	500	53.98	62.87	71.43	52.98	61.90	70.03
DCM	25	38.08	47.51	56.01	37.50	46.70	55.91
	50	44.65	53.57	62.43	45.00	54.01	63.07
	100	50.23	59.60	68.22	51.89	60.90	67.32
	250	57.42	66.68	75.19	56.86	65.02	74.00
	500	64.21	73.76	82.34	63.01	72.98	81.03
Ethyl acetate	25	27.43	36.21	45.45	26.76	35.08	44.14
	50	33.60	42.98	51.12	32.86	41.16	50.87
	100	39.09	48.76	57.98	40.00	49.83	58.72
	250	45.43	54.23	63.09	44.87	53.98	62.43
	500	51.66	60.65	69.22	50.94	59.98	68.88

TABLE 4: Sedative effect of crude and various fractions of *Syzygium cumini* in open-field screening.

Samples	Dose (mg/ml)	Number of lines crossed
Control	5 ml	130.00 ± 3.65
Diazepam	0.5	9.23 ± 0.55***
Methanolic extract	25	88.32 ± 3.01
	50	82.04 ± 2.79
	100	75.54 ± 2.70*
	250	67.09 ± 2.65**
	500	60.21 ± 1.40***
<i>n</i> -Hexane	25	112.09 ± 2.09
	50	108.32 ± 2.30
	100	101.87 ± 2.44
	250	95.32 ± 2.54
	500	89.01 ± 2.05
Chloroform	25	80.23 ± 2.13
	50	74.98 ± 2.12
	100	68.23 ± 2.30
	250	62.09 ± 2.34***
	500	57.12 ± 2.88***
DCM	25	43.98 ± 2.11*
	50	37.01 ± 2.73**
	100	32.32 ± 2.60***
	250	26.21 ± 2.43***
	500	20.90 ± 2.00***
Ethyl acetate	25	75.8 ± 3.00
	50	69.65 ± 2.83
	100	63.87 ± 2.50*
	250	57.23 ± 2.12**
	500	52.56 ± 1.82***

* $P < 0.05$; ** $P < 0.01$. *** $P < 0.001$.

significant safety profile of natural products as therapeutic agents, the researchers got interested in screening these potential medicinal plants to validate their folkloric uses and claims [24–26]. In the current research work, the crude extract and various fractions of *S. cumini* were tested for various pharmacological activities. *S. cumini* is traditionally used for various inflammatory, painful conditions, sedation, and muscle relaxant [27–29]. The toxicity profile of *S. cumini* exhibited slight sedation and cessation of locomotion at a higher dosage of 500 mg/kg with zero mortality at maximum applied dose of 1000 mg/kg. The safe dose range for in vivo activities of the crude extracts and fractions was ascertained to be 25–500 mg/kg bodyweight. The tested *S. cumini* extracts and various fractions significantly attenuated edema induced by carrageenan. Crude methanolic extract of *S. cumini* inhibited paw edema more effectively followed by ethyl acetate, dichloromethane, chloroform, and n-hexane fractions, respectively. The analgesic activity of *S. cumini* extract exhibited dose-dependent analgesia with the same pattern of activity across various fractions, i.e., more effective methanolic extract followed by ethyl acetate, dichloromethane, chloroform, and n-hexane fractions, respectively. The inflammation induced by carrageenan is related to the release of various inflammatory mediators such as prostaglandins (PGs), bradykinin, and histamine [30]. Among these mediators, majorly, PGs are responsible for induction of pain, inflammation, and fever [31]. *S. cumini* probably inhibits cyclo-oxygenase (COX) and thus blocks the production of PGs and other intracellular cascade that leads to pain, inflammation, and pyrexia. In addition to the inhibition of PGs, *S. cumini* also exhibited sedative and muscle relaxant effects, which reflects its capability to modify some other pharmacodynamics pathways. *S. cumini* extracts exhibited potent muscle relaxant and sedative effects. The sedative and muscle relaxant effects suggested that the chemical constituents of *S. cumini* keep the anion neuronal channels open, especially the chloride channels, which leads to the depression of the central nervous system. The induction of anion influx is mostly related to stimulation of GABA (gamma aminobutyric acid) receptors, thereby hyperpolarizing the neuronal membrane via elevated chloride influx. These results further suggest that the crude extract or fractions might accelerate the action of GABA neurotransmitters, which is responsible for sedation and muscle relaxant effects [32]. However, further mechanistic studies should be conducted on various isolated constituents of *S. cumini* to know the exact mechanism of its activities.

5. Conclusion

S. cumini is a folklore medicinal plant traditionally, which is used in various health conditions. The present study substantiates the folklore medicinal claims about *S. cumini* as an anti-inflammatory, analgesic, sedative, and muscle relaxant and concludes that *S. cumini*, especially its crude methanol extract, has a significant role as anti-inflammatory, analgesic, sedative, and muscle relaxant. This study provides leads for researchers to isolate new and novel compounds from

S. cumini, which have the biological potential for the treatment of various diseases.

Data Availability

The data used to support this study are included within the article.

Conflicts of Interest

The authors declare that they have no conflicts of interest.

Acknowledgments

The authors are grateful to the Higher Education Commission of Pakistan for funding this research project (7343 NRPU/R&D/HEC/2017).

References

- [1] M. É. A. Stefanello, A. C. R. F. Pascoal, and M. J. Salvador, "Essential oils from neotropical Myrtaceae: chemical diversity and biological properties," *Chemistry & Biodiversity*, vol. 8, no. 1, pp. 73–94, 2011.
- [2] M. Ayyanar and P. Subash-Babu, "Syzygium cumini (L.) Skeels: a review of its phytochemical constituents and traditional uses," *Asian Pacific Journal of Tropical Biomedicine*, vol. 2, no. 3, pp. 240–246, 2012.
- [3] P. D. Sadawarte, K. H. Pujari, S. K. Sonawane, and S. S. Arya, "Potential food applications and health benefits of jambhul (*Syzygium cumini* L.)," *Indian Journal of Nutrition and Dietetics*, vol. 53, no. 3, Article ID 5340, 2016.
- [4] J. B. Harborne, "Indian medicinal plants. A compendium of 500 species," in *Journal of Pharmacy & Pharmacology*, P. K. Warriar, V. P. K. Nambiar, and C. Ramankutty, Eds., vol. 46, no. 11, 935 pages, 1994.
- [5] A. Helmstadter, "Syzygium cumini (L.) SKEELS (Myrtaceae) against diabetes—125 years of research," *Pharmazie*, vol. 63, no. 2, pp. 91–101, 2008.
- [6] M. S. Baliga, H. P. Bhat, B. R. V. Baliga, R. Wilson, and P. L. Palatty, "Phytochemistry, traditional uses and pharmacology of Eugenia jambolana Lam. (black plum): a review," *Food Research International*, vol. 44, no. 7, pp. 1776–1789, 2011.
- [7] E. Kumar, S. Mastan, K. R. Reddy, G. A. Reddy, N. Raghunandan, and G. Chaitanya, "Anti-arthritis property of the methanolic extract of Syzygium cumini seeds," *International Journal of Integrative Biology*, vol. 4, pp. 55–61, 2008.
- [8] N. Rekha, R. Balaji, and M. Deecaraman, "Effect of aqueous extract of Syzygium cumini Pulp on antioxidant defense system in streptozotocin induced diabetic rats," *Iranian Journal of Pharmacology & Therapeutics*, vol. 7, no. 2, pp. 137–145, 2008.
- [9] B. Sharma, G. Viswanath, R. Salunke, and P. Roy, "Effects of flavonoid-rich extract from seeds of Eugenia jambolana (L.) on carbohydrate and lipid metabolism in diabetic mice," *Food Chemistry*, vol. 110, no. 3, pp. 697–705, 2008.
- [10] R. Arun, M. V. D. Prakash, S. K. Abraham, and K. Premkumar, "Role of Syzygium cumini seed extract in the chemoprevention of in vivo genomic damage and oxidative stress," *Journal of Ethnopharmacology*, vol. 134, no. 2, pp. 329–333, 2011.

- [11] R. S. Tanwar, S. B. Sharma, U. R. Singh, and K. M. Prabhu, "Antiatherosclerotic potential of active principle isolated from *Eugenia jambolana* in streptozotocin-induced diabetic rats," *Evidence-Based Complementary and Alternative Medicine*, vol. 2011, Article ID 127641, 9 pages, 2011.
- [12] A. Rauf, I. A. Khan, N. Muhammad et al., "Phytochemical composition, *in vitro* urease, α -glucosidase and phosphodiesterase inhibitory potency *Syzygium cumini* (Jamun) Fruits," *South African Journal of Botany*, vol. 143, 2021.
- [13] I. I. Mahmoud, M. S. A. Marzouk, F. A. Moharram, M. R. El-Gindi, and A. M. K. Hassan, "Acylated flavonol glycosides from *Eugenia jambolana* leaves," *Phytochemistry*, vol. 58, no. 8, pp. 1239–1244, 2001.
- [14] A. K. Timbola, B. Szpoganicz, A. Branco, F. D. Monache, and M. G. Pizzolatti, "A new flavonol from leaves of *Eugenia jambolana*," *Fitoterapia*, vol. 73, no. 2, pp. 174–176, 2002.
- [15] Z. P. Ruan, L. L. Zhang, and Y. M. Lin, "Evaluation of the antioxidant activity of *Syzygium cumini* leaves," *Molecules*, vol. 13, no. 10, pp. 2545–2556, 2008.
- [16] I. S. Bhatia and K. L. Bajaj, "Chemical constituents of the seeds and bark of *Syzygium cumini*," *Planta Medica*, vol. 28, no. 4, pp. 346–352, 1975.
- [17] S. Ramya, K. Neethirajan, and R. Jayakumararaj, "Profile of bioactive compounds in *Syzygium cumini*—a review," *Journal of Pharmacy Research*, vol. 5, no. 8, pp. 4548–4553, 2012.
- [18] Y. S. Al-Awthan, A. Rauf, U. Rashid et al., "Sedative-hypnotic effect and *in silico* study of dinaphthodiospyrrols isolated from *Diospyros lotus* Linn," *Biomedicine & Pharmacotherapy*, vol. 140, Article ID 111745, 2021.
- [19] A. Rauf, T. Abu-Izneid, F. A. Alhumaydhi et al., "In vivo analgesic, anti-inflammatory, and sedative activity and a molecular docking study of dinaphthodiospyrol G isolated from *Diospyros lotus*," *BMC Complementary Medicine and Therapies*, vol. 20, no. 1, p. 237, 2020.
- [20] S. Bawazeer and A. Rauf, "In vivo anti-inflammatory, analgesic, and sedative studies of the extract and naphthoquinone isolated from *Diospyros kaki* (persimmon)," *ACS Omega*, vol. 6, no. 14, pp. 9852–9856, 2021.
- [21] T. Abu-Izneid, A. Rauf, S. U. A. Shah et al., "In Vivo study on analgesic, muscle-relaxant, sedative activity of extracts of *Hypochoeris radicata* and *in silico* evaluation of certain compounds present in this species," *BioMed Research International*, vol. 10, Article ID 3868070, , 2018.
- [22] R. Sharma and P. K. Prajapati, "Remarks on "herbal immune booster-induced liver injury in the COVID-19 pandemic - a case series"," *Journal of Clinical and Experimental Hepatology*, vol. 12, no. 1, pp. 247–248, 2022.
- [23] R. Sharma, R. Bolleddu, J. K. Maji, G. Ruknuddin, and P. K. Prajapati, "In-Vitro α -amylase, α -glucosidase inhibitory activities and *in-vivo* anti-hyperglycemic potential of different dosage forms of guduchi (*tinospora cordifolia* [willd.] miers) prepared with ayurvedic bhavana process," *Frontiers in Pharmacology*, vol. 12, 2021.
- [24] R. Sharma and N. Martins, "Telomeres, DNA damage and ageing: potential leads from ayurvedic rasayana (Anti-Ageing) drugs," *Journal of Clinical Medicine*, vol. 9, no. 8, p. 2544, 2020.
- [25] D. Shah, M. Gandhi, A. Kumar, N. Cruz-Martins, R. Sharma, and S. Nair, "Current insights into epigenetics, noncoding RNA interactome and clinical pharmacokinetics of dietary polyphenols in cancer chemoprevention," *Critical Reviews in Food Science and Nutrition*, vol. 61, pp. 1–37, 2021.
- [26] R. Sharma and P. K. Prajapati, "Predictive, preventive and personalized medicine: leads from ayurvedic concept of Prakriti (human constitution)," *Current Pharmacology Reports*, vol. 6, no. 6, pp. 441–450, 2020.
- [27] L. Chanudom and J. Tangpong, "Anti-inflammation property of *Syzygium cumini* (L.) skeels on indomethacin-induced acute gastric ulceration," *Gastroenterology Research and Practice*, vol. 12, Article ID 343642, 2015.
- [28] V. T. Chagas, L. M. França, S. Malik, and A. M. A. Paes, "*Syzygium cumini* (L.) skeels: a prominent source of bioactive molecules against cardiometabolic diseases," *Frontiers in Pharmacology*, vol. 6, 2015.
- [29] L. C. D. S. Assunção Carvalho, M. C. De Freitas, A. S. Silva et al., "Syzygium cumini nectar supplementation reduced biomarkers of oxidative stress, muscle damage, and improved psychological response in highly trained young handball players," *Frontiers in Physiology*, vol. 9, Article ID 1508, 2018.
- [30] L. A. Abdulkhaleq, M. A. Assi, R. Abdullah, M. Zamri-Saad, Y. H. Taufiq-Yap, and M. N. M. Hezme, "The crucial roles of inflammatory mediators in inflammation: a review," *Veterinary World*, vol. 11, no. 5, pp. 627–635, 2018.
- [31] J. R. Vane, "Inhibition of prostaglandin synthesis as a mechanism of action for aspirin-like drugs," *Nature New Biology*, vol. 231, no. 25, pp. 232–235, 1971.
- [32] E. Dailly and M. Bourin, "The use of benzodiazepines in the aged patient: clinical and pharmacological considerations," *Pakistan Journal of Pharmaceutical Sciences*, vol. 21, pp. 144–150, 2008.

Review Article

Biogenic Phytochemicals Modulating Obesity: From Molecular Mechanism to Preventive and Therapeutic Approaches

Vikram Kumar ¹, **Desh Deepak Singh**,¹ **Sudarshan Singh Lakhawat**,¹
Nusrath Yasmeen ¹, **Aishwarya Pandey**,² and **Rajeev K. Singla** ^{3,4}

¹Amity Institute of Biotechnology, Amity University Rajasthan, Jaipur 303002, Rajasthan, India

²INRS, Eau Terre Environnement Research Centre, Québec, QC, Canada

³Institutes for Systems Genetics, Frontiers Science Center for Disease-Related Molecular Network, West China Hospital, Sichuan University, Chengdu 610041, Sichuan, China

⁴Global Research and Publishing Foundation, New Delhi, India

Correspondence should be addressed to Rajeev K. Singla; rajeevsingla26@gmail.com

Received 6 January 2022; Accepted 5 March 2022; Published 27 March 2022

Academic Editor: Gabriel A. Agbor

Copyright © 2022 Vikram Kumar et al. This is an open access article distributed under the Creative Commons Attribution License, which permits unrestricted use, distribution, and reproduction in any medium, provided the original work is properly cited.

The incidence of obesity and over bodyweight is emerging as a major health concern. Obesity is a complex metabolic disease with multiple pathophysiological clinical conditions as comorbidities are associated with obesity such as diabetes, hypertension, cardiovascular disorders, sleep apnea, osteoarthritis, some cancers, and inflammation-based clinical conditions. In obese individuals, adipocyte cells increased the expression of leptin, angiotensin, adipocytokines, plasminogen activators, and C-reactive protein. Currently, options for treatment and lifestyle behaviors interventions are limited, and keeping a healthy lifestyle is challenging. Various types of phytochemicals have been investigated for antiobesity potential. Here, we discuss pathophysiology and signaling pathways in obesity, epigenetic regulations, regulatory mechanism, functional ingredients in natural antiobesity products, and therapeutic application of phytochemicals in obesity.

1. Introduction

Globally, according to the World Health Organization (WHO), obesity is a major metabolic and heritable disorder, in which more than 1.9 billion adults are suffering from overweight and more than 600 million of them are having the issues of being clinically obese [1, 2]. It is one of the most severe metabolic disorder conditions, which generally develop due to improper energy intake versus energy workout [3–7], stress [8], sedentary lifestyle [9], alcohol consumption [10], depression [11], insufficient nutritional knowledge about the food supplements, and then, ultimately these leads to the accumulation of excessive fats in adipose tissues, which is one of the most prominent factors behind the various chronic disorders such as hypertension, hyperlipidemia, type 2 diabetes, coronary heart disease, and many others [2]. Primarily obesity is an endocrine disorder [12], and interestingly, a

recent study also reveals that obesity is not caused by overeating [13].

Food field research that has recently aroused considerable interest is the potential of natural products to counteract obesity [2, 14, 15]. Nature represents an enormous reservoir of biologically active compounds to treat various ailments from times immemorial [16]. Because of the side effects encountered with long time usage of synthetic drugs and due to stringent guidelines to be fulfilled during drug approvals, plant-herbal drugs have gained much attention as a reliable option to clinical remedy, and the claim for these herbal remedies has greatly increased recently. A variety of phytochemicals are investigated such as polyphenols, alkaloids, terpenoids, flavonoids, tannins, saponins, glycosides, steroids, and proteins present in plants, and their products are key factors in the treatment of several disorders [2]. These products contain dietary phytochemicals with a high

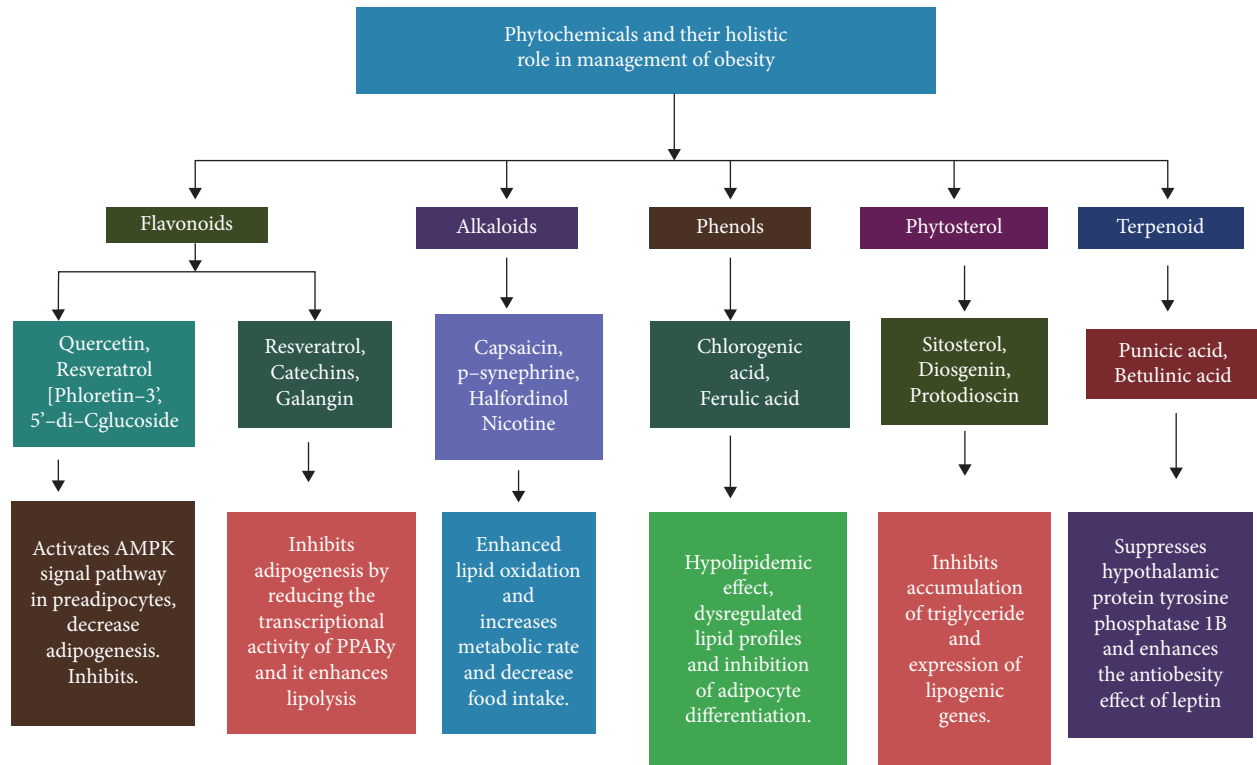


FIGURE 1: Phytochemicals and their role in obesity to preventive and therapeutic approaches.

potential for health promotion and disease prevention [17, 18]. Multiple phytochemicals combinations may result in synergistic activity that increases their bioavailability and their action on multiple molecular targets, thus offering advantages over treatments with single chemicals [15, 19]. The antiobesity effects of these compounds are mediated by the regulation of various pathways, including lipid absorption, intake, and expenditure of energy, increasing lipolysis, and decrease lipogenesis, and differentiation and proliferation of preadipocytes as shown in Figure 1 [15]. A good number of phytoconstituents such as guggulsterone, hydroxycitric acid, apigenin, genistein, gymnemic acid, caffeine, theophylline, ephedrine, capsaicin, piperine, ellagic acid, and catechins have been reported to possess antilipidaemic and prohealth properties [15, 20, 21]. Although some of these compounds are used in preparing antiobesity drugs/formulations, they lack adequate clinical investigations and scientific validation to be authentic and recommended for obesity therapy.

In other words, the potential of plants, herbs, and their derivatives for the treatment of obesity is still largely unexplored and can be an excellent alternative to develop safe and effective natural product-based antiobesity drugs [22]. The potential of phytochemicals as a source of new drugs opens a wide field for scientific investigation owing to the abundant availability of (250,000–500,000) known species, of which only a small percentage has been phytochemically investigated and evaluated for pharmacological potential [23]. Even from the plants known for traditional medicinal use, many still have not been studied for their effectiveness and safety. Therefore, a necessity has arisen for alternative

therapies, especially based on natural products with minimal or no side effects in place of the present therapeutics.

2. Pathophysiology and Signaling Pathways in Obesity

The pathophysiology of obesity is contributed by different endocrine factors and one of the most studied is leptin hormone deficiency. The leptin deficiency triggers hyperphagia mediated through the arcuate nucleus of the hypothalamus. This region expresses neurocircuits involved in the control of feeding process which is regulated by complicated signaling pathways. The variation in nutrition during the gestation period is strongly associated with the onset of neonatal and postnatal obesity. The thrifty gene hypothesis and predation release are two opposite theories that link the evolution process as a cause of obesity. The genome and epigenome studies have associated different genes with obesity. The hypomethylation and hypermethylation of genes and transcriptional factors have been linked with the pathogenesis of obesity. The endocrine-disrupting chemicals (EDC) induce obesity by interfering with various transcriptional factors which regulate fatty acid metabolism, fat absorption, adipocyte differentiation, and adipogenesis as discussed in Figure 2.

2.1. Endocrinology of Obesity. The free fatty acids (FFA) are long chains of hydrocarbons with terminal carboxylic acid which bind to glycerol via the esterification process to form fats. The excess amount of energy is stored in form of fat in

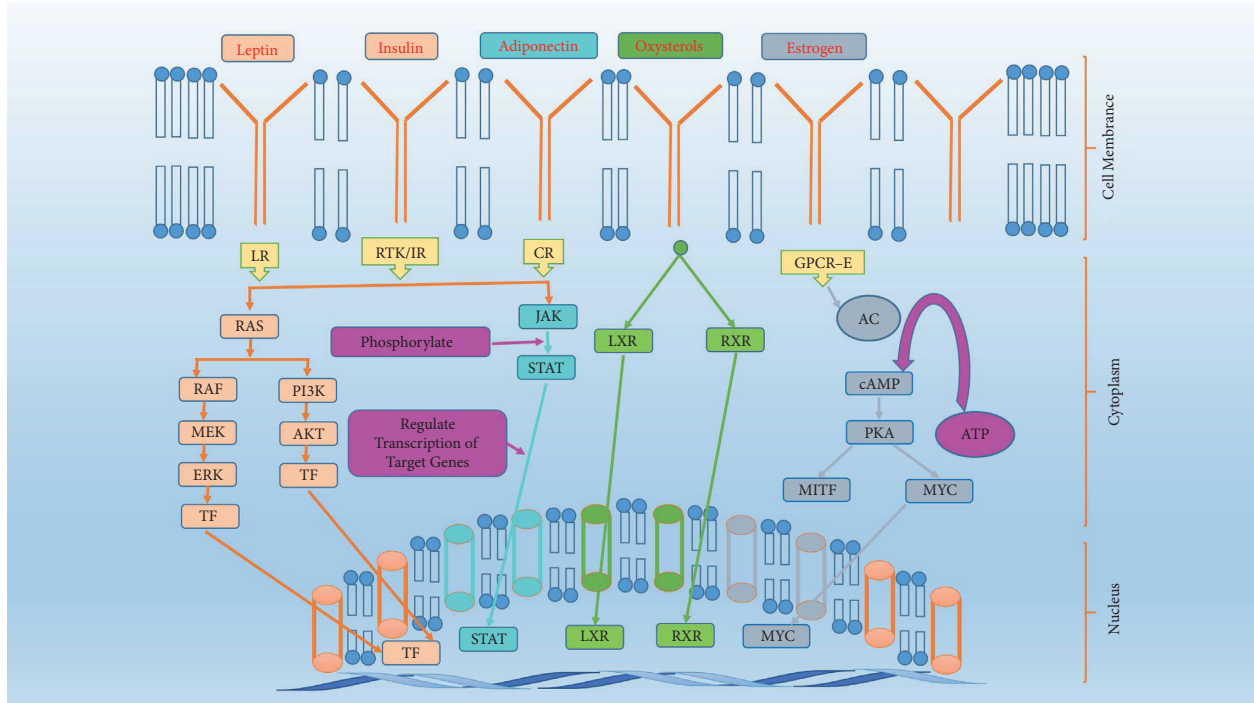


FIGURE 2: Pathophysiology and signaling pathways in obesity, illustrating different endocrine signaling interactions affected in the progression of obesity. The leptin, insulin, and adiponectin bind to LR, IR, and CR, respectively, and activate different TFs via PI3K and STAT pathways. The estrogen activates cAMP signaling via GPCR-E receptor while oxysterol bind with cell receptors to induce activation of signaling cascade and activate through LXR and RXR transcription factors. The activated transcription factors translocate to the nucleus and bind with DNA to regulate thousands of genes and associated gene expressions. LR: leptin receptor; IR: insulin receptor; CR: cytokines receptor; GPCR-E: G-protein coupled receptor for estrogen; RTK: receptor tyrosine kinase; AC: adenyl cyclase; cAMP: cyclic adenosine 3',5'-monophosphate; TF: transcription factor; PKA: protein kinase A; MYC: myc proto-oncogene; MITF: microphthalmia-associated transcription factor; RAF: RAF family of serine/threonine kinases; ERK: extracellular-signal-regulated kinase; MEK: mitogen-activated protein kinase kinase; PI3K: phosphoinositide-3-kinase; JAK: Janus kinase; STAT: signal transducer and activator of transcription; AKT: protein kinase B; LXR: liver X receptor; RXR: retinoid X receptor.).

adipocytes of adipose tissues. During energy-deprived conditions such as fasting, adipocytes release FFA and glycerol which are oxidized aerobically to form ATP [24]. The adipose tissue can be classified as brown adipose tissue (BAT) which is good fat and white adipose tissue (WAT) which is bad fat. This attribute is because BAT is highly vascularised, rich in mitochondria, and is associated with thermogenesis. WAT is most abundant, low in mitochondria, and is least vascularised [25]. The interscapular BAT is utilized for thermoregulation apart from shivering and sweating to control the body temperature. The adipose tissue not responds to endocrine signals as well as it is involved in the generation of endocrine signals such as leptin and associated cytokines.

The leptin hormone is secreted by adipocytes and is an important link between obesity and homeostasis of energy as shown in Figure 2. The leptin deficiency causes less expenditure of energy and is associated with obesity but exceptionally in many individuals, who are obese, elevated leptin concentrations are found. This probably indicates the prevalence of leptin resistance behind the pathogenesis of obesity [26]. The full effect of leptin in regulating obesity is governed by the central nervous system and particularly important is the hypothalamus.

The hypothalamus consists of agouti-related protein (AgRP) neurons in the arcuate nucleus region. These neurons produce endocrine signals such as neuropeptide Y (NPY), AgRP protein, and gamma-aminobutyric acid which is an inhibitory neurotransmitter [27]. These neurons get activated during fasting due to the reduction of leptin and insulin hormone which induce hunger. The high concentration of leptin and insulin inhibits AgRP neurons. Abnormal activation of AgRP neurons causes hyperphagic, i.e., excessive feeding behavior. Clustered near AgRP neurons, there are Proopiomelanocortin (POMC) neurons in the arcuate nucleus which release α -melanocortical stimulating hormone. The activation of these neurons induces satiety [28]. In the deficiency of leptin hormone, POMC neurons are inhibited while AgRP neurons are activated, therefore causing uncontrollable feeding and still induces the feeling of hunger. The genetic mutations in the melanocortin system hence cause hyperphagic obesity. Exceptionally, the calcitonin gene-related protein (CGRP) neurons located in the para branchial nucleus surrounding the superior cerebellar peduncle cause anorexia which is potentially fatal. CGRP-PBN neurons are inhibited by AgRP neurons which increases the meal volume [29].

Since the concentration of leptin is directly proportional to the body fat volume, therefore, generally low leptin concentration is unable to fully activate neurocircuits involved in feedback inhibition of the feeding process and causes obesity [30]. Insulin deficiency or insulin resistance also contributes to obesity by lowering the levels of phospholipase enzyme while the excess phospholipase D1 and D2 expressed in rodents suppress obesity [31]. The postprandial concentration of glucose is regulated by the release of insulin from the pancreatic beta islet of Langerhans which also activates phospholipases [32, 33]. Obesity is a major risk factor for the development of insulin resistance and progression to diabetes which may cause hyperglycemia and leads to cardiovascular disease, sleep apnea, and renal failure [34]. The transition of obesity to diabetes is complex and involves signaling pathways such as Janus kinases (JAK)/signal transducers and activators of transcription factors (STAT) pathway. The binding of growth factor/cytokine on plasma membrane receptors of adipocytes causes stimulation of receptor-associated JKA. The JKA are of 3 types JAK1, JAK2, and JAK3. The signal transducers and transcription factors proteins are of seven types STAT1, STAT2, STAT3, STAT4, STAT5a, STAT5b, and STAT6 containing tyrosine residues that are phosphorylated during activation [22]. The phosphorylated receptor subunit contains specific binding sites for the SH2 (Src homology 2) domain of STAT proteins. After binding to the cytoplasmic tail of JAK proteins in adipocytes, the STAT proteins are phosphorylated at the carboxyl terminus of tyrosine residues. This causes a conformational change in STAT dimer units further to dissociate from JAK and promote their transport to the nucleus. Upon binding with DNA, the STAT proteins activate thousands of genes [35, 36]. The feedback inhibition of this important cytokine signaling involves the suppression of cytokine signaling (SOCS) molecules and protein tyrosine phosphatases (PTP) as shown in Figure 2.

The leptin binds to the beta isoform of leptin receptors, causes activation of JAK-2 by autophosphorylation which further carries phosphorylation of its cytoplasmic tail at tyrosine (Tyr or Y) residues, i.e., Tyr-985, Tyr-1077, and Tyr-1138. This initiates phosphorylation of STAT-3 and STAT-5. The phosphorylation of STAT proteins causes alteration in their conformation and their accumulation in the nucleus to regulate gene transcription [37]. The STAT-3 activation increases gene expression of proopiomelanocortin (POMC) and inhibits AgRP/NPY expression in the arcuate nucleus region of the hypothalamus, thus inducing satiety and inhibiting hyperphagic behavior. The STAT-3 activation parallelly induces the SOCS-3 feedback inhibition loop for the leptin signaling pathway [38]. The protein tyrosine phosphatase (PTP) performs dephosphorylation of JAK and inhibits the JAK/STAT pathway as shown in Figure 2. Experimentally targeted STAT locus deletion in mice causes severe obesity due to probable induction of leptin resistance. The importance of leptin is also indicated by early mutation studies of the *ob/ob* gene and *ob/db* gene in mice. The *ob* gene encodes leptin hormone and the *db* gene encodes leptin receptor. It is observed that mutations in the *ob/db* gene reduce responsiveness to leptin presence and may contribute

to leptin resistance [39] in individuals. Thus, the absence of leptin in individuals with sufficient energy due to inborn error promotes obesity. The leptin acts on two types of neurons: (a) orexigenic or feed-inducing neurons which expresses NPY and AgRP and (b) anorexigenic or feed-suppressing neurons which expresses cocaine- and amphetamine-related transcript (CART) and α -melanocyte stimulating hormone (α -MSH). In the arcuate nucleus, leptin-regulated proopiomelanocortin (POMC) is an important precursor for the α -MSH hormone which binds to the melanocortin-4 receptor (MC4R) and induces anorexic and feeding suppression properties. The AgRP and α -MSH are antagonistic for the MC4R receptor and produce opposite effects upon binding [40]. The MC4R receptor is activated by α -MSH and hence suppresses feeding behavior. MC4R inhibition by AgRP promotes feeding and decreases leptin response. Similar to AgRP, the NPY also increases the feeding process while suppresses catabolism and promotes anabolism [41]. The insulin suppresses both food intake and expression of NPY in the arcuate nucleus. The study of agouti mice revealed that the agouti protein mimics the structural properties of α -MSH, and therefore, it inhibits α -MSH binding to MC4R receptors. A similar heterozygous mutation at this locus reported in four to five percent of human beings causes severe obesity. The regulation of paraventricular hypothalamic nuclei by leptin-controlled arcuate nucleus neuron terminals is strongly involved in the pathogenesis of obesity.

2.2. Neonatal Development. The intake of food is regulated by stomach distention in infants. In neonates, the arcuate nucleus projects into the brain and expresses the POMC gene. During development, arcuate nucleus then sequentially express NPY followed by GABA and then AgRP [42].

Random axonal growth occurs from the first to the third week of the postnatal period. During the gestation period, depending upon the metabolic state, the signals from mother to fetus influences the property of AN neurons to increase the volume of POMC neurons or NPY forms, i.e., anorexigenic or orexigenic forms. Both overnourishment as well as undernourishment of mother during pregnancy is associated with a risk factor of obesity in the offspring. Incidentally, maternal obesity during pregnancy reduces the mass of neurons that expresses leptin receptors and may cause leptin resistance, while undernutrition or malnutrition causes the delayed response to presynaptic GABA and postsynaptic AgRP neurons to stimulus [42, 43].

The leptin deficiency is also associated with decreases in BAT stores. The most accepted yet controversial hypothesis of thrifty genes in human beings states that obese individuals are evolutionarily superior to survive in starving conditions such as famine or flood. Hence, it is the normal approach of the body to defend against stressful conditions by storing more energy in form of fats. This energy in obese individuals may be used in adverse conditions [44]. In opposition to the thrifty gene hypothesis, predation release theory hypothesizes that societal development and invent of weapons by humans have resulted in superiority over much stronger

predators of the ancient era which removed the pressure of natural selection and survival of the fittest against predators. This resulted in the drifting of obesity traits overcoming generations [45]. The genome-wide association study (GWAS) is a new technique used to associate specific genotypes with diseased phenotypes. The method involves analysis of the genome in masses and then identification of genetic markers to envisage the disease. It has recognized different gene variants for obesity. The GWAS analysis in mice has associated gene mutations in *ApoE*, *Ppm1l*, *Lpl*, and *Lactb* genes with obesity. These mutations cause defective apolipoprotein E, protein phosphatase 1 like protein, lipoprotein lipase, and lactamase b, respectively, that are strongly associated with obesity [46]. Some of the literature also indicates that genetic engineering of wheat and other cereal crops is responsible for causing obesity. It is predicted that the genetic engineering of wheat varieties has caused a modification in starch content and therefore induce obesity [47]. The interaction between genes and environment and particularly the sedentary lifestyle along with elevated stress levels also are associated with obesity. Fat mass and obesity (FTO) associated gene is expressed in adipocytes and hypothalamus which encodes FTO protein (alpha-ketoglutarate dependent dioxygenase). A single base pair variation within the first intronic sequence of FTO proteins is associated with obesity in individuals [48]. This means that not only the disruption of coding sequences of DNA but also noncoding sequences play a major role in obesity.

2.3. Epigenetic Modifications. Epigenetics is the study of heritable phenotypic traits caused by modifications in chromosomes without significant variations in sequences of DNA. The epigenome-wide association analysis (EWAS) has associated hypermethylation and hypomethylation of DNA in WAT with proinflammatory pathways and obesity. The hypermethylation of β -adrenoceptor (*ADRB3*) and hypomethylation in the leptin (*Lep*) gene are associated with obesity. The folic acid deficiency also suppresses methylation by inhibiting the DNA methylase enzyme. Endocrine-disrupting chemicals (EDCs) induce hypermethylation of DNA sequences and promote obesity [49]. EDCs are environmental chemicals that interfere with the endocrine system and promote obesity. Some of the EDCs are tributyltin, diethylstilbesterol, dichlorodiphenyltrichloroethane (DDT), phytoestrogens, parabens, etc. The transcription factors such as peroxisome proliferator-activated receptors (PPARs) are classified into PPAR gamma, alpha, and epsilon, which regulate and control genome throughout the life wherein EDCs binding with nuclear receptors of PPAR gamma is related to obesity. The PPARs are ligand-activated transcription factors that cause the formation of the dimer with retinoid X receptors (RXRs) and promote adipocyte differentiation and adipogenesis. Maternal obesity as well as maternal malnutrition both are associated with risk factors of obesity in the offspring. During gestation, maternal obesity is associated with a high risk of being transferred to offspring caused by decreased methylation of developmental gene *Znf483*. Likewise, early gestation exposure to

malnutrition increases risk factors of obesity [50–52]. The gut microflora dysbiosis is also the most important contributor to obesity. The bacterial strains of Gram-positive Firmicutes and Gram-negative Bacteroidetes form general gut microflora. The higher ratio of Firmicutes : Bacteroidetes is associated with the risk of obesity [53].

2.4. Metabolism of Fatty Acids. During starvation and low glucose levels, the adipose tissue releases FFA in blood which are then utilized as an energy source by starving cells and tissues. The fat synthesis in the body occurs in two ways via ingestion of a fat-rich diet and by biosynthesis of fat [54]. Upon ingestion, the fat undergoes lipolysis by forming FFA and glycerol by intestinal lipases. They are then transported to intestinal enterocytes cells through transporter protein. Once inside the enterocyte cells, the FFA and glycerol are reassembled to form triglycerides [55]. At the same time, the cholesterol is converted to cholesterol esters. Finally, the association of triglycerides, cholesterol, and lipoprotein in form of chylomicrons is completed. The very low-density lipoprotein and triglycerides are produced in the liver. Both chylomicron and very-low-density lipoprotein under the stimulation of insulin hormone and lipoprotein lipase enzyme transports FFA and triglycerides into muscles and adipose tissues via the blood. The residual chylomicrons and very-low-density lipoprotein decrease in size and then forms low-density lipoprotein. They are then consumed by hepatocytes which lower cholesterol levels and low-density lipoprotein levels. The HDL or high-density lipoprotein removes cholesterol from extrahepatic peripheral tissues and transports it to the liver [56]. During fat biosynthesis, the glucose under energy-rich conditions is converted into fatty acids via the formation of malonyl coenzyme A and involving fatty acid synthase complex [57]. The adipocytes hypertrophy is a condition in which there is an increase in the size of the adipocytes which leads to obesity while adipocyte hyperplasia is a condition in which there is an increase in numbers of adipocytes caused by differentiation of preadipocytes which also leads to obesity. Mild obesity involves adipocyte hypertrophy Severe obesity involves both hypertrophy and hyper plasticity [58]. Hyperplastic adipocytes are metabolically active and generally harmless but hypertrophic adipocytes are pathogenic and store unhealthy fat. Due to hypoxia and low space, they produce inflammatory cytokines such as interleukin-6, tumor necrosis factor-alpha, and leptin but downregulate production of adiponectin hormone [59]. Adiponectin is an anti-inflammatory hormone that is released by adipocytes. It is important in the regulation of the sugar level and fatty acid breakdown [60]. At the same time, obesity and overweight are the main carters of metabolic syndromes and nonalcoholic fatty liver disease (NAFLD).

NAFLD is a continuum of hepatic ailments linked with metabolic and cardiovascular disorders, such as obesity, dyslipidemia, type 2 diabetes, insulin resistance, and hypertension. It is characterised by increase in liver fat contents (>5%) followed by inflammation and fibrosis [61, 62]. In this condition, the FFA release rate from adipose tissue and

delivery to skeletal muscle and liver is also increased in obese subjects with NAFLD, which outcomes in escalation in muscle and hepatic FFA uptake. Other than this, intrahepatic de novo lipogenesis (DNL) of FFA is more in subjects suffered with NAFLD as compared with normal intrahepatic triglyceride (IHTG), which promote the accretion of intracellular fatty acids [61]. The formation and release of TG in VLDL is amplified in subjects with NAFLD, which provides a mechanism for removing IHTG. Augmented blood sugar and insulin accompanying with NAFLD stimulate DNL and slow down the fatty acid oxidation, by distressing sterol regulatory element binding proteins (SREBP-1c) and carbohydrate responsive element binding proteins (ChREBP). All these abnormal metabolic progression proliferate the intracellular fatty acids that are not oxidized or disseminated within VLDL-TG, and which are subsequently esterified to TG and deposited within lipid vesicles and at the same time, some lipid metabolites of fatty acid can impair the insulin signaling process which leads to the tissue insulin resistance [61, 62].

2.5. Adipogenesis. The preadipocytes convert into mature adipocytes via two processes: preadipocyte proliferation and adipocyte differentiation. The adipocyte differentiation involves sequential morphological changes: (a) growth arrest, (b) mitotic clonal expansion, (c) early differentiation, and (d) terminal differentiation. All the above steps are triggered by preadipocyte factor 1 (pref-1) and CCAAT enhancer-binding protein (C/EBP) [63, 64]. The C/EBP-beta and -delta are transcription factors that induce activity and expression of peroxisome proliferator-activated receptor-gamma (PPAR-gamma). The PPAR-gamma is an inducer of C/EBP-alpha that binds to the promoter of PPAR-gamma and -alpha and promotes the differentiation process [64]. After completion of the differentiation process, all markers of mature adipocytes are well expressed. To produce energy, the triglycerides degrade into FFA and glycerol in absence of glucose as a carbon source. There is a natural hierarchy for catabolic activities to generate energy. In this hierarchy, carbohydrates reserves are first consumed to generate energy followed by lipids and then the proteins [65]. The WAT performs the breakdown of triglycerides into FFA and glycerol during lipolysis. In the cytoplasm of WAT, the adipose triglyceride lipase, monoacylglycerol lipase, and hormone-sensitive lipases in acute energy need to convert triglycerides into FFA and glycerol. These FFA are used as energy sources in organs and tissues via beta-oxidation [66]. The energy imbalance within the adipocytes produces endoplasmic reticulum stress and mitochondrial stress. The free fatty acid oxidation occurs in two sites namely peroxisomes and mitochondria. The free fatty acid oxidation in peroxisomes is strictly utilized for free fatty acid biosynthesis; on the other hand, mitochondrial free fatty acid oxidation is used for energy production during the crisis. The obese individual tends to depend upon glucose oxidation more than fatty acid oxidation revealing that mitochondrial fatty acid oxidation is compromised [67].

3. Progression of Antiobesity Pharmaceuticals

Obesity is now a global problem [68] and is associated with several chronic conditions including osteoarthritis, obstructive sleep apnea, gallstones, fatty liver disease, reproductive and gastrointestinal cancers, dyslipidemia, hypertension, type 2 diabetes, heart failure, coronary artery disease, and stroke [69]. However, many medications have been used to manage obesity over the years. For research scientists, there are now numerous molecular targets for antiobesity drugs: central receptors for biogenic amines, cannabinoids, hypothalamic neuropeptides, peripheral β 3-adrenoceptor, and UCPs; and dominating all obesity research is leptin—a tantalizing but frustrating obesity target. However, most of the antiobesity drugs that were approved and marketed have now been withdrawn due to serious adverse effects. In the 1990s, fenfluramine and dexfenfluramine were withdrawn from the market because of heart valve damage [70]. In 2000, the European Medicines Agency (EMA) recommended the market withdrawal of several antiobesity drugs, including phentermine, diethylpropion, and mazindol, due to an unfavorable risk-to-benefit ratio [71]. The first selective CB1 receptor blocker, rimonabant, was available in 56 countries from 2006 but was never approved by the U.S. Food and Drug Administration (FDA) due to an increased risk of psychiatric adverse events, including depression, anxiety, and suicidal ideation [72]. Subsequently, rimonabant was withdrawn from the European market in 2009. Recently, many newer agents have been tried, though only orlistat and sibutramine have been approved for long-term use. In October 2010, sibutramine, widely used after approval by the U.S. FDA in 1997, was withdrawn from the market because of an association with increased cardiovascular events and strokes [73]. More recently, in February 2011, the U.S. FDA rejected approval of the bupropion/naltrexone combination marketed as Contrave due to concerns over potential cardiovascular risks. Currently, some of the US-FDA approved antiobesity active pharmaceutical ingredients, i.e., phentermine, lorcaserin, naltrexone, orlistat, and liraglutide are clinically tested (Table 1) and available in the market [74].

The long-term safety and efficacy of newly developed drugs should also be evaluated in the management of obesity, which often requires continuous treatment to achieve and maintain weight loss, though the rigidity of a regulatory committee for the approval of novel antiobesity drugs and the regulatory guidelines for antiobesity therapy represents a significant limitation to developing drugs [75, 76].

Antiobese drugs generally have the potentials to decrease appetite or increase satiety, such as sibutramine; those that are adrenergic and also reduce the appetite, such as the amphetamines; and those that alter the digestion, such as orlistat. Besides, most of the treatments available have only revealed short-term assistances and are not recommended for sustained weight loss due to the liver enzyme abnormalities and liver disease. Fenfluramine is an example of a drug that is no longer approved for the treatment of obesity

TABLE 1: A comparison of FDA-approved antiobesity drugs [74].

Drug	Dose concentration	Approving bodies	Mechanism of action	Weight reduces up to kg/year	Side effects
Phentermine	46 mg–92 mg once daily.	Approved by FDA in 2012.	Reduces appetite	8.6	Dizziness, pulmonary hypertension
Lorcaserin	10 mg twice daily	Approved by FDA in 2012.	5-HT _{2C} receptor activation	3.6	Headache, dizziness
Naltrexone	64 mg/720 mg tablets two times daily	Approved by FDA in 2014.	Noradrenaline and dopamine reuptake inhibitor.	4.8	Vomiting, dizziness
Orlistat	60–120 mg three times daily	Approved by FDA in 1999.	Pancreatic lipase inhibitor	3.4	Hepatotoxic, steatorrhea
Liraglutide	3.0 mg injection once daily	Approved by FDA in 2014.	GLP-1 receptor agonist	5.9	Nausea, pancreatitis

because of safety concerns. Elevations of aminotransferases and/or alkaline phosphatase have been reported with sibutramine use in placebo-controlled trials [77]. Drugs used for the management of obesity comorbidity disease such as NAFLD, diabetes, hypertension, and hyperlipidemia also have serious hepatotoxicity. Antidiabetic drugs, i.e., glibenclamide/glyburide, chlorpropamide, tolbutamide, tolazamide, metformin, pioglitazone, and rosiglitazone are reported for hepatotoxicity in terms of cholestasis, hepatitis, and liver failure.

Antihypertensive drugs, i.e., nifedipine, diltiazem, amlodipine, losartan, candesartan, valsartan, enalapril, ramipril, captopril, and fosinopril are also reported for severe hepatitis in liver [78]. At the same time, some natural products or phytochemicals are also reported for hepatotoxicity, which have been widely used for the obesity management since last many decades [79]. The extract of *Germander* causes the drug-induced liver injury (DILI), which is probably mediated by furano neoclerodane diterpenoids. The desert shrub *Chaparral* was marketed for weight loss, but its active phytochemical nordihydroguaiaretic acid is reported to have the liver toxicity in recent studies. *Kava* preparation of rhizome of *Piper methysticum* marketed for anxiolytic and mood enhancer, but some studies described the kava associated immune-mediated liver toxicity, with CYP2D6 deficiency. The roots of “*Chelidonium majus*” herb contain the biologically active phytoconstituents chelerythrine and sanguinarine, and their principia are similar to the opium and reported for hepatotoxic effects. Phytochemicals of “*Lycopodium serratum*” also reported for idiosyncratic or hypersensitivity reaction based cholestatic type hepatotoxicity [80]. In view of such serious toxicity of herbal or natural products, there is a great need of authenticated safe and effective treatment for obesity and its comorbidity diseases.

4. Obesity Regulating Mechanisms of Natural Phytochemicals

4.1. Proliferation in Energy Outflow. The BAT is highly vascularised, rich in mitochondria, and is strongly associated with heat generation or thermogenesis. During low-temperature conditions, the BAT helps in the

regulation of body temperature [81]. The BAT consumes excess energy for heat generation by a process that involves leakage of protons produced during the electron transport chain and oxidative phosphorylation [81, 82]. Interestingly, BAT escapes ATP formation and results in leakage of protons from perimitochondrial space through uncoupling protein (UCP-1 or UCP-3) which generates excess energy in form of metabolic heat and also promotes higher oxidation rates of FFA [82]. The WAT which stores unhealthy fat can be converted into BAT in a process of adipocyte differentiation known as browning. Therefore, the proliferation of BAT and browning of WAT can contribute towards the treatment of obesity by releasing excess stored energy in form of heat [83]. Natural phytochemicals have been found helpful in the treatment of obesity. Particularly, the phytochemicals rutin, naringenin, luteolin, and quercetin promote browning of WAT and prevents obesity (Table 2). The genistein and myricetin cause prevention of obesity by elevation of UCP-1 expression, peroxisome proliferator-activated receptor gamma coactivator 1-alpha (PGC-1a), and PRDM-16 which promotes brown adipogenesis through PPAR-gamma as shown in Figure 3 [84].

4.2. Craving Suppressant Influence. The reduction of appetite or induction of satiety can be of great significance in the regulation of obesity. The studies revealed that certain systems in the central nervous system are modulators of metabolic activities. The hypothalamus is one such major modulator in regulating hunger [85]. The uncontrolled hunger in which satiety is not achieved due to inborn errors of metabolism is related to obesity. The arcuate nucleus in the hypothalamus expresses NPY and AgRP which induces hunger and food craving while the CART and POMC pathway suppresses hunger [86]. The recent advances in obesity treatment have considered apigenin flavonoid to regulate hyperphagia or excessive feeding behavior. The apigenin activates POMC and CART pathways in the brain [87]. The other similar phytochemicals include isoflavone genistein and flavonoid cyanidin which also suppresses feeding by regulation of leptin concentration in the brain (Table 2). These approaches shall be greatly helpful in controlling obesity in the future [88, 89] as shown in Figure 3.

TABLE 2: Antiobesity phytochemicals' mechanism of action, signaling pathway, and their classification.

Mechanism of action	Signaling pathway	Classification	Phytochemical	Reference
Proliferation in energy outflow	(1) Browning of WAT into BAT (2) Thermogenesis via UCP 1/UCP 3 (3) Escaping ATP formation	Flavanoid	Rutin, naringenin, luteolin, quercetin, genistein, and myricetin	[81–84]
	(4) PPAR-gamma, PGC 1 a, PRDM 16	Phenols	p-hydroxybenzoic, cinnamic acid, ferulic acid, caffeic acid, p-coumaric, and cinnamic acid	[139–141]
Craving suppressant influence	(1) Upregulation of POMC and CART pathway	Flavanoid	Apigenin, genistein, and cyanidin	[1–89]
	(2) Downregulation of AgRP and NPY pathway	Alkaloid	Halfordinol	[136–138]
Inhibition of lipase and other enzyme activity	(1) Inhibition of pancreatic phosphor lipase enzyme	Flavanoid	Epigallocatechin-3,5-digallate and other related flavan-3-ol-digallate esters, catechins, resveratrol, and galangin	[90–92]
	(2) Inhibition of alpha amylase enzyme	Anthocyanin	Cyanidin	
Adipocyte differentiation control	(1) Regulation of adipogenesis by PPAR-gamma, C/EBP families such as C/EBP alpha, beta, and epsilon (2) The SREBP 1a, SREBP 1c, and SREBP 2 induce cholesterol biosynthesis. The SREBP 1c promotes differentiation of adipocytes and may activate PPAR-gamma. The inhibition of C/EBP alpha, PPAR-gamma, and SREBP may be effective for obesity treatment (3) Adipocyte differentiation by apigenin is linked with inhibition of interleukin 6, leptin production, and monocyte chemoattractant protein 1(MCP-1). The suppression of the expression of PPAR-gamma, SREBP-1c, and GLUT-4 via JNK signaling (4) Interaction with PPAR- gamma and decreases adipocyte differentiation	Flavanoid	Apigenin, guggul sterols, naringenin, genistein, hesperidin, myricetin, kaempferol, and rutin	[98–102]
		Alkaloid	Synephrine, nuciferine, piperine, and piperlongumine	
Regulation of fat metabolism activity	(1) Downregulation of perilipin-1 (2) Promoting lipolysis and inhibition of insulin-dependent lipogenesis (3) The downregulation of PPAR-gamma/EBP beta, SREBP-1, and genes of triglyceride biosynthesis (4) The lowering of triacylglycerol concentrations in adipocytes by regulating lipolysis	Flavanoid	Genistein, daidzein, kaempferol, apigenin, hesperidin, and berberine	[104, 105]
		Phytosterols	Ampesterol, brassicasterol, guggulsterone, sitosterol, diosgenin, and stigmasterol	

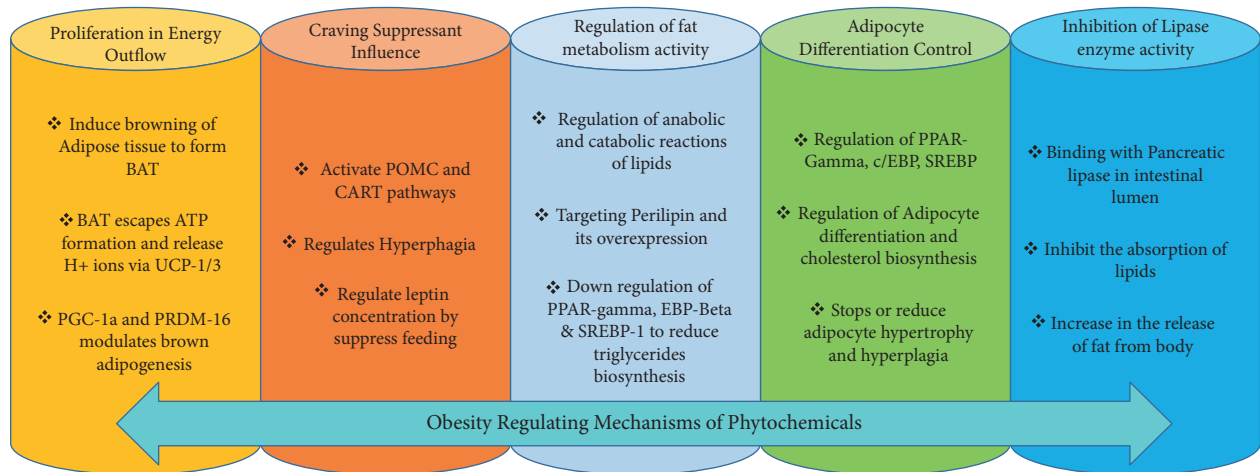


FIGURE 3: Obesity-regulating mechanisms of natural phytochemicals.

4.3. Inhibition of Lipase Enzyme Activity. One of the important factors which contribute to obesity is the elevated absorption of lipids and carbohydrates via the gastrointestinal tract. The inhibition of such digestive enzymes which carry absorption of carbohydrate and lipid from the intestine shall reduce obesity [90]. The enzyme phospholipase is secreted in pancreatic juice which triggers the breakdown of triglycerides into FFA and monoglycerides in the intestinal lumen. After absorption of FFA and monoglycerides in blood, they are transported towards chylomicrons for reassembly of the triglycerides and the formation of cholesterol esters [91]. The inhibition of the pancreatic phospholipase enzyme can be promising for the treatment of obesity. The side effects studies of such inhibition processes must be thoroughly performed, since it may cause stomach flatulence and distention. An inhibitor of the alpha-amylase enzyme may prevent fatty acid biosynthesis under excess consumption of glucose and related sugars [92]. Generally, under low energy requirements, excess glucose is converted into fatty acids via the formation of malonyl CoA. In this process, the mitochondrial citrate is transported to the cytoplasm where it is used to regenerate acetyl coenzyme A. The acetyl coenzyme A is converted to malonyl coenzyme A by acetyl-coenzyme A carboxylase enzyme. The cytoplasmic fatty acid synthase complex uses malonyl CoA and synthesizes fatty acid chains [93]. The plant-derived flavonoid luteolin is a strong phospholipase inhibitor. Similarly, epigallocatechin-3,5-digallate and other related flavan-3-ol-digallate esters offer very high phospholipase inhibition properties [94] (Table 2). One of the latest isolated flavone compounds has shown the highest inhibition level alpha-amylase enzyme, as shown in Figure 3 [95].

4.4. Adipocyte Differentiation Control. Certain phytochemicals possess adipocyte proliferation and differentiation regulatory properties. The formation of new adipocytes is referred to as adipogenesis. It is regulated by adipocyte-specific genes belonging to PPAR-gamma, C/EBP families such as C/EBP alpha, beta, and epsilon. Interdependence of C/EBP alpha and PPAR-gamma controls adipocyte differentiation process [96]. Sterol regulatory element-binding proteins (SREBPs) also play important role in cholesterol balance, free fatty acid metabolism, and differentiation of adipocytes. The SREBP 1a, SREBP 1c, and SREBP 2 induce cholesterol biosynthesis. SREBP 1c promotes differentiation of adipocytes and may activate PPAR-gamma. The inhibition of C/EBP alpha, PPAR-gamma, and SREBP may be effective for obesity treatment [97]. The phytochemicals such as apigenin [98], guggul sterols [99], naringenin, genistein [100], hesperidin, myricetin, kaempferol, and rutin [101] have been proven effective in downregulating the differentiation of adipocytes (Table 2). This inhibition of adipocyte differentiation by apigenin is linked with possible inhibition of interleukin 6, leptin production, and monocyte chemoattractant protein 1 (MCP-1). The genistein suppresses the expression of PPAR-gamma, SREBP-1c, and GLUT-4 via JNK signaling. Myricetin interacts with PPAR-gamma and

decreases adipocyte differentiation, as shown in Figure 3 [102].

4.5. Regulation of Fat Metabolism Activity. The release of FFA and glycerol in adipocytes is controlled by several mechanisms. The stores of WAT are determinants for the plasma concentrations of FFA. The elevated rates of lipolysis during feeding process contribute to the high ratio of circulating fatty acid level. Therefore, the phytochemical which may target the important steps in the catabolism of fats shall prevent obesity [101]. Likewise, perilipin lipid droplet coating protein blocks the lipases to reach triglycerides present in adipocytes. The enzymes protein kinase A causes phosphorylation of perilipin and induces conformational change. This promotes the binding of protein lipase A and initiates lipolysis. The low perilipin has been proven helpful for the treatment of obesity in high-fat-diet-fed rats [103]. The genistein along with daidzein downregulated perilipin-1. It also promoted lipolysis and inhibited insulin-dependent lipogenesis [104]. The kaempferol downregulated PPAR-gamma/EBP beta, SREBP-1, and genes of triglyceride biosynthesis [105]. Apigenin, kaempferol, and hesperidin (Table 2) decrease triacylglycerol concentrations in adipocytes by regulating lipolysis, as shown in Figure 3 [106].

5. Functional Ingredients in Natural Antiobesity Products

5.1. Plant Metabolites/Phytochemicals. The plethora of investigations conducted on plant metabolites provides ample evidence that demonstrates the therapeutic potential of these phytochemicals in treating obesity and the related diseases. Millions of phytochemicals exist that are broadly classified under polyphenols, alkaloids, and terpenoids. These phytochemicals/plant metabolites exert their antiobesity effects (Table 3) either alone or synergistically via the following mechanisms: (a) enhancing energy expenditure, thermogenesis, lipolysis, and lipid metabolism, modulating adipose tissue, acting as appetite suppressants, regulating adipogenesis, inhibiting the activity of the enzyme pancreatic lipase, acting as antioxidants, and preventing oxidative damage in living systems [107].

5.2. Polyunsaturated Fatty Acids (PUFAs). One of the most important ingredients used to combat obesity is the type of dietary fat being used. Although people opine that fat is the main reason for obesity but that does not hold true as the amount and type of fat being used plays a crucial role in weight management via modulating metabolism and adipose tissue function [108]. Consequently, dietary fats rich in monounsaturated fatty acids (MUFAs) and polyunsaturated fatty acids (PUFAs) are considered to enhance body metabolism. PUFAs are known to show excellent antiobesity effects and are further classified into ω -3 and ω -6 groups. ω -3 PUFAs consist of two types of fatty acids, one is eicosapentaenoic acid (EPA) and the other one is docosahexaenoic acid (DHA). There is an intermediate fatty acid between EPA and DHA known as docosapentaenoic acid (DPA) [109].

TABLE 3: Chemical structure and therapeutic application of phytochemicals in obesity.

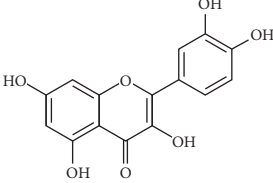
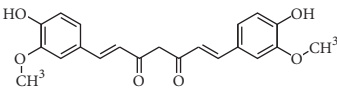
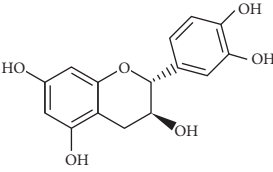
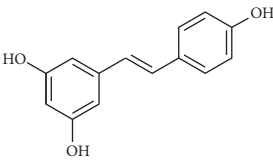
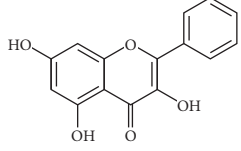
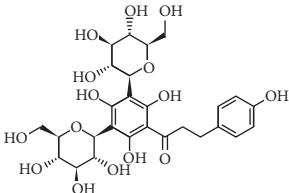
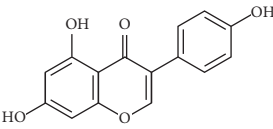
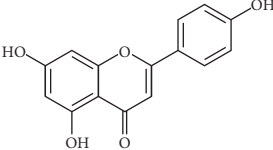
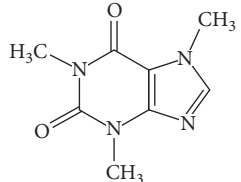
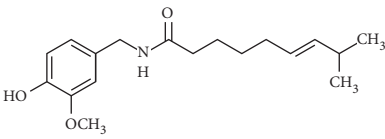
Plant source	Name of phytochemical	Structure	Antiobesity effect	Phyto molecules	Reference
<i>Coriandrum sativum</i>	Quercetin		Reduces the process of adipogenesis by activation AMPK signaling mechanism	Flavonoids	[131]
<i>Curcuma longa</i>	Curcumin		Enhanced β -oxidation, inhibition of fatty acid synthesis, and decreased fat storage	Flavonoids	[132]
<i>Vitis vinifera</i>	Catechins		Prevents α -glucosidase activity and micelle formation in reducing carbohydrates absorption in the small intestine	Flavonoids	[133]
<i>Arachis hypogaea, Vitis vinifera, and Cyanococcus</i>	Resveratrol		Prevents transcriptional activity and reduce adipogenesis	Flavonoids	[134]
<i>Alpinia galangal and Helichrysm aureonitens</i>	Galangin		Reduces the collection of hepatic triglycerides	Flavonoids	[131–134]
<i>Cyclopia falcata and Cyclopia subternata</i>	Phloretin-3',5'-di-c-glucoside		Inhibits the expression of peroxisome proliferator-activated receptor-2 (PPAR-2) and adipogenesis.	Flavonoids	[131–134]
<i>Glycine max</i>	Genistein		Antiadipogenic effects by suppressing PPAR- α and causing	Flavonoids	[131–134]
<i>Matricaria chamomilla</i>	Apigenin		Antiobesity effect in visceral adipose tissue	Flavonoids	[136]
<i>Camellia sinensis and Coffea arabica</i>	Caffeine		Exerts lipolytic and thermogenic actions	Alkaloids	[136]
<i>Capsicum annuum</i>	Capsaicin		Enhanced lipid oxidation and increased energy expenditure	Alkaloids	[138]

TABLE 3: Continued.

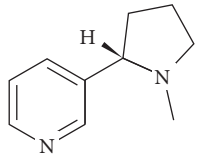
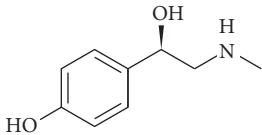
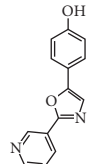
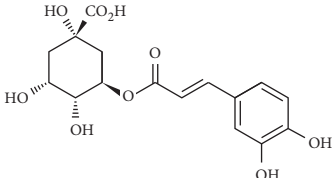
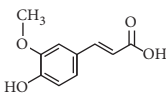
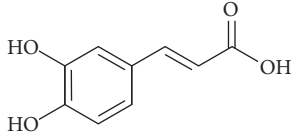
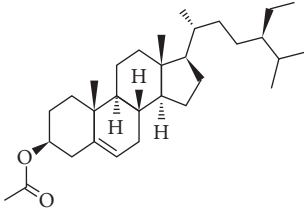
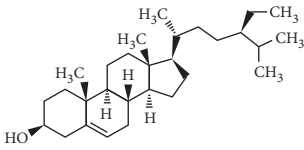
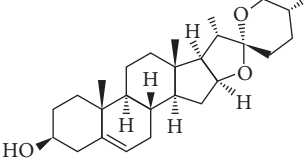
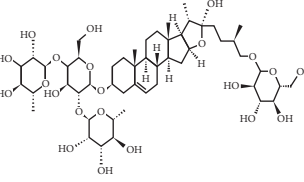
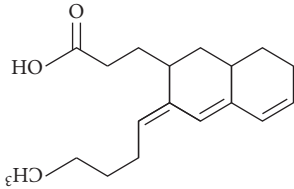
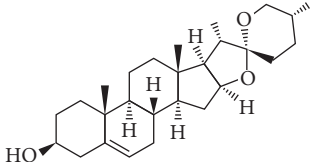
Plant source	Name of phytochemical	Structure	Antiobesity effect	Phyto molecules	Reference
<i>Nicotiana tabacum</i> and <i>Capsicum annuum</i>	Nicotine		Prevents food intake and increase metabolic rate	Alkaloids	[136–138]
<i>Citrus aurantium</i>	p-synephrine		Increases metabolic rate and reduces weight loss	Alkaloids	[136–138]
<i>Aegle marmelos</i>	Halfordinol		Prevents food intake and increase metabolic rate	Alkaloids	[136–138]
<i>Glycine max</i> and <i>Coffea canephora</i>	Chlorogenic acid		Reduces the absorption of carbohydrate	Phenols	[141]
<i>Hordeum vulgare</i> and <i>Asparagus officinalis</i>	Ferulic acid		Improves the glucose and lipid homeostasis in a high-fat diet and reduce obesity	Phenols	[139]
<i>Coffea arabica</i>	Caffeic acid		Modulated gut microbiota dysbiosis	Phenols	[140]
<i>Arachis hypogaea</i> , <i>Citrullus Colocynth</i> , and <i>Bauhinia variegata</i>	Sitosterol		Reduce the absorption of cholesterol by lowering the level of cholesterol and LDL (low-density lipoprotein)	Phytosterol	[142]
<i>Dioscorea villosa</i>	β -sitosterol		Exhibited antiobesity effects by suppressing sterol regulatory elements	Phytosterol	[143]
<i>Trigonella foenumgraecum</i> and <i>Dioscorea villosa</i>	Diosgenin		Inhibits accumulation of triglyceride and expression of lipogenic genes	Phytosterol	[144]
<i>Trapa natans</i> and <i>Tribulus terrestris</i>	Protodioscin		Reduces blood levels of triglyceride, cholesterol, LDL	Phytosterol	[142–144]

TABLE 3: Continued.

Plant source	Name of phytochemical	Structure	Antiobesity effect	Phyto molecules	Reference
<i>Punica granatum</i> and <i>Momordica</i>	Punicic acid		Enhances the activity of PPAR- α , PAR γ -responsive genes and reduces the deposition of adipose tissue	Terpenoid	[145–148]
<i>Orthosiphon aristatus</i>	Betulinic acid		Suppresses tyrosine phosphatase 1B and enhances the antiobesity potential	Terpenoid	[145–148]

PUFAs can be obtained from fish and fish oils. Numerous investigational studies reported that dietary fatty acids are involved in modulating adipose tissue properties and homeostasis between glucose and insulin. Substantial evidence from literature quote several mechanisms by which ω -3PUFAs could exert their antiobesity effects: (a) increase in fatty acid β -oxidation, (b) enhanced energy expenditure via thermogenesis, (c) alteration in epigenetic effects and gene expression in fat tissue, (d) modulation in adipokine pathways leading to altered adipokines release, and (e) reduction in enzymatic activity of fatty acid synthase and stearoyl-CoA desaturase-1 (lipid synthesizing enzymes) finally appetite suppression [110]. However, a balanced ω -6/ ω -3 ratio of 1:2/1 along with physical activity of some degree is identified to be a key factor in the treatment of obesity and related diseases [111].

5.3. Dietary Fiber. The role of dietary fibers (DFs) in treating obesity and related disorders has become prominent. DFs are either analogous carbohydrates or edible plant parts that exhibited altered digestion patterns in the human intestine. DF is of two types: soluble dietary fiber (SDF) and insoluble dietary fiber (IDF). SDF is generally fermented by the microbiota of the gut releasing short-chain fatty acids (SCFAs) metabolites. SDFs (especially guar gum, pectin, psyllium, and β -glucans) are viscous [112]. This physico-chemical property of SDFs helps them to form a barrier like gel in the small intestine which enables to delay absorption and gastric emptying altering postprandial metabolism. On the other hand, IDF which is seen in cellulose, hemicellulose, and lignin is regarded as fecal bulk-forming agents [113]. The physiological mechanisms contributing to weight loss strategies include (a) appetite suppression through satiating properties of the fiber, (b) delayed gastric emptying, (c) alteration in the transport mechanism involving glucose and fat, (d) its fiber regulates the defecation rhythm, and (e) it has a role in the growth of gut microbiota [114]. Evidence from studies reported that DF is fermentable by the gut microbiota which in turn helps in the production of SCFAs which are known to enhance satiating properties of DF that is inversely proportional to the weight gain in humans [115].

DF also altered blood lipid concentrations and glycemic response in humans. There exists robust epidemiologic evidence that proves that dietary fiber intake can help overcome overweight and obesity; however, many more interventional studies are needed to ascertain these effects removing all the practical interventional hurdles.

5.4. Proteins. A balanced diet essentially consists of dietary proteins. A diet that has 1.2–1.6 gm of protein/kg/day and which has approximately 25–30 gm of the protein-rich meal regarded as higher protein. A high-protein diet (HPD) is generally associated with weight loss strategies, improved satiety, fat mass loss, etc. Evidence from scientific studies has put forth several mechanisms by which dietary protein can help in weight loss and management: (1) improved satiety that is associated with enhanced thermic effects and (2) enhanced energy expenditure [116]. Dietary proteins also enhance the fat-free mass which is attributed to an improvement in body composition. It is evident from research data that HPD elevates levels of anorexigenic hormones such as glucagon-like peptide-1, cholecystokinin, and peptide tyrosine-tyrosine whilst reducing levels of orexigenic hormones (such as ghrelin), ultimately increasing satiety and reduction in food intake. HPD induced thermic effects also called diet-induced thermogenesis (DIT) might be due to increased amino acid oxidation levels postprandial resulting in increased oxygen demand essential for the movement of proteins and finally enhanced satiety. Hence, it can be concluded that HPD can be used as a safe tool for efficacious weight reduction and weight management to overcome obesity and the related diseases. However, to confirm the beneficial effects of HPD, in-depth clinical trials for a longer period must be conducted [117].

5.5. Antiobesity Effect of Dietary Calcium. Calcium (Ca) is regarded as the most versatile nutrient that acts as a prolific second messenger in several physiological processes and a signaling agent. Calcium helps in the fertilization and development process, nerve signal transduction, cell proliferation, neuronal plasticity, flexibility in mammals through

muscular movements, skeletal integrity, bone metabolism, blood coagulation, cellular differentiation, and cell death [118, 119]. The array of diverse functions exhibited by Ca^{2+} led scientists to investigate its role in diseases. Epidemiologic data from several studies indicate that there exists a strong association between dietary calcium intake and the prevalence of obesity [120]. The plausible mechanisms by which the amount calcium intake can regulate the bodyweight or modulate obesity are as follows: (1) high Ca^{2+} intake increases fecal fat and EE (energy expenditure). This is probably due to increased dietary calcium which binds to more fatty acids and or to bile salts in the colon, leading to the formation of insoluble calcium-fatty acid soaps and thereby inhibiting fat absorption and hence reducing weight [121]. (2) Intracellular calcium levels are regulated by hormones, such as parathyroid hormone (PTH) and 1,25-hydroxyvitamin D (1,25-(OH)(2)-D). High dietary calcium intake could stimulate lipolysis, inhibit fat accumulation mainly by preventing the release of parathyroid hormones and 1,25-(OH)(2)-D. Hence, it is opined that calcium intake can influence lipogenesis or lipolysis based on the influx of Ca^{2+} in adipocytes [122]. Several studies in both humans and animals were conducted but the data reported are inconsistent related to the impact of Ca^{2+} intake on anthropometric measurements and the prevalence of obesity warranting further elaborative investigation with conclusive results.

5.6. Probiotics. Microbes that are commensals in the human intestines play a crucial role in the absorption, lysis, and storage of nutrients. They are also essential in several physiological processes of humans such as metabolism, digestion, circadian rhythms, and vitamin synthesis [123]. Additional roles of gut microbiota are to influence tissue-fatty acid composition, stimulate energy production, and inflammation. Gut microbiota dysbiosis is found to be inherently associated with metabolic disorders leading to obesity. Modulation of gut microbiota using nutraceuticals (probiotics and prebiotics) has shown promising effects in the treatment of obesity [124]. Probiotics are nutraceuticals composed of live bacteria, especially Lactobacilli and Bifidobacteria, which help in improving gut microbiome and health status. The gut microbiome along with the probiotic supplementation has a positive impact on health conditions such as type 2 diabetes, immune, infectious diseases, and also cardiovascular diseases. Its impact on the neurotransmission signaling and functionality of the brain has a significant influence on weight management and obesity. Probiotics help in weight loss by inhibiting fat accumulation, leading to inflammation reduction, and also have the capability to reduce insulin resistance. Apart from this, they influence gastrointestinal peptides and neuropeptides [125]. Prebiotics are dietary substrates defined as “dietary ingredients that on selective fermentation lead to changes, gut microbiota especially its composition and function those of which are associated with potential health benefits to the host” [126]. Several studies conducted reported that usage of prebiotics especially insulin-type fructans help in the colonization of

arabinoxylan, *Roseburia*, and *Clostridium* cluster XIVa, which further increases species such as *Bacteroides* and *Bifidobacterium* along with *Roseburia* exhibiting the anti-adipogenic effect in obese mice fed with the high-fat diet. Although these findings prove the importance of prebiotics and probiotics in obesity management with experimental evidence from animal studies, significant supportive data from human clinical trials are unavailable [127, 128].

6. Therapeutic Application of Phytochemicals in Obesity

Some clinically important secondary metabolites are used as antiobesity agents [129]. Several phytochemicals are employed to reduce the process of adipogenesis, carbohydrates absorption in the small intestine, collection of hepatic triglycerides, deposition of adipose tissue, weight loss, and enhances the antiobesity potential, activity of PPAR- α and PAR γ -responsive genes (Table 3) [130, 131]. Flavonoids have the potential to inhibit lipase activity and control adipogenesis, such as quercetin, catechins, resveratrol, and galangin. Cyanidin and cyanidin 3-glucoside molecules isolated from *Ribes nigrum* and *Morus alba*, respectively, both molecules reduce triglycerides and normalized adipocytokine secretion [131–134]. Adipogenic transcription factor (C/EBP) increases lipolysis and fatty acid oxidation and normalizes adipocytokine secretion. Some other flavonoids and genistein increase the HDL (high-density lipoprotein) and decrease the BMI (body mass index). Naringin and berberine reduce the hypercholesterolemic level, decrease the blood lipid and quercetin molecules, and increase the blood HDL [134, 135]. Alkaloid with antiobesity property isolated, synephrine from *Citrus aurantium*, nuciferine from *Nelumbo nucifera*, piperine and piperlongumine from *Piper nigrum*. Green coffee reduced body fat by decreasing the absorption of glucose [136–138]. Phenols are an important phytochemical and reduce the risk of obesity such as p-hydroxybenzoic, cinnamic acid, ferulic acid, caffeic acid, p-coumaric, and cinnamic acid [139–141]. Phytosterols are naturally occurring phytochemicals and reduce obesity and decrease LDL-cholesterol such as campesterol, brassicasterol, guggulsterone, sitosterol, diosgenin, and stigmasterol and appear to reduce obesity, and high intakes of these compounds decrease LDL-cholesterol levels in the intestinal lumen. Phytosterols compete with cholesterol for micelle [142–144]. Chemically modified terpenes are found in plants and consist of both primary and secondary metabolites [145–148]. Some terpene molecules are ligands with hermeneutic potential to stimulate PPAR and act as dietary sensors and regulate glucose metabolism and control energy homeostasis metabolism [145–148]. In the recent era of research and development, the natural phytochemicals are also playing very important role for the treatment of NAFLD. Epidemiological evidence recommends that a healthy dietary habits with cumulative intake of several plant-based natural phytochemicals, i.e., spirulina, berberine, oleuropein, garlic, curcumin, resveratrol, coffee, ginseng, glycyrrhizin, cocoa powder, bromelain, and epigallocatechin-3-gallate could lower the risk of NAFLD

TABLE 4: Efficacy of natural products-based antiobesity bioactive components.

S. N.	Name of the natural product	Bioactive component	Duration of HFD (high-fat diet) in male mice	Reduction in body weight in (%)	References
1	<i>Morus alba</i>	Resveratrol anthocyanin	HFD (fat: 45%, w/w) for 12 weeks	53.5%	[151]
2	<i>Curcuma longa</i>	Curcumin	HFD (fat: 60%, w/w) for 12 weeks	15.9%	[152]
3	<i>Rhizoma coptidis</i>	Berberine	HFD (fat: 16.2%, w/w) for 6 weeks	13.2%	[153]
4	<i>Capsicum annuum</i>	Capsicin	HFD (fat: 45%, w/w) for 9 weeks	8%	[154]
5	<i>Acacia mollissima</i>	Robinetinidol	HFD (fat: 60%, w/w) for 7 weeks	23.2%	[155]
6	<i>Zingiber officinale</i>	Gingerol, paradol, d shogol	HFD (fat: 30%, w/w) for 5 weeks	38.6%	[156]
7	<i>Nelumbo nucifera</i>	Alkaloids	HFD (fat: 20%, w/w) for 6 weeks	9.81%	[157]
8	<i>Camellia sinensis</i>	Caffeine	HFD (10%, w/w) for 6 weeks	11.3%–16.9%	[107]
9	<i>Coffea Arabica</i>	Caffeoyl, quinic acids	HFD (fat: 30%, w/w) for 2–15 weeks	14.3%	[158]
10	<i>Glycine max</i>	Protein isolated	HFD (25%, w/w) for 12 weeks	10.0%	[159]
11	<i>Vaccinium ashei</i>	Anthocyanins	HFD (45%, w/w) for 12 weeks	9.81%	[160]
12	<i>Citrus depressa</i>	Flavonoids	HFD (35%, w/w) for 4 weeks	10.0%	[161]

[149, 150], and researchers are working to develop the phytochemicals based on conventional, safe, and effective dose formulations via the clinical studies. Some of the important bioactive components of antiobesity preclinical screening details are discussed in Table 4.

7. Clinical Studies: Translational Potential of Natural Products from Bench to Bedside

There are very limited clinical studies reported on the antiobesogenic activity of numerous herbal plant extracts and their active phytochemicals. Hydroxyl citric acid isolated from the herbal plant *Garcinia cambogia* has been reported to have potent lipogenesis and ATP citrate lyase inhibitor activity and decreased serum triglyceride in obese women [162]. Isolated natural phytoconstituent curcumin from *Curcuma longa*, polyphenols from *Salacia oblonga*, terpenoids from *Embllica officinalis* exposed to have hypolipidemic, blood glucose-lowering, and antioxidant activity in diabetic and obese patients during the clinical studies [163]. Herbal tea extract of *Salacia oblonga* has the potential to improve the lipid profile and decrease fasting blood glucose and HbA1c levels in obese and diabetic patients [164]. Crude extract of *Portulaca oleracea* L. seeds also has a significant role in ameliorating lipid profiles in obese adolescents [165]. *Hibiscus sabdariffa* plant extract is stated to decrease the body weight, BMI, body fat, and waist-to-hip ratio in clinical studies with a BMI of ≥ 27 and aged 18–65 [166]. Dietary supplement with *Phaseolus vulgaris* extracts was also reported to have the α -amylase-inhibiting activity, which significantly reduced the body weight, fat mass, and waist/hip perimeters [167]. The antiobesity mechanisms reported for *C. annuum*, in which the effect on fat oxidation was observed, are due to the stimulation of catecholamine secretion, promoting energy expenditure and reducing the accumulation of body fat mass [168]. In the catechines class, green tea and coffee were also reported for the significant reduction of body weight and maintenance of the body weight in average condition. *Sorghum bicolor* L. has been demonstrated to be a worthy substitute to control obesity in weighty men because it reduces body fat fraction and

amplifies daily carbohydrate and dietary fiber consumption when compared to wheat consumption [169]. Nowadays, people are having a great interest in herbal plant compositions or phytochemicals due to safer and efficacious effects, and the clinical studies must not be limited to *in vitro* or *in vivo* levels for their development.

8. Conclusions and Current and Future Inclinations on Biogenic Antiobesity Agents

Obesity is a multifaceted, long-lasting disorder triggered by an interaction of causative aspects such as lifestyle, dietary pattern, and environmental and genetic factors [140]. Healthy lifestyle and behavioral interventions are the main aspects of body weight loss and natural product-based treatment is more beneficial than synthesized molecules-based treatment in terms of toxicity [139–142]. Natural product-based molecules are also more beneficial in hyperlipidaemic activities, antidiabetic, cancer due to obesity, and hypercholesteremia [141, 142]. It is indeed that natural product-based molecules will provide the new and more appropriate platform for antiobesity treatment.

Abbreviations

JAK:	Janus kinase
STAT:	Signal transducer and activator of transcription
SH2:	Src homology 2
SOCS:	Suppression of cytokine signaling
PTP:	Protein tyrosine phosphatase
POMC:	Proopiomelanocortin
NPY:	Neuropeptide Y
CART:	Cocaine- and amphetamine-related transcript
MSH:	Melanocyte stimulating hormone
AgRP:	Agouti-related protein
MC4R:	Melanocortin 4 receptor
CGRP:	Calcitonin gene-related protein
BAT:	Brown adipose tissue
WAT:	White adipose tissue
GWAS:	Genome-wide association studies
FTO:	Fat mass and obesity

EDC:	Endocrine disrupting chemicals
C/EBP:	CCAAT enhancer binding protein
PPAR:	Peroxisome proliferator-activated receptor
US-FDA:	U.S. Food and Drug Administration
UCP:	Uncoupling protein
SREBP:	Sterol regulatory element binding protein
MUFA:	Monounsaturated fatty acid
PUFA:	Polyunsaturated fatty acid
EPA:	Eicosapentaenoic acid
DHA:	Docosahexaenoic acid
DPA:	Docosapentaenoic acid
DF:	Dietary fibers
SDF:	Soluble dietary fiber
IDF:	Insoluble dietary fiber
SCFAs:	Short-chain fatty acids
HPD:	High-protein diet.

Data Availability

All the key information is already available in the manuscript. Still, the authors are ready to share the raw data if the proper channel for the inquiry will be followed which will be routed through journal and affiliation authorities.

Conflicts of Interest

The authors declare that there are no conflicts of interest.

Acknowledgments

The authors would like to thank Amity University, Rajasthan, for providing the needful platform to write this important review paper.

References

- [1] A. Waxman, "WHO global strategy on diet, physical activity and health," *Food and Nutrition Bulletin*, vol. 25, no. 3, pp. 292–302, 2004.
- [2] R. Mopuri and M. S. Islam, "Medicinal plants and phytochemicals with anti-obesogenic potentials: a review," *Bio-medicine & Pharmacotherapy*, vol. 89, pp. 1442–1452, 2017.
- [3] C. Willyard, "Heritability: the family roots of obesity," *Nature*, vol. 508, no. 7496, pp. S58–S60, 2014.
- [4] A. Hruby and F. B. Hu, "The epidemiology of obesity: a big picture," *PharmacoEconomics*, vol. 33, no. 7, pp. 673–689, 2015.
- [5] A. Bhadoria, K. Sahoo, B. Sahoo, A. Choudhury, N. Sofi, and R. Kumar, "Childhood obesity: causes and consequences," *Journal of Family Medicine and Primary Care*, vol. 4, no. 2, pp. 187–192, 2015.
- [6] K. D. Hall, S. B. Heymsfield, J. W. Kemnitz, S. Klein, D. A. Schoeller, and J. R. Speakman, "Energy balance and its components: implications for body weight regulation," *The American Journal of Clinical Nutrition*, vol. 95, no. 4, pp. 989–994, 2012.
- [7] J. O. Hill, H. R. Wyatt, and J. C. Peters, "Energy balance and obesity," *Circulation*, vol. 126, no. 1, pp. 126–132, 2012.
- [8] E. S. Van der Valk, M. Savas, and E. F. C. van Rossum, "Stress and obesity: are there more susceptible individuals?" *Current Obesity Reports*, vol. 7, no. 2, pp. 193–203, 2018.
- [9] F. W. Booth, C. K. Roberts, and M. J. Laye, "Lack of exercise is a major cause of chronic diseases," *Comprehensive Physiology*, vol. 2, no. 2, pp. 1143–1211, 2012.
- [10] G. Traversy and J.-P. Chaput, "Alcohol consumption and obesity: an update," *Current Obesity Reports*, vol. 4, no. 1, pp. 122–130, 2015.
- [11] Y. Milaneschi, W. K. Simmons, E. F. C. van Rossum, and B. W. Penninx, "Depression and obesity: evidence of shared biological mechanisms," *Molecular Psychiatry*, vol. 24, no. 1, pp. 18–33, 2019.
- [12] J. U. Weaver, "Classical endocrine diseases causing obesity," *Obesity and Metabolism*, vol. 36, pp. 212–228, 2008.
- [13] D. S. Ludwig, L. J. Aronne, A. Astrup et al., "The carbohydrate-insulin model: a physiological perspective on the obesity pandemic," *The American Journal of Clinical Nutrition*, vol. 114, no. 6, pp. 1873–1885, 2021.
- [14] S. M. Bahijri, L. Alsheikh, G. Ajabnoor, and A. Borai, "Effect of supplementation with chitosan on weight, cardiometabolic, and other risk indices in Wistar rats fed normal and high-fat/high-cholesterol diets ad libitum," *Nutrition and Metabolic Insights*, vol. 10, 2017.
- [15] S. Rayalam, M. Dellafera, and C. Baile, "Phytochemicals and regulation of the adipocyte life cycle," *The Journal of Nutritional Biochemistry*, vol. 19, no. 11, pp. 717–726, 2008.
- [16] Y. Panahi, M. S. Hosseini, N. Khalili, E. Naimi, M. Majeed, and A. Sahebkar, "Antioxidant and anti-inflammatory effects of curcuminoid-piperine combination in subjects with metabolic syndrome: a randomized controlled trial and an updated meta-analysis," *Clinical Nutrition*, vol. 34, no. 6, pp. 1101–1108, 2015.
- [17] J. Krzyzanowska, A. Czubacka, and W. Oleszek, "Dietary phytochemicals and human health," *Advances in Experimental Medicine & Biology*, vol. 698, pp. 74–98, 2010.
- [18] F. Dehghani Firouzabadi, A. Jayedi, E. Asgari et al., "The association of dietary phytochemical index with metabolic syndrome in adults," *Clinical Nutrition Research*, vol. 10, no. 2, pp. 161–171, 2021.
- [19] Z. Li, H. Jiang, H. Yan, X. Jiang, Y. Ma, and Y. Qin, "Carbon and nitrogen metabolism under nitrogen variation affects flavonoid accumulation in the leaves of *Coreopsis tinctoria*," *PeerJ*, vol. 9, Article ID e12152, 2021.
- [20] S. Wolfram, Y. Wang, and F. Thielecke, "Anti-obesity effects of green tea: from bedside to bench," *Molecular Nutrition & Food Research*, vol. 50, no. 2, pp. 176–187, 2006.
- [21] R. S. Karunakaran, O. Lokanatha, G. Muni Swamy et al., "Anti-obesity and lipid lowering activity of bauginiastatin-1 is mediated through PPAR- γ /AMPK expressions in diet-induced obese rat model," *Frontiers in Pharmacology*, vol. 12, Article ID 704074, 2021.
- [22] Y. Bustanji, I. M. Al-Masri, M. Mohammad et al., "Pancreatic lipase inhibition activity of trilactone terpenes of *Ginkgo biloba*," *Journal of Enzyme Inhibition and Medicinal Chemistry*, vol. 26, no. 4, pp. 453–459, 2011.
- [23] S. M. Rates, "Plants as source of drugs," *Toxicon*, vol. 39, no. 5, pp. 603–613, 2001.
- [24] H. Zhang, S. Yan, B. Khambu et al., "Dynamic mTORC1-TFEB feedback signaling regulates hepatic autophagy, steatosis and liver injury in long-term nutrient oversupply," *Autophagy*, vol. 14, no. 10, pp. 1779–1795, 2018.
- [25] A. E. Pollard and D. Carling, "Thermogenic adipocytes: lineage, function and therapeutic potential," *Biochemical Journal*, vol. 477, no. 11, pp. 2071–2093, 2020.
- [26] T. Gao, D. Ma, S. Chen, X. Zhang, Y. Han, and M. Liu, "Acupuncture for the treatment of leptin resistance in

- obesity: a protocol for systematic review and meta-analysis," *Medicine*, vol. 100, no. 28, Article ID e26244, 2021.
- [27] K. Timper and J. C. Brüning, "Hypothalamic circuits regulating appetite and energy homeostasis: pathways to obesity," *Disease Models & Mechanisms*, vol. 10, no. 6, pp. 679–689, 2017.
- [28] R. S. Ahima and D. A. Antwi, "Brain regulation of appetite and satiety," *Endocrinology and Metabolism Clinics of North America*, vol. 37, no. 4, pp. 811–823, 2008.
- [29] R. D. Palmiter, "The parabrachial nucleus: CGRP neurons function as a general alarm," *Trends in Neurosciences*, vol. 41, no. 5, pp. 280–293, 2018.
- [30] J. L. Trevaskis and A. A. Butler, "Double leptin and melanocortin-4 receptor gene mutations have an additive effect on fat mass and are associated with reduced effects of leptin on weight loss and food intake," *Endocrinology*, vol. 146, no. 10, pp. 4257–4265, 2005.
- [31] S. Khoury, V. Gudziol, S. Grégoire et al., "Lipidomic profile of human nasal mucosa and associations with circulating fatty acids and olfactory deficiency," *Scientific Reports*, vol. 11, no. 1, Article ID 16771, 2021.
- [32] M. A. McArdle, O. M. Finucane, R. M. Connaughton, A. M. McMorrow, and H. M. Roche, "Mechanisms of obesity-induced inflammation and insulin resistance: insights into the emerging role of nutritional strategies," *Frontiers in Endocrinology*, vol. 4, p. 52, 2013.
- [33] U. Galicia-Garcia, A. Benito-Vicente, S. Jebari et al., "Pathophysiology of type 2 diabetes mellitus," *International Journal of Molecular Sciences*, vol. 21, no. 17, p. 6275, 2020.
- [34] A. Algoblan, M. Alalfi, and M. Khan, "Mechanism linking diabetes mellitus and obesity," *Diabetes, Metabolic Syndrome and Obesity: Targets and Therapy*, vol. 7, pp. 587–591, 2014.
- [35] E. Bousoik and H. Montazeri Aliabadi, "Do we know jack about JAK? a closer look at JAK/STAT signaling pathway," *Frontiers in Oncology*, vol. 8, p. 287, 2018.
- [36] S.-A. Manea, A. Manea, and C. Heltianu, "Inhibition of JAK/STAT signaling pathway prevents high-glucose-induced increase in endothelin-1 synthesis in human endothelial cells," *Cell and Tissue Research*, vol. 340, no. 1, pp. 71–79, 2010.
- [37] M. S. Poetsch, A. Strano, and K. Guan, "Role of leptin in cardiovascular diseases," *Frontiers in Endocrinology*, vol. 11, p. 354, 2020.
- [38] M. Thon, T. Hosoi, and K. Ozawa, "Possible integrative actions of leptin and insulin signaling in the hypothalamus targeting energy homeostasis," *Frontiers in Endocrinology*, vol. 7, p. 138, 2016.
- [39] L. Xu, H. Li, G. Zhou et al., "DNA-binding activity of STAT3 increased in hypothalamus of DIO mice; the reduction of STAT3 phosphorylation may facilitate leptin signaling," *Biochemical and Biophysical Research Communications*, vol. 505, no. 1, pp. 229–235, 2018, [doi:].
- [40] A. M. Ramos-Lobo and J. Donato Jr., "The role of leptin in health and disease," *Temperature*, vol. 4, no. 3, pp. 258–291, 2017.
- [41] T. Boswell and I. C. Dunn, "Regulation of agouti-related protein and pro-opiomelanocortin gene expression in the avian arcuate nucleus," *Frontiers in Endocrinology*, vol. 8, p. 75, 2017.
- [42] M. Desai, M. G. Ferrini, G. Han, K. Narwani, and M. G. Ross, "Maternal high fat diet programs male mice offspring hyperphagia and obesity: mechanism of increased appetite neurons via altered neurogenic factors and nutrient sensor AMPK," *Nutrients*, vol. 12, no. 11, p. 3326, 2020.
- [43] B. Bradford and R. Maude, "Fetal response to maternal hunger and satiation - novel finding from a qualitative descriptive study of maternal perception of fetal movements," *BMC Pregnancy and Childbirth*, vol. 14, no. 1, p. 288, 2014.
- [44] R. Acín-Perez, A. Petcherski, M. Veliova et al., "Recruitment and remodeling of peridroplet mitochondria in human adipose tissue," *Redox Biology*, vol. 46, Article ID 102087, 2021.
- [45] J. R. Speakman, "A nonadaptive scenario explaining the genetic predisposition to obesity: the "predation release" hypothesis," *Cell Metabolism*, vol. 6, no. 1, pp. 5–12, 2007, [doi:].
- [46] K. Wang, W.-D. Li, C. K. Zhang et al., "A genome-wide association study on obesity and obesity-related traits," *PLoS One*, vol. 6, no. 4, Article ID e18939, 2011.
- [47] P. R. Shewry and S. J. Hey, "Do we need to worry about eating wheat?" *Nutrition Bulletin*, vol. 41, no. 1, pp. 6–13, 2016.
- [48] K. A. Fawcett and I. Barroso, "The genetics of obesity: FTO leads the way," *Trends in Genetics*, vol. 26, no. 6, pp. 266–274, 2010, [doi:].
- [49] S. Li, M. Chen, Y. Li, and T. O. Tollefsbol, "Prenatal epigenetics diets play protective roles against environmental pollution," *Clinical Epigenetics*, vol. 11, no. 1, p. 82, 2019.
- [50] P. E. Panchenko, S. Voisin, M. Jouin et al., "Expression of epigenetic machinery genes is sensitive to maternal obesity and weight loss in relation to fetal growth in mice," *Clinical Epigenetics*, vol. 8, no. 1, p. 22, 2016.
- [51] S. D. Parlee and O. A. MacDougald, "Maternal nutrition and risk of obesity in offspring: the Trojan horse of developmental plasticity," *Biochimica et Biophysica Acta - Molecular Basis of Disease*, vol. 1842, no. 3, pp. 495–506, 2014.
- [52] R. Raab, S. Michel, J. Günther, J. Hoffmann, L. Stecher, and H. Hauner, "Associations between lifestyle interventions during pregnancy and childhood weight and growth: a systematic review and meta-analysis," *International Journal of Behavioral Nutrition and Physical Activity*, vol. 18, no. 1, p. 8, 2021.
- [53] M. A. Stanislawski, D. Dabelea, L. A. Lange, B. D. Wagner, and C. A. Lozupone, "Gut microbiota phenotypes of obesity," *npj Biofilms and Microbiomes*, vol. 5, no. 1, p. 18, 2019.
- [54] M. Coelho, T. Oliveira, and R. Fernandes, "State of the art paper Biochemistry of adipose tissue: an endocrine organ," *Archives of Medical Science*, vol. 2, no. 2, pp. 191–200, 2013.
- [55] L. Liu, P. Li, Y. Liu, and Y. Zhang, "Efficacy of probiotics and synbiotics in patients with nonalcoholic fatty liver disease: a meta-analysis," *Digestive Diseases and Sciences*, vol. 64, no. 12, pp. 3402–3412, 2019.
- [56] B. A. Ference, J. J. P. Kastelein, and A. L. Catapano, "Lipids and lipoproteins in 2020," *JAMA*, vol. 324, no. 6, pp. 595–596, 2020.
- [57] M. Alves-Bezerra and D. E. Cohen, "Triglyceride metabolism in the liver," *Comprehensive Physiology*, vol. 8, no. 1, pp. 1–22, 2017.
- [58] M. Longo, F. Zatterale, J. Naderi et al., "Adipose tissue dysfunction as determinant of obesity-associated metabolic complications," *International Journal of Molecular Sciences*, vol. 20, no. 9, p. 2358, 2019.
- [59] M. S. Burhans, D. K. Hagman, J. N. Kuzma, K. A. Schmidt, and M. Kratz, "Contribution of adipose tissue inflammation to the development of type 2 diabetes mellitus," *Comprehensive Physiology*, vol. 9, no. 1, pp. 1–58, 2018.

- [60] A. Achari and S. Jain, "Adiponectin, a therapeutic target for obesity, diabetes, and endothelial dysfunction," *International Journal of Molecular Sciences*, vol. 18, no. 6, p. 1321, 2017.
- [61] G. Tarantino, V. Citro, and D. Capone, "Nonalcoholic fatty liver disease: a challenge from mechanisms to therapy," *Journal of Clinical Medicine*, vol. 9, no. 1, p. 15, 2019.
- [62] E. Fabbrini, S. Sullivan, and S. Klein, "Obesity and nonalcoholic fatty liver disease: biochemical, metabolic, and clinical implications," *Hepatology*, vol. 51, no. 2, pp. 679–689, 2010.
- [63] Y.-L. Cho, J.-K. Min, K. M. Roh et al., "Phosphoprotein phosphatase 1CB (PPP1CB), a novel adipogenic activator, promotes 3T3-L1 adipogenesis," *Biochemical and Biophysical Research Communications*, vol. 467, no. 2, pp. 211–217, 2015.
- [64] Y. Zuo, L. Qiang, and S. R. Farmer, "Activation of CCAAT/Enhancer-binding protein (C/EBP) α expression by C/EBP β during adipogenesis requires a peroxisome proliferator-activated receptor- γ -associated repression of HDAC1 at the C/ebp α gene promoter," *Journal of Biological Chemistry*, vol. 281, no. 12, pp. 7960–7967, 2006.
- [65] N. Stefan, A. L. Birkenfeld, and M. B. Schulze, "Global pandemics interconnected - obesity, impaired metabolic health and COVID-19," *Nature Reviews Endocrinology*, vol. 17, no. 3, pp. 135–149, 2021.
- [66] H. M. Nagy, M. Paar, C. Heier et al., "Adipose triglyceride lipase activity is inhibited by long-chain acyl-coenzyme A," *Biochimica et Biophysica Acta (BBA) - Molecular and Cell Biology of Lipids*, vol. 1841, no. 4, pp. 588–594, 2014.
- [67] R. J. A. Wanders, H. R. Waterham, and S. Ferdinandusse, "Metabolic interplay between peroxisomes and other subcellular organelles including mitochondria and the endoplasmic reticulum," *Frontiers in Cell and Developmental Biology*, vol. 3, p. 83, 2016.
- [68] W. P. T. James, "The epidemiology of obesity: the size of the problem," *Journal of Internal Medicine*, vol. 263, no. 4, pp. 336–352, 2008.
- [69] H. S. Park, C. Y. Park, S. W. Oh, and H. J. Yoo, "Prevalence of obesity and metabolic syndrome in Korean adults," *Obesity Reviews*, vol. 9, no. 2, pp. 104–107, 2008.
- [70] H. M. Connolly, J. L. Crary, M. D. McGoon et al., "Valvular heart disease associated with fenfluramine-phentermine," *New England Journal of Medicine*, vol. 337, no. 9, pp. 581–588, 1997.
- [71] G. Glazer, "Long-term pharmacotherapy of obesity 2000: a review of efficacy and safety," *Archives of Internal Medicine*, vol. 161, no. 15, pp. 1814–1824, 2001.
- [72] M. MacMillan, K. Cummins, and K. Fujioka, "What weight loss treatment options do geriatric patients with overweight and obesity want to consider?" *Obesity Science & Practice*, vol. 2, no. 4, pp. 477–482, 2016.
- [73] W. P. T. James, I. D. Caterson, W. Coutinho et al., "Effect of sibutramine on cardiovascular outcomes in overweight and obese subjects," *New England Journal of Medicine*, vol. 363, no. 10, pp. 905–917, 2010.
- [74] A. K. Singh and R. Singh, "Pharmacotherapy in obesity: a systematic review and meta-analysis of randomized controlled trials of anti-obesity drugs," *Expert Review of Clinical Pharmacology*, vol. 13, no. 1, pp. 53–64, 2020.
- [75] L. Bahia, C. W. Schaan, K. Sparrenberger et al., "Overview of meta-analysis on prevention and treatment of childhood obesity," *Jornal de Pediatria*, vol. 95, no. 4, pp. 385–400, 2019.
- [76] C. Haddock, W. Poston, P. Dill, J. Foreyt, and M. Ericsson, "Pharmacotherapy for obesity: a quantitative analysis of four decades of published randomized clinical trials," *International Journal of Obesity*, vol. 26, no. 2, pp. 262–273, 2002.
- [77] K. S. Czepiel, N. P. Perez, K. J. Campoverde Reyes, S. Sabharwal, and F. C. Stanford, "Pharmacotherapy for the treatment of overweight and obesity in children, adolescents, and young adults in a large health system in the US," *Frontiers in Endocrinology*, vol. 11, p. 290, 2020.
- [78] P. Ghali and K. D. Lindor, "Hepatotoxicity of drugs used for treatment of obesity and its comorbidities," *Seminars in Liver Disease*, vol. 24, no. 04, pp. 389–397, 2004.
- [79] E. X. Zheng and V. J. Navarro, "Liver injury from herbal, dietary, and weight loss supplements: a review," *Journal of Clinical and Translational Hepatology*, vol. 3, no. 2, pp. 93–98, 2015.
- [80] G. Tarantino, M. G. Pezzullo, M. N. D. d. Minno et al., "Drug-induced liver injury due to "natural products" used for weight loss: a case report," *World Journal of Gastroenterology*, vol. 15, no. 19, pp. 2414–2417, 2009.
- [81] B. Cannon and J. Nedergaard, "Brown adipose tissue: function and physiological significance," *Physiological Reviews*, vol. 84, no. 1, pp. 277–359, 2004.
- [82] A. D. Flouris, P. C. Dinas, A. Valente, C. M. B. Andrade, N. H. Kawashita, and P. Sakellariou, "Exercise-induced effects on UCP1 expression in classical brown adipose tissue: a systematic review," *Hormone Molecular Biology and Clinical Investigation*, vol. 31, no. 2, 2017.
- [83] H. El Hadi, A. Di Vincenzo, R. Vettor, and M. Rossato, "Food ingredients involved in white-to-Brown adipose tissue conversion and in calorie burning," *Frontiers in Physiology*, vol. 9, p. 1954, 2019.
- [84] X. Zhang, X. Li, H. Fang et al., "Flavonoids as inducers of white adipose tissue browning and thermogenesis: signalling pathways and molecular triggers," *Nutrition and Metabolism*, vol. 16, no. 1, p. 47, 2019.
- [85] K. S. de Fluiter, G. F. Kerkhof, I. A. L. P. van Beijsterveldt et al., "Appetite-regulating hormone trajectories and relationships with fat mass development in term-born infants during the first 6 months of life," *European Journal of Nutrition*, vol. 60, no. 7, pp. 3717–3725, 2021.
- [86] L. M. Holsen, C. R. Savage, L. E. Martin et al., "Importance of reward and prefrontal circuitry in hunger and satiety: prader-Willi syndrome vs simple obesity," *International Journal of Obesity*, vol. 36, no. 5, pp. 638–647, 2012.
- [87] T. Su, C. Huang, C. Yang et al., "Apigenin inhibits STAT3/CD36 signaling axis and reduces visceral obesity," *Pharmacological Research*, vol. 152, Article ID 104586, 2020.
- [88] A. E. Valsecchi, S. Franchi, A. E. Panerai, A. Rossi, P. Sacerdote, and M. Colleoni, "The soy isoflavone genistein reverses oxidative and inflammatory state, neuropathic pain, neurotrophic and vasculature deficits in diabetes mouse model," *European Journal of Pharmacology*, vol. 650, no. 2-3, pp. 694–702, 2011.
- [89] S.-M. Lim, H. S. Lee, J. I. Jung et al., "Cyanidin-3-O-galactoside-enriched Aronia melanocarpa extract attenuates weight gain and adipogenic pathways in high-fat diet-induced obese C57BL/6 mice," *Nutrients*, vol. 11, no. 5, p. 1190, 2019.
- [90] S. Tucci, E. J. Boyland, and J. C. Halford, "The role of lipid and carbohydrate digestive enzyme inhibitors in the management of obesity: a review of current and emerging therapeutic agents," *Diabetes, Metabolic Syndrome and Obesity: Targets and Therapy*, vol. 3, pp. 125–143, 2010.

- [91] G. Hu, D. Liu, H. Tong, W. Huang, Y. Hu, and Y. Huang, "Lipoprotein-associated phospholipase A2 activity and mass as independent risk factor of stroke: a meta-analysis," *BioMed Research International*, vol. 2019, pp. 1–11, 2019.
- [92] N. A. Lunagariya, N. K. Patel, S. C. Jagtap, and K. K. Bhutani, "Inhibitors of pancreatic lipase: state of the art and clinical perspectives," *EXCLI journal*, vol. 13, pp. 897–921, 2014.
- [93] F. Pietrocola, L. Galluzzi, J. M. Bravo-San Pedro, F. Madeo, and G. Kroemer, "Acetyl coenzyme A: a central metabolite and second messenger," *Cell Metabolism*, vol. 21, no. 6, pp. 805–821, 2015.
- [94] S. Kumar and A. K. Pandey, "Chemistry and biological activities of flavonoids: an overview," *The Scientific World Journal*, vol. 2013, pp. 1–16, 2013.
- [95] C. Proença, M. Freitas, D. Ribeiro et al., "Evaluation of a flavonoids library for inhibition of pancreatic α -amylase towards a structure-activity relationship," *Journal of Enzyme Inhibition and Medicinal Chemistry*, vol. 34, no. 1, pp. 577–588, 2019.
- [96] T. Hishida, M. Nishizuka, S. Osada, and M. Imagawa, "The role of C/EBPdelta in the early stages of adipogenesis," *Biochimie*, vol. 91, no. 5, pp. 654–657, 2009.
- [97] X. Zhao and F. Yang, "Regulation of SREBP-mediated gene expression," *Acta Biophysica Sinica*, vol. 28, no. 4, pp. 287–294, 2012.
- [98] X.-L. Qiu and Q.-F. Zhang, "Chemical profile and pancreatic lipase inhibitory activity of *Sinobambusa tootsik* (Sieb.) Makino leaves," *PeerJ*, vol. 7, 2019.
- [99] J.-Y. Yang, M. A. Della-Fera, and C. A. Baile, "Guggulsterone inhibits adipocyte differentiation and induces apoptosis in 3T3-L1 cells," *Obesity*, vol. 16, no. 1, pp. 16–22, 2008.
- [100] Y. R. Choi, J. Shim, and M. J. Kim, "Genistin: a novel potent anti-adipogenic and anti-lipogenic agent," *Molecules*, vol. 25, no. 9, p. 2042, 2020.
- [101] M. Khalilpourfarshbafi, K. Gholami, D. D. Murugan, M. Z. Abdul Sattar, and N. A. Abdullah, "Differential effects of dietary flavonoids on adipogenesis," *European Journal of Nutrition*, vol. 58, no. 1, pp. 5–25, 2019.
- [102] B. Ahmad, C. J. Serpell, I. L. Fong, and E. H. Wong, "Molecular mechanisms of adipogenesis: the anti-adipogenic role of AMP-activated protein kinase," *Frontiers in Molecular Biosciences*, vol. 7, p. 76, 2020.
- [103] S. Patel, W. Yang, K. Kozusko, V. Saudek, and D. B. Savage, "Perilipins 2 and 3 lack a carboxy-terminal domain present in perilipin 1 involved in sequestering ABHD5 and suppressing basal lipolysis," *Proceedings of the National Academy of Sciences*, vol. 111, no. 25, pp. 9163–9168, 2014.
- [104] M.-H. Kim, J.-S. Park, M.-S. Seo, J.-W. Jung, Y.-S. Lee, and K.-S. Kang, "Genistein and daidzein repress adipogenic differentiation of human adipose tissue-derived mesenchymal stem cells via Wnt/ β -catenin signalling or lipolysis," *Cell Proliferation*, vol. 43, no. 6, pp. 594–605, 2010.
- [105] T. Li, X. Li, H. Meng, L. Chen, and F. Meng, "ACSL1 affects triglyceride levels through the PPAR γ pathway," *International Journal of Medical Sciences*, vol. 17, no. 6, pp. 720–727, 2020.
- [106] S. Gómez-Zorita, A. Lasa, N. Abendaño et al., "Phenolic compounds apigenin, hesperidin and kaempferol reduce in vitro lipid accumulation in human adipocytes," *Journal of Translational Medicine*, vol. 15, no. 1, p. 237, 2017.
- [107] Y. Xu, M. Zhang, T. Wu, S. Dai, J. Xu, and Z. Zhou, "The anti-obesity effect of green tea polysaccharides, polyphenols and caffeine in rats fed with a high-fat diet," *Food & Function*, vol. 6, no. 1, pp. 296–303, 2015.
- [108] M. Konstantinidi and A. E. Koutelidakis, "Functional foods and bioactive compounds: a review of its possible role on weight management and obesity's metabolic consequences," *Medicines*, vol. 6, no. 3, p. 94, 2019.
- [109] S. D'Angelo, M. L. Motti, and R. Meccariello, " ω -3 and ω -6 polyunsaturated fatty acids, obesity and cancer," *Nutrients*, vol. 12, no. 9, p. 2751, 2020.
- [110] A. Bouyanfif, S. Jayarathne, I. Koboziev, and N. Moustaid-Moussa, "The Nematode *Caenorhabditis elegans* as a model organism to study metabolic effects of ω -3 polyunsaturated fatty acids in obesity," *Advances in Nutrition*, vol. 10, no. 1, pp. 165–178, 2019.
- [111] G. Astarita, J. H. McKenzie, B. Wang et al., "A protective lipidomic biosignature associated with a balanced omega-6/omega-3 ratio in fat-1 transgenic mice," *PLoS One*, vol. 9, no. 4, Article ID e96221, 2014.
- [112] M. C. W. Myhrstad, H. Tunsjø, C. Charnock, and V. H. Telle-Hansen, "Dietary fiber, gut microbiota, and metabolic regulation-current status in human randomized trials," *Nutrients*, vol. 12, no. 3, p. 859, 2020.
- [113] S. Chang, X. Cui, M. Guo et al., "Insoluble dietary fiber from pear pomace can prevent high-fat diet-induced obesity in rats mainly by improving the structure of the gut microbiota," *Journal of Microbiology and Biotechnology*, vol. 27, no. 4, pp. 856–867, 2017.
- [114] E. Jovanovski, N. Mazhar, A. Komishon et al., "Effect of viscous fiber supplementation on obesity indicators in individuals consuming calorie-restricted diets: a systematic review and meta-analysis of randomized controlled trials," *European Journal of Nutrition*, vol. 60, no. 1, pp. 101–112, 2021.
- [115] J. E. Drew, N. Reichardt, L. M. Williams et al., "Dietary fibers inhibit obesity in mice, but host responses in the cecum and liver appear unrelated to fiber-specific changes in cecal bacterial taxonomic composition," *Scientific Reports*, vol. 8, no. 1, Article ID 15566, 2018.
- [116] L. Kjølbæk, L. B. Sørensen, N. B. Søndergaard et al., "Protein supplements after weight loss do not improve weight maintenance compared with recommended dietary protein intake despite beneficial effects on appetite sensation and energy expenditure: a randomized, controlled, double-blinded trial," *The American Journal of Clinical Nutrition*, vol. 106, no. 2, pp. 684–697, 2017.
- [117] J. Moon and G. Koh, "Clinical evidence and mechanisms of high-protein diet-induced weight loss," *Journal of Obesity & Metabolic Syndrome*, vol. 29, no. 3, pp. 166–173, 2020.
- [118] H. Alomaim, P. Griffin, E. Swist et al., "Dietary calcium affects body composition and lipid metabolism in rats," *PLoS One*, vol. 14, no. 1, Article ID e0210760, 2019.
- [119] P. Li, X. Chang, X. Fan et al., "Dietary calcium status during maternal pregnancy and lactation affects lipid metabolism in mouse offspring," *Scientific Reports*, vol. 8, no. 1, Article ID 16542, 2018.
- [120] O. Sadeghi, A. H. Keshteli, F. Doostan, A. Esmailzadeh, and P. Adibi, "Association between dairy consumption, dietary calcium intake and general and abdominal obesity among Iranian adults," *Diabetes & Metabolic Syndrome: Clinical Research Reviews*, vol. 12, no. 5, pp. 769–775, 2018, [doi:..
- [121] J. Y. Hong, J. S. Lee, H. W. Woo, A. S. Om, C. K. Kwock, and M. K. Kim, "Meta-analysis of randomized controlled trials on calcium supplements and dairy products for changes in body weight and obesity indices," *International Journal of Food Sciences & Nutrition*, vol. 72, no. 5, pp. 615–631, 2021.

- [122] J. Z. Ilich, O. J. Kelly, P.-Y. Liu et al., "Role of calcium and low-fat dairy foods in weight-loss outcomes revisited: results from the randomized trial of effects on bone and body composition in overweight/obese postmenopausal women," *Nutrients*, vol. 11, no. 5, p. 1157, 2019.
- [123] F. De Filippis, L. Paparo, R. Nocerino et al., "Specific gut microbiome signatures and the associated pro-inflammatory functions are linked to pediatric allergy and acquisition of immune tolerance," *Nature Communications*, vol. 12, no. 1, p. 5958, 2021.
- [124] S. M. Harakeh, I. Khan, T. Kumosani et al., "Gut microbiota: a contributing factor to obesity," *Frontiers in Cellular and Infection Microbiology*, vol. 6, p. 95, 2016.
- [125] A. Aoun, F. Darwish, and N. Hamod, "The influence of the gut microbiome on obesity in adults and the role of probiotics, prebiotics, and synbiotics for weight loss," *Preventive Nutrition and Food Science*, vol. 25, no. 2, pp. 113–123, 2020.
- [126] P. De Marco, A. C. Henriques, R. Azevedo et al., "Gut microbiome composition and metabolic status are differently affected by early exposure to unhealthy diets in a rat model," *Nutrients*, vol. 13, no. 9, p. 3236, 2021.
- [127] Z. Y. Kho and S. K. Lal, "The human gut microbiome - a potential controller of wellness and disease," *Frontiers in Microbiology*, vol. 9, p. 1835, 2018.
- [128] E. M. Dewulf, P. D. Cani, A. M. Neyrinck et al., "Inulin-type fructans with prebiotic properties counteract GPR43 overexpression and PPAR γ -related adipogenesis in the white adipose tissue of high-fat diet-fed mice," *The Journal of Nutritional Biochemistry*, vol. 22, no. 8, pp. 712–722, 2011.
- [129] C. I. Gamboa-Gómez, N. E. Rocha-Guzmán, J. A. Gallegos-Infante, M. R. Moreno-Jiménez, B. D. Vázquez-Cabral, and R. F. González-Laredo, "Plants with potential use on obesity and its complications," *EXCLI J*, vol. 14, pp. 809–831, 2015.
- [130] M. B. Shehadeh, G. A. R. Y. Suaifan, and A. M. Abu-Odeh, "Plants secondary metabolites as blood glucose-lowering molecules," *Molecules*, vol. 26, no. 14, p. 4333, 2021.
- [131] M. González-Castejón and A. Rodríguez-Casado, "Dietary phytochemicals and their potential effects on obesity: a review," *Pharmacological Research*, vol. 64, no. 5, pp. 438–455, 2011.
- [132] M. García-Barrado, M. Iglesias-Osma, E. Pérez-García et al., "Role of flavonoids in the interactions among obesity, inflammation, and autophagy," *Pharmaceuticals*, vol. 13, no. 11, p. 342, 2020.
- [133] J. Park, H. L. Kim, Y. Jung, K. S. Ahn, H. J. Kwak, and J. Y. Um, "Bitter orange (*Citrus aurantium* linné) improves obesity by regulating adipogenesis and thermogenesis through AMPK activation," *Nutrients*, vol. 11, no. 9, p. 1988, 2019.
- [134] C.-L. Hsu and G.-C. Yen, "Induction of cell apoptosis in 3T3-L1 pre-adipocytes by flavonoids is associated with their antioxidant activity," *Molecular Nutrition & Food Research*, vol. 50, no. 11, pp. 1072–1079, 2006.
- [135] D. J. García-Martínez, M. Arroyo-Hernández, M. Posada-Ayala, and C. Santos, "The high content of quercetin and catechin in airen grape juice supports its application in functional food production," *Foods*, vol. 10, no. 7, p. 1532, 2021.
- [136] S. Ghosh, S. Manchala, M. Raghunath, G. Sharma, A. K. Singh, and J. K. Sinha, "Role of phytomolecules in the treatment of obesity: targets, mechanisms and limitations," *Current Topics in Medicinal Chemistry*, vol. 21, no. 10, pp. 863–877, 2021.
- [137] E. Thom, "The effect of chlorogenic acid enriched coffee on glucose absorption in healthy volunteers and its effect on body mass when used long-term in overweight and obese people," *Journal of International Medical Research*, vol. 35, no. 6, pp. 900–908, 2007.
- [138] T. Soifoini, D. Donno, V. Jeannoda et al., "Phytochemical composition, antibacterial activity, and antioxidant properties of the artocarpus altilis fruits to promote their consumption in the Comoros islands as potential health-promoting food or a source of bioactive molecules for the food industry," *Foods*, vol. 10, no. 9, p. 2136, 2021.
- [139] S. Nobili, D. Lippi, E. Witort et al., "Natural compounds for cancer treatment and prevention," *Pharmacological Research*, vol. 59, no. 6, pp. 365–378, 2009, [doi].
- [140] M. Jin Son, C. Rico, S. Hyun Nam, and M. Young Kang, "Influence of oryzanol and ferulic Acid on the lipid metabolism and antioxidative status in high fat-fed mice," *Journal of Clinical Biochemistry & Nutrition*, vol. 46, no. 2, pp. 150–156, 2010.
- [141] T. S. de Melo, P. R. Lima, K. M. M. B. Carvalho et al., "Ferulic acid lowers body weight and visceral fat accumulation via modulation of enzymatic, hormonal and inflammatory changes in a mouse model of high-fat diet-induced obesity," *Brazilian Journal of Medical and Biological Research*, vol. 50, no. 1, Article ID e5630, 2017.
- [142] A. Salehi-Sahlabadi, H. K. Varkaneh, F. Shahdadian et al., "Effects of Phytosterols supplementation on blood glucose, glycosylated hemoglobin (HbA1c) and insulin levels in humans: a systematic review and meta-analysis of randomized controlled trials," *Journal of Diabetes and Metabolic Disorders*, vol. 19, no. 1, pp. 625–632, 2020.
- [143] A. Berger, P. J. Jones, and S. S. Abumweis, "Plant sterols: factors affecting their efficacy and safety as functional food ingredients," *Lipids in Health and Disease*, vol. 3, no. 1, pp. 3–5, 2004.
- [144] M. C. Izar, D. M. Tegani, S. H. Kasma, and F. A. Fonseca, "Phytosterols and phytosterolemia: gene-diet interactions," *Genes & Nutrition*, vol. 6, no. 1, pp. 17–26, 2011.
- [145] M. Payab, S. Hasani-Ranjbar, N. Shahbal et al., "Effect of the herbal medicines in obesity and metabolic syndrome: a systematic review and meta-analysis of clinical trials," *Phytotherapy Research*, vol. 34, no. 3, pp. 526–545, 2020.
- [146] I. Romieu, L. Dossus, L. Dossus et al., "Energy balance and obesity: what are the main drivers?" *Cancer Causes & Control*, vol. 28, no. 3, pp. 247–258, 2017.
- [147] J. Zheng, S. Zheng, Q. Feng, Q. Zhang, and X. Xiao, "Dietary capsaicin and its anti-obesity potency: from mechanism to clinical implications," *Bioscience Reports*, vol. 37, no. 3, Article ID BSR20170286, 2017.
- [148] L. Carrera-Quintanar, R. I. López Roa, S. Quintero-Fabián, M. A. Sánchez-Sánchez, B. Vizmanos, and D. Ortuño-Sahagún, "Phytochemicals that influence gut microbiota as prophylactics and for the treatment of obesity and inflammatory diseases," *Mediators of Inflammation*, vol. 2018, pp. 1–18, 2018.
- [149] G. Tarantino, C. Balsano, S. J. Santini et al., "It is high time physicians thought of natural products for alleviating NAFLD. Is there sufficient evidence to use them?" *International Journal of Molecular Sciences*, vol. 22, no. 24, Article ID 13424, 2021.
- [150] T. M. do Moinho, S. L. Matos, and C. R. O. Carvalho, "A comprehensive review on phytochemicals for fatty liver: are they potential adjuvants?" *Journal of Molecular Medicine*, 2022.

- [151] H. H. Lim, S. O. Lee, S. Y. Kim, S. J. Yang, and Y. Lim, "Anti-inflammatory and antiobesity effects of mulberry leaf and fruit extract on high fat diet-induced obesity," *Experimental Biology and Medicine*, vol. 238, no. 10, pp. 1160–1169, 2013.
- [152] J. H. Kim, O.-K. Kim, H.-G. Yoon et al., "Anti-obesity effect of extract from fermented *Curcuma longa* L. through regulation of adipogenesis and lipolysis pathway in high-fat diet-induced obese rats," *Food & Nutrition Research*, vol. 60, no. 1, Article ID 30428, 2016.
- [153] W. Xie, D. Gu, J. Li, K. Cui, and Y. Zhang, "Effects and action mechanisms of berberine and rhizoma coptidis on gut microbes and obesity in high-fat diet-fed c57bl/6j mice," *PLoS One*, vol. 6, no. 9, Article ID e24520, 2011.
- [154] J. I. Joo, D. H. Kim, J.-W. Choi, and J. W. Yun, "Proteomic analysis for antiobesity potential of capsaicin on white adipose tissue in rats fed with a high fat diet," *Journal of Proteome Research*, vol. 9, no. 6, pp. 2977–2987, 2010.
- [155] N. Ikarashi, T. Toda, T. Okaniwa, K. Ito, W. Ochiai, and K. Sugiyama, "Anti-obesity and anti-diabetic effects of acacia polyphenol in obese diabetic KKAY mice fed high-fat diet," *Evidence-based Complementary and Alternative Medicine*, vol. 2011, pp. 1–10, 2011.
- [156] R. H. Mahmoud and W. A. Elnour, "Comparative evaluation of the efficacy of ginger and orlistat on obesity management, pancreatic lipase and liver peroxisomal catalase enzyme in male albino rats," *European Review for Medical and Pharmacological Sciences*, vol. 17, no. 1, pp. 75–83, 2013.
- [157] H. Du, J.-S. You, X. Zhao, J.-Y. Park, S.-H. Kim, and K.-J. Chang, "Antiobesity and hypolipidemic effects of lotus leaf hot water extract with taurine supplementation in rats fed a high fat diet," *Journal of Biomedical Science*, vol. 17, no. 1, p. S42, 2010.
- [158] T. Murase, K. Misawa, Y. Minegishi et al., "Coffee polyphenols suppress diet-induced body fat accumulation by downregulating srebp-1c and related molecules in C57BL/6J mice," *American Journal of Physiology-Endocrinology and Metabolism*, vol. 300, no. 1, pp. E122–E133, 2011, [doi:].
- [159] I. Torre-Villalvazo, A. R. Tovar, V. E. Ramos-Barragán, M. A. Cerbón-Cervantes, and N. Torres, "Soy protein ameliorates metabolic abnormalities in liver and adipose tissue of rats fed a high fat diet," *Journal of Nutrition*, vol. 138, no. 3, pp. 462–468, 2008.
- [160] T. Wu, Q. Tang, Z. Gao et al., "Blueberry and mulberry juice prevent obesity development in C57BL/6 mice," *PLoS One*, vol. 8, no. 10, Article ID e77585, 2013.
- [161] Y.-S. Lee, B.-Y. Cha, K. Saito et al., "Effects of a Citrus depressa Hayata (shiikuwasa) extract on obesity in high-fat diet-induced obese mice," *Phytomedicine*, vol. 18, no. 8-9, pp. 648–654, 2011.
- [162] Y. Ono, E. Hattori, Y. Fukaya, S. Imai, and Y. Ohizumi, "Anti-obesity effect of *Nelumbo nucifera* leaves extract in mice and rats," *Journal of Ethnopharmacology*, vol. 106, no. 2, pp. 238–244, 2006.
- [163] C. Ma, J. Wang, H. Chu et al., "Purification and characterization of aporphine alkaloids from leaves of *Nelumbo nucifera* Gaertn and their effects on glucose consumption in 3T3-L1 adipocytes," *International Journal of Molecular Sciences*, vol. 15, no. 3, pp. 3481–3494, 2014.
- [164] T. Ogawa, H. Tabata, T. Katsube et al., "Suppressive effect of hot water extract of wasabi (*Wasabia japonica* Matsum.) leaves on the differentiation of 3T3-L1 preadipocytes," *Food Chemistry*, vol. 118, no. 2, pp. 239–244, 2010.
- [165] H. Kim and S.-Y. Choung, "Anti-obesity effects of *Bos-singaulti gracilis* Miers var. *pseudobaselloides* Bailey via activation of AMP-activated protein kinase in 3T3-L1 cells," *Journal of Medicinal Food*, vol. 15, no. 9, pp. 811–817, 2012.
- [166] H.-C. Chang, C.-H. Peng, D.-M. Yeh, E.-S. Kao, and C.-J. Wang, "Hibiscus sabdariffa extract inhibits obesity and fat accumulation, and improves liver steatosis in humans," *Food & Function*, vol. 5, no. 4, pp. 734–739, 2014.
- [167] L. Celleno, M. V. Tolaini, A. D'Amore, N. V. Perricone, and H. G. Preuss, "A Dietary supplement containing standardized *Phaseolus vulgaris* extract influences body composition of overweight men and women," *International Journal of Medical Sciences*, vol. 4, no. 1, pp. 45–52, 2007.
- [168] S. Snitker, Y. Fujishima, H. Shen et al., "Effects of novel capsinoid treatment on fatness and energy metabolism in humans: possible pharmacogenetic implications," *The American Journal of Clinical Nutrition*, vol. 89, no. 1, pp. 45–50, 2009.
- [169] P. C. Anunciação, L. d. M. Cardoso, R. d. C. G. Alfenas et al., "Extruded sorghum consumption associated with a caloric restricted diet reduces body fat in overweight men: a randomized controlled trial," *Food Research International*, vol. 119, pp. 693–700, 2019.